Role of extracellular polymeric substances on biocorrosion initiation or inhibition

Dissertation

zur Erlangung des akademischen Grades eines
Doktors der Naturwissenschaften
– Dr. rer. nat. –

vorgelegt von

Agata Joanna WIKIEŁ

geboren in Sokołów Podlaski

Biofilm Centre – Aquatische Biotechnologie

Fakultät für Chemie
der
Universität Duisburg–Essen

2013

Die vorliegende Arbeit wurde im Zeitraum von April 2010 bis Juli 2013 im Arbeitskreis von Prof. Dr. Wolfgang Sand am Biofilm Centre der Universität Duisburg–Essen durchgeführt.

Tag der Disputation: 26.08.2013

Gutachter:	Prof. Dr. Wolfgang Sand
	Prof. Dr. José J. G. Moura
Vorsitzender:	Prof. Dr. Christian Mayer

Those, whose love, experience, common sense and support led me, through the times of sadness and joy to this day

I dedicate this work.
I love you.

Tym, ktorych miłość, doświadczenie, rozsądek i wsparcie doprowadziły mnie, przez czasy smutku i radości, do dnia dzisiejszego

Pracę tą dedykuje.

Kocham Was.

ACKNOWLEDGEMENTS

Working on the Ph.D. has been a wonderful experience. It is hard to say whether it has been grappling with the topic itself, which has been the real learning experience, or grappling with how to write, give talks, work in a group, and stay focussed till the late night hours ... In any case, I am indebted to many people for making the time working on my Ph.D. an unforgettable experience.

First of all, I am deeply grateful to my advisors **Prof. Dr. Wolfgang SAND** and **Dr. Mario VERA** for introducing me into the fascinating world of microbiology. Working with them has been a real honour to me. They had oriented and supported me with care, and had always been patient and encouraging in times of new ideas and difficulties. Their ability to select and approach compelling research problems, their high scientific standards, and their hard work set an example. I appreciate it from all my heart.

I also want to thank to all current and former colleagues from the **Aquatic Biotechnology group**, and to whole **Biofilm Centre,** because they provided a great atmosphere and lots of fun. Thank you for your motivation and support.

The research leading to these results has received funding from the Marie Curie European Community's Seventh Framework Programme (FP7/2007–2013) under grant agreement n°238579, BIOCOR Initial Training Network (www.biocor.eu/ip4). The BIOCOR project gave me this tremendous opportunity to collaborate with research institutes across Europe and to work with the best scientists within the field of biocorrosion. I am very grateful for all BIOCOR network meetings, trainings and scientific discussions. All that was possible thanks to an excellent project coordination and management and I want to thank for that **Dr. Régine BASSEGUY**, **Mr. Vincent BIRRIEN** and **Mrs. Jennifer STEPHENSON**. In this place I would like to thank also all BIOCOR students, especially **Yaryna DATSENKO, Omar Rosas CAMACHO and Marko STIPANICEV** for effective brainstorming during our workshops and for great time we had together during informal meetings.

I will be forever thankful to **Prof**. **Dr. José J.G. Moura, Leonardo Dall'Agnol** and the **Bion/Bioprot group** from Universidade Nova de Lisboa, Portugal not only for the fantastic and fruitful time, I have spent there during my secondment, for their scientific advice, knowledge, many insightful discussions and suggestions. But also for their heart, inspiration, positive energy and "travesseiros".

I would like to sincerely acknowledge **Dr. Isabelle FRATEUR, Blanca Estela TORRES BAUTISTA** and **Prof. Dr. Philip MARCUS** from Centre National de la Recherche Scientifique, Laboratoire de Physico–Chimie des Surfaces (CNRS–LPCS), France for provision of equipment and laboratory, extensive training, scientific support and very

intensive electrochemical discussions. They were my primary resource for getting my electrochemical questions answered.

I would like to express my thankfulness to **Prof. Dr. Christine DUPONT–GILLAIN, Prof. Paul ROUXHET** and **Yi YANG** from Université Catholique de Louvain, Belgium for the opportunity to carry out various surface analyses, for fruitful discussions and their life wisdom.

I would like to thank **Prof. Dr. Iwona BEECH** and **Jemimah DOMA** for their help in microbial diversity studies, for their open minds and open hearts.

I am also grateful to **Dr. Justyna E. JOŃCA** from the Centre Nationale de la Recherche Scientifique – Laboratoire de Chimie de Coordination (CNRS–LCC) for her help in performing Transmission Electron Microscopy images.

I would like to thank **Dr. Larysa PURISH** from the General and Soil Microbiology Department, Zabolotny Institute of Microbiology and Virology, Ukraine for the open laboratory doors and sharing her experience in the lipid analyses.

*I will be forever grateful to my **Parents** and **Siblings: Rafał, Łukasz, Kasia, Ewa** and **Mateusz** because I would not have gone so far without their love, support, trust and faith.*

*I thank my friends and my family **Danuta**, **Paolo** and **Jessica**, who took me with open hearts and supported in the good and bad days.*

*I would like to thank my friend **Zosia** for sharing her experience and motivation, for being for me whenever I needed it and for always fruitful conversations.*

*I thank my best friend **Justynka** for having faith in me and my intellect, for shaping my character and not only … and forher attention, understanding and unlimited energy for our talks.*

*Finally, I would like to thank my boyfriend and soul mate **Adrian** for his unlimited patience and support when times were rough, for sharing with me his heart and every second of his life, independently of the distance. For being with me.*

Your unconditional love, attention and faith led me to this day.

Kocham Was.

TABLE OF CONTENTS

LIST OF FIGURES

LIST OF TABLES

LIST OF ABBREVIATIONS

AAS	Atomic absorption spectrophotometer
AC	Alternating current
AFM	Atomic force microscopy
AmOx	Ammonia oxidisers
AP	Acid producers
APB	Acid producing bacteria
ASW	Artificial seawater
b	Tafel constant
b_a	Anodic Tafel constant
b_c	Cathodic Tafel constant
BSA	Bovine serum albumin
CE*	Counter electrode
CE**	18-crown-6 ether
CFU	Colony-forming unit
CLSM	Confocal laser scanning microscopy
D N A	Deoxyribonucleic acid
DAPI	4',6-diamidino-2-phenylindole
DC	Direct current
DGGE	Denaturing gradient gel electrophoresis
DMSO	Dimethyl sulfoxide
E	Electrode potential
E_b	Binding energy
E_c	Charging effect (in XPS studies)
E_{corr}	Corrosion potential
eDNA	Extracellular DNA
EDTA	Ethylenediaminetetraacetic acid
EFM	Epiflurescence microscopy
EIS	Electrochemical impedance spectroscopy
E_k	Kinetic energy
EOR	Enhanced oil recovery
EPS	Extracellular polymeric substances
ER	Extraction reagent
FAME	Fatty acids methyl esters
FeOx	Iron ixidisers
FeRed	Iron reducers
FITC	Fluorescein-isothiocyanate
GC	Gas chromatography
h	Planck's constant
HF	High frequency
hNRB	Heterotrophic nitrate reducing bacteria
HOB	Hydrocarbon oxidising bacteria
Hz	Hertz
i	Current
i_a	Cathodic current
i_c	Anodic current
i_{corr}	Corrosion current
IRB	Iron reducing bacteria
KDO	2–keto–3–deoxyoctonate
LB	Luria Bertani growth medium

LB EPS	Loosely bound EPS
LP	Linear polaristion
MIC	Microbially influenced corrosion
MnOx	Manganese oxidisers
MnRB	Manganese reducing bacteria
MnRed	Manganese reducers
MOB	Metal oxidising bacteria
MPN	Most probable number
MRB	Metal reducing bacteria
MRB	Metal reducng bacteria
mVMN	VMN medium mineral salts solution
NCBI	National Center for Biotechnology Information
NiOx	Nitrite oxidisers
Nred	Nitrate reducers
NR-SOB	Nitrate reducing sulfide oxidising bacteria
O&G	Oil and gas
OCP	Open cirquit potential
OD	Optical density
Ox	Oxidant
PBS	Phosphate buffer saline
PCR	Polymerase chain reaction
PIPES	10 mM piperazine–N,N′–bis(2–ethanesulfonic acid)
R	Resistance
rDNA	Ribosomal DNA
RE	Reference electrode
Red	Reductant
RT	Room temperature
S^0Ox	Sulfur oxidisers
S_2O_3Ox	Thiosulfate oxidisers
SCE	Standard calomel electrode
SDS PAGE	Sodium dodecyl sulfate polyacrylamide gel electrophoresis
SOB	Sulfur oxidising bacteria
SO-Nred	Sulfide oxidising nitrate reducers
SPV	Sulfo–phospho–vanillin
SRA	Sulfate reducing archea
SRB	Sulfate reducing bacteria
SRP	Sulfate reducing prokaryotes
t	Time
TB EPS	Tightly bound EPS
TEA	Tris base, acetic acid and EDTA buffer
TEM	Transmission electron microscopy
TRITC	Tetramethyl rhodamine isothiocyanate
TVL	Total volatile solids
v	Frequency of an associated electromagnetic wave
VBNC	Viable but nonculturable
VMN	Growth medium for SRP
WE	Working electrode
XPS	X–ray photoelectron spectroscopy
Z	Impedance
ZJ	Imaginary part of the impedance
ZR	Real part of the impedance

φ	Phase
Φ_{sp}	Work needed to brng the electron from the zero attraction to the entrance of the energy analyser (in XPS studies)
ω	Frequency
*	Electrochemical studies
**	EPS investigations

GENERAL INTRODUCTION

The oil and gas industry experience financial losses originated from deterioration processes affecting the production operations. Carbon steel, commonly applied as a construction material for the oil transport and storage facilities, undergoes corrosion processes induced by various environmental factors. Abiotic factors, such as oxygen availability, presence of certain chemical compounds (e.g. hydrogen sulfide or chlorides), flow conditions, deposits formation are well known (Beech and Gaylarde, 1999). However, biotic factors, neglected for a long time, can significantly contribute to the corrosiveness of the environment, decreasing the oil quality as well as efficiency of mitigation strategies. Production and injection systems harbour diverse microbial communities that can participate in deleterious processes such as microbially influenced corrosion (MIC). Microorganisms are able to initiate, facilitate or accelerate corrosion reactions through the interaction with the metal and/or solution. They may influence the kinetics of corrosion processes of metals (Little and Lee, 2007).

Microorganisms accumulate at the interfaces and form biofilms. Life within the biofilm is beneficial for microorganisms, as it protects them against various environmental stresses, biocides, lack of nutrition and desiccation. It is a diverse structure stabilised by the extracellular polymeric substances (EPS). The organisation of the biofilm, or more specifically the extracellular matrix, in which cells are embedded, needs to be carefully evaluated. EPS is known to form and stabilise the biofilm through weak physicochemical interactions, being also an important factor of metal–microbe interactions, providing the reaction space for the corrosion processes. Thus, EPS characterisation and evaluation of its influence on biodeterioration has been the core part of this research work.

MIC is a very complex problem, thus it is urgent to apply a multidisciplinary approaches to support the industry with a proper feedback. Combination of microbiological and physico–chemical methods creates a powerful tool to reach this goal. The experimental approach of this work, shown in the **FIG.1**, was divided in two theoretical chapters, which highlighted the field of interest as well as five experimental sections.

The first theoretical section (Chapter I) describes the oil and gas industry. Here a special interest was focused on the recovery processes. Later on biodeterioration

problems, affecting this field were specified and the strategies against MIC recalled. Description of biofilms and EPS closes this chapter.

The second chapter is a review of various techniques applied in this study. First, the fundamentals of several electrochemical techniques were described. This included the characteristics of the corrosion potential (E_{corr}), linear polarisation (LP) and electrochemical impedance spectroscopy (EIS). A special attention was paid to the latter technique, as it is a very difficult subject and researches just recently started to use it for EPS investigations. Later on, X–ray photoelectron spectroscopy was presented. This technique was used to characterise which EPS components can adsorb to the steel surface. Additionally, various microscopic techniques were described, as indispensable tools for the biofilm formations studies.

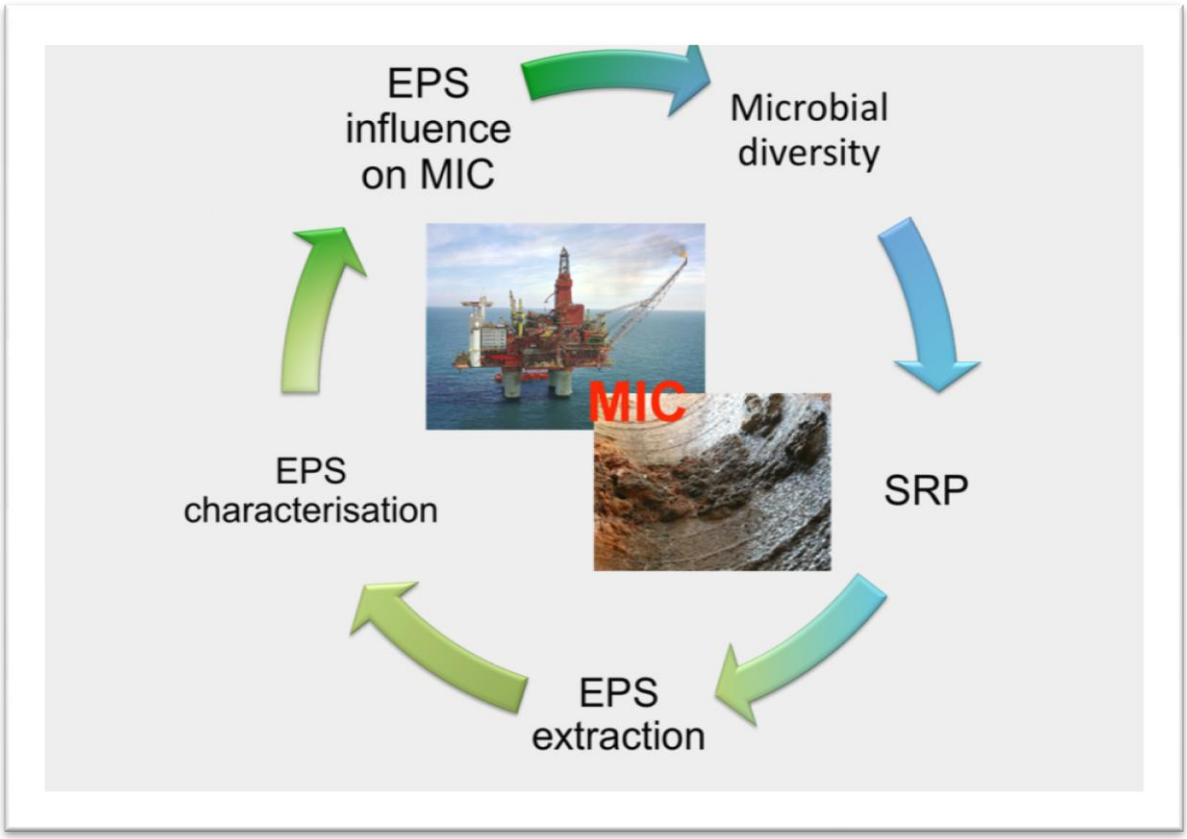

FIG. 1. EXPERIMENTAL SCHEME APPLIED IN THIS STUDY. USED PICTURES SHOW AN OIL PRODUCTION PLATFORM AND IRON SULFIDES DEPOSITS DUE TO MIC. SRP – SULFATE REDUCING PROKARYOTES, EPS – EXTRACELLULAR POLYMERIC SUBSTANCES.

The third chapter focused on the characterisation of the microbial diversity present at the corrosion sites from various water injection and oil production systems. Here culture–dependent and molecular techniques were used. Additionally, the

dynamics of microbial attachment and biofilm formation on the carbon steel surface were visualised.

The potential involvement of the sulfate reducing bacterium, *Desulfovibrio alaskensis* AL1, in the steel corrosion was characterised in the fourth chapter. This included monitoring of corrosion potential, microscopic studies of the biofilm formation and investigations of effects of its biofilm on the carbon steel surface. EPS extracted from this model microorganism was used for further investigations.

In the fifth chapter, an EPS extraction protocol for *D. alaskensis* AL1 was optimised. The reason for that was the need of isolation of sufficient amounts of pure EPS suitable for the studies presented in other chapters. A special attention was focused on avoiding EPS contamination with remaining extraction reagents and the cell lysis products.

The diversity of *D. alaskensis* AL1 EPS secretion in various conditions was shown in the Chapter VI. Studies of the influence of carbon steel and flow conditions in a bioreactor on the EPS secretion were performed. These results were compared with EPS secreted under static conditions in absence of the mentioned carbon steel plates. This included quantitative analyses of the EPS composition, extracellular protein profiles, fatty acids methyl esters and EPS visualisation techniques.

The final chapter focused on the investigations of EPS behaviour on the steel surface. This included monitoring of electrochemical response of carbon steel to the presence of EPS. The chemical nature of the surface–active molecules present in the EPS was complementarily investigated with use of X–ray photoelectron spectroscopy and surface tension measurements.

REFERENCES

Beech, I.B., Gaylarde, C.C., 1999. Recent advances in the study of biocorrosion: an overview. Rev. Microbiol. 30, 117–190.

Little, B.J., Lee, J.S., 2007. Microbiologically Influenced Corrosion. John Wiley & Sons.

CHAPTER I: BIODETERIORATION OF STEEL

Corrosion refers to the deterioration of a material as a result of chemical reactions with its surrounding environment. It is an ubiquitous problem, affecting various areas of a daily life. Corrosion process can be influenced by microbial activities, especially when the organisms are in close contact with the metal surface forming a biofilm. The resulting metal deterioration is known as biocorrosion, or microbially influenced corrosion (MIC). All industrial facilities are susceptible of microbial contamination, especially those that use or are in contact with non–sterile fluids, such as petroleum industry.

This chapter was focused on describing the oil and gas (O&G) field, with the special interest on the oil recovery processes. The effect of living organisms on the O&G structures and applied mitigation techniques against them are described. Later on, the corrosion fundamentals are recalled. The complexity of biocorrosion problems and microorganisms involved in this process are shown, to finally focus on the biofilms, as a microbial existence and survival strategy. The role of EPS in the biofilm formation and MIC is also presented.

1.1. Oil and Gas industry

1.1.1. Field characterisation – the recovery processes

Important reserves of oil and gas (O&G) are located under the sea floor in many parts of the globe. Offshore drilling platforms are composite systems able to pump tons of barrels of oil daily, being very dynamic and cost–effective investments. Production, transportation and storage processes of hydrocarbons mixed with highly corrosive and biologically active seawater are the subjects of high biodeterioration problems, as they provide adequate conditions for microbial growth.

The life cycle of an oil reservoir generally consists of three phases of production. The primary phase utilises natural reservoir pressures and lift equipment to produce the oil. As it flows through the formation rock into the well bore, oil is pumped to the surface and recovered. After some period of time, the well naturally empties and the secondary phase technology or water flooding is applied (**FIG. 1.1**). Large volumes of water are injected into the oil reservoir to sweep the remaining oil into the well bore before being pumped out to the surface. Finally, a tertiary phase technology, called also enhanced oil recovery (EOR) or improved oil recovery, is applied. This technology lifts oil from low–pressure reservoirs due to carbon dioxide injection. This approach is applied to further enhance water flooding. The cyclical process begins when water injection is temporarily suspended and replaced with the injection of large volumes of carbon dioxide. After some period of time, the injection switches back to water. The alternating carbon dioxide and water slogs are then pumped into the reservoir to sweep the residual oil, not recovered by the primary and secondary phases of production. The carbon dioxide reduces the oil viscosity and increases the relative permeability, so the trapped oil is mobilised and can flow easily through the rocks. The production stream consisting of oil, water and carbon dioxide is gathered by the flow lines and than processed through the separation equipment. The recovered oil is stored for further transport and sale, while the water and carbon dioxide are then returned in separate streams to the injection systems repeating the cycle.

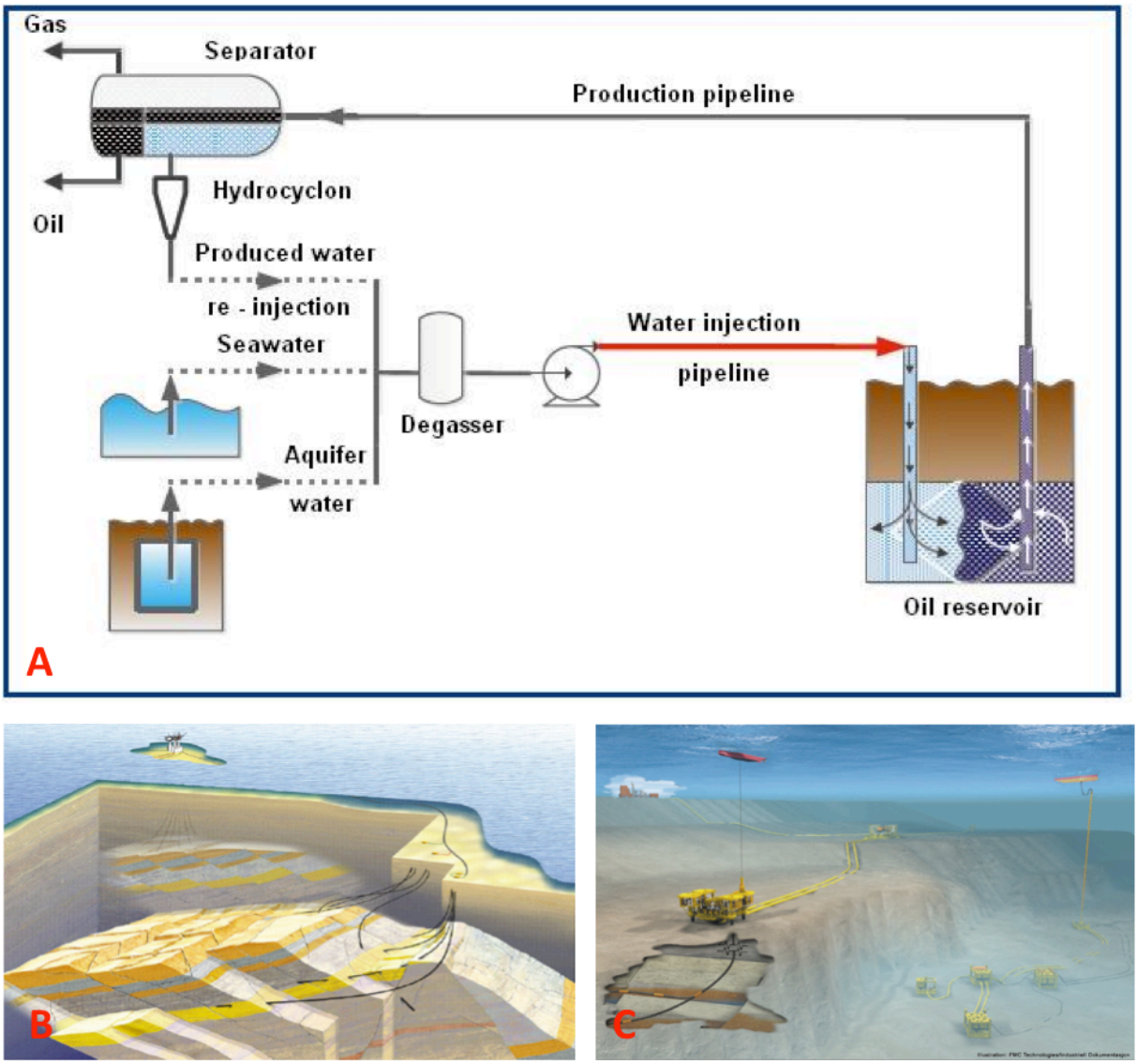

FIG 1.1. OIL AND GAS RECOVERY PROCESS: WATER INJECTION PIPELINE SCHEME (A), ADAPTED FROM (COMANESCU ET AL., 2012); THE OIL RESERVOIR (B) AND SUBSEA INSTALLATION (C). DOTTED LINES IN THE UPPER SCHEME INDICATE INJECTION OF EITHER PRODUCED, AQUIFER, SEAWATER OR A MIXTURE OF THEM IN THE DIFFERENT COMBINATIONS.

Different types of water are injected to the well. One of the possibilities is to use produced water, which is any water that is produced during the secondary or tertiary oil recovery. Alternatively, seawater or aquifer water may also be used. Finally, a mixture of them in different proportions can be used for enhancement of recovery rates of extracted oil. The choice of water to be used is mainly based on availability and economic reasons. The water used for the injection is treated in various ways. Commonly, as presented in **FIG. 1.2** it is first mechanically cleaned and filtered for the removal of sand particles. Further on, it is treated with sodium hypochlorite and UV–light, followed by the use of oxygen scavengers (degassing package) to reduce its oxygen content. Very often, at the end of the process nitrate is added to reduce

reservoir souring by the hydrogen sulfide produced by sulfate reducing prokaryotes (SRP).

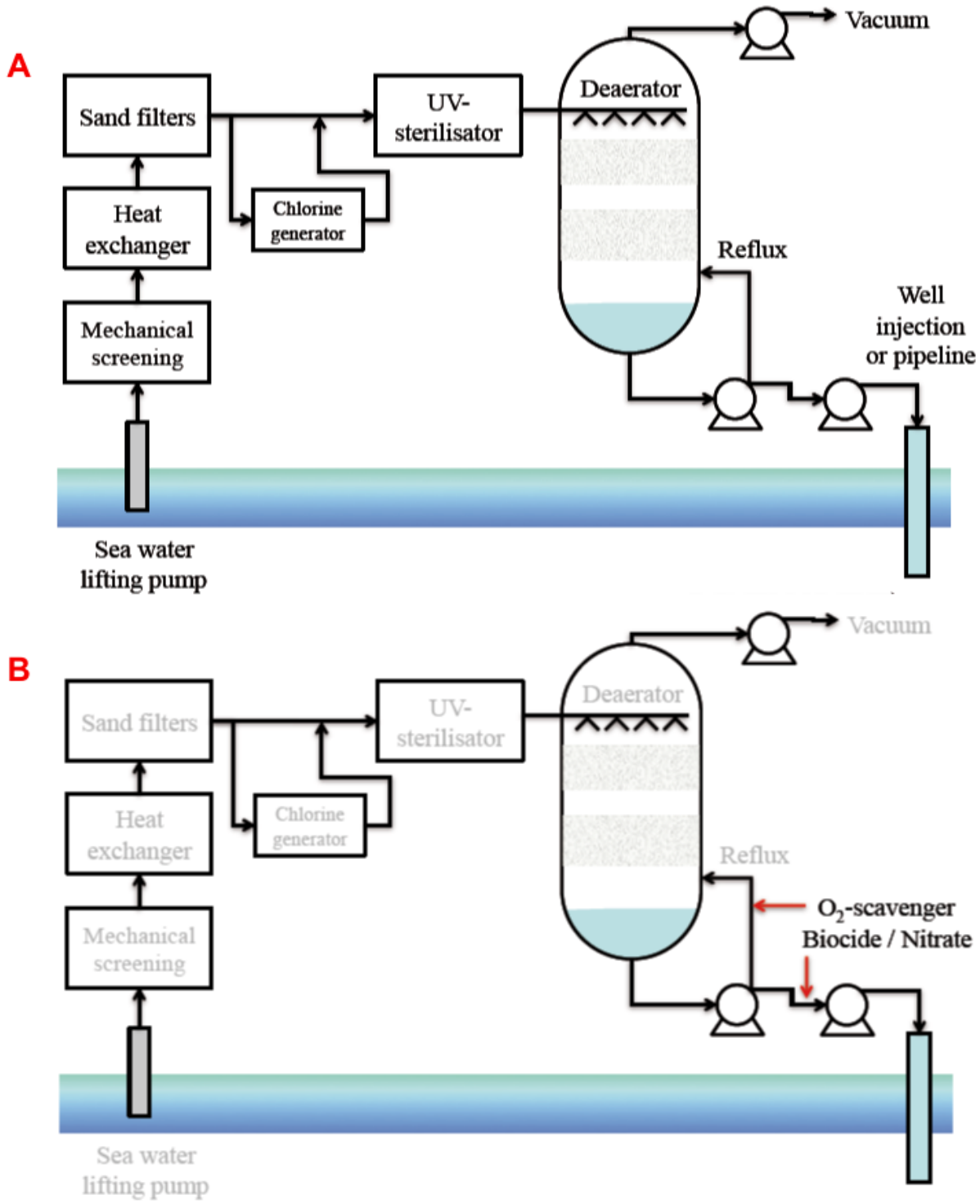

FIG. 1.2. SEAWATER TREATMENT BEFORE THE INJECTION: MECHANICAL CLEANING AND STERILISATION (A) AND BIOCIDE / NITRATE TREATMENT (B).

In order to decrease the likelihood of localised corrosion caused by oxygen presence and to reduce the microbial growth, the water treatment process is repeated before each injection to the well.

1.1.2. Biocorrosion problems and mitigation strategies

Despite the water treatment, O&G production plants perennially suffer from MIC. Another industrial problems of microbial origin are linked to souring, i.e. the hydrogen sulfide content in oil or water and biofouling, referred as unwanted deposition and growth of biofilms (Flemming, 2002). Biocorrosion, as well as biofouling of industrial systems, generate microbiological contamination, which brings energy and production efficiency losses. However, many industrial sites neglected or overlooked these circumstances, until the irreversible damages were a source of serious system failures and environmental destruction. Biodeterioration problems have been underestimated since they usually need time to be directly visible and therefore taken under consideration. While designing the systems, the priority was put on oil recovery processes more than on its transportation and storage cases.

Offshore structures suffer from living organisms, which cover the submerged surfaces of the platform, both in the seawater and in the mud at the base of the structures. However, there is a little concern in the industry about corrosion of the external structures under marine fouling. Microbial activity at the pipeline interior is more dynamic. The biggest deterioration problems occur in water injection pipelines and oil production systems. In the production wells at the beginning of an oil reservoir's lifespan, oil rises through the production wells under the internal drive pressure of the reservoir. Primarily, it contains very little amounts of water, being almost inert for the establishment of the biodeterioration problems. As the reservoir is gradually depleted of oil, the amount of water increases, creating an ideal environment for the microbial growth.

In turn, water injection systems are affected by several problems associated mainly with the use of seawater to maintain the reservoir pressure. In practice, the water source chosen for secondary recovery operations is typically the easiest and cheapest source of water for offshore flooding operations. It contains contaminants, which can block the reservoir and are corrosive to the equipment and plant components. Especially vulnerable to the damage are the parts situated in the water

uptake, filtration and subsequent pipe–work. Seawater typically contains 25–30 mM sulfate, thus providing abundant electron acceptor for SRP activity (Gieg et al., 2011). For that reason, mixtures of seawater and aquifer water are used to decrease these problems.

The golden rule, which is applied to the industrial systems, in order to prevent and control biocorrosion and biofouling is “Keep the system clean” (Videla, 2002). Here the main attention is focused on the removal of deposits from the metallic surfaces. Thus, a wide range of chemical, mechanical and other methods are used to control biological activity on offshore structures. This includes the use of *inter alia* mineral and organic acids, chelating compounds, such as EDTA, biocides and coatings. Another procedure of special interest is a mechanical treatment, such as the periodic „pigging“ process. A pipeline inspection gauge, or “pig”, is a tool with which pipelines are cleaned and/or inspected internally. One of the advantages of using pigs comes from removing more debris and solid products. “Pigging” improves also the flow efficiency of the pipeline and water quality. It lowers the pumping pressure and allows avoiding piping modifications. Their design allows “pigs” to create a tide seal in the line and to be most often propelled by the existing pressure in the pipeline. When an adequate pressure and volume are applied behind the pig, it forms the sliding seal passing through the line. Pig sizes differ among the systems. They can be from 5 cm small in diameter, but when requested they can be made up to 160 cm. Depending on the needs, pipeline pigging can range from few to tens of pigs, when the system is strongly deposited. Also the pigs used for cleaning usually differ from each other. The first pigs are made of the soft foam swab to collect the easiest removable sludge. Hard scale deposits are then removed with devices equipped with cleaning wire brushes, as shown in the **FIG. 1.3**. The last pig running through the system (called the "intelligent pig") is used for the system inspection, failure and damage monitoring. Use of “pigging” system does not require a lot of time and the service is interrupted only for several hours. Further on, the collected debris can be used for microbial diversity studies.

FIG. 1.3. CLEANING PIG (LEFT) AND PIGGING DEBRIS (RIGHT).

However, "pigging" process can only be applied to these systems, which have been previously specially adapted to this treatment. In other cases chemical cleaning is the only alternative. The usual industrial practice, if possible, includes both procedures: mechanical cleaning and chemical treatment.

1.2. Corrosion fundamentals

Corrosion is referred as the destructive attack of a metal by a chemical or electrochemical reaction with its environment (Uhlig and Revie, 1985; Fontana, 1986). When a metallic material is exposed to an aqueous environment it can donate electrons if an electrical circuit is completed. When an important amount of electrons migrate from the anode to the cathode and consequently the formation of positively charged metal ions is enhanced, then corrosion occurs. The electrons, generated in the primary metallic dissolution process (anodic reaction), are consumed in a secondary process (cathodic reaction). The anodic or oxidation reaction of a metal M is:

$$M \rightarrow M^{n+} + ne^{-} \tag{1.1}$$

Where the electron flow constitutes the anodic current, I_a. For iron this reaction is:

$$Fe \rightarrow Fe^{2+} + 2e^{-} \tag{1.2}$$

In the cathodic reaction an oxidant (Ox) in the electrolyte is reduced to a reductant (Red):

$$Ox^{q+} + ne^{-} \rightarrow \mathrm{Re}\, d^{(q-n)+} \tag{1.3}$$

Where the electron flow constitutes the cathodic current, I_c. In aerated water solutions the dominant cathodic reaction is the reduction of dissolved oxygen. In anaerobic solutions the reduction of protons dominates, what is represented as the reduction of water (Lewandowski et al., 1997). In the latter (anaerobic) conditions this can be described as:

$$2H_2O + 2e^- \rightarrow H_2 + 2OH^- \quad (1.4)$$

The corresponding net reaction is:

$$2H_2O + Fe \rightarrow Fe(OH)_2 + H_2 \quad (1.5)$$

In aerobic solutions, the basic anodic reaction is the same as the one described in equation 1.2, dissolution of iron. The products of the reaction – ferrous ions, react with oxygenated water (equation 1.7, below) and are further oxidised by the available oxygen (equation 1.8):

$$O_2 + 2H_2O + 4e^- \rightarrow 4OH^- \quad (1.6)$$

$$2Fe + O_2 + 2H_2O \rightarrow 2Fe(OH)_2 \quad (1.7)$$

$$4Fe(OH)_2 + O_2 + 2H_2O \rightarrow 4Fe(OH)_3 \quad (1.8)$$

For corrosion to occur an anodic reaction, a cathodic reaction, an ionic conductor (electrolyte, culture media) and an electrical intermediary between the two reactions are needed; the latter is an electronic conductor (metal e.g. iron or carbon steel). The rate of corrosion is depending on the rate of the partial reactions and their current densities, respectively.

1.3. Types of corrosion

Corrosion takes many different forms. The uniform (or general) corrosion is characterised by a corrosive attack proceeding evenly over the entire surface area, or a large fraction of the area of the metal under attack. Uniform corrosion results in

loss of material until failure. This is the most widespread form of corrosion that is observed.

However, corrosion process can occur also locally. Pitting corrosion is a localised form of corrosion by which pits or "pin holes" are produced in the material. Pitting is considered to be more dangerous than uniform corrosion damage, because it is more difficult to predict and counterattack. Corrosion products often cover the pits, making the detection step very difficult. A small, narrow pit with minimal overall metal loss can lead to the failure of an entire engineered system.

Similar to pitting, crevice corrosion occurs at a specific location. This type of corrosion is often associated with a stagnant microenvironment, like the ones found under gaskets, washers and clamps. Acidic conditions, or a depletion of oxygen in a crevice can lead to this type of corrosion.

Galvanic corrosion refers to corrosion damage induced when two dissimilar materials are coupled in a corrosive electrolyte. It occurs, for example when they are brought into electrical contact under water. When a galvanic couple forms, one of the metals in the couple becomes the anode and corrodes faster than it would do by itself, while the other becomes the cathode and corrodes slower than it would alone.

1.4. Microbially influenced corrosion

Microbial communities attached to the surface, referred as biofilms, cause MIC. When biofilms accumulate on metal surfaces, reactants and products of microbial activity are entrapped in the biofilm space, influencing both the solution and the surface chemistry. These modifications may interfere with the electrochemical processes naturally occurring at the interface between the substratum and the environment. Modifications in the biofilm may include the microbial community structure and the composition of extracellular polymeric substances (EPS). Each of these modifications is complex and may affect the corrosion reactions in various ways. For example, biofilm created heterogeneities lead to the concentration gradients (Lewandowski and Beyenal, 2009). Also these structural heterogeneities established over metallic surfaces induce the separation of anodes and cathodes – favouring localised corrosion processes. An example of this phenomenon is when a non–uniform microbial colonisation occurs. As a consequence, differential aeration cells are formed, generating potential differences due to oxygen gradients, and

hence, corrosion current. The corrosion reactions may be also modified by the metabolic reactions on the metallic substratum, occurring in the biofilms. Other factors include the increase in the mass transport resistance near the metal surface or the generation of aggressive chemical species for steel substances, modifications in the conductivity of the interface, chelating of metallic ions in the polymeric matrix and destabilisation of corrosion inhibitors.

Microorganisms can attack various materials. Some ones provide nutrients and some act as a substratum for their growth and biofilm formation (Sand, 1994). Thus MIC comprises diverse types of failures, occurring at different materials, including metal, plastics or concrete. Microbes can promote reactions, which would not occur naturally under abiotic conditions. This is a consequence of the great variety of physiological activities that can take place by different types of microorganisms – that do not act isolated, but associated to the chemical and electrochemical forces of particular environments (Beech and Gaylarde, 1999). Consequently, biofilms can be formed under these conditions, under the presence or the absence of oxygen, creating oxic or anoxic gradients depending on the environmental conditions (Videla and Characklis, 1992).

MIC was shown to be an important reason for the failure of pipelines in the O&G industry under several environments (Brondel et al., 1994). In these industries, the problems originated by microbial activity are particularly difficult to diagnose, evaluate and control. The characterisation of the microbial communities within these industrial environments is important in order to establish their possible interactions, their multicellular strategies and their bioelectrochemical influence on industral metallic facilities.

1.4.1. Microorganisms involved in MIC

Biodeterioration at metal surfaces is associated with microorganisms, or the products of their metabolic activity including enzymes, EPS, organic and inorganic acids, as well as volatile compounds such as ammonia or hydrogen sulfide (Beech and Gaylarde, 1999). Microbes are ubiquitous in the environment and are fundamental to the biogeochemical cycling of nutrients in marine, freshwater and terrestrial ecosystems. Their ability to influence the corrosion of many materials normally considered as resistant to destruction, in a variety of environments, makes

microorganisms a real threat to the stability of those metals. The sub–surface microbial community structure is highly diverse and able to adapt to different conditions. Thus, MIC is rarely associated to one single mechanism or to one single species of microorganisms (Videla, 2005; Lewandowski and Beyenal, 2009).

Within a very rich microbial flora metal oxidising / reducing microorganisms (MOB and MRB, respectively), especially these of iron and manganese cycle, methanogens, microorganisms of nitrogen cycle, as well as mineral acid producers (APB), fungi and other slime producers have been implicated in the steel deterioration (Beech and Coutinho, 2003).

However, the most often discussed and considered to have the highest influence on MIC processes and oil field losses are microbes able to produce hydrogen sulfide (H_2S), which is the key souring agent. It occurs in the environment when sulfate, sulfite, thiosulphate or elemental sulfur are reduced by microbes to gain energy for growth (Liamleam and Annachhatre, 2007). Such biological sulfide production is a detrimental, widespread phenomenon in the petroleum industry, occurring within oil reservoir and topside processing facilities under various temperatures in any offshore or onshore operations (Gieg et al., 2011). The most investigated microorganisms known to produce H_2S are sulfate reducers. Most of them are bacteria, typically *Deltaproteobacteria* and *Firmicutes*, and are designated as Suflate Reducing Bacteria (SRB). Some sulfate reducers phylogenetically affiliate with the Archaea and are designated as Sulfate Reducing Archaea (SRA). In order to characterise sulfate respiring microbes, independently of their phylogenetic affiliation, they will be further described as Sulfate Reducing Prokaryotes (SRP). These microorganisms are anaerobes, ubiquitous to marine fouling communities and most other anaerobic environments (such as marine mud, inside platform legs, oil storage tanks, as well as water and production systems). H_2S is particularly aggressive, as the sulfide ions directly attack metal surfaces leading to anaerobic corrosion and pit formation (Hamilton, 1985). Additionally, production of sulfide leads to air quality lowering, provoking health and safety problems, environmental hazards (Tang et al., 2009; Williamson, 2011) and a wide range of economic losses due to reservoir souring and corrosion of metals. They are easily introduced into any system and become active in the areas of low oxygen concentration. Sulfur or thiosulfate reducing organisms can also produce sulfide as end product and potentially contribute to souring. Iron sulfide production in combination with bacterial cell

masses provokes pipe plugging, decreases heat exchange efficiency, and may clog filters, valves and other control equipment. H_2S can sour oil and gas by increasing their sulfur content, reduce the value of the related product and extending the corrosive effects along the pipeline. More information about the SRP activity can be found in the Chapter IV.

Nevertheless, there are other microorganisms able of secrete sulfides. Various culture media for the enumeration of SRP support the growth of facultative sulfide producers such as *Shewanella putrefaciens* and *Aeromonas veronni* (Lutterbach and Contador, 2011). *Shewanella* are facultative iron reducing bacteria (IRB), able to grow under both aerobic and anaerobic conditions, what gives them an advantage at the oxic–anoxic interfaces within a biofilm. In aerobic conditions *Shewanella* uses oxygen as the final electron acceptor. *Shewanella* can also use manganese, nitrate, nitrite, thiosulfate, elemental sulfur as terminal electron acceptors (Lovley et al., 1989; Myers and Myers, 1994; Moser and Nealson, 1996). Because of their ability to reduce ferric iron and sulfite, oxidise hydrogen gas, and produce sulfide they may also contribute considerably to MIC generation (Dawood and Brözel, 1998; Videla et al., 2008). Due to their versatile metabolism, these bacteria are strong competitors within the biofilm community. Some studies have shown a rival behaviour between SRP and IRB (Lutterbach et al., 2009; Roden et al., 2000). Other microorganisms influencing MIC are metal reducers, such as iron and manganese reducing bacteria (MnRB), which can attack the protective passive layers on metal surfaces. They dissolve the oxide film and replace it by less stable and corrosion resistant metal layers. This results in the loss of protective passive layers on e.g. stainless steel surface, allowing further corrosion to occur. Bacterial oxidation of Fe^{2+} and Mn^{2+}, present either in the bulk medium or at metal surface, promote corrosive reactions by accumulation of cathodically reactive ferric and manganese oxides. These slimy precipitates of hydrated ferric oxide, that are further formed will reduce filter efficiency and, if they reach the reservoir, may decrease the permeability of the reservoir rock. Although the major problem associated with iron bacteria is plugging, their growth may also result in increased corrosion rates by differential aeration.

APB and fungi produce inorganic and organic acids. Sulfur, ammonia, nitrite oxidation leads to the occurrence of sulfuric and nitric acids, which solubilise metals, and cause surface deterioration. Sulfur oxidising bacteria oxidise sulfur compounds, such as sulfide, to sulfur or sulfate. They are often found in association with SRB

where they can form corrosive 'sulfureta', alternating oxidised and reduced sulfur environments (Moosavi and Hamilton, 1987).

In the oil field it is also not surprising to find hydrocarbon oxidising bacteria (HOB), able to degrade oil and reduce the available oxygen (Rosenberg, 2006). The ratio of HOB to the total population of heterotrophic bacteria, as well as their variety may change according to the time of sampling or the extent of oil content. Their presence in the field will provide both nutrients and suitable conditions for sulfate reducing microbial activity.

Nitrate treatment for prevention or decrease of reservoir souring can have as a consequence a shift of the indigenous microbial communities away from sulfide production. Many microbes such as heterotrophic nitrate reducing bacteria (hNRB) and nitrate reducing sulfide oxidising bacteria (NR–SOB), found in nitrate treated systems can be involved in sulfide attenuation strategies (Hubert et al., 2003; Nemati et al., 2001). One of the primary mechanisms is believed to be due to microbial competition between hNRB (reaction [4], **FIG. 1.4**) and SRP for available electron donors (Grigoryan et al., 2008; Hubert et al., 2009), as shown in the reaction [1], **FIG. 1.4**. Some SRP as well as many hNRB and NR–SOB can reduce nitrate to ammonia (Moura et al., 1997). NR–SOB can help decrease the concentrations of existing sulfide by oxidising it to sulfate and elemental sulfur (S°), using nitrate as the electron acceptor to produce primarily nitrite and/or N_2 (reaction [3], **FIG. 1.4**). Nitrite can also chemically oxidise the existing soluble sulfide (reaction [5], **FIG. 1.4**) to yield a mixture of products, including ammonium, polysulfides, S°, and sulfate (Kaster et al., 2007; Lin et al., 2009).

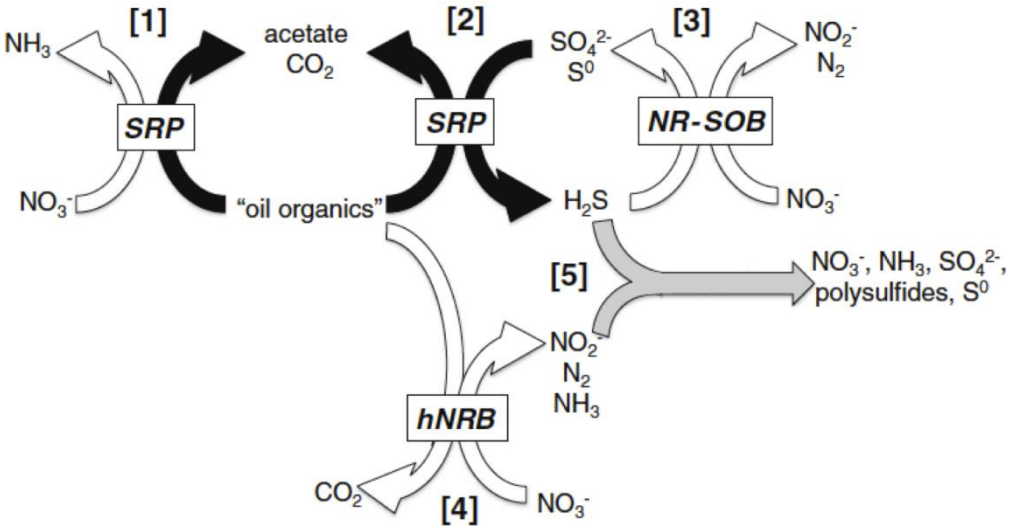

FIG. 1.4. SCHEME OF THE INTERSECTIONS OF SULFUR AND NITROGEN BIOGEOCHEMICAL CYCLES THAT CAN OCCUR IN OIL RESERVOIRS. BLACK ARROWS DENOTE SULFUR–CYCLE REACTIONS; WHITE ARROWS DENOTE NITROGEN CYCLE REACTIONS; GRAY ARROWS DENOTE NON–BIOLOGICAL CHEMICAL REACTIONS. SRP DENOTES REACTIONS CONDUCTED BY SULFATE–REDUCING PROKARYOTES, HNRB DENOTES REACTIONS PRIMARILY CONDUCTED BY HETEROTROPHIC NITRATE OR NITRITE–REDUCING BACTERIA, NR–SOB DENOTES REACTIONS PRIMARILY CONDUCTED BY NITRATE–REDUCING SULFIDE–OXIDIZING BACTERIA. REACTIONS: [1] AMMONIFICATION; [2] SULFIDOGENESIS; [3] COMPLETE AND PARTIAL SULFIDE OXIDATION; [4] HNRB COMPETITION WITH SRP FOR ELECTRON DONORS, COUPLED TO INCOMPLETE REDUCTION OF NITRATE TO NITRITE; [5] CHEMICAL REACTION OF NITRITE WITH SULFIDE; ADAPTED FROM (GIEG ET AL., 2011).

Other bacteria utilising nitrogen are involved in its cycling by oxidising aerobically ammonia to nitrite and nitrate, which is used by anaerobic nitrate reducers. Additionally, in anaerobic environments produced ammonia combined with nitrite production is used for denitrification driven by anammox activity (Shartau et al., 2010).

All these microorganisms, as mentioned, can jointly coexist in naturally occurring biofilms, often forming synergistic communities, able to affect MIC processes through co–operative metabolism not seen in the individual species (Dowling et al., 1991).

1.5. Biofilms

Biofilms are interface – associated colonies of microorganisms embedded in a self – produced organic polymeric matrix (Dunne, 2002), containing also molecules derived from the bulk aqueous phase, absorbed matter, organic solutes, metallic ions, inorganic particles and/or corrosion products of the metal substratum. They can be found in a great variety of conditions: aquatic and soil environments, living tissues,

medical devices or industrial piping systems. Approximately 95% of the microorganisms build up biofilms, as long as there is at least a minimum amount of water, containing nutrients for their growth, adjacent to the surface or interface in which they establish (Evans, 2004). In most natural environments, the association to the surfaces or interfaces is the predominant microbial lifestyle. It provides a favourable microenvironment, where the cells will not be compromised by free displacement and shear stresses (Watnick and Kolter, 2000). Therefore, biofilm formation can be regarded as a universal microbial survival strategy (Beech and Cheung, 1995; Costerton et al., 1995, 1987; Flemming and Wingender, 2010).

Biofilm formation is a very complex process (**FIG. 1.5**). The first components that bind to the surface or interface are organic molecules, salts and solvated ions present in the solution. These components can be used by bacteria as nutrients, electron acceptors, enzymatic cofactors or trace elements. They become adsorbed and subsequently retained by the heterogeneous structure of the surface, forming a conditioning layer on it. Later on, some planktonic (free floating) cells, attracted by the electrostatic and physical forces, are moved from the bulk liquid to the preconditioned surface. At this stage no chemical, firm binding occurs (Dreeszen, 2003). Cell reversible attachment occurs, and is followed by the desorption, caused by the shear stresses of a flowing electrolyte. Afterwards, the cells, which did not detach, become irreversibly attached to the surface. This process is followed by the biofilm development, maturation and increase in its thickness. The biofilm stability and firm binding to the surface is facilitated by an intensive EPS secretion. Finally, daughter cells from the biofilm detach and return to their planktonic lifestyle in the liquid environment. These ones might reattach to a new surface or interface and to develop a new biofilm (Videla, 1996).

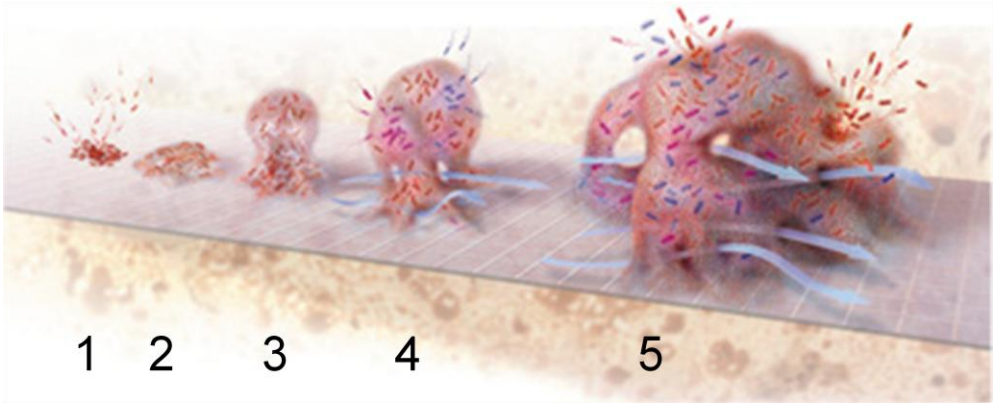

FIG. 1.5. SCHEMATIC REPRESENTATION OF THE BIOFILM FORMATION: 1 – POPULATION OF INDIVIDUAL FREE–FLOATING (PLANKTONIC) MOTHER CELLS THE SURFACE (REVERSIBLE PROCESS); 2 – IRREVERSIBLE CELL ATTACHMENT; 3 AND 4 – BIOFILM DEVELOPMENT AND MATURATION. 5 – DETACHMENT AND DISPERSAL OF INDIVIDUAL DAUGHTER CELLS FROM THE BIOFILM. THE IMAGE WAS TAKEN FROM: WWW.WVLC.UWATERLOO.CA/BIOLOGY447/BIOFILMS.

The biofilm structure is affected by various factors, such as pH, temperature, nutrient availability, medium viscosity, availability and distribution of oxygen or terminal electron acceptors, etc. The biofilm is also not a continuous layer or a planar structure, but a gradient driven three–dimensional microbial consortium, containing a heterogeneous cellular distribution, with voids, water and nutrient channels. Biofilm stability is a consequence of diverse physical, chemical and biological processes that occur simultaneously (Videla, 1996; Picioreanu et al., 2001).

The development of a microbial biofilm offers several advantages in contrast to planktonic growth. Beneficial properties of a biofilm are strongly related to its heterogeneous structure, supported by a massive EPS production (Davey and O'Toole, 2000). Due to the gradients of gases and nutrients within the biofilm, spatial distribution of the representatives of different metabolic groups occurs and, thus, cooperative relations establishment becomes possible (Stewart and Franklin, 2008). These gradient zones enhance the establishment of these complex symbiotic communities (Harrison et al., 2005). By providing microorganisms protection against biocides, desiccation, predators and other stress factors, biofilms are for the microorganisms of high importance.

1.6. Extracellular polymeric substances

The variety of the biofilm matrix molecules (polysaccharides, proteins, lipids, DNA, humic substances and others) referred as EPS, play a fundamental role in its structural stability as well as nutrition. Each of its components has a particular importance on the different stages of biofilm maturation (Karatan and Watnick, 2009). The content of these macromolecules in a given EPS varies, depending on bacterial species and their growth conditions (Marshall, 1992). The composition of a certain extracellular matrix is controlled by different processes like active secretion, cell lysis, and adsorption of substances from the environment (Laspidou and Rittmann, 2002).

EPS is an integral part of the biofilm matrix, mediating the cell adhesion to the surface, facilitating a strong binding of the microbes to each other, as well as to the surface. Exopolymeric material composed of macromolecules with varying hydrophilicity, or of macromolecules that have both hydrophilic and hydrophobic regions can adhere to a wide range of surfaces. Polysaccharides, proteins, and lipids present in microbial EPS have all been implicated in microbial cell adhesion to hydrophobic substrates, whereas acidic and neutral polysaccharides have been proposed to facilitate attachment to hydrophilic materials (Neu and Marshall, 1991).

EPS are also known to provide anchoring sites for extracellular enzymes, which may help to access different substances, or to degrade inhibitory compounds (Flemming and Wingender, 2010). The EPS matrix is also responsible for the water retention. It maintains a highly hydrated microenvironment around biofilm organisms, enhancing their tolerance to desiccation in water–deficient environments.

In case of corrosion–associated biofilms, EPS compounds are also an important factor in metal–microbe interactions, providing the reaction space for these processes and contributing to the early steps of the biofilm development. Exopolymers presence on the metal surface can modify the morphology and chemistry of corrosion products, often giving these products more aggressive properties. Exopolymers secreted by adherent bacteria can enhance corrosion of the surfaces to which they are associated (Geesey et al., 2011). The capacity of EPS to bind metal ions is important to MIC (Comte et al., 2006) and depends both on the bacterial species and on the type of metal ion. It may lead to the formation of complexes with a range of redox potentials, probably participating in the electron–transfer processes that drive corrosion reactions. Some data supporting the idea of a corrosion promoting effect of EPS has been published (Fang et al., 2002; Dong et al.,

2011). Comparison of EPS obtained from two strains of SRP belonging to the same genus (and similar by the most their physiological parameters), demonstrated that EPS with a higher ion–binding capacity was produced by the more corrosive strain (Beech et al., 1999). In acidophilic leaching bacteria, it was proposed that *Acidithiobacillus ferrooxidans* EPS concentrate ferric iron ions by complexing them through uronic acids or other residues, being essential for the chemical attack to metal sulfides such as pyrite (Sand and Gehrke, 2006). Some proposed MIC models also describe the potential involvement of SRP exopolymers in the metal deterioration (Beech et al., 2005). Here a mechanism, involving Fe^{3+} – EPS complexes into electron transfer has been suggested, which may explain the observed corrosion acceleration in an oxygenated biofilm (Beech and Sunner, 2004). Subsequently, questions arising from the proven abundance of extracellular proteins were related to the role of their enzymatic activities. The importance of reactions mediated by EPS proteins has started to be also considered as relevant to the biodeterioration (Busalmen et al., 2002).

From the other side a protective role of EPS due to hindering of the corrosion products diffusion from the metal surface has been reported (Videla and Herrera, 2009). Evaluation of EPS produced by several bacterial strains confirmed that some of them might possess candidate compounds to be potentially used for a further development of “green” corrosion mitigation strategies (Stadler et al., 2008).

REFERENCES

Beech, I., Zinkevich, V., Tapper, R., Gubner, R., Avci, R., 1999. Study of the interaction of sulphate–reducing bacteria exopolymers with iron using X–ray photoelectron spectroscopy and time–of–flight secondary ionisation mass spectrometry. J. Microbiol. Methods 36, 3–10.

Beech, I.B., Cheung, C.W.S., 1995. Interactions of exopolymers produced by sulphate–reducing bacteria with metal ions. Int. Biodeterior. Biodegrad. 35, 59–72.

Beech, I.B., Coutinho, C., 2003. Biofilms on corroding materials, in: Biofilms in Medicine, Industry and Environmental Biotechnology Characteristics, Analysis and Control. IWA Publishing of Alliance House, London, pp. 115–131.

Beech, I.B., Gaylarde, C.C., 1999. Recent advances in the study of biocorrosion: an overview. Rev. Microbiol. 30, 117–190.

Beech, I.B., Sunner, J.A., Hiraoka, K., 2005. Microbe–surface interactions in biofouling and biocorrosion processes. Int. Microbiol. Off. J. Span. Soc. Microbiol. 8, 157–168.

Brondel, D., Edwards, R., Hayman, A., Hill, D., Mehta, S., Semerad, T., 1994. Corrosion in the Oil Industry. Oilfield Rev. 6 2 4–18.

Busalmen, J., Vázquez, M., de Sánchez, S., 2002. New evidences on the catalase mechanism of microbial corrosion. Electrochimica Acta 47, 1857–1865.

Comanescu, I., Melchers, R.E., Taxen, C., 2012. Correlation between MIC and water quality, pigging frequency and biocide dosing in oil field water injection pipelines. Eur. Corros. Congr. Paper No.: 1527 (in press).

Comte, S., Guibaud, G., Baudu, M., 2006. Biosorption properties of extracellular polymeric substances

(EPS) resulting from activated sludge according to their type: Soluble or bound. Process Biochem. 41, 815–823.
Costerton, J.W., Cheng, K.J., Geesey, G.G., Ladd, T.I., Nickel, J.C., Dasgupta, M., Marrie, T.J., 1987. Bacterial biofilms in nature and disease. Annu. Rev. Microbiol. 41, 435–464.
Costerton, J.W., Lewandowski, Z., Caldwell, D.E., Korber, D.R., Lappin–Scott, H.M., 1995. Microbial biofilms. Annu. Rev. Microbiol. 49, 711–745.
Dawood, Brözel, 1998. Corrosion–enhancing potential of Shewanella putrefaciens isolated from industrial cooling waters. J. Appl. Microbiol. 84, 929–936.
Dong, Z.H., Liu, T., Liu, H.F., 2011. Influence of EPS isolated from thermophilic sulphate–reducing bacteria on carbon steel corrosion. Biofouling 27, 487–495.
Dowling, N.J.E., Mittelman, M.W., White, D.C., 1991. The role of consortia in micobially influenced corrosion, in: Mixed Cultures in Biotechnology. McGraw Hill, New York, pp. 341–372.
Dreeszen, P.H., 2003. Biofilm: the key to understanding and controlling bacterial growth in automated drinking water systems, Edstrom Industries, Inc, Waterford, WI.
Dunne, W.M., 2002. Bacterial Adhesion: Seen Any Good Biofilms Lately? Clin. Microbiol. Rev. 15, 155–166.
Evans, L.V., 2004. Biofilms: Recent Advances in their Study and Control. CRC Press.
Fang, H.H.P., Xu, L.–C., Chan, K.–Y., 2002. Effects of toxic metals and chemicals on biofilm and biocorrosion. Water Res. 36, 4709–4716.
Flemming, H.–C., 2002. Biofouling in water systems—cases, causes and countermeasures. Appl. Microbiol. Biotechnol. 59, 629–640.
Flemming, H.–C., Wingender, J., 2010. The biofilm matrix. Nat. Rev. Microbiol. 8, 623–633.
Fontana, M.G., 1986. Corrosion engineering. McGraw–Hill.
Geesey, G.G., Jang, L., Jolley, J.G., Hankins, M.R., Iwaoka, T., Griffiths, P.R., 2011. Binding of Metal Ions by Extracellular Polymers of Biofilm Bacteria [WWW Document]. URL http://www.iwaponline.com/wst/02011/wst020110161.htm (accessed 7.12.13).
Gieg, L.M., Jack, T.R., Foght, J.M., 2011. Biological souring and mitigation in oil reservoirs. Appl. Microbiol. Biotechnol. 92, 263–282.
Grigoryan, A.A., Cornish, S.L., Buziak, B., Lin, S., Cavallaro, A., Arensdorf, J.J., Voordouw, G., 2008. Competitive Oxidation of Volatile Fatty Acids by Sulfate– and Nitrate–Reducing Bacteria from an Oil Field in Argentina. Appl. Environ. Microbiol. 74, 4324–4335.
Hamilton, W.A., 1985. Sulphate–Reducing Bacteria and Anaerobic Corrosion. Annu. Rev. Microbiol. 39, 195–217.
Harrison, J., Turner, R., Marques, L., Ceri, H., 2005. Biofilms. A new understanding of these microbial communities is driving a revolution that may transform the science of microbiology. Am. Sci. 93, 508.
Hubert, C., Nemati, M., Jenneman, G., Voordouw, G., 2003. Containment of biogenic sulfide production in continuous up–flow packed–bed bioreactors with nitrate or nitrite. Biotechnol. Prog. 19, 338–345.
Hubert, C., Voordouw, G., Mayer, B., 2009. Elucidating microbial processes in nitrate– and sulfate–reducing systems using sulfur and oxygen isotope ratios: The example of oil reservoir souring control. Geochim. Cosmochim. Acta 73, 3864–3879.
Karatan, E., Watnick, P., 2009. Signals, regulatory networks, and materials that build and break bacterial biofilms. Microbiol. Mol. Biol. Rev. Mmbr 73, 310–347.
Kaster, K.M., Grigoriyan, A., Jenneman, G., Jennneman, G., Voordouw, G., 2007. Effect of nitrate and nitrite on sulfide production by two thermophilic, sulfate–reducing enrichments from an oil field in the North Sea. Appl. Microbiol. Biotechnol. 75, 195–203.
Laspidou, C.S., Rittmann, B.E., 2002. A unified theory for extracellular polymeric substances, soluble microbial products, and active and inert biomass. Water Res. 36, 2711–2720.
Lewandowski, Z., Beyenal, H., 2009. Mechanisms of Microbially Influenced Corrosion, in: Flemming, P.D.H.–C., Murthy, D.P.S., Venkatesan, D.R., Cooksey, P.D.K. (Eds.), Marine and Industrial Biofouling, Springer Series on Biofilms. Springer Berlin Heidelberg, pp. 35–64.
Lewandowski, Z., Dickinsony, W., Leey, W., 1997. Electrochemical interactions of biofilms with metal surfaces. Water Sci. Technol. 36, 295–302.
Liamleam, W., Annachhatre, A.P., 2007. Electron donors for biological sulfate reduction. Biotechnol. Adv. 25, 452–463.
Lin, S., Krause, F., Voordouw, G., 2009. Transformation of iron sulfide to greigite by nitrite produced by oil field bacteria. Appl. Microbiol. Biotechnol. 83, 369–376.
Lovley, D.R., Phillips, E.J.P., Lonergan, D.J., 1989. Hydrogen and Formate Oxidation Coupled to Dissimilatory Reduction of Iron or Manganese by Alteromonas putrefaciens. Appl. Environ. Microbiol. 55, 700–706.
Lutterbach, M.T.S., Contador, L.S., 2011. Problems Caused by Microbes and Treatment Strategies:

Identification of H2S–Producing Bacteria in Corrosion Product of a Gas Pipeline, in: Applied Microbiology and Molecular Biology in Oilfield Systems. pp. 125–131.
Lutterbach, M.T.S., Contador, L.S., Chaves Oliveira, A.L., De França IV, F.P., Pimenta, G.D.., Galvão, M.M., 2009. Iron Sulfide Production by Shewanella Strain Isolated from Black Powder. Nace Int. Pap. No 09391.
Marshall, K.C., 1992. Biofilms: an overview of bacterial adhesion, activity, and control at surfaces 202–207.
Moser, D.P., Nealson, K.H., 1996. Growth of the facultative anaerobe Shewanella putrefaciens by elemental sulfur reduction. Appl. Environ. Microbiol. 62, 2100–2105.
Moura, I., Bursakov, S., Costa, C., Moura, J.J.., 1997. Nitrate and Nitrite Utilization in Sulfate–Reducing Bacteria. Anaerobe 3, 279–290.
Myers, C.R., Myers, J.M., 1994. Ferric iron reduction–linked growth yields of Shewanella putrefaciens MR–1. J. Appl. Bacteriol. 76, 253–258.
Nemati, M., Jenneman, G.E., Voordouw, G., 2001. Mechanistic study of microbial control of hydrogen sulfide production in oil reservoirs. Biotechnol. Bioeng. 74, 424–434.
Neu, T.R., Marshall, K.C., 1991. Microbial “footprints” - A new approach to adhesive polymers. Biofouling 3, 101–112.
Picioreanu, C., van Loosdrecht, M.C., Heijnen, J.J., 2001. Two–dimensional model of biofilm detachment caused by internal stress from liquid flow. Biotechnol. Bioeng. 72, 205–218.
Roden, E.E., Urrutia, M.M., Mann, C.J., 2000. Bacterial Reductive Dissolution of Crystalline Fe(III) Oxide in Continuous–Flow Column Reactors. Appl. Environ. Microbiol. 66, 1062–1065.
Rosenberg, E., 2006. Hydrocarbon–Oxidizing Bacteria, in: Dworkin, M., Falkow, S., Rosenberg, E., Schleifer, K.–H., Stackebrandt, E. (Eds.), The Prokaryotes. Springer New York, New York, NY, pp. 564–577.
Sand, W., 1994. Mikrobielle Werkstoffzerstörung – Grundlagen: Mikrobielle Schädigungsmechanismen. Mater. Corros. 45, 10–16.
Sand, W., Gehrke, T., 2006. Extracellular polymeric substances mediate bioleaching/biocorrosion via interfacial processes involving iron(III) ions and acidophilic bacteria. Res. Microbiol. 157, 49–56.
Shartau, S.L.C., Yurkiw, M., Lin, S., Grigoryan, A.A., Lambo, A., Park, H.–S., Lomans, B.P., van der Biezen, E., Jetten, M.S.M., Voordouw, G., 2010. Ammonium concentrations in produced waters from a mesothermic oil field subjected to nitrate injection decrease through formation of denitrifying biomass and anammox activity. Appl. Environ. Microbiol. 76, 4977–4987.
Stadler, R., Fuerbeth, W., Harneit, K., Grooters, M., Woellbrink, M., Sand, W., 2008. First evaluation of the applicability of microbial extracellular polymeric substances for corrosion protection of metal substrates. Electrochimica Acta 54, 91–99.
Tang, K., Baskaran, V., Nemati, M., 2009. Bacteria of the sulphur cycle: An overview of microbiology, biokinetics and their role in petroleum and mining industries. Biochem. Eng. J. 44, 73–94.
Uhlig, H.H., Revie, R.W., 1985. Corrosion and corrosion control: an introduction to corrosion science and engineering. Wiley.
Videla, H.A., 1996. Manual of Biocorrosion. CRC Press/Lewis Publishers.
Videla, H.A., 2002. Prevention and control of biocorrosion. Int. Biodeterior. Biodegrad. 49, 259–270.
Videla, H.A., 2005. An Updated Overview of SRB Induced Corrosion and Protection of Carbon Steel. Nace Int. Pap. No 05488.
Videla, H.A., Characklis, W.G., 1992. Biofouling and microbially influenced corrosion. Int. Biodeterior. Biodegrad. 29, 195–212.
Videla, H.A., Herrera, L.K., 2009. Understanding microbial inhibition of corrosion. A comprehensive overview. Int. Biodeterior. Biodegrad. 63, 896–900.
Videla, H.A., Le Borgne, S., Panter, C., Raman, R.K.S., 2008. MIC of steels by iron reducing bacteria. Nace Int. Papaer No 08505.
Watnick, P., Kolter, R., 2000. Biofilm, city of microbes. J. Bacteriol. 182, 2675–2679.
Williamson, N., 2011. Health and safety issues from the production of hydrogen sulphide, in: Applied Microbiology and Molecular Biology of Oilfield Systems. pp. 151–157.

CHAPTER II. TECHNIQUES FOR MIC AND BIOFILMS INVESTIGATIONS

Various methods described in this chapter were used for characterising the influence of sulfate reducers biofilms on carbon steel behaviour (Chapter IV). Additionally, electrochemical and X–ray photoelectron spectroscopy (XPS) were applied to study the influence of extracellular polymeric substances (EPS) on steel corrosion (Chapter VII). This chapter aimed to describe the above – mentioned methods for a better understanding of the results presented in further chapters. Firstly, electrochemical methods, such as corrosion potential monitoring, linear polarisation and electrochemical impedance spectroscopy are presented. Particular attention was paid to the latter technique, as it is a very complex method with a challenging interpretation of the results. Further, XPS is described. Aditionally, a general overview of various microscopic methods for biofilm studies closes this chapter. These approaches allowed the systematic study of EPS properties and their function in this thesis.

1.1. Electrochemical approaches

Electrochemistry studies involve chemical reactions, which take place at the interface between an electronic conductor (the electrode / in this study carbon steel) and an ionic conductor (the electrolyte), with electron transfer between the electrode and the electrolyte or species in solution.

Most corrosion phenomena are of electrochemical nature and consist of reactions on the surface of the corroding metal. Therefore, electrochemical methods must be used to characterise corrosion processes on the surface of interest. The advantage of applying these techniques is providing complex results in relatively short periods of time and providing useful information to elucidate mechanistic information about the processes studied.

1.1.1. Corrosion potential measurements

The corrosion potential (E_{corr}) measurements are related to the open circuit potential (OCP) recording of a corroding metal. The potential is recorded at zero net current, which is a non – intrusive method for the corrosion studies. When a specimen is placed in a cell, E_{corr} can be immediately measured. OCP is measured by means of the potential difference between the material of study (working electrode, WE) and a reference electrode (RE, e.g. standard calomel electrode (SCE) etc.) immersed in an electrolyte. The magnitude of the measured potential depends on the nature of the metallic substratum and its chemical composition, the temperature and the hydrodynamic characteristics of the electrolyte (Monfort, 2001). The application of this technique is simple. It can be applied outside laboratory conditions, and it allows the differentiation between a passivation phenomenon or a localised corrosion process, which occur under the presence of some types of biofilms. Since with E_{corr} the separate contributions are monitored together, these measurements do not provide mechanistic information and it is recommended to apply this technique in parralel with other techniques to determine the cathodic and anodic influences of the electrochemical processes.

1.1.2. Linear polarisation

Linear polarisation (LP) curve is a graphical relationship between the electrode current density (i) expressed as the logarithm of the current density, log (i) and the potential of the electrode (E). Measurements consist of changing the potential of the electrode linearly and recording the current as a function of the potential. Measurement of the polarisation curves is carried out in the three – electrode system. While registering polarisation curves in a wide anodic range ($E > E_{corr}$) it is possible to determine the ranges corresponding to active metal deterioration (corrosion) or its passivation. While applying the cathodic potentials ($E < E_{corr}$) it is possible to observe various reduction processes on the surface.

Cathodic and anodic polarisation curves recorded around the corrosion potential provide valuable information about the corrosion processes taking place in the metal – solution system. When polarising the electrode close to $E_{corr,}$ a linear change of current density with varying potential is observed in a wide potential range then the Tafel behaviour/relationship is observed (Dominguez–Benetton, 2007; Orazem and Tribollet, 2008). The Tafel equation can be written in the following form (Orazem and Tribollet, 2008):

$$\log(i) = \log(i_{corr}) + \frac{1}{b}(E - E_{corr}) \tag{2.1}$$

where: i_{corr} is the corrosion current and b is the Tafel constant. For cathodic and anodic reactions this equation can be written with use of b_c and b_a, which correspond to the cathodic and anodic Tafel constants, respectively. This formula shows clearly the linear dependence between log (i) and $E – E_{corr}$, with 1/b being the slope of it. Thus, it is possible to estimate directly the value of i_{corr} by reading it from the LP curve or calculate it indirectly using the Stern and Geary equation (Frateur, 1997; Landolt, 2003).

It is possible to extrapolate the anodic and cathodic linear portions of the polarisation curves to E_{corr}, where, under ideal conditions, they should intersect. The relative values of the slopes of the anodic or cathodic polarisation curves, determine whether the anodic, cathodic, or both reactions control the rate of the corrosion process. As b_c value increases, reduction is favoured and oxidation is not favoured and vice versa for b_a (Landolt, 2003).

1.1.3. Electrochemical Impedance Spectroscopy

Another way to approach electrochemical systems is applying a minimal perturbation to an electrochemical cell by means of an alternate electrical signal of a low amplitude, which allows observing the behaviour of the system in a pseudo – steady state.

Ohm's law states that the current through a conductor between two points is directly proportional to the potential difference across the two points. While considering the Ohm's law, the resistance R [Ω] can be described as:

$$I = \frac{E}{R} \tag{2.2}$$

where I is the current through the conductor in amperes [A] and E is the potential difference measured across the conductor in volts [V]. The applied current in this case is a direct current (DC). If an alternating sinusoidal voltage E(t) = Esinωt is applied, the current can be described as:

$$I = \frac{E}{R}\sin \omega t \tag{2.3}$$

or in the phasor notation:

$$\dot{I} = \frac{\dot{E}}{R} \tag{2.4}$$

A passive complex electrical system comprises both energy dissipater (resistor, R) and energy storage (capacitor, C) elements. If they will be considered to be connected in series and the voltage $\dot{E}$ is applied across them, then the voltage of the system will be the sum of the resistor voltage $\dot{E}_R$ and the capacitor voltage $\dot{E}_C$:

$$\dot{E} = \dot{E}_R + \dot{E}_C \tag{2.5}$$

and

$$\dot{E} = \dot{I}Z \tag{2.6}$$

In this way it was shown that the sinusoidal voltage is linked to the measured current by a vector Z, called impedance. The impedance is a kind of generalised resistance and the equation (2.6) is a generalised version of Ohm's law (Bard and Faulkner, 2001). The impedance is a complex parameter, with the real (Z_R) and the imaginary (Z_J) part of it (both parts are real in the sense of being measurable). The real part describes the resistance to current flowing in phase with the applied voltage while the imaginary part describes the resistance to the electric shock shifted in phase.

Electrochemical Impedance Spectroscopy (EIS) is a technique, in which the frequency response of an electrochemical system to an alternate signal is analysed in a transfer function, between an input signal (e.g. voltage) and the resulting output signal (e.g. current), that is processed by instrumentation to yield the frequency–depended transfer function (Bard & Faulkner, 2001; Orazem & Tribollet, 2008). Impedance experiments involve the conversion of the time–domain input and output signals into a complex quantity that is a function of frequency (Orazem and Tribollet, 2008).

EIS is well established as a powerful technique for investigating corrosion processes and other electrochemical systems. Recently it has been also successfully applied to study the EPS influence on carbon steel (Dong et al., 2011). Among the advantages of this technique is that it is not intrusive, a big amount of mechanistic information is obtained, it offers high precision on the measurements, and allows performing measurements in a wide range of frequencies. However, it has a serious disadvantage that the interpretation of the results is complex (Greef et al., 1990).

The frequency range that this technique often uses (10^{-4} to 10^{5} Hz), allows identifying the elements comprising the electrochemical cell when the current is out of phase with the voltage. For example, at high frequencies (e.g. 10 kHz) the resistance of the electrolyte can be measured, while at low frequencies (e.g. 1 mHz) diffusional effects, adsorption phenomena and interfacial desorption can be identified (Gabrielli, 1998). However, the selection of the frequency domain mainly depends on the system to be studied and the characteristics of the equipment to use.

This technique is based on the frequency response analysis of the electrochemical system to a sinusoidal variation superposed to a continuous potential or a direct current. As above presented, at the entrance of the system – for

potentiostatic experiments – a sinusoidal potential perturbation E (t) of low amplitude E_0 is imposed over the working electrode, at a given frequency range (ω). The obtained response for each frequency is a sinusoidal current I (t) of phase ϕ and amplitude I_0.

The impedance transfer function defined as the relation between an input voltage signal E (t) and an output current I (t), as shown in the equation 2.6, can defined in complex notation as:

$$Z(\omega) = |Z|e^{j\phi} = Z_R + jZ_J \tag{2.7}$$

where Z is the impedance, Z_R is the real part of the impedance, Z_J the imaginary part of the impedance, ϕ is the current phase and j the imaginary number $\sqrt{-1}$. Respectively, the impedance modulus |Z| and the phase angle ϕ are defined as:

$$|Z| = \sqrt{Z_R^2 + (jZ_j)^2} \tag{2.8}$$

$$\phi = \tan^{-1}\frac{Z_J}{Z_R} \tag{2.9}$$

In corrosion studies, two types of plots known as Nyquist and Bode diagrams are used to describe these relationships. Plots of the opposed imaginary part of the impedance – Z_J versus the real part Z_R (Nyquist diagrams), tend to give characteristic behaviours such as semicircles or slopes, according to the phenomena taking place in the electrochemical system. Bode plots show the system's frequency response; here the modulus and the phase are plotted versus the logarithm of the frequency. For electrochemical work, the choice between the two types of display is not obvious, although most workers favour complex plane plotting (Gabrielli, 1997). In recent years, other representations have been reported, allowing visualising and extracting more information from the impedance data.

In general, EIS plays an important role in the study of biofilm formation and MIC. One of the aims of this study was to extend its applicability on the studies of EPS behaviour on the carbon steel.

1.2. X – ray Photoelectron Spectroscopy

X–ray photoelectron spectroscopy, XPS is a quantitative technique, which allows to investigate a thin layer of adsorbed matter on the surface, in contrast to the bulk solution (Andrade, 1985). XPS may be applied to surface chemical analysis of minerals (Seyama and Soma, 2003), catalysts (Venezia, 2003), metals (Asami and Hashimoto, 1987), and polymers (Briggs, 1998) as well as living systems, e.g. biofilms (Rouxhet et al., 1994; van der Mei et al., 2000; Rouxhet et al., 2003).

The principle of XPS is based on irradiation by a given energy *hv* (X radiation), where h is the Planck's constant and v is a frequency of an associated electromagnetic wave of an atom A, which consequently generates an ion in an excited state A^{+*} and a free electron ē emitted with a fixed amount of kinetic energy (E_k).

$$A + hv \rightarrow A^{+*} + \bar{e} \qquad (2.10)$$

The kinetic energy of the emitted electron is related to its binding energy (E_b) by the equation:

$$E_k = hv - E_b \qquad (2.11)$$

Further on, it is required to first apply work to bring the electron from the zero attraction to the entrance of the energy analyser, Φ_{sp}, which is constant and characteristic for the spectrometer. Secondly, the sample charges while expelling the electrons and contributes to the primary E_k (charging effect E_c). In the consequence, measured kinetic energy can be described as follows:

$$E_k = hv - E_b - \Phi_{sp} - E_c \qquad (2.12)$$

Parameters *hv*, Φ_{sp} and E_c are fixed. Therefore, the position of the peak of each investigated atom is settled by the binding energy, $\underline{\mathbf{E_b}}$, specific for a certain energy level of a certain element. A scheme of an XPS spectrophotometer system is shown in **FIG. 2.1**.

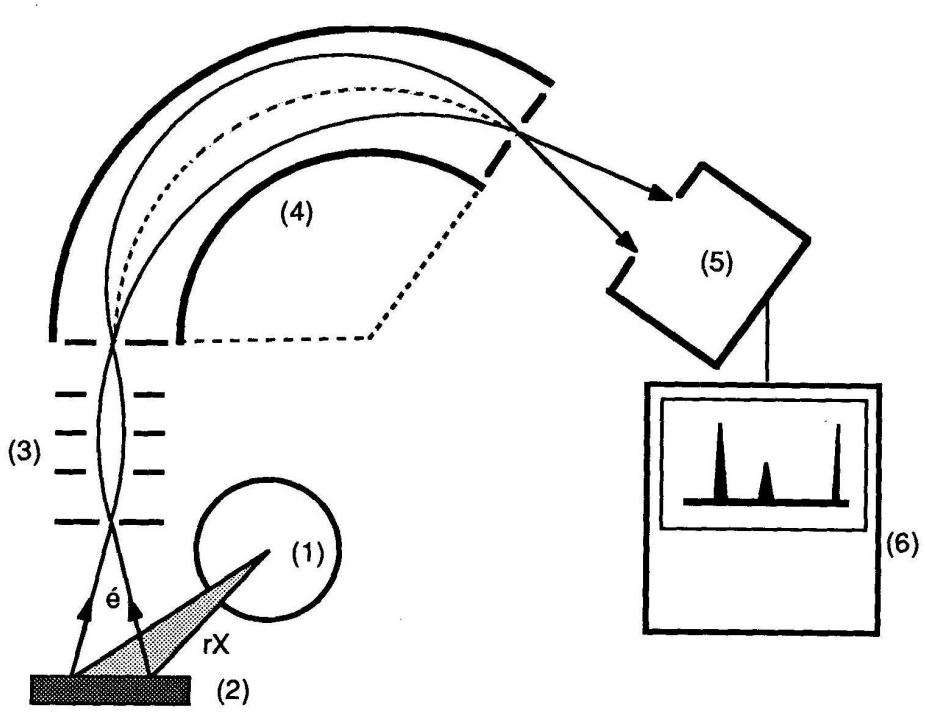

FIG. 2.1. DIAGRAM OF A X–RAY PHOTOELECTRON SPECTROMETRY SYSTEM. (1) X–RAY TUBE FROM WHICH THE X–RAY ENERGY IS EMITTED; (2) SAMPLE; (3) ELECTRONIC FOCUSING SYSTEM; (4) SPECTROMETER; (5) ELECTRONS DETECTOR (CHANNELTRON); (6) DATA ACQUISITION. THE WHOLE SYSTEM IS UNDER THE ULTRA–HIGH VACUUM (UHV).

1.3. Microscopic techniques for biofilm investigations

The importance of investigating the scale and spatial arrangement of biofilms, including the distribution and composition of microorganisms and their EPS, within the biofilm matrix, is crucial for understanding the function of biofilms. Light microscopy (e.g. epifluorescence and confocal laser scanning microscopies, EFM and CLSM, respectively), electron microscopy (e.g. transmission electron microscopy, TEM), and atomic force microscopy (AFM) are very extensively applied to investigate the biofilm structure in various stages of its development and its influence on the surface. Each of these techniques offers possibilities to visualise the overall appearance and/or specific features of biofilms, e.g. microbial colonies, individual cells and/or EPS.

1.3.1. Light microscopy (EFM and CLSM)

Light microscopy uses glass lenses to bend and focus light rays in order to produce enlarged images of small subjects, such as bacterial cells. Fluorescent microscopes work on the principle that an object is emitting light. Exposing a fluorescent specimen to ultraviolet, violet, or blue light results in the emission of the absorbed energy at a longer, specific wavelength. The emitted light is used to form an image.

Additionally, CLSM is now established as an important tool for obtaining high resolution images and 3–D reconstructions of biofilms. Confocal imaging can only be performed with point–wise illumination and detection, which is the most important advantage of using CSLM. Scanning is achieved by either deflection of the laser beam or movement of the sample on a stage. Stacking of 2–D optical sections collected in series can generate a 3–D reconstruction of a specimen, including its surface, when required. The combination of CSLM, image analysis and fluorescent probes provides the tools for analysing changes in 3D biofilm structure, offering also a great potential for the analysis of the physico–chemical microenvironment surrounding microorganisms.

Usually, specimens are stained with fluorochromes that fluoresce brightly upon exposure to light of a specific wavelength. DAPI or 4',6–diamidino–2–phenylindole is a fluorescent stain that binds to single and double stranded nucleic acids. DAPI stains all DNA and RNA containing microorganisms, including algae, protozoans and nucleic acid containing cell structures (Porter and Feig, 1980). DAPI can pass through an intact cell membrane therefore it can be used to stain both live and fixed cells.

Lectins are naturally occurring proteins, which bind carbohydrates with considerable specificity (Michael et al., 1995). In recent years, fluorescently labelled lectins have been used to study biological systems e.g., the distribution of EPS in biofilms or the detection of fungi in tissue sections (Kennedy et al., 1995). Fluorescein–isothiocyanate (FITC)–labeled lectins were used to stain part of the glycoconjugate fraction of biofilm (Michael et al., 1995; Lawrence et al., 1998; Neu, 2000), flocs, and granules (Beer et al., 1996; Wang et al., 2005) (De Beer et al. 1996; Wang et al. 2005). FITC itself is also often used to stain proteins (Chen et al., 2007; Schmid et al., 2003). In recent years, there is an increased interest in multicolor

fluorescence experiments for exploring how the EPS and/or cells distribute in the bioaggregates. This can be achieved by combining differently labelled lectins with other staining methods like DAPI or FITC.

1.3.2. Atomic force microscopy

The atomic force microscope (AFM) is a type of scanning probe microscopes (SPM). SPMs are designed to measure various local properties with a probe. To acquire an image, the SPM scans the probe over a small area of the sample, in order to produce an image. AFM utilises a sharp tip (generally made of silicon nitride or silicon) to produce a topographical map of the surface. The tip is mounted on the underside of a cantilever, the flexing of which is generally detected by the deflection of a laser beam. The reflected laser beam strikes a position–sensitive photodetector consisting of a four–segment photo–detector. The differences between the segments of the photo–detector of signals indicate the position of the laser spot on the detector and thus the angular deflections of the cantilever (**FIG. 2.2**).

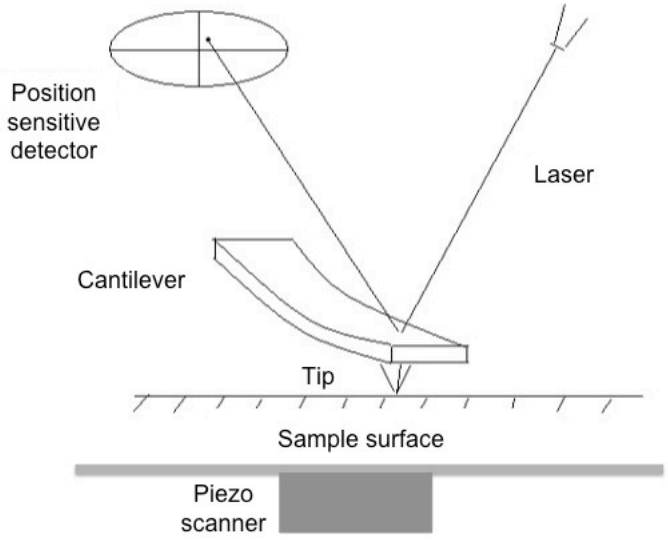

FIG. 2.2. SCHEME OF AFM.

A piezo scanner positions the tip with a high resolution. Piezoelectric ceramics are a class of materials that expand or contract when in the presence of a voltage gradient. Piezo–ceramics make it possible to create three–dimensional positioning devices of a high precision.

There are several modes of AFM operation, each one has been introduced to extend the variety of samples, which can be imaged. The choice of each mode is influenced by the sample, its topography, and the conditions of imaging, e.g. in air or in fluid. The contact mode is the standard mode of AFM imaging. The probe operates in the repulsive force region. The cantilever deflects as the tip encounters variations in surface topography. This mode of operation was improved by noncontact AFM, where a vibrating tip is oscillated at its resonant frequency to produce an image. In this mode, the tip of the cantilever does not contact the sample surface. The cantilever is instead oscillated. In non–contact mode, images may be made of very soft surfaces that are not well adhered to their substrates. The third mode of operation is known as tapping mode and is a compromise between the contact and non–contact AFM. The cantilever is oscillated with larger amplitude than in non–contact mode. The mode was developed as a method to achieve high resolution without frictional forces. The cantilever is oscillated near its resonance frequency as it is scanned over the sample surface. As the tip is brought closer to the sample at some point, it will begin to intermittently contact (‘tap’) on the surface.

AFM can be used to determine the depth and angle of pits formed on surfaces, and the data collected during the scanning process can be processed to determine the effect of biofilms on surface roughness of the metal (Steele et al., 1994). Application of AFM in a high–resolution topographical imaging of bacterial biofilms, corroded steel surfaces, and in the quantification of localised corrosion (Xu et al., 2002; Yuan and Pehkonen, 2007) is of high importance for biocorrosion studies.

1.3.3. Transmission electron microscopy

Transmission electron microscopy uses high–energy electrons (up to 300 kV accelerating voltage), which are accelerated to nearly the speed of light. The beam of high velocity electrons accelerated under the vacuum, focused by condenser lens, passes through a thin–section specimen of a material, and electrons are scattered. A sophisticated system of electromagnetic lenses focuses the scattered electrons into an image. The imaging mode provides a highly magnified view of the micro– and nanostructure. The resolution of TEM can reach even 0.2 nm, which is about 1000 times higher than in a classical light microscope. This enables the instrument's user to examine fine details, thousands of times smaller than the smallest resolvable

object in a light microscope, what may be of high importance, while focusing on e.g. EPS visualisation (Lawrence et al., 2003).

REFERENCES

Andrade, J.D., 1985. X–ray Photoelectron Spectroscopy (XPS), in: Andrade, J.D. (Ed.), Surface and Interfacial Aspects of Biomedical Polymers. Springer US, pp. 105–195.

Asami, K., Hashimoto, K., 1987. X–ray photoelectron spectroscopy for corrosion studies. Langmuir 3, 897–904.

Bard, A.J., Faulkner, L.R., 2001. Chapter 10. techniques based on concepts of Impedance, in: Electrochemical Methods: Fundamentals and Applications. John Wiley and Sons, Inc., pp. 368–416.

Beer, D. de, O'Flaharty, V., Thaveesri, J., Lens, P., Verstraete, W., Beer, D. de, 1996. Distribution of extracellular polysaccharides and flotation of anaerobic sludge. Appl. Microbiol. Biotechnol. 46, 197–201.

Briggs, D., 1998. Surface Analysis of Polymers by XPS and Static SIMS. Cambridge University Press.

Chen, M.–Y., Lee, D.–J., Tay, J.–H., Show, K.–Y., 2007. Staining of extracellular polymeric substances and cells in bioaggregates. Appl. Microbiol. Biotechnol. 75, 467–474.

Dominguez–Benetton, X., 2007. Biocomplexity and Bioelectrochemical Influence of Biofilms in Carbon Steel Deterioration A Transmission Line Approach for Electrochemical Impedance Analysis. Time. Mexican Petroleum Institute.

Dong, Z.H., Liu, T., Liu, H.F., 2011. Influence of EPS isolated from thermophilic sulphate–reducing bacteria on carbon steel corrosion. Biofouling 27, 487–495.

Frateur, I., 1997. Incidence de la corrosion des materiaux ferreux sur la demande en chlore libre en reseaux de distribution d'eau potable. Université Pierre et Marie Curie, Paris 6.

Gabrielli, C., 1997. Use and Application of Electrochemical Impedance Techniques. France.

Gabrielli, C., 1998. Identification of electrochemical processes by frequency response analysis, Solartron, Technical report number 004/83.

Greef, R., Peat, R., Peter, L.M., Pletcher, D., Robinson, J., 1990. Instrumental mehods in electrochemistry, Southampton Electrochemistry Group, Ellis Horwood (Ed.), Chapter 8.

Kennedy, J.F., Palva, P.M.G., Corella, M.T.S., Cavalcanti, M.S.M., Coelho, L.C.B.B., 1995. Lectins, versatile proteins of recognition: a review. Carbohydr. Polym. 26, 219–230.

Landolt, D., 2003. Corrosion et chimie des surfaces des métaux. Presses polytechniques et universitaires romandes.

Lawrence, J.., Neu, T.., Swerhone, G.D.., 1998. Application of multiple parameter imaging for the quantification of algal, bacterial and exopolymer components of microbial biofilms. J. Microbiol. Methods 32, 253–261.

Lawrence, J.R., Swerhone, G.D.W., Leppard, G.G., Araki, T., Zhang, X., West, M.M., Hitchcock, A.P., 2003. Scanning Transmission X–Ray, Laser Scanning, and Transmission Electron Microscopy Mapping of the Exopolymeric Matrix of Microbial Biofilms. Appl. Environ. Microbiol. 69, 5543–5554.

Michael, T, Smith, M, C., 1995. Lectins probe molecular films in biofouling: characterization of early films on non–living and living surfaces. Mar. Ecol. Prog. Ser. 119, 229–236.

Monfort, N.M., 2001. Localised corrosion of carbon steels induced by sulphate–reducing bacteria. Development of a specific sensor. PhD thesis. Université Paris VI, Electrochimie.

Neu, T.R., 2000. In situ cell and glycoconjugate distribution in river snow studied by confocal laser scanning microscopy 85–95.

Orazem, M.E., Tribollet, B., 2008. Electrochemical Impoedance Spectroscopy. Wiley.

Porter, K.G., Feig, I.S., 1980. The use of DAPI for identifying and counting aquatic microflora 943–948.

Rouxhet, P.G., Dupont–Gillain, C.C., Genet, M.J., Dufrêne, Y.F., 2003. Use of X–ray photoelectron spectroscopy and atomic force microscopy for studying interfaces in biofilms, in: Biofilms in Medicine, Industry and Environmental Biotechnology: Characteristics, Analysis and Control. IWA Publishing.

Rouxhet, P.G., Mozes, N., Dengis, P.B., Dufrêne, Y.F., Gerin, P.A., Genet, M.J., 1994. Application of X–ray photoelectron spectroscopy to microorganisms. Colloids Surf. B Biointerfaces 2, 347–369.

Schmid, M., Thill, A., Purkhold, U., Walcher, M., Bottero, J.Y., Ginestet, P., Nielsen, P.H., Wuertz, S., Wagner, M., 2003. Characterization of activated sludge flocs by confocal laser scanning microscopy and image analysis. Water Res. 37, 2043–2052.

Seyama, H., Soma, M., 2003. Surface–analytical Studies on Environmental and Geochemical Surface Processes. Anal. Sci. 19, 487–497.

Steele, A., Goddard, D.T., Beech, I.B., 1994. An atomic force microscopy study of the biodeterioration of stainless steel in the presence of bacterial biofilms. Int. Biodeterior. Biodegrad. 34, 35–46.

Van der Mei, H.C., de Vries, J., Busscher, H.J., 2000. X–ray photoelectron spectroscopy for the study of microbial cell surfaces. Surf. Sci. Reports 39, 1–24.

Venezia, A.M., 2003. X–ray photoelectron spectroscopy (XPS) for catalysts characterization. Catal. Today 77, 359–370.

Wang, Z.–W., Liu, Y., Tay, J.–H., 2005. Distribution of EPS and cell surface hydrophobicity in aerobic granules. Appl. Microbiol. Biotechnol. 69, 469–473.

Xu, L.–C., Chan, K.–Y., Fang, H.H.., 2002. Application of atomic force microscopy in the study of microbiologically influenced corrosion. Mater. Charact. 48, 195–203.

Yuan, S.J., Pehkonen, S.O., 2007. Microbiologically influenced corrosion of 304 stainless steel by aerobic Pseudomonas NCIMB 2021 bacteria: AFM and XPS study. Colloids Surf. B Biointerfaces 59, 87–99.

CHAPTER III. MICROBIAL DIVERSITY STUDIES IN THE OIL AND GAS INDUSTRY

Water injection and oil production systems are inhabited by diverse microbial communities, which can participate in biocorrosion. This study applied culture–dependent and molecular approaches to examine the microbial diversity at corrosion sites from various water injection and oil production systems.

It was observed that in one of the investigated water injection systems, where samples came from biocoupons and injected water, only anaerobically grown cultures were enriched. Within them sulfate, manganese, nitrate and iron reducers were detected. The latter two enrichments were shown to contain species able to grow in Postgate E medium and to reduce sulfate. The results of the most probable number (MPN) experiments, showed similar cell numbers in all enriched cultures. 16S rDNA gene cloning and sequencing revealed presence of *Desulfovibrio, Thalassospira* and *Pseudomonas* species. In the debris received from the "cleaning pigs", used in the second water injection system and in a production pipeline, aerobic and anaerobic microorganisms from the sulfur, nitrogen, iron and manganese cycles were found. Some of the DGGE profiles within single tested metabolic group differed among samples from the cleaning pigs from one pipeline. However, profiles obtained from other enrichments were very similar. It was also found that 3 groups of microorganisms enriched in different media had exactly the same profiles. The first group included sulfate reducers, neutrophilic H_2SO_4 producers and nitrite oxidisers – all thermophilic; the second had thermophilic nitrate reducers and manganese oxidisers and the third one had both meso– and thermophilic iron reducers and acidophilic H_2SO_4 producers. Their parallel presence in various media was discussed.

The high diversity of bacterial groups at the corrosion sites, suggested that the corrosion was probably a consequence of an integrated microbial community action, introducing corrosive metabolites able to accelerate corrosion and facilitating electron transfer between pipe surfaces and microorganisms.

1. INTRODUCTION

Microbial development occurs in almost all environments and may be responsible for microbiologically influenced corrosion (MIC). This process occurs at the interface between the metal and electrolyte, involving anodic and cathodic reactions at the metal surface. However, MIC is not a new corrosion mechanism but it integrates the role of microbial flora in deterioration processes. Thus, an inherently abiotic process can be influenced by various biological behaviours (Beech and Gaylarde, 1999).

Biocorrosion is well recognised in many offshore oil operations (Sanders and Hamilton, 1986) and can be induced by both direct and indirect action of microorganisms. While directly attaching to the surface and colonising it, microorganisms cause differential oxygen distribution or production of iron sulfides. Localised attack in the form of pitting is a typical feature of MIC. Indirect activities observed in the form of e.g. acid secretion, provoking the reservoir souring, causes corrosion problems downstream of the areas of microbial growth.

Basing on the data obtained from individual case histories, it was suggested that overall losses to oil and gas industry due to microbial activity could be over 100 million dollars per annum (Maxwell et al., 2004). Biodeterioration is related to the adhesion of microorganisms on the surface of materials, and their subsequent colonisation. The microbial structures formed at the interior of the pipelines, known as biofilms, are composed of cellular aggregates, extracellular polymeric substances (EPS), inorganic and organic matter, and mainly water (Davey and O'toole, 2000).

As presented in Chapter I, bacterial groups with diverse metabolic properties are involved in MIC, by wining energy through oxidation/reduction of a wide range of compounds. MIC due to sulfate reducing prokaryotes (SRP) presence is nowadays the major problem in the oil and gas industry. They are a group of ubiquitous, diverse anaerobes able to use sulfate ions as the terminal electron acceptor, producing H_2S. Several SRP can reduce nitrate, sulfite or thiosulphate. Biogenic production of H_2S in oil reservoirs subjected to water flooding (souring) is a serious concern for the oil industry. Toxicity of H_2S, accelerated corrosion of pipelines, production and processing equipment, and decrease in efficiency of secondary oil recovery due to plugging of the oil bearing strata by biomass and precipitated metal sulfides, are some of the problems associated with souring. Furthermore, the necessity for the

removal of H_2S prior to the use of oil and gas, and before recycling the produced water, increases production costs.

Other major players in the MIC process include acid producing microorganisms, sulfur oxidising microorganisms, metal – reducing/oxidising microorganisms and microorganisms from the nitrogen cycle.

By creating microenvironments with different aeration, pH and nutrient availability, microorganisms can not only survive next to each other, but often forming synergistic communities, able to affect MIC processes through co–operative metabolism (Dowling et al., 1991). A model of microbial interactions between acid producers, bacteria from the sulfur cycle and metal oxidisers and reducers is shown in **FIG. 3.1**.

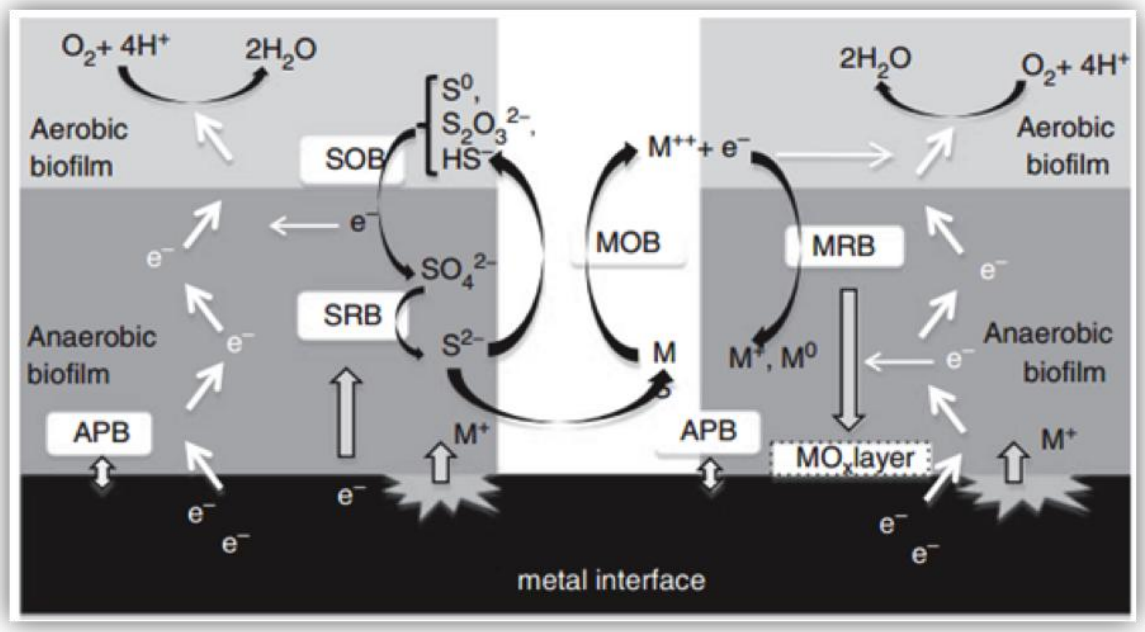

FIG. 3.1. SCHEMATIC DESCRIPTION OF MIC AND ELECTRON FLOW FROM METAL TO MICROORGANISMS. APB (ACID PRODUCING BACTERIA), SRB (SULFATE–REDUCING BACTERIA), SOB (SULFUR OXIDISING BACTERIA), MRB (METAL REDUCING BACTERIA), MOB (METAL OXIDIZING BACTERIA); ADAPTED FROM (KAN ET AL., 2011).

The complementarity of biological functions makes these consortia very resistant against environmental stresses.

2. MATERIALS AND METHODS

2.1. Industrial samples

Analyses of microbial diversity in oil and gas industry were performed from the field samples, provided by one of the leading energy companies. The following samples were received: 3 samples from the installation A, water injection system A (pigging debris from Pigs number 1, 4 and 9), 2 water and 2 biocoupon samples from Installation B, water injection pipeline B and 3 pigging samples (Pigs 1, 2 and 3) from Installation C, production pipeline. The details of each investigated installation, including their construction material are presented in **TABLE 3.1**.

Water samples from the Installation B received numbers 1 and 2, while biocoupon samples were numbered as 3 and 4. Each pigging sample number, as above shown, corresponded to its injection order into the system. Received biocoupons (**FIG. 3.2**) were part of the corrosion monitoring of the different systems. These coupons are small rod shaped steel samples, made of the most vulnerable to MIC material in the given system (**TABLE 3.1**). In total five biocoupons of 40 mm^2 were situated in one bioprobe, introduced to the system and incubated for approximately 6 months.

FIG. 3.2. INDUSTRIAL BIOPROBE FOR MIC MONITORING. FROM LEFT: PROBE BEFORE INTRODUCTION TO THE SYSTEM; AFTER ITS EXPOSURE; AND THE BIOCOUPON IN ORIGINAL FLUID.

Installation A corresponded to the water injection system made of carbon steel. The temperature inside the pipe was around 30°C. Injected water was a mixture of aquifer and produced water. Samples were from the pigging operations. Cleaning operation was done with 3 pigs only and the debris of each of them was analysed. Biocoupons and water from the installation B were from the water injection pipeline

B1. This system experienced severe corrosion problems while injecting seawater only. Later injection of aquifer and produced water didn't solve corrosion problems. Replacement of carbon steel for a stainless steel brought a decrease of corrosion rates. The temperature in the pipeline B1 was around 30°C. The production stream from the installation C contained a mixture of oil and seawater in the rate 2:5 (v/v). The temperature at the inlet was of approx. 80°C, while at the outlet decreased to 65°C. In this installation injected seawater was treated with nitrate. The production line was made of carbon steel. Received debris was collected from the first, fourth and ninth cleaning pig (from total 45 pigs used for the pipeline cleaning). All samples, after their removal, were immediately flushed with nitrogen and dispatched.

TABLE 3.1. OVERVIEW OF VARIOUS SAMPLES DELIVERED BY THE INDUSTRIAL PARTNER.

Installation	System	Medium transported through the system	T [°C]	Type of received sample	Construction material	Comments
A	Water injection pipeline A	Mixture of produced and aquifer water	30°C	Pigging debris	Carbon steel (C_{max} 0.16%)	Corrosion has been a problem. Iron sulfides as corrosion product found
B	Water injection pipeline B1	Mixture of produced and aquifer water	30°C	Biocoupons and water	Carbon steel (C_{max} 0.16%)	Severe corrosion took place in the mixture of produced and aquifer water or aquifer water only with carbon steel as construction material; SRP detected
C	Production pipeline	Reservoir fluid: mixture of oil and seawater	80 – 65°C	Pigging debris	Carbon steel (C_{max} 0.16%)	Sever corrosion took place. Nitrate treatment performed. Iron sulfides as corrosion product found

2.2. Sample preparation and enrichment tests

Received samples were directly processed and diverse enrichment tests were performed. For samples from the installation B the MPN procedure was applied. Chosen MPN protocol delivered semi–quantitative data on concentrations of the cells in analysed samples. It involved performing 10–fold serial dilutions of a microbial culture or an environmental sample into media until the sample was diluted to extinction. Cultures were incubated and assessed for growth by either eye, based on turbidity changes, media colour change and cell counts. Thermophilic samples were inoculated with the pigging debris prepared as described below without applying the MPN protocol due to the rapid medium evaporation from the reagent tubes. Pigging

debris from the Installation A was not processed for MPN because of the insufficient sample amount.

Biofilms from the biocoupons were scratched with sterile cotton swabs and stirred in the original fluid (50 mL) at 30°C for 2 h before the inoculation. Pigging debris from Installations A and C was prepared in analogous manner with the difference that for each g of pigging mud, 10 mL of artificial seawater, ASW (Berglin and Elwing, 2008) was added, and then stirred as described above. For the MPN analysis, water samples were diluted in 10 fold dilution steps until 10^{-7} and coupon samples until 10^{-4}. Aliquots of the dilutions were inoculated in triplicate (10 %, v/v) to the test tubes containing fresh growth media. Growth temperature was the same as in the installation. For Installation C samples (T = 80°C), special long neck Erlenmeyer flasks were prepared (**FIG 3.3**). This operation helped to decrease the evaporation of growth media. All cultures were incubated in the Stackable Shaker (Thermo Scientific®) with stirring velocity of 140 rpm.

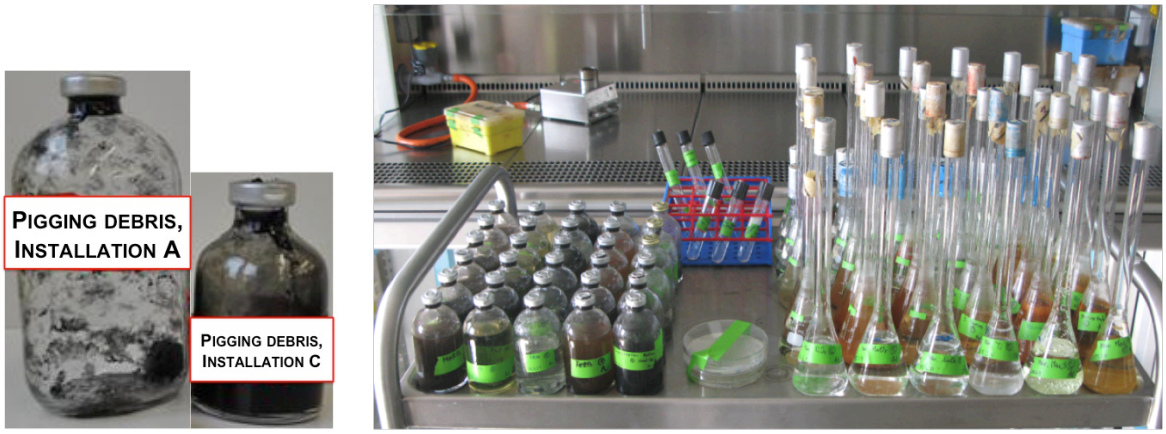

FIG. 3.3. PIGGING DEBRIS AND INOCULATED MEDIA FROM THE INSTALLATION A AND C.

Enrichment tests were performed for acid producers (AP), iron and manganese oxidisers and reducers (FeOx, MnOx, FeRed, MnRed, respectively), ammonia and nitrite oxidisers (AmOx, NiOx, respectively), chemoorganotrophs, nitrate and sulfate reducers (NRed, SRP, respectively), as well as for sulfide oxidising nitrate reducing microorganisms (SO–NRed). The information about bacterial cultivation media is shown in **TABLE 3.2**. Anaerobically grown mesophilic microorganisms were inoculated in reagent tubes and incubated in the Whitley A85 Anaerobic Workstation, (Don Whitley) under the atmosphere of nitrogen, hydrogen and carbon dioxide in the 88:10:2 $v_{N2}/v_{H2}/v_{CO2}$ ratio. Anaerobic thermophiles, grown in the 100 mL serum

bottles, after the inoculation under anaerobic conditions, as mentioned, were tightly closed with the rubber septa and incubated at 80°C under stirring (140 rpm).

In order to assess the growth of microorganisms the following actions were undertaken. Measurement of pH decrease for AP was done with use of Merck pH tests strips. Mn^{2+} and Fe^{2+} ions concentration changes were monitored with use of 1100B Atomic Absorption Spectrometer, AAS (Perkin Elmer). Samples from MRB cultures were taken under anaerobic conditions and mixed with 1N H_2SO_4 in the 1:1 (v/v) ratio. Later on, they were centrifuged at 13000 × g for 2 min and the collected supernatant was used for the measurements. In MnOx cultures, samples were diluted with sterile filtered deionised water at 1:40 (v/v) ratio and further measured with AAS. Nitrite presence was detected by the stipple test with the sulphanilamide/N–(naphthyl)–ethylenediamine–dihydrochloride reaction (Alaburda and Nishihara, 1998). The filter paper was first soaked dropwise with the reagent and then a drop of AmOx, NiOx or NRed culture was applied. The test was positive if pink colour appeared. Sulfide depletion was checked as described (Cord–Ruwisch, 1985). All measurements were done against abiotic controls, incubated in parallel with the inoculated media.

TABLE 3.2. SUMMARY OF ALL ENRICHMENT TESTS PERFORMED ON INDUSTRIAL SAMPLES.

GROUP OF MICROORGANISMS	MEDIUM*	INCUBATION TIME [WEEK]	ASSESSMENT OF BACTERIAL GROWTH BY	AEROBIC / ANAEROBIC CONDITIONS
Acidophilic H_2SO_4 producers = sulfur oxidisers	Sulfur amended Mackintosh medium (Mackintosh, 1978)	3	Decrease of pH (below pH = 2)	Aerobic
Neutrophilic H_2SO_4 producers = neutrophilic thiosulfate oxidisers	(Matin and Rittenberg, 1971)	3	Decrease of pH (below pH = 6)	Aerobic
Fungi	Sabouraud agar	1	Observation of fungal colonies on plates	Aerobic
Acidophilic Fe^{2+} oxidisers	Fe (II) supplemented Mackintosh medium (1 g $FeSO_4 \times 7H_2O$ / L medium)	3	Change of medium colour	Aerobic
Neutrophilic Fe^{2+} oxidisers/ *Gallionella*	(Kucera and Wolfe, 1957) modified by (Hanert, 1992)	3	Change of medium colour	Microaerophilic
Neutrophilic Fe^{2+} oxidisers/ *Leptotrix*	(Mulder and Veen, 1963)	1	Observation of bacterial colonies on plates	Micro–aerophilic
Mn^{2+} oxidisers	(Bromfield, 1956) modified by (Tyler and Marshall, 1967)	3 – 4	Decrease of Mn^{2+} ions (AAS)	Aerobic
Fe^{3+} reducers	(Lovley and Phillips, 1988)	4	Increase of Fe^{2+} ions (AAS)	Anaerobic
Mn^{4+} reducers	Like Fe^{3+} reducers, only instead of Fe^{3+}, MnO_2 was added	4	Increase of Mn^{2+} ions (AAS)	Anaerobic
Ammonia oxidisers	(Krümmel and Harms, 1982)	4 – 6	Production of nitrite and/or nitrate	Aerobic
Nitrite oxidisers	(Carlucci and Strickland, 1968)	4 – 6	Production of nitrate, disappearance of nitrite	Aerobic
Nitrate reducers	(Schippers et al., 1995)	4 – 6	Production of nitrite, depletion of nitrate	Anaerobic
Sulfate reducers	Postgate E medium (Postgate, 1979)	3	Black precipitates and H_2S production	Anaerobic
Nitrate–reducing, sulfide–oxidisers	(Nemati et al., 2001)	3 – 6	Nitrate and sulfide depletion,	Anaerobic
Chemoorganotrophs	R2A agar	1	Observation of bacterial colonies on plates	Aerobic

* ALL MEDIA CONTAINED 2% SODIUM CHLORIDE

Additionally, NRed and FeRed enrichments from the installation B were subsequently inoculated in Postgate E medium in order to detect SRP. Later on these cultures were named as N SRP and Fe SRP, respectively.

2.3. Bacterial treatment after cultivation

2.3.1. Strains isolation and their characterisation

For the strains isolation, enriched cultures were inoculated in the respective growth medium, diluted in 10 fold steps until $1 \cdot 10^{-6}$ (10 % inoculum, v/v) and incubated for 1 week. The sample with the highest dilution, in which the growth was observed, was used as inoculum for the next dilution set. This procedure was repeated thrice. Afterwards, microorganisms were platted on agar plates containing the mixture of 15 g/L agar–agar and the growth medium. Further on, a single colony was picked up and inoculated into the growth medium. This whole procedure was repeated once more.

Characterisation of isolated microorganisms was done by 16S rDNA analyses. The samples were centrifuged at 11180 × g for 10 min. The supernatant was discarded and the cells were washed with 1 mL 1 M sodium chloride. DNA was extracted as described (Aljanabi and Martinez, 1997). DNA quality was analysed using agarose gel electrophoresis and absorbance measurements at 230 nm, 260 nm, 280 nm and 340 nm were done with BioPhotometer plus (Eppendorf).

PCR amplification of DNA fragments was performed in a final reaction volume of 25 µL using 20 ng of genomic DNA as a template, 5 x Green Flexi buffer, 2.5 mM $MgCl_2$, 1 mM dNTPs, 4 % DMSO, 15 pmol of each single universal 16S bacterial primer 27F and 1492R, respectively (Lane, 1991) and 1 U GoTaq®DNA polymerase (Promega®). The following temperature program was used: 3 min initial denaturation at 94 ºC, followed by 35 cycles of: denaturation for 30 s at 94 ºC, primer annealing for 30 s at 57ºC and 1.5 min extension at 72 ºC. The final extension step was done for 3 min at 72ºC.

PCR products were run in agarose gel electrophoresis (1 % agarose gels in TAE buffer (20 mM Tris–acetate pH = 8; 0.5 mM EDTA) at 110 V for 30–*35* min (Amersham Biosciences, Electrophoresis power supply 301). For all electrophoresis the 1 kb plus DNA Ladder (Invitrogen™) was used. Gels were stained for 10 min by incubation in 0.2 µg/ml ethidium bromide in TAE buffer (40 mM Tris – base, 20mM acetic acid, 1mM EDTA), rinsed in water and photographed using a Biorad® GelDoc™ station.

PCR products were purified with Promega® Gel extraction kit. DNA concentration and purity were estimated using BioPhotometer plus (Eppendorf). Afterwards, PCR products were cloned using the pGEM®–T vector system (Promega®) following the ligation protocol of the manufacturer in 10 µL reactions. Ligation mixtures were incubated at 16 °C for 24 h or at 4°C 48 h. The ligation reactions were transformed in *E. coli* DH5α competent cells before being sent for sequencing.

Competent *E. coli* cells were prepared as follows. An overnight culture of *E. coli* DH5α in the was prepared and 100 µL were inoculated to 6 mL in fresh LB medium. Cells were grown at 37 °C until OD_{600} reached the value of 0.4. Further on they were incubated on ice for 10 min and centrifuged for 7 min at 2655 × g at 4°C. Collected pellet was carefully resuspended in 250 µL ice–cold $CaCl_2$ solution (60 mM $CaCl_2$, 10 mM piperazine–N,N′–bis(2–ethanesulfonic acid) (PIPES), 15% (v/v) glycerin) and centrifuged for 5 min in the same conditions as before. In the next step, cell pellet was resuspended in 200 µL of ice–cold $CaCl_2$ solution and incubated for 30 min on ice for competence induction. Afterwards, the whole (10 µL) ligation mix was added to *E. coli* cells. Part of cells was incubated without ligation mix (negative control). After the incubation at 4°C for 30 min, cells were heat shocked for 2 min at 42 °C. 0.8 ml of LB medium was added and cells were grown for 1 h at 37°C, with 150 rpm stirring. Afterwards cells were plated on LB with Amp/X–gal/IPTG plates and grown for 14–16 h at 37 °C.

Plasmids containing an insert were isolated using the Roti®–Prep Plasmid MINI Kit (Carl Roth). Concentrations of plasmids were analysed using BioPhotometer plus (Eppendorf). The presence of an insert cloned on pGEM–T vector was confirmed by PCR using T7 and SP6 primers, adjacent to its cloning site. Plasmids with a cloned insert were sent for sequencing to “Zentraler DNA–Sequenzierservice” of the Medical Faculty of the Institute for Human Genetics, Universitätsklinikum Essen. Electropherograms were evaluated with BioEdit program (version 7.1.3) and DNA sequences were analysed in NCBI database by using BLAST comparisons.

2.3.2. Denaturing Gradient Gel Electrophoresis and functional genes tests of the mixed cultures

The microbiological diversity of oil field samples was analysed by Denaturing Gradient Gel Electrophoresis (DGGE). This was performed in collaboration with M.Sc. Jemimah Doma and Prof. Dr. Iwona B. Beech from the University of Portsmouth, UK (UoP) and Oklahoma University (OU). For the DNA extraction of all enriched cultures either Power Biofilm Kit (MOBIO®), NucleoSpin® tissue (Macherey–Nagel) or QIAGEN DNeasy Blood and Tissue Kit (QIAGEN) were used, following the manufacturers protocol. PCR reactions were performed to verify the presence of bacteria and archea, as well as *apsA* gene (encoding for the alpha subunit of adenosine–5'–phosphosulfate reductase), *dsrAB* (genes encoding for the alpha and beta subunits of the dissimilatory sulfite reductase), *nirK* (gene encoding for the nitrite reductase) and *Shewanella* 16S rDNA gene. PCR reaction mixtures (V=25 µL or its multiplication), as well as used temperature programs are shown in **TABLE 3.3** and **TABLE 3.4**, respectively. PCR products were checked on 0.9% agarose gels run at on 140 V for 40 min. Afterwards these were stained with 4µL SYBR® Safe DNA gel stain (Invitrogen) acc. to the manufacturer manual. 30 – 80% denaturing gradient DGGE was carried out from a successful bacterial 16S rRNA PCR with 6% (w/v) polyacrylamide gel prepared with TAE buffer. 40 µL of PCR product were loaded per lane. After the DGGE gel was prepared, samples were loaded and run in TAE buffer at 60°C in Ingeny Gel Apparatus (Ingeny, Netherlands) for 18–20 h (15 min at the voltage of 200 V, and further at 90 V, until the end of experiment). After running, staining was performed with 12µL of SYBR® Safe DNA stain incubated in the dark for 15 min. Further on, gels were rinsed with distilled water and exposed to UV to record the gel image with use of NucleoCam Digital Image Documentation System™ (NucleoTech).

TABLE 3.3. PCR REACTION MIXTURES USED FOR ENRICHMENTS CHARACTERISATION.

Reagent	Bacterial 16S rDNA mix (550bp size)		Archeal 16S rDNA mix (600bp size)		apsA PCR mix, (658 bp size)		dsrAB PCR mix, (1900 bp size)		nirK PCR mix, (165 bp size)		Shewanella PCR mix, (1048 bp size)	
		V [µL]		V [µL]		V [µL]		V [µL]		V [µL]		V [µL]
Water		6.5		8.85		6.5		6.5		6.5		6.5
Master Mix [A]		12.5	10x conc.	2.5		12.5		12.5		12.5		12.5
Forward (F) Primer	341F+GC[1]	0.5	Arch333F +GC[2]	2.0	9 P1F[3]	0.5	DSR1F[4]	0.5	nirK876[5]	0.5	She211F[6]	0.5
Reverse (R) Primer	907R[1]	0.5	Arch958R[2]	2.0	10 P1R[3]	0.5	DSR4R[4]	0.5	nirK1040[5]	0.5	She1259R[6]	0.5
Go Taq Polymerase				0.15								
5M Betaine				2.5								
2.5 mM $MgCl_2$				1.5								
dNTPs (10mM)				0.5								
DNA		5.0		5.0		5.0		5.0		5.0		5.0

[A] GoTaq® Green Master Mix, 2x concentrated (conc), Promega® (Components: GoTaq Polymerase, 2X Green GoTaq® Reaction Buffer (pH 8.5), 400µM dATP, 400µM dGTP, 400µM dCTP, 400µM dTTP, 3 mM MgCl2)

[1] (Schäfer and Muyzer, 2001)

[2] (Struchtemeyer et al., 2005)

[3] (Al–Humam et al., 2010)

[4] (Loy et al., 2004)

[5] (Henry et al., 2004)

[6] (Todorova and Costello, 2006)

TABLE 3.4. PCR TEMPERATURE PROGRAMS USED FOR ENRICHMENTS CHARACTERISATION.

	Bacterial 16S rDNA Touch down PCR		Archeal 16S rDNA		*apsA*		*dsrAB*		*nirK*		*Shewanella*	
	t [min]	T [°C]	t [min]	T [°C]	t [min]	T [°C]	t [min]	T [°C]	t [min]	T [°C]	t [min]	T [°C]
Initial denaturation	4.0	94	4.0	94	5.0	95	4.0	94	4.0	94	1.5	94
Number of cycles	1											
Denaturation	1.0	94	X									
Annealing	1.0	63–54*										
Extension	1.0	72										
Number of cycles	20											
Denaturation	1.0	94	1.0	94	1.0	94	1.0	94	0.75	94	1.0	92
Annealing	1.0	53	1.0	53	1.0	62	1.0	54	0.75	54	1.5	53
Extension	1.0	72	1.0	72	1.0	72	1.0	72	2.0	72	1.0	72
Final extension	10.0	72	10.0	72	10	72	10	72	10	72	5.0	72
Cooling	∞	6	∞	6	∞	6	∞	6	∞	6	∞	6
Number of cycles	15		35		35		35				24	

* WITH EACH SUBSEQUENT CYCLE THE TEMPERATURE WAS DECREASING FOR 0.5°C

2.4. Biofilm formation studies of enriched cultures with use of Epifluorescence Microscopy

The dynamics of biofilm formation of SRP cultures enriched from the biocoupons material (installation B, water injection pipeline B1) was investigated. The detailed description of the coupons used for this study and their preparation are given in the Chapter IV. The preparation procedure and material used in whole study was unified. The cultures were anaerobically grown in the same medium, as the one used for the enrichment tests. All experiments were performed at 30°C with 5% (v/v) inoculum (initial cell number of 10^7 cells / ml) of the enriched culture in exponential growth phase. The coupons were incubated for 1, 12, 24, 72 and 168 h and afterwards stained under anaerobic conditions in the following way. Each coupon was rinsed with 4 ml of sterile filtered deionised water, in order to exclude the influence of the medium compounds. Cell staining was done with 0.02% (w/v) 4',6–diamidino–2–phenylindole (DAPI) aqueous solution for 10 min. Subsequently, after rinsing coupons with deionised water, they were anaerobically dried, removed from the anaerobic chamber and directly visualised under the epifluorescence microscope (EFM). The whole procedure was performed avoiding direct sunlight. DAPI solution and water used for washing the coupons were flushed under the sterile conditions with nitrogen for 20 min.

Visualisation of fluorescently stained specimens was performed using an upright EFM (Zeiss®, AxioImager™ A1m) equipped with a HBO 100 mercury vapour lamp, using Zeiss® filterset 49. Air–objectives (Zeiss®, EC plan NEOFLUAR 440480/9903 and EC epiplan NEOFLUAR 422393/9900) and a digital microscope camera (Zeiss®, AxioCam™ MRm). Images were processed using the Zeiss® AxioVert™ Software.

3. RESULTS

3.1. Enrichment tests of industrial samples – assessment of cultivable microbial populations

Enrichment tests for 15 (or 13 in case of thermophiles) different metabolic groups of microorganisms originated from diverse pipelines with various corrosion failures were performed. For the installations A and C, the results are summarised in **TABLE 3.5**. In case of installation B, the results of MPN tests are presented separately (**TABLE 3.6**).

TABLE 3.5. ENRICHMENT TESTS RESULTS FROM PIGGING SAMPLES.

GROUP OF MICROORGANISMS	INSTALLATION A			INSTALLATION C		
	PIG 1	PIG 4	PIG 9	PIG 1	PIG 2	PIG 3
ACIDOPHILIC H_2SO_4 PRODUCERS	+	+	–	+	+	+
NEUTROPHILIC H_2SO_4 PRODUCERS	–	–	–	–	+	+
FUNGI	+	+	+	*	*	*
ACIDOPHILIC Fe^{2+} OXIDISERS	+	–	–	+	+	+
NEUTROPHILIC Fe^{2+} OXIDISERS/ *GALLIONELLA*	–	–	–	–	–	–
NEUTROPHILIC Fe^{2+} OXIDISERS/ *LEPTOTRIX*	–	–	–	–	–	–
Mn^{2+} OXIDISERS	+	–	+	+	+	+
Fe^{3+} REDUCERS	+	+	+	+	+	+
Mn^{4+} REDUCERS	+	+	+	+	+	+
NH_4^+ OXIDISERS	+	+	+	+	+	+
NO_2^- OXIDISERS	+	+	+	+	+	+
NO_3^- REDUCERS	+	–	+	–	+	+
SO_4^{2-} REDUCERS	+	+	+	+	+	+
NO_3^- REDUCING S^{2-}OXIDISERS	–	–	–	–	–	–
CHEMOORGANOTROPHS	+	+	+	*	*	*

\+ – GROWTH OBSERVED – – NO GROWTH OBSERVED

* BECAUSE OF HIGH TEMPERATURE TESTS NOT PERFORMED

In installations A and C the microbial flora was very rich and diverse. Despite multiple cleaning steps, microbial growth was observed even after the ninth cleaning pig passed through the system. Microorganisms able to grow with and without oxygen presence were detected, however the former ones were observed mainly in the pigging debris from the first running pigs. Among the microorganisms of the sulfur cycle, acidophilic sulfur oxidisers (S^0Ox) and SRP were found. Neutrophilic thiosulfate oxidisers (S_2O_3Ox) were not enriched. Not many types of FeOx were found. These were mainly acidophiles found in the first pig sample from Installation A and in all three pigs from the production pipelines of Installation C. FeRed were

present in all pigging samples, independently of the biofilm depth. Microorganisms of the manganese cycle, both MnOx and MnRed were ubiquitous, as well as the ones of the nitrogen cycle. However nitrate reduction was observed on different levels of the pipeline biofilms. Various chemoorganotrophs and fungi were detected in the Installation A. These tests were not done for the Installation C because of the high growth temperatures required.

TABLE 3.6. ENRICHMENT TESTS RESULTS WITH SAMPLES THE INSTALLATION B.

GROUP OF MICROORGANISMS	WATER SAMPLES		BIOCOUPON SAMPLES	
	NO. 1	NO. 2	NO. 3	NO. 4
	CELL NUMBER/mL		CELL NUMBER/cm^2	
ACIDOPHILIC H_2SO_4 PRODUCERS	No growth			
NEUTROPHILIC H_2SO_4 PRODUCERS				
FUNGI				
ACIDOPHILIC Fe^{2+} OXIDISERS				
NEUTROPHILIC Fe^{2+} OXIDISERS/ *GALLIONELLA*				
NEUTROPHILIC Fe^{2+} OXIDISERS/ *LEPTOTRIX*				
Mn^{2+} OXIDISERS				
Fe^{3+} REDUCERS	2.9×10^4	2.9×10^4	3.0×10^3	3.0×10^3
Mn^{4+} REDUCERS	2.9×10^4	2.9×10^4	3.0×10^3	3.0×10^3
NH_4^+ OXIDISERS	No growth			
NO_2^- OXIDISERS				
NO_3^- REDUCERS	2.9×10^4	2.9×10^4	3.0×10^3	3.0×10^3
SO_4^{2-} REDUCERS	2.9×10^4	2.9×10^4	3.0×10^3	3.0×10^3
NO_3^- REDUCING S^{2-}OXIDISERS	No growth			
CHEMOORGANOTROPHS	3.0×10^9	3.2×10^9	1.4×10^8	5.2×10^7

Analyses of the samples from Installation B revealed presence of anaerobic microorganisms in both types of samples. The only aerobically grown cultures were chemoorganotrophic microorganisms. After the second passage SRP and MnRed enrichments lost their culturability. The same phenomenon was observed for FeRed enrichments from one water sample (No. 2) and two biocoupons, but this appeared after the fourth subcultivation in 2 week intervals. However, before that happened, living cultures of NRed and FeRed were also inoculated in Postgate E medium and growth of SRP was successful. MPN results disclosed supplementary information about the initial number of the different physiological groups representatives in the field samples processed. For the water samples they reached 2.9×10^4 cells/mL and 3.0×10^3 cells/cm^2 enriched from the coupon independently of the type of anaerobic culture. For chemoorganotrophs, 3.0×10^9 to 3.2×10^9 colony forming units (CFU) / mL were found in the water samples and 5.2×10^7 to 1.4×10^8 CFU / cm^2 in biocoupons. None of the enrichments contained SO–NRB.

3.2. Bacterial isolates identification

Through the use of 16S rDNA analysis and cloning approach it was possible to characterise some strains present in enrichments from Installation B samples. From above 30 clones, the following microorganisms were found: *Desulfovibrio dechloracetivorans* (Sun et al., 2000), (98% identity, SRP), *Desulfovibrio caledoniensis* (Cetin and Aksu, 2013), (99% identity, SRP).

In case of NRB cultures *Thalassospira spp.* was present in enriched samples. *Thalassospira xiamenensis* (Liu et al., 2007), (97% identity) and *Thalassospira lucentensis* (López–López et al., 2002), (98% identity) were identified. *Pseudomonas stutzeri* (Lalucat et al., 2006), (98% identity, marine denitrifying bacterium) and *Pseudomonas putida* (93% identity) were also detected.

3.3. DGGE and PCR results

The summary of all results obtained from the PCR analyses are summarised in **Table 3.7**.

TABLE 3.7. SUMMARY OF PCR RESULTS OBTAINED WITH DNA FROM ENRICHED CULTURES. *APSA*

NO.	METABOLIC GROUP	INSTALLATION	PIG/ SAMPLE NO.	BACTERIAL 16S RDNA	ARCHEAL 16S RDNA	*FUNCTIONAL GENES*			
						APSA	*DSRAB*	*NIRK*	*SH**
1	Mn^{4+} reducers	A	1	+	–	+	–	–	–
2			4	+	–	+	–	–	–
3			9	+	–	+	–	–	–
4		C	1	+	–	–	–	–	–
5			2	+	+	–	–	–	–
6			3	+	+	–	–	–	–
7	Acid.** Fe^{2+} oxidisers	A	1	+	–	–	–	–	–
8		C	1	+	–	–	–	–	–
9			2	+	–	–	–	–	–
10			3	+	–	+	–	–	–
11	SO_4^{2-} reducers	A	1	+	–	+	–	–	–
12			4	+	–	+	–	–	–
13			9	+	–	+	+	–	–
14		C	1	+	–	+	–	–	–
15			2	+	–	+	–	–	–
16			3	+	–	+	–	–	–
17	Neutr.*** H_2SO_4 producers	C	2	+	–	+	–	–	–
18			3	+	–	+	–	–	–
19	NO_2^- oxidisers	C	1	+	–	+	–	–	–
20			2	+	–	+	–	–	–
21			3	+	–	–	–	–	–
22		A	1	+	–	–	–	–	–
23			4	+	–	–	–	–	–
24			9	+	–	–	–	–	–
25	NH_4^+ oxidisers	C	1	+	–	–	–	–	–
26			2	+	–	–	–	–	–
27			3	+	–	–	–	–	–
28		A	1	+	–	–	–	–	–
29			4	+	–	–	–	–	–
30			9	+	–	+	–	–	–
31	Mn^{2+} oxidisers	A	1	+	–	–	–	–	–
32			9	+	–	+	–	–	–
33		C	1	+	–	–	–	–	–
34			2	+	–	+	–	–	–
35			3	+	–	–	–	–	–
36	NO_3^- reducers	C	2	+	+	–	–	–	–
37			3	+	+	–	–	–	–
38		A	1	+	–	–	–	–	–
39			9	+	–	–	–	–	–

* SH – *SHEWANELLA* 16S RDNA GENE

\+ – POSITIVE RESULT

– – NEGATIVE RESULT

** ACID. – ACIDOPHILIC

*** NEUTR. – NEUTROPHILIC

40	Fe^{3+} reducers	A	1	+	+	–	–	–	–
41			4	+	–	–	–	–	–
42			9	+	–	+	–	–	–
43		C	1	+	–	–	–	–	–
44			2	+	–	–	–	–	–
45			3	+	–	–	–	–	–
46	Acid.* H_2SO_4 producers	A	1	+	–	+	–	–	–
47			4	+	–	+	–	–	–
48		C	1	+	–	+	–	–	–
49			2	+	–	+	–	–	–
50			3	+	–	–	+	–	–
51	(Fe) SO_4^{2-} reducers	B	1	+	–	+	+	–	–
52			2	+	–	+	+	–	–
53			4	+	–	+	+	–	–
54	(N) SO_4^{2-} reducers		1	+	–	+	+	–	–
55			2	+	–	+	+	–	–
56			3	+	–	+	–	–	–
57	NO_3^- reducers		1	+	–	+	–	–	–
58			2	+	–	+	–	–	–
59			3	+	–	–	–	–	–
60			4	+	–	+	–	–	–
61	Fe^{3+} reducers		1	+	–	+	–	–	–

\+ – POSITIVE RESULT

– – NEGATIVE RESULT

** ACID. – ACIDOPHILIC

*** NEUTR. – NEUTROPHILIC

All enrichments were positive for bacterial 16S rDNA. 28 enrichments were grown at 80°C, however only 4 of them were positive for Archaeal 16S rDNA. One enrichment, which gave an amplicon for the Archeal 16S rDNA was found in the enrichment culture from FeRed medium inoculated with the debris from the Pig 1, installation A. 32 enrichments were positive for *apsA* marker, from which only 6 were also positive for the *dsrAB* marker. Five of these having both *apsA* and *dsrAB* genes were detected in the enrichments from the Installation B (the one with the most severe corrosion problems). The sixth one was found in the SRP enrichment from the Installation A Pig 9. Other enrichments containing *apsA* gene (but no *dsrAB* gene), were coming from the media for S^0Ox (4 samples, Installation A and C), S_2O_3Ox (2 samples, Installation C) and SRP (6 samples, Installations A – C); AmOx (1 sample, Installation A), NiOx (2 samples, Installation C) and NRed (3 samples, Installation B);

MnOx (2 samples, Installations A and C) and MnRed (3 samples, Installation A); acidophilic FeOx (1 sample Installation C) and FeRed (2 samples, Installation A and B).

Only one enriched culture was positive for dsrAB marker, and negative for *apsA* gene (acidophilic H_2SO_4 producers medium inoculated with the debris from the Pig 3, Installation C). *Shewanella* 16S rDNA and *nirK* (NRed marker) were not detected in any of the samples.

DGGE was performed for all 61 samples with 30 to 80% denaturing gradient gels. Amplicons obtained with universal bacterial 16S rDNA primers were loaded. The results are shown in the Fig. 3.4. In total from 2 to even 21 bands per lane were detected in the enriched cultures.

Lanes No. 1–6 were from manganese reducers. The first 3 were enriched under mesophilic conditions, while the next 3 ones were enriched under thermophilic conditions. The number of bands in samples 1–3 increased with the respective pig number. An opposite trend was observed in the next 3 bands. No bands repeated between thermophilic and mesophilic samples. Lanes from 7 to 10 corresponded to acidophilic iron oxidisers, 7^{th} was grown at 30°C and 8 – 10 at 80°C. These profiles showed higher similarity to each other. Two bands at the upper part also appeared in the manganese reducers' profiles. Lanes 11 – 16 corresponded to SRP, and 17 – 24 to NiOx. From these, samples in lanes 14 to 21 were thermophilic. With the increasing lane number in the mesophilic samples, number of bands increased. However, lane 13 significantly differed from two former lanes. This one was also more similar to the next 7 lanes (14 to 20) and gave positive results for both the presence *apsA* and *dsrAB* genes. Lanes from 14 to 20 had identical profiles, although the samples were coming from different media. However, all of them were grown at the same temperature (80°C), all had *apsA* gene only (no *dsrAB* gene) and both media contained sulfate. Lanes 21 to 23 had identical DGGE profiles and lane 24 varied from the former three, having less bands with their different migration. Lanes 25 to 30 corresponded to the samples enriched for AmOX, while 25–27 and 28–30 were thermophiles and mesophiles, respectively. Lanes 25–27 had almost identical profiles, but the last lane had weaker bands than other two. Also lane 29 showed high similarity to the lanes 25 to 27. However, DGGE profiles from mesophilic AmOx varied significantly from each other with the band path, as well as lanes 31 and 32, which were coming from the DNA of mesophilic manganese

oxidisers. Lanes 33 to 35 corresponded to thermophilic manganese oxidisers and 36 and 37 to thermophilic NRed. Lanes 38th and 39th were from mesophilic NRed. From lanes 33 – 37 lane DNA profiles were identical. The sample, in lane 38 was more related to the sample 40, than sample 39. The only observed similarity was shown in the upper gel part. Samples from 40 to 45 were from FeRed enrichments and 40–42 were mesophiles. These lanes showed similar profiles, but the middle lane had no bands in the bottom part of the gel. Next three lanes (43–45) showed partial similarity in the upper part of the gel. The least number of bands was this time in the lane 45. Lanes from 46th to 50th were from S^0Ox, with last three samples grown at 80°C. Their profiles showed a very high level of similarity, with the difference that bands were fading with each subsequent sample.

The last 11 lanes, were from enrichment samples from the installation B (temperature of 30°C), 51st to 56th were linked to diversely obtained SRP, the next four to NRed and the last one came from iron reducers enrichments. Here bands 51–54 were identical, 55th had an additional band at the bottom of the gel. This band was the only one present in the lane 56. Samples 57 and 60 were highly similar, and 58 and 59 differed with the band distribution on the top of the gel with variation of one band. Iron reducers lane had only 2 well separated bands, and some smears. It was not similar to any of the samples enrichments from the installation B.

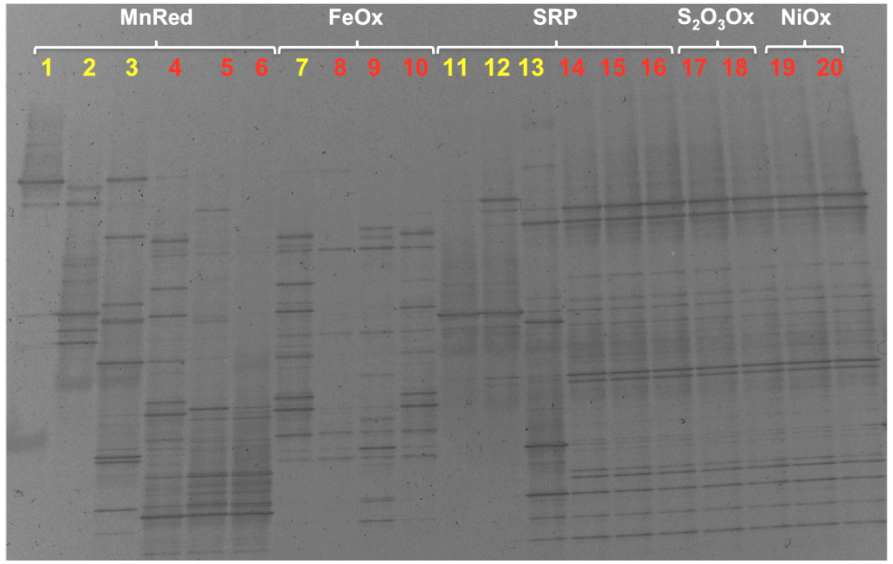

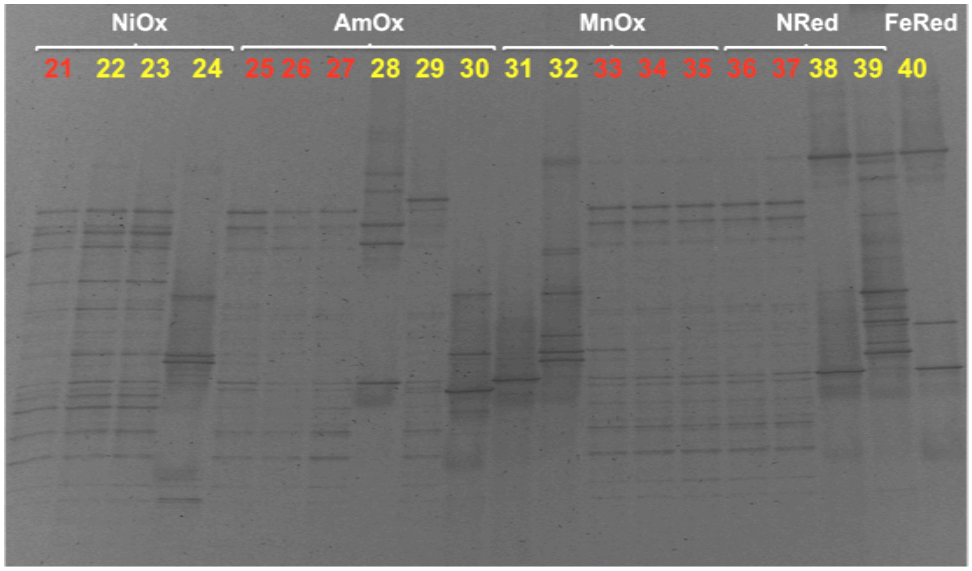

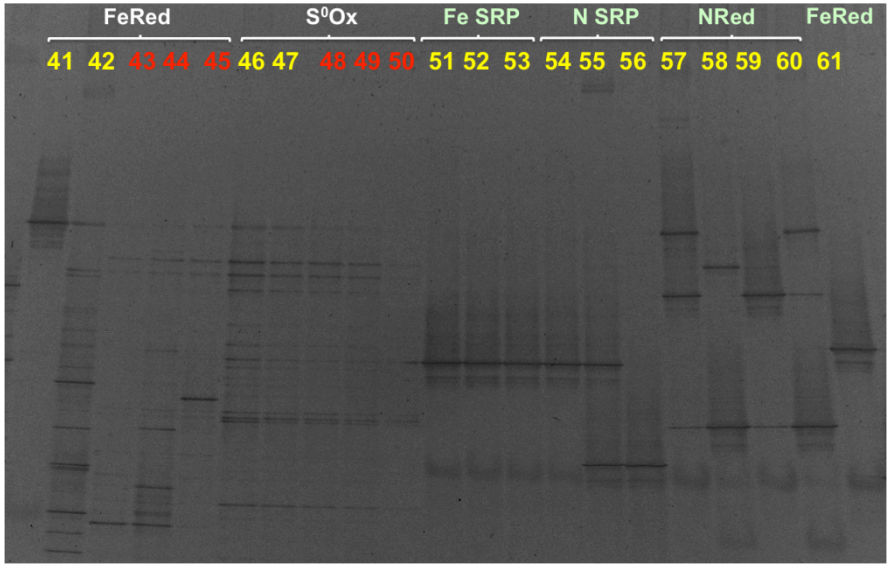

FIG. 3.4. DGGE GELS FROM ENRICHMENTS OF INDUSTRIAL SAMPLES. NUMBERS 1 TO 61 CORRESPOND TO THE SAMPLES NUMBERS AS IN TABLE 3.7. RED COLOUR REFERS TO THE THERMOPHILIC, AND YELLOW COLOUR TO THE MESOPHILIC ENRICHMENTS. SAMPLES WRITTEN IN WHITE CORRESPOND TO INSTALLATIONS A AND C AND IN LIGHT GREEN TO INSTALLATION B.

3.4. Biofilm formation studies by EFM

The attachment dynamics of SRP enrichments from the Installation B to the carbon steel surface were studied by EFM microscopy and DAPI staining. It was observed that the initial cell adhesion appeared already within the first hour of incubation. After 12 h, a random cell distribution was detected and after 24 h cell aggregates occurred. After 3 days of incubation coupons were fully covered and within one week a thick multilayer biofilm was formed (**FIG. 3.5**).

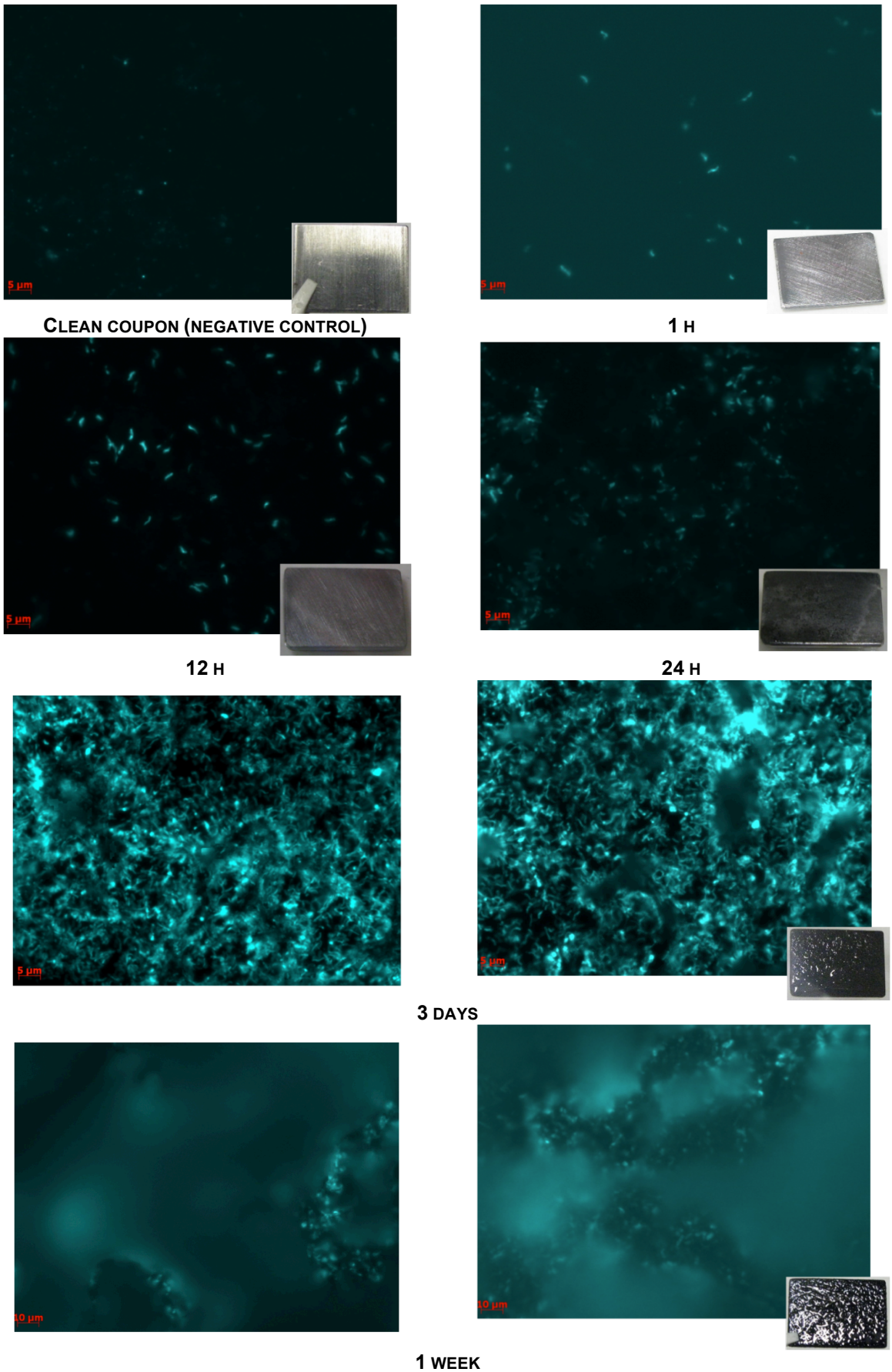

FIG. 3.5. BIOFILM FORMATION OF A SRP ENRICHMENT CULTURE FROM THE BIOCOUPON (INSTALLATION B, WATER INJECTION PIPELINE B1). COUPONS AFTER 3 DAYS AND ONE WEEK OF INCUBATION WERE VISUALISED ON THE DIFFERENT HEIGHT LEVELS IN ORDER TO SHOW CELLS AT VARIOUS VERTICAL POSITIONS.

4. DISCUSSION

Culture dependent methods for characterisation of microbial diversity of the oil field revealed that the most microbiologically diverse samples were the pigging debris ones, containing both aerobic and anaerobic microorganisms, independently of the pigging gauge origin or number. Aerobic microorganisms were present even in the deepest layers of collected biofilm mud, where the oxygen levels were below the detection limit. Despite the fact that many organisms can also grow in the presence or absence of oxygen, one cannot exclude the possibility that while performing pigging procedure some aerobic consortia were mechanically shifted to the deeper biofilm layers.

In the installation B, with severe corrosion problems, the cultivable fraction of the resident microbial flora was found to be mainly anaerobic. Similar results were reported after investigation of the microbial populations in production waters of a low–temperature biodegraded oil reservoir (Grabowski et al., 2005). Observed growth rates, independently of inoculated medium, were very similar; assessing the cell numbers by a semi–quantitative technique, such as MPN, 2.9×10^4 cells were found in 1 mL of SRP, NRed, MnRed and FeRed media inoculated with the injection water, while 3.2×10^3 cells were found on 1 cm^2 of the biocoupon. Possibly all enriched consortia could be able to reduce in parallel sulfate, nitrate, iron or manganese. Such cases of microorganisms able to use Fe (III), Mn (IV), nitrate or sulfate as an electron acceptor in various combinations have been already reported in the literature (Lovley et al., 1993; Tebo and Obraztsova, 1998; Weelink et al., 2009).

Enriched NRed and FeRed cultures were additionally inoculated to Postgate E medium in order to address their sulfate reducing abilities. This trial gave positive growth. DGGE profiles of these enrichments named as N SRP (sulfate reducing cultures from nitrate reducers enrichments) and Fe SRP (sulfate reducing cultures from iron reducers enrichments) were very similar (**FIG. 3.4**, lanes 51–56).

Enriched samples were analysed by PCR for the presence of *apsA*, *dsrAB*, *nirK* and 16S rDNA *Shewanella* genes, which are accepted as the markers for SRP, NRed and FeRB (*Shewanella)*. *NirK* gene was not detected; nevertheless, it did not exclude the presence of NRB in the system. Other genes, such as *nirS* or *nfr* gene, which were found in SRP able to reduce nitrite (Al–Humam et al., 2010; Greene et al.,

2003) may be more suitable for this system. Moreover, cloning and sequencing revealed the presence of clones with 98% identity to *Pseudomonas stutzeri*. *P. stutzeri* is a marine denitrifying bacterium. Several strains of this species are also able to fix nitrogen and some participate in the degradation of pollutants or resist against toxic metals (Lalucat et al., 2006). None of them had been regarded as a reducer of Fe (III) (Naganuma et al., 2006).

Subsequently, clones with 97% and 98% identity to *Thalassospira xiamenensis* (Liu et al., 2007), and *Thalassospira lucentensis* (López–López et al., 2002) were found. Members of this genus were primarily isolated from the surface water of a waste–oil pool and marine oligotrophic conditions, respectively. These microorganisms can grow under anaerobic conditions by reducing nitrate. They are halophiles, able to grow in the presence of up to 10% sodium chloride. Carbohydrates, organic acids or aminoacids are used as the carbon source and both nitrate and ammonium as nitrogen source. Furthermore *T. xiamenensis* is able to degrade petroleum. Consequently, the presence of these microorganisms may significantly affect oil quality, increase availability of various carbon sources for the growth of other microorganisms and decrease the effectiveness of nitrate treatment.

Through the use of 16S rDNA analysis and cloning approach it was possible to characterise also some SRP strains. The most often found clones were *Desulfovibrio dechloracetivorans* and *Desulfovibrio caledoniensis*. The later one was isolated from an oil production well, where it caused severe corrosion of low alloyed steel (Cetin and Aksu, 2013). *D. dechloracetivorans* is able to grow by coupling the reductive dechlorination of 2–chlorophenol to the oxidation of acetate. This bacterium is also able to reduce sulfate, sulfite, thiosulfate, and nitrate using acetate, fumarate, lactate, propionate, pyruvate, alanine, and ethanol as electron donors. Frequently, various culture media for the enumeration of SRP support the growth of facultative sulfide producers, e.g. *Shewanella* (Lutterbach et al., 2009). These facultative H_2S – producing bacteria might contribute considerably towards MIC (Dawood and Brözel, 1998). However, tests for functional genes presence gave negative results and no iron reducers were found among the sequenced clones.

Samples from two production plants (A and C) showed differences in their cultivable fraction compared to microorganisms from these observed in the installation B. These differences could be attributed to the type of samples received. While the biofilm on the biocoupon was very thin and hardly visible, the cleaning mud

was black and had an intensive sulfide smell with oily consistence. The first signs of microbial growth from the latter samples were observed within few days, while when inoculating with the biological material scratched from the biocoupon, the maximal incubation time (6 weeks) was needed to detect microbial growth.

SRP are the major organisms involved in carbon steel corrosion enhancement. However, more often the role of other sulfide producing microorganisms has been emphasised (Crolet and Magot, 1996; Magot et al., 1997). Presence of thiosulfate and its utilisation has been shown to represent one of the major risk factors, leading to penetration rates greater than a centimetre per year (Campaignolle et al., 1996). The common presence of diverse bacterial groups at corrosion sites suggests high complexity of electron transfer processes between metal–microbes and microbes–microbes (Kan et al., 2011). These reactions could involve various microorganisms organisms, including SRP (or more generally sulfide producers), but not limited to them. AP, MnRed, FeRed, MnOx, FeOx and SOB are more and more often emphasised as simultaneously causing surface deterioration (Little and Lee, 2007). Here, other mechanisms for MIC have been proposed (i.e. producing sulfuric acid, ammonia and hydrogen, metal oxidation, or reduction), where for each mechanism, many different causative microorganisms might be involved.

By using selective culture media, physiologically diverse bacterial groups have been identified as major players in the MIC process (Kan et al., 2011). Acetic acid produced by *Clostridium aceticum and* sulfuric acid produced by *Acidithiobacillus thioxidans*, are significant contributors to the corrosion. The impact of acidic metabolites is intensified when they are trapped at the biofilm–metal interface. *Shewanella* or *Geobacter* (metal reducing bacteria) as well as *Gallionella*, *Leptothrix*, *Sphaerotilus*, *Crenothrix* and *Clonothrix* (iron and manganese oxidising bacteria), were very often found in the areas with MIC risks (Beech and Gaylarde, 1999; Dexter, 2003; Little and Lee, 2007). However, culture–dependent approaches may underestimate the microbial populations at MIC sites because of their selective nature. This could probably explain the lack of aerobic enrichments in the installation B. They could be present as well as the anaerobic microorganisms, but being dominated by other ones, they were not enriched. Media biases may also select for the fastest growing or for the most abundant microorganisms. Another possible scenario could be the occurrence of viable but not culturable (VBNC) microorganisms. VBNC microorganisms are in a state of very low metabolic activity

and do not divide, but are alive and have the ability to become culturable once "resuscitated" (Oliver, 2005). Bacteria in a VBNC state cannot grow on standard growth media and it is proposed that they can enter the VBNC state as a response to stress.

To support the culture dependent approach, molecular microbiology tests were performed. DGGE profiles of enriched cultures revealed significant differences within one test (e.g. MnRed). Sometimes the number of bands increased; in other cases it was the opposite. It also appeared that the band patherns were identical, like for thermophilic AmOx. However, between enrichments for different metabolic groups, DGGE profiles were found to be identical. That was the case of thermophilic nitrate reducers with thermophilic manganese oxidisers. The existence of a microbial group catalysing nitrate dependent Mn^{2+} oxidation is not yet clear. However, this redox process was reported to occur under anaerobic conditions in soil samples (Pyzola, 2013) and in deep–sea sediments (Luther III et al., 1997). Detection of anaerobes able to oxidise ferrous iron with simultaneous nitrate reduction was documented (Schädler et al., 2009; Straub and Buchholz–Cleven, 1998; Straub et al., 1996). However, as mentioned, there is a lack of information about the use of manganese with nitrate as an electron acceptor.

Other groups of enrichments, in which identical DGGE profiles were found, were the thermophilic SRP, neutrophilic sulfuric acid producers and nitrite oxidisers. It is not clear which microorganisms could be enriched and only sequencing could support these investigations. It might be possible that DGGE biased towards the dominant populations within the consortia. Nevertheless, in all these enrichments the *apsA* gene was present but no *dsrAB*. PCR assays have been developed for the amplification of *dsr*AB genes, however the primers designed for its amplification were successful to detect only pure SRP strains from a culture collection (Al–Humam et al., 2010). As further shown in this study, an attempt to detect the presence of an SRP strain isolated and purified from the oil field and grown in nitrate–enrichments, using these primers, failed. Thus, it was concluded that analysis based on employing the *dsr*AB gene failed to confirm the presence of SRP in media supplemented with nitrate. As a consequence *dsrAB* gene was assessed as unsuitable marker for universal detection of SRP populations in the oil field environment. In addition to sulfate, some SRP species can also utilise thiosulfate, sulfite and elemental sulfur as electron acceptors. Other non sulfur–containing electron acceptors utilised by SRP

include nitrate and nitrite (Moura et al., 1997). It is also known that nitrite can have an inhibitory effect on SRP growth, however SRP which contain a periplasmic nitrite reductase (*nrf*) could overcome this inhibition by further reducing nitrite to ammonia (Greene et al., 2003). The existence of the same consortia under aerobic and anaerobic conditions at high temperatures may be caused by the fact that at 80°C oxygen levels in water were low and tolerated by the SRP/thiosulfate reducers. Additionally, the media to enrich NRed contained sulfate. It could be possible that these enriched cultures were able to use both sulfate and thiosulfate as electron acceptors. In parallel, not only NiOx could use nitrite, but the microorganisms of the sulfur cycle as well. NiOx could be present, but presumably they were overgrown by SRP in the enrichments.

The last groups of enrichments with the same DGGE profiles were iron reducers and acidophilic sulfuric acid produces, both thermo– and mesophiles. The chemolithoautotrophic bacterium *Acidithiobacillus ferrooxidans* is able to perform aerobic respiration with H_2, iron or sulfur as electron donors. However, it has also been shown that this bacterium can grow on H_2/Fe^{3+}, H_2/S^0, or S^0/Fe^{3+} under anaerobic conditions (Brock and Gustafson, 1976; Ohmura et al., 2002; Pronk and Johnson, 1992; Pronk et al., 1992). Anaerobic respiration using Fe^{3+} or S^0 as an electron acceptor and H_2 or S^0 as an electron donor served as a primary energy source of the bacterium. The potential for dissimilatory ferric iron reduction in acidophilic heterotrophic bacteria was also reported (Coupland and Johnson, 2008).

Finally, the attention was also paid to NR–SOB cultures, as these microorganisms have high potential for reservoir souring control. It was reported that the addition of nitrate and an NR–SOB culture dominated by *Thiomicrospira* sp. CVO to a growing SRP consortium inhibited the production of sulfide by this consortium immediately (Nemati et al., 2001). This was followed by oxidation and removal of the present sulfide. For that purpose the same medium was used to enrich these cultures, however in this study none of these microorganisms were enriched.

5. CONCLUSIONS

The most aggressive biocorrosion phenomenon takes place in the presence of microbial consortia, in which various physiological types of organisms interact in complex ways within biofilms. The list of specific microorganisms responsible for MIC is constantly growing and the detection techniques improve. Thus new mechanisms are postulated (Kan et al., 2011). However, some groups of bacteria are consistently identified as causative MIC organisms. These organisms known to influence corrosion are physiologically diverse and have frequently been grouped by either a common electron acceptor or an energy source that is linked to the resulting corrosion.

The current study was consistent with these reports. Observed populations were extremely diverse, with a high ability of adaptation and resistance to the dynamically varying environmental conditions. Furthermore, a single type of microorganism can simultaneously affect corrosion via several mechanisms and possible candidates were shown here. The ability of microorganisms to colonise the surface is very strong, and as shown it may appear within few days. This should be taken into account while planning MIC mitigation activities, as these have to face many defence mechanisms developed by synergistic consortium. In recent years, characterising the physiological properties of microbes isolated from corroding sites has been a high priority. The logic is simple: a basic knowledge of the microbial species involved in microbial corrosion will provide the background for detection, monitoring and control of MIC.

6. REFERENCES

Al–Humam, A.A., Rizik, T.Y., Sunner, J.A., Beech, I.B., 2010. Effects of Nitrate on Bacterial Communities in an Oil Field Environment. Nace Int. Pap. No 10249.

Alaburda, J., Nishihara, L., 1998. [Presence of nitrogen compounds in well water]. Rev. Saúde Pública 32, 160–165.

Aljanabi, S.M., Martinez, I., 1997. Universal and rapid salt–extraction of high quality genomic DNA for PCR–based techniques. Nucleic Acids Res. 25, 4692–4693.

Beech, I.B., Gaylarde, C.C., 1999. Recent advances in the study of biocorrosion: an overview. Rev. Microbiol. 30, 117–190.

Berglin, M., Elwing, H., 2008. Erosion of a model rosin–based marine antifouling paint binder as studied with quartz crystal microbalance with dissipation monitoring (QCM–D) and ellipsometry. Prog. Org. Coatings 61, 83–88.

Brock, T.D., Gustafson, J., 1976. Ferric iron reduction by sulfur– and iron–oxidizing bacteria. Appl. Environ. Microbiol. 32, 567–571.

Bromfield, S., 1956. Oxidation of Manganese by soil Microorganisms. Aust. J. Biol. Sci. 9, 238–252.

Campaignolle, X., Caumette, P., Dabosi, F., Crolet, J.L., 1996. The Role of Thiosulfate on the Microbially Induced Pitting of Carbon Steel. Nace Int. Pap. No 96273.

Carlucci, A.F., Strickland, J.D.H., 1968. The isolation, purification and some kinetic studies of marine nitrifying bacteria. J. Exp. Mar. Biol. Ecol. 2, 156–166.

Cetin, D., Aksu, M.L., 2013. Corrosion behavior of low–alloy steel in the presence of Desulfovibrio caledoniensis. Mater. Corros. 64, 236–241.

Cord–Ruwisch, R., 1985. A quick method for the determination of dissolved and precipitated sulfides in cultures of sulfate–reducing bacteria. J. Microbiol. Methods 4, 33–36.

Coupland, K., Johnson, D.B., 2008. Evidence that the potential for dissimilatory ferric iron reduction is widespread among acidophilic heterotrophic bacteria. Fems Microbiol. Lett. 279, 30–35.

Crolet, J.L., Magot, M.F., 1996. Non–Srb Sulfidogenic Bacteria in Oilfield Production Facilities. Mater. Perform. 35.

Davey, M.E., O'toole, G.A., 2000. Microbial biofilms: from ecology to molecular genetics. Microbiol. Mol. Biol. Rev. Mmbr 64, 847–867.

Dawood, Brözel, 1998. Corrosion–enhancing potential of Shewanella putrefaciens isolated from industrial cooling waters. J. Appl. Microbiol. 84, 929–936.

Dexter, S.C., 2003. Microbiologically influenced corrosion, in: Corrosion: Fundamentals, Testing and Protection. Metals Park, OH: ASM Internatioinal, pp. 1–400.

Dowling, N.J.E., Mittelman, M.W., White, D.C., 1991. The role of consortia in micobially influenced corrosion, in: Mixed Cultures in Biotechnology. McGraw Hill, New York, pp. 341–372.

Grabowski, A., Nercessian, O., Fayolle, F., Blanchet, D., Jeanthon, C., 2005. Microbial diversity in production waters of a low–temperature biodegraded oil reservoir. Fems Microbiol. Ecol. 54, 427–443.

Greene, E.A., Hubert, C., Nemati, M., Jenneman, G.E., Voordouw, G., 2003. Nitrite reductase activity of sulphate–reducing bacteria prevents their inhibition by nitrate–reducing, sulphide–oxidizing bacteria. Environ. Microbiol. 5, 607–617.

Hanert, H.H., 1992. The genus Gallionella, in: The Prokaryotes. 2nd Edition. Springer Verlag Berlin, New York, pp. 4082–4088.

Henry, S., Baudoin, E., López–Gutiérrez, J.C., Martin–Laurent, F., Brauman, A., Philippot, L., 2004. Quantification of denitrifying bacteria in soils by nirK gene targeted real–time PCR. J. Microbiol. Methods 59, 327–335.

Kan, J., Chellamuthu, P., Obraztsova, A., Moore, J.E., Nealson, K.H., 2011. Diverse bacterial groups are associated with corrosive lesions at a Granite Mountain Record Vault (GMRV). J. Appl. Microbiol. 111, 329–337.

Krümmel, A., Harms, H., 1982. Effect of organic matter on growth and cell yield of ammonia–oxidizing bacteria. Arch. Microbiol. 133, 50–54.

Kucera, S., Wolfe, R.S., 1957. A SELECTIVE ENRICHMENT METHOD FOR GALLIONELLA FERRUGINEA1. J. Bacteriol. 74, 344–349.

Lalucat, J., Bennasar, A., Bosch, R., García–Valdés, E., Palleroni, N.J., 2006. Biology of Pseudomonas stutzeri. Microbiol. Mol. Biol. Rev. 70, 510–547.

Lane, D.J., 1991. 16S／23S rRNA sequencing, in: Nucleic Acid Techniques in Bacterial Systematics. John Wiley & Sons, New York, pp. 115–175.

Little, B.J., Lee, J.S., 2007. Microbiologically Influenced Corrosion. John Wiley & Sons.

Liu, C., Wu, Y., Li, L., Ma, Y., Shao, Z., 2007. Thalassospira xiamenensis sp. nov. and Thalassospira profundimaris sp. nov. Int. J. Syst. Evol. Microbiol. 57, 316–320.

López–López, A., Pujalte, M.J., Benlloch, S., Mata–Roig, M., Rosselló–Mora, R., Garay, E., Rodríguez–Valera, F., 2002. Thalassospira lucentensis gen. nov., sp. nov., a new marine member of the alpha–Proteobacteria. Int. J. Syst. Evol. Microbiol. 52, 1277–1283.

Lovley, D.R., Phillips, E.J.P., 1988. Novel Mode of Microbial Energy Metabolism: Organic Carbon Oxidation Coupled to Dissimilatory Reduction of Iron or Manganese. Appl. Environ. Microbiol. 54, 1472–1480.

Lovley, D.R., Roden, E.E., Phillips, E.J.., Woodward, J.., 1993. Enzymatic iron and uranium reduction by sulfate–reducing bacteria. Mar. Geol. 113, 41–53.

Loy, A., Küsel, K., Lehner, A., Drake, H.L., Wagner, M., 2004. Microarray and functional gene analyses of sulfate–reducing prokaryotes in low–sulfate, acidic fens reveal cooccurrence of recognized genera and novel lineages. Appl. Environ. Microbiol. 70, 6998–7009.

Luther III, G.W., Sundby, B., Lewis, B.L., Brendel, P.J., Silverberg, N., 1997. Interactions of manganese with the nitrogen cycle: Alternative pathways to dinitrogen. Geochim. Cosmochim. Acta 61, 4043–4052.

Lutterbach, M.T.S., Contador, L.S., Chaves Oliveira, A.L., De França IV, F.P., Pimenta, G.D.., Galvão, M.M., 2009. Iron Sulfide Production by Shewanella Strain Isolated from Black Powder. Nace Int. Pap. No 09391.

Mackintosh, M.E., 1978. Nitrogen Fixation by Thiobacillus ferrooxidans. J. Gen. Microbiol. 105, 215–218.

Magot, M., Ravot, G., Campaignolle, X., Ollivier, B., Patel, B.K.C., Fardeau, M.–L., Thomas, P., Crolet, J.–L., Garcia, J.–L., 1997. Dethiosulfovibrio peptidovorans gen. nov., sp. nov., a New Anaerobic, Slightly Halophilic, Thiosulfate–Reducing Bacterium from Corroding Offshore Oil Wells. Int. J. Syst. Bacteriol. 47, 818–824.

Matin, A., Rittenberg, S.C., 1971. Enzymes of Carbohydrate Metabolism in Thiobacillus species. J. Bacteriol. 107, 179–186.

Maxwell, S., Devine, C., Rooney, F., 2004. Monitoring and Control of Bacterial Biofilms in Oilfield Water Handling Systems. Nace Int. Papaer No 04752.

Moura, I., Bursakov, S., Costa, C., Moura, J.J.., 1997. Nitrate and Nitrite Utilization in Sulfate–Reducing Bacteria. Anaerobe 3, 279–290.

Mulder, E.G., Veen, W.L. van, 1963. Investigations on theSphaerotilus–Leptothrix group. Antonie Van Leeuwenhoek 29, 121–153.

Naganuma, T., Sato, M., Hoshii, D., Amano–Murakami, Y., Iwatsuki, T., Mandernack, K., 2006. Isolation and Characterization of Pseudomonas Strains Capable of Fe(III) Reduction with Reference to Redox Response Regulator Genes. Geomicrobiol. J. 23, 145–155.

Nemati, M., Jenneman, G.E., Voordouw, G., 2001. Mechanistic study of microbial control of hydrogen sulfide production in oil reservoirs. Biotechnol. Bioeng. 74, 424–434.

Ohmura, N., Sasaki, K., Matsumoto, N., Saiki, H., 2002. Anaerobic Respiration Using Fe3+, S0, and H2 in the Chemolithoautotrophic Bacterium Acidithiobacillus ferrooxidans. J. Bacteriol. 184, 2081–2087.

Oliver, J.D., 2005. The viable but nonculturable state in bacteria. J. Microbiol. Seoul Korea 43 Spec No, 93–100.

Postgate, J.R.F., 1979. The sulphate–reducing bacteria. CUP Archive.

Pronk, J.T., Bruyn, J.C. de, Bos, P., Kuenen, J.G., 1992. Anaerobic Growth of Thiobacillus ferrooxidans. Appl. Environ. Microbiol. 58, 2227–2230.

Pronk, J.T., Johnson, D.B., 1992. Oxidation and Reduction of Iron by Acidophilic Bacteria. Geomicrobiol. J. 10, 153–171.

Pyzola, S., 2013. Nitrate reduction coupled to iron (II) and manganese (II) oxidation in an agricultural soil. Theses Diss.—Plant Soil Sci.

Sanders, P.F., Hamilton, W.A., 1986. Biological and Corrosion Activities of Sulphate–Reducing Bacteria in Industrial Process Plant. National Association of Corrosion Engineers, Houston, TX, p. 47.

Schädler, S., Burkhardt, C., Hegler, F., Straub, K.L., Miot, J., Benzerara, K., Kappler, A., 2009. Formation of Cell–Iron–Mineral Aggregates by Phototrophic and Nitrate–Reducing Anaerobic Fe(II)–Oxidizing Bacteria. Geomicrobiol. J. 26, 93–103.

Schäfer, H., Muyzer, G., 2001. Denaturing gradient gel electrophoresis in marine microbial ecology, in: Methods in Microbiology. Elsevier, pp. 425–468.

Schippers, A., Hallmann, R., Wentzien, S., Sand, W., 1995. Microbial Diversity in Uranium Mine Waste Heaps. Appl. Environ. Microbiol. 61, 2930–2935.

Straub, K.L., Benz, M., Schink, B., Widdel, F., 1996. Anaerobic, nitrate–dependent microbial oxidation of ferrous iron. Appl. Environ. Microbiol. 62, 1458–1460.

Straub, K.L., Buchholz–Cleven, B.E.E., 1998. Enumeration and Detection of Anaerobic Ferrous Iron–Oxidizing, Nitrate–Reducing Bacteria from Diverse European Sediments. Appl. Environ. Microbiol. 64, 4846–4856.

Struchtemeyer, C.G., Elshahed, M.S., Duncan, K.E., McInerney, M.J., 2005. Evidence for aceticlastic methanogenesis in the presence of sulfate in a gas condensate–contaminated aquifer. Appl. Environ. Microbiol. 71, 5348–5353.

Sun, B., Cole, J.R., Sanford, R.A., Tiedje, J.M., 2000. Isolation and Characterization of Desulfovibrio dechloracetivorans sp. nov., a Marine Dechlorinating Bacterium Growing by Coupling the Oxidation of Acetate to the Reductive Dechlorination of 2–Chlorophenol. Appl. Environ. Microbiol. 66, 2408–2413.

Tebo, B.M., Obraztsova, A.Y., 1998. Sulfate–reducing bacterium grows with Cr(VI), U(VI), Mn(IV), and Fe(III) as electron acceptors. Fems Microbiol. Lett. 162, 193–198.

Todorova, S.G., Costello, A.M., 2006. Design of Shewanella–specific 16S rRNA primers and application to analysis of Shewanella in a minerotrophic wetland. Environ. Microbiol. 8, 426–432.

Tyler, P.A., Marshall, K.C., 1967. Form and function in manganese–oxidizing bacteria. Arch. Fuer Mikrobiol. 56, 344–353.

Weelink, S.A.B., van Doesburg, W., Saia, F.T., Rijpstra, W.I.C., Röling, W.F.M., Smidt, H., Stams, A.J.M., 2009. A strictly anaerobic betaproteobacterium Georgfuchsia toluolica gen. nov., sp. nov. degrades aromatic compounds with Fe(III), Mn(IV) or nitrate as an electron acceptor. Fems Microbiol. Ecol. 70, 575–585.

CHAPTER IV: CHARACTERISATION OF THE CORROSIVE BEHAVIOUR OF *D. ALASKENSIS* ON CARBON STEEL

Sulfate Reducing Prokaryotes (SRP) have been associated with the steel deterioration by building heterogeneous biofilms, capable of accelerating corrosion processes. In this study, biofilm development of *Desulfovibrio alaskensis* AL1 was investigated. A correlation was made between the electrochemical response of a carbon steel surface to the presence of SRP and their metabolic activity. In the exponential growth phase, sulfide concentration reached its maximum of about 10 mM. This phenomenon was assigned to the simultaneous appearance of a corrosion potential (E_{corr}) peak of –720 mV. Subsequently, during the intensive biofilm formation and development another E_{corr} peak (–710 mV) occurred. A decrease in the potential was registered during the biofilm maturation and kept stable, being 25 mV lower than in the control. While carbon steel was protected from the SRP attachment but exposed to their metabolic products, only one potential maximum (–730 mV) was recorded. E_{corr} variations coincided with sulfide concentration changes and remained 120 mV lower *vs*. the control. Weight loss examinations revealed lower corrosion rates compared to the control, which did not exceed 0.05 mmpy. Confocal laser scanning studies microscopy suggested importance of extracellular proteins in *D. alaskensis* biofilm formation. The carbon steel surface after the exposure to the SRP biofilm or to its metabolic products was visualised, revealing the influence of attached microorganisms in the localised corrosion development.

1. INTRODUCTION

Marine environment is a highly corrosive and biologically active habitat. It became a touchstone for microbially induced corrosion (MIC) issues (Sanders and Stott, 1987). MIC depends on metal type (host location), nutrients present in the environment and groups of organisms found in the bulk. Microorganisms alter the conditions at the interface between the metal and the substratum, modifying electrochemical reactions, which are fundamental for corrosion processes (Beech, 2003). Being widely distributed in nature and industrial systems, including *inter alia* petroleum reservoirs and oil production facilities, SRP became well recognised as probably one of the most influent members of microbial communities associated with MIC of metals.

SRP are a group of phylogenetically diverse microorganisms of several genera, which carry out dissimilatory reduction of sulfur compounds such as sulfate, sulfite, thiosulfate and/or sulfur to sulfide (Bak and Cypionka, 1987; Lovley and Phillips, 1994). They are also sources of serious health and safety hazards as well as environmental risks (Odom et al., 1993). SRP can be easily introduced into water injection and oil production systems and become active in areas of low oxygen concentration (Edyvean, 1987). Most genera are described as strictly anaerobic, although some are able to tolerate oxygen (Cypionka et al., 1985; Hardy and Hamilton, 1981). The main carbon sources for SRP are lactate, pyruvate, and malate, which are oxidised either fully to carbon dioxide or incompletely to acetate and CO_2 (Barton, 1995; Postgate, 1984; Rabus et al., 2006). During their growth, SRP produce large amounts of hydrogen sulfide, which contributes to the maintenance of anaerobic conditions.

Comprehensive studies of SRP–driven corrosion described several mechanisms by which they can influence this process. Direct mechanisms involve certain microbial metabolic reactions or their products in the electrochemical corrosion process (Hamilton, 2003). For example removal of hydrogen at cathodic sites, employing hydrogenases, facilitates cathodic depolarisation, leading to the increase in corrosion rates (Bryant et al., 1991). Anodic reactions can be stimulated by microbially produced sulfide. Iron sulfides formed, also contribute to the corrosion, decreasing hydrogen overvoltage and/or adsorbing the cathodically produced hydrogen (Lee et al., 1995; Lewandowski et al., 1997). Other direct mechanisms

include sulfide and hydrogen induced cracking and volatile phosphorus compounds production (Beech and Gaylarde, 1999). Indirect influence of SRP on corrosion is related with the bacterial tendency to attach to the surfaces and to form biofilms, in this way altering the physico–chemical environment, where the biocorrosion reactions take place.

SRP are able to grow in different physicochemical conditions, thus inhabiting the most extreme environments of our planet such as the cold, hot, saline and/or alkaline ecosystems. The menace arising from their ubiquity became the motivation to investigate in–depth biofilm formation of these microorganisms with particular attention to the biocorrosion problems within the oil and gas industry. In particular the activity of SRP has considerable influence on various industrial processes, resulting in extensive and costly damages for equipment, additional production losses due to the shutting down of the transport and production units for several weeks and decrease in petroleum quality. *D. alaskensis* AL1, isolated from soured oil wells, has been chosen as a model for SRP corrosive activity on carbon steel surfaces, material widely used in the industry. Application of a multidisciplinary approach of electrochemical, analytical, biochemical and advanced microscopic tools has a potential to deeper understanding of the biofilm formation mechanisms, which are crucial in MIC processes.

2. MATERIALS AND METHODS

2.1. Microorganisms and growth media

In this study, the marine bacterium *Desulfovibrio alaskensis* AL1, isolated from a soured oil well in Purdu Bay, Alaska (Feio et al., 2004) was used. It was anaerobically grown in VMN sulfate growth medium (Zinkevich and Beech, 2000). Furthermore sodium chloride concentration in the medium was increased up to 0.34 M as required for the optimal growth of this marine strain. Medium sterilisation was done by autoclaving at 121°C for 30 min. All experiments were performed at 30°C, with a starting pH of 7.4 and 5% (v/v) inoculum (initial cell number of 10^7 cells / ml) from *D. alaskensis* AL1 culture in exponential growth phase.

2.2. Specimens preparation

Working electrodes (WE) used for electrochemical studies were prepared from 2 cm diameter St37–2 (S235–JR) carbon steel rods (3.14 cm^2 active exposed surface). Its chemical composition is shown in the **TABLE 4.1**. WE was polished up to grit 600 and sterilised by UV light (253.7 nm) in an Airflow workstation for 1 h, directly before being introduced into the electrochemical reactor. Coupons for microscopic surveys and weight loss experiments were from the same type of carbon steel, prepared equally. For these experiments St 37–2 coupons were of the 10 x 20 x 2 mm size.

TABLE 4.1. CHEMICAL COMPOSITION IN % OF ST 37–2 (S235–JR) CARBON STEEL.

Element	*C*	*Mn*	*N*	*S*	*P*
Mass percentage	max. 0.2	max. 1.4	max. 0.009	max. 0.045	max. 0.045

2.3. Microbial activity and corrosion behaviour monitoring

Electrochemical tests were performed in a 1L single compartment MultiPort™ Corrosion Cell Kit (Gamry®), previously sterilised by autoclaving (121°C, 30 min) prior to use. The medium was purged with sterile filtered humidified argon for 1 h prior to the experiment. To maintain strict anoxic conditions and avoid contamination, a permanent flow of sterile humidified argon was kept in the headspace of the cell, ensuring a positive pressure during all tests. Electrochemical experiments were performed in a three–electrode configuration using an Autolab 30® potentiostat / galvanostat and data acquisition was performed using the GPES® software. After inoculation with *D. alaskensis* AL1, data were acquired in 90 s time intervals. Monitoring of corrosion potential in function of time (E_{corr}) was done for 6 days. Additionally E_{corr} was measured in two conditions: (a) with direct exposure to the microbial environment and (b) with an isolated WE (wrapped with a cellulose acetate membrane of 0.2 µm pore size). The latter prevented direct cell–surface interactions. This setup allowed us to investigate the influence of only microbial metabolic products and secreted EPS on the carbon steel surface. Graphite served as a counter electrode (CE) and Saturated Calomel Electrode (SCE) as a reference (RE),

which was in contact to the system through a bridge tube filled with the same electrolyte as in the experiment.

In parallel, bacterial growth was monitored by light absorbance (optical density at 600 nm, OD_{600}) with a Shimadzu® UV–VIS Spectrophotometer model UV–1800 and data were complemented with pH measurements. Lactate and sulfate consumption were determined with DIONEX® ICS 3000 HPLC with Ionpac AS11 HC and AG11 HC pre–column. Sulfide production was determined by a colorimetric assay as described elsewhere (Cline, 1969). For OD_{600} as well as sulfate and lactate consumption samples were taken in 4 h intervals until 32 h and afterwards starting from 48 h daily; pH from the beginning of the survey was measured each 24 h. In case of samples used for sulfide determination sampling was done daily during the whole period of the survey. Before the determination of sulfide concentration, each sample was mixed in the ratio 1:1 (v/v) with 2 M zinc acetate immediately after its collection, in order to precipitate it and avoid further loss.

2.4. Weight loss tests and corrosion rate determination

Carbon steel coupons prepared as described above (Section 2.2. Specimens preparation) were used for the weight loss measurements after 6 days of exposure to SRP. As in the electrochemical tests, coupons were either in direct contact with microorganisms or covered with the 0.2 µm membrane. Sterile VMN sulfate growth medium was used as negative control. After removing the coupons from the cultivation media, the removal of corrosion products was performed according to the ASTM G1–03 (2011) standard (G01 Committee, 2011). Briefly, the cleaning procedure was done with of 0.25 M hexamethylentetramine in 5.8 M hydrochloric acid for 5 min, followed by rinsing with sterile deionised water. The entire weight loss procedure was done anaerobically with all solutions flushed with nitrogen prior to use.

The corrosion rate was calculated using the formula below:

$$Corrosion\ rate[mmpy] = 0.465\frac{X}{t \cdot A} \quad (4.1)$$

where:

0.465 –factor accounting for the dimensional analysis and the density of carbon steel

X –difference between initial and final weight after cleaning in milligrams (weight loss)

t –exposure time in days

A –total area of the coupon in cm^2

2.5. Surface analysis

In order to reveal the role of *D. alaskensis* AL1 and their metabolic products in localised corrosion, coupons of carbon steel St37–2 were incubated anaerobically for 6 days under the following conditions: (a) in VMN medium, inoculated with 5% (v/v) *D. alaskensis* AL1, (b) under the same conditions but covered with the 0.2 µm pore size membrane, (c) in VMN medium containing EPS previously extracted from *D. alaskensis* AL1 culture with Dowex® Marathon® C (Chapter V). Extracted EPS was twice concentrated and mixed in 1:1 (v/v) ratio with the growth medium, (d) in sterile VMN medium. After incubation, corrosion products were removed as described above (Section 2.4), rinsed with deionised water and dried with hot air. Surface analyses were performed with a NanoWizard® II Atomic Force Microscope, AFM (JPK Instruments, Germany). A silicon cantilever MicroMash® CSC37/no Al, with typical spring constant 0.3 N/m and resonance frequency 21 kHz was used for the surface imaging. Scanning was performed in contact mode, with a set–point of 1.00 V and line–rate of 1.000 Hz. Images were acquired and processed with JPK SPM v.3 and JPK Image processing v.3 softwares, respectively.

2.6. Biofilm formation experiments and staining procedures

Confocal Laser Scanning Microscope (CLSM) was applied for the biofilm formation studies on the carbon steel surface. Coupons were incubated with SRP for 1, 2, 4, 8, 12, 24, 72 and 144 h. In order to exclude the influence of the medium compounds, each coupon was rinsed with 4 ml of sterile filtered deionised water before staining. In order to visualise proteins, sugars (possessing α–D–mannosyl and α–D–glucosyl groups) and DNA, respectively, samples were stained sequentially with 2.6 mM fluorescein isothiocyanate (FITC) for 30 min, 50µg/ml tetramethyl rhodamine isothiocyanate (TRITC) – conjugated lectin Concanavalin A (Con A) for 45 min and with 0.36 mM DAPI for 15 min. Each staining step was completed by rinsing the coupon with deionised water. Afterwards a drop of Citifluor® AF–2, an anti–fading agent was applied. All staining procedures were performed avoiding the direct sunlight.

CLSM was performed using LSM 510 Carl Zeiss® Jena laser scanning microscope. The objective used for the imaging was Carl Zeiss® EC Plan–Neofluar 100x/1.30 Oil Pol. Scanning was performed in multichannel mode. DAPI was excited at the wavelengths of 364 nm and 351 nm with the main dichroic mirror HFT UV 375 and band pass filter BP 385–470. FITC was excited at the wavelength of 488 nm with HFT 488 mirror and BP 505–530 filter. TRITC excitation was performed at 543 nm and for observation of the light reflected from the surface a wavelength of 633 nm was applied. Here the main dichroic mirrors HFT 488/543 and HFT UV/488/568/633 and high pass filter LP 560 were used. In case of TRITC, a secondary dichroic beam, splitter NFT 570 was applied to reduce the background noise from the metal surface. The pinhole during the scanning was adjusted in the way to obtain similar optical slice thickness. For three–dimensional (3D) images, Z–scanning with an interval of 0.3 µm was performed. The software used to acquire and process the images was LSM 510 Release 3.2 (Zeiss®).

3. RESULTS

3.1. Microbial activity and corrosion behaviour monitoring

D. alaskensis AL1 was used to monitor the corrosive behaviour of SRP in contact with the carbon steel and to correlate it with the bacterial metabolic activity. Changes in pH, lactate and sulfate consumption with parallel sulfide production together with Ecorr were monitored for 144 h (**FIG. 4.1**).

An intensive lactate and sulfate concentration depletion occurred within the first 24 h of SRP growth. Afterwards, a lack of their utilisation was recorded (**FIG. 4.1B**). While the biomass production took place, the energy winning from the oxidation processes was observed, and stopped when the bacterial growth reached its plateau. Furthermore, sulfide concentration reached its maximum within the first 24 h and subsequently started to diminish until near zero. In parallel a pH increase was observed (**FIG. 4.1A**).

Simultaneous electrochemical studies with carbon steel either unprotected or covered with a 0.2 µm membrane were carried out (**FIG. 4.1C**). Two potential ennoblement maxima were observed in absence of the membrane around 24 and 48 h, reaching the value of approx. –720 and –710 mV (*vs*. SCE), respectively. After this time the bacterial activity started to decrease, correlating with a decrease in the potential. Additionally, the biotically driven augmentation observed here was comparable to the negative control. In case of E_{corr} monitoring with the WE covered by the membrane, the potential behaviour was different. Its pattern correlated to the sulfide concentration changes. After reaching a maximal potential of –730 mV (*vs*. SCE) at 24 h, strong decrease was observed.

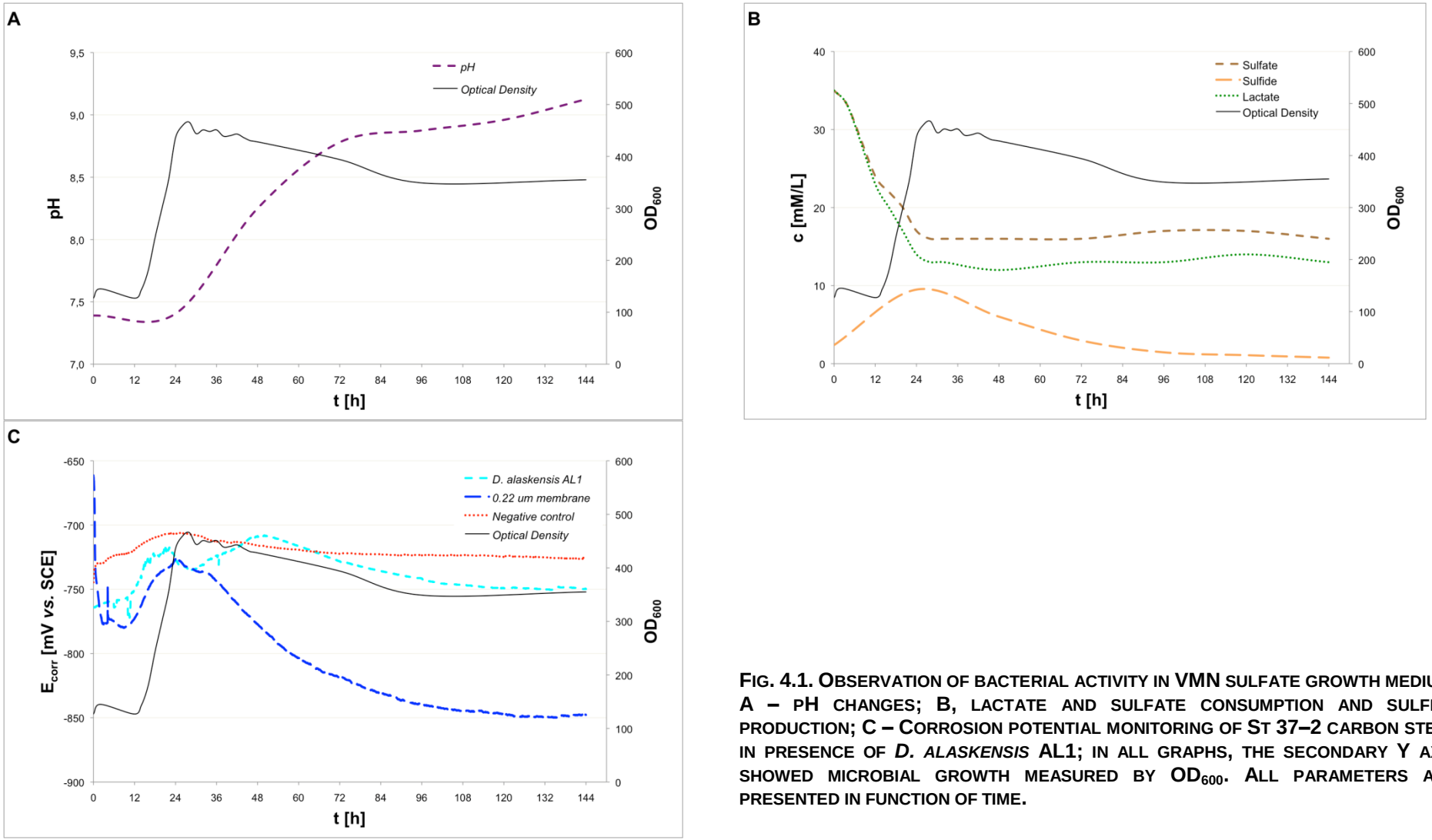

FIG. 4.1. OBSERVATION OF BACTERIAL ACTIVITY IN VMN SULFATE GROWTH MEDIUM. A – PH CHANGES; B, LACTATE AND SULFATE CONSUMPTION AND SULFIDE PRODUCTION; C – CORROSION POTENTIAL MONITORING OF ST 37–2 CARBON STEEL IN PRESENCE OF *D. ALASKENSIS* AL1; IN ALL GRAPHS, THE SECONDARY Y AXIS SHOWED MICROBIAL GROWTH MEASURED BY OD_{600}. ALL PARAMETERS ARE PRESENTED IN FUNCTION OF TIME.

In both, electrochemical measurements and weight loss experiments it was observed, that the SRP biofilm was slightly more aggressive than just its metabolic products. Calculated corrosion rates were equal to 0.048 and 0.042 mmpy for biofilm and membrane covered coupons, respectively (**FIG. 4.2**). The negative control provoked a slightly higher mass decrease of carbon steel in comparison to the former conditions.

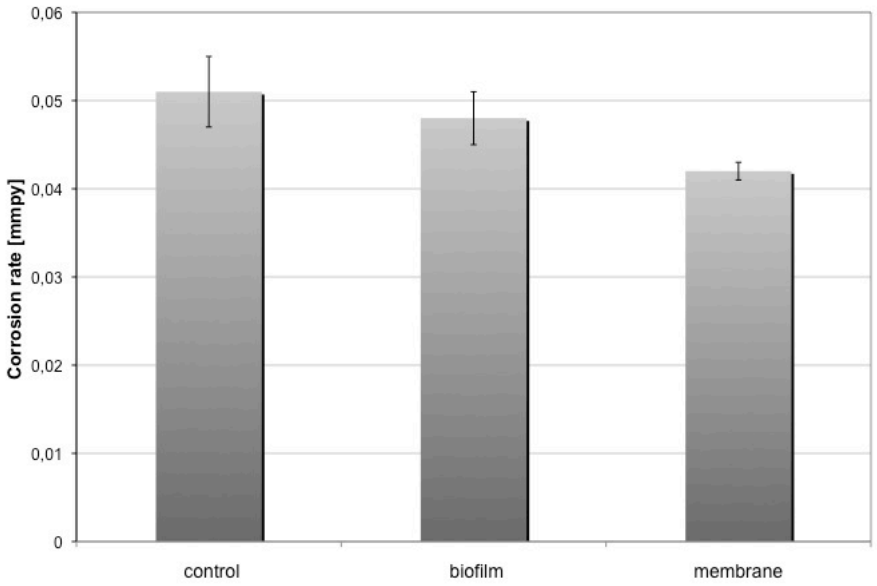

FIG. 4.2. CORROSION RATES OF ST37–2 CARBON STEEL AFTER 6 DAYS INCUBATION WITH *D. ALASKENSIS*.

3.2. Surface analysis

AFM examination of St 37–2 carbon steel coupons previously exposed to SRP or their metabolic products revealed a difference of surface effects observed under the conditions tested (**FIG. 4.3**). Biofilm development (**FIG. 4.3A**) on the surface resulted in pitting formation, in agreement with other reports (Miranda et al., 2006; Padilla–Viveros et al., 2006; Rao et al., 2000). Another distinguishing feature of the surface exposed to the direct impact of attached microorganisms was a fine preservation of the polishing traces compared to the control incubated in the sterile medium. When the metal coupon was protected from bacterial colonisation by the membrane (**FIG. 4.3B**), AFM analyses also showed an increase in surface roughness. Formation of precipitates was also observed, which were almost irremovable by the applied cleaning procedures. Measured pit depths were in the range from 1.3 ± 0.2 µm to 1.4 ± 0.3 µm in the coupons directly exposed to *D. alaskensis* and covered with the

membrane, respectively. No damages were found on the surface of the coupons exposed to the medium with addition of EPS (**FIG. 4.3C**). In the latter case, the initial surface structure was preserved better as compared to the control (**FIG. 4.3D**).

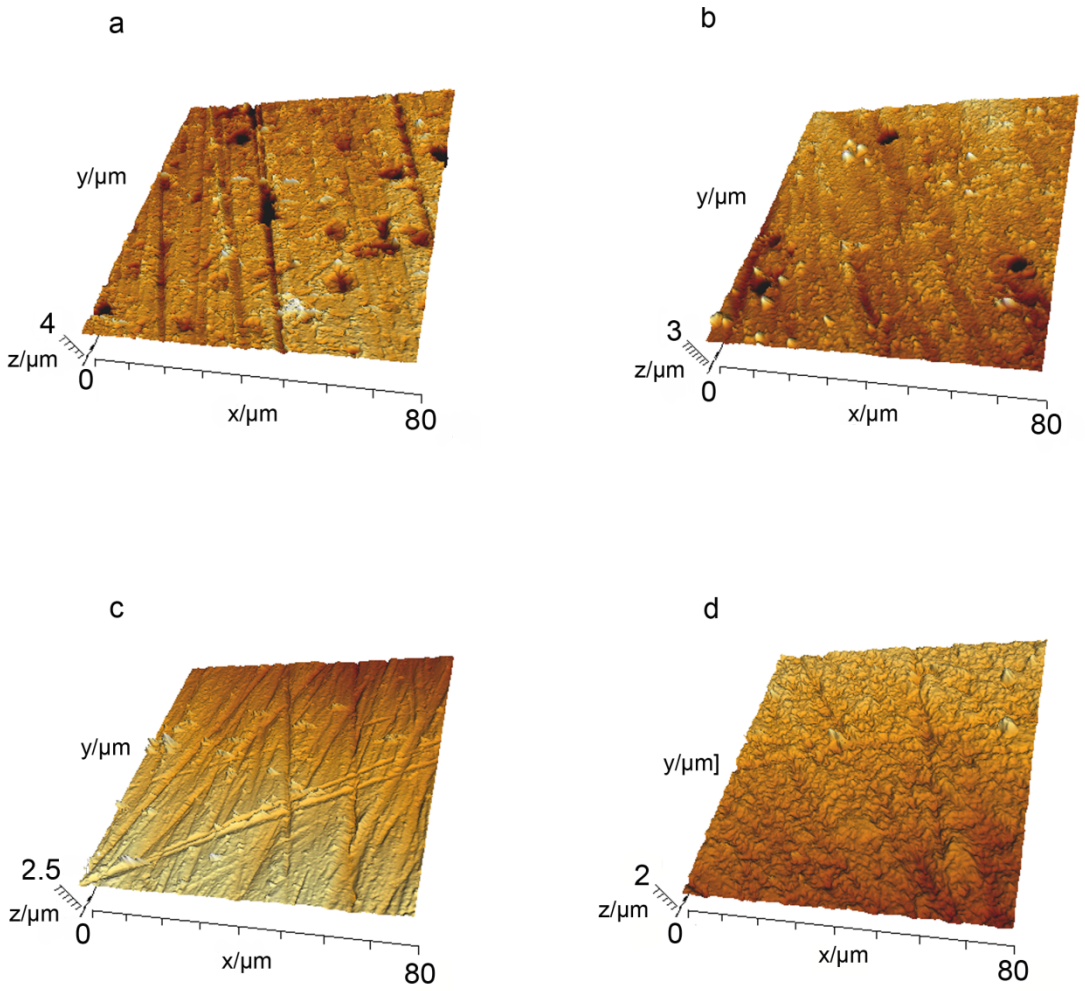

FIG. 4.3. VISUALISATION OF A STEEL SURFACE AFTER 6 DAYS INCUBATION IN VARIOUS CONDITIONS (AFM): (A) D. ALASKENSIS IN VMN MEDIUM, (B) D. ALASKENSIS AL1 ISOLATED FROM THE SURFACE BY THE MEMBRANE WITH 0.2 MM PORE SIZE, (C) STERILE VMN MEDIUM ENRICHED WITH BACTERIAL EPS, (D) STERILE VMN MEDIUM.

3.3. Biofilm formation

CLSM observations of the coupons (**FIG. 4.4**) showed that irreversible attachment of *D. alaskensis* AL1 to the carbon steel surface occurred very rapidly. Extracellular proteins might be involved in this process, as protein signal was detected on the surface, although other EPS components may also contribute to the formation of the conditioning layer. Signal from TRITC–conjugated ConA, recognising α–D–mannosyl and α–D–glucosyl– containing sugars, appeared during the second hour of incubation and was merely associated with the cells. During this stage cells were still randomly distributed on the surface.

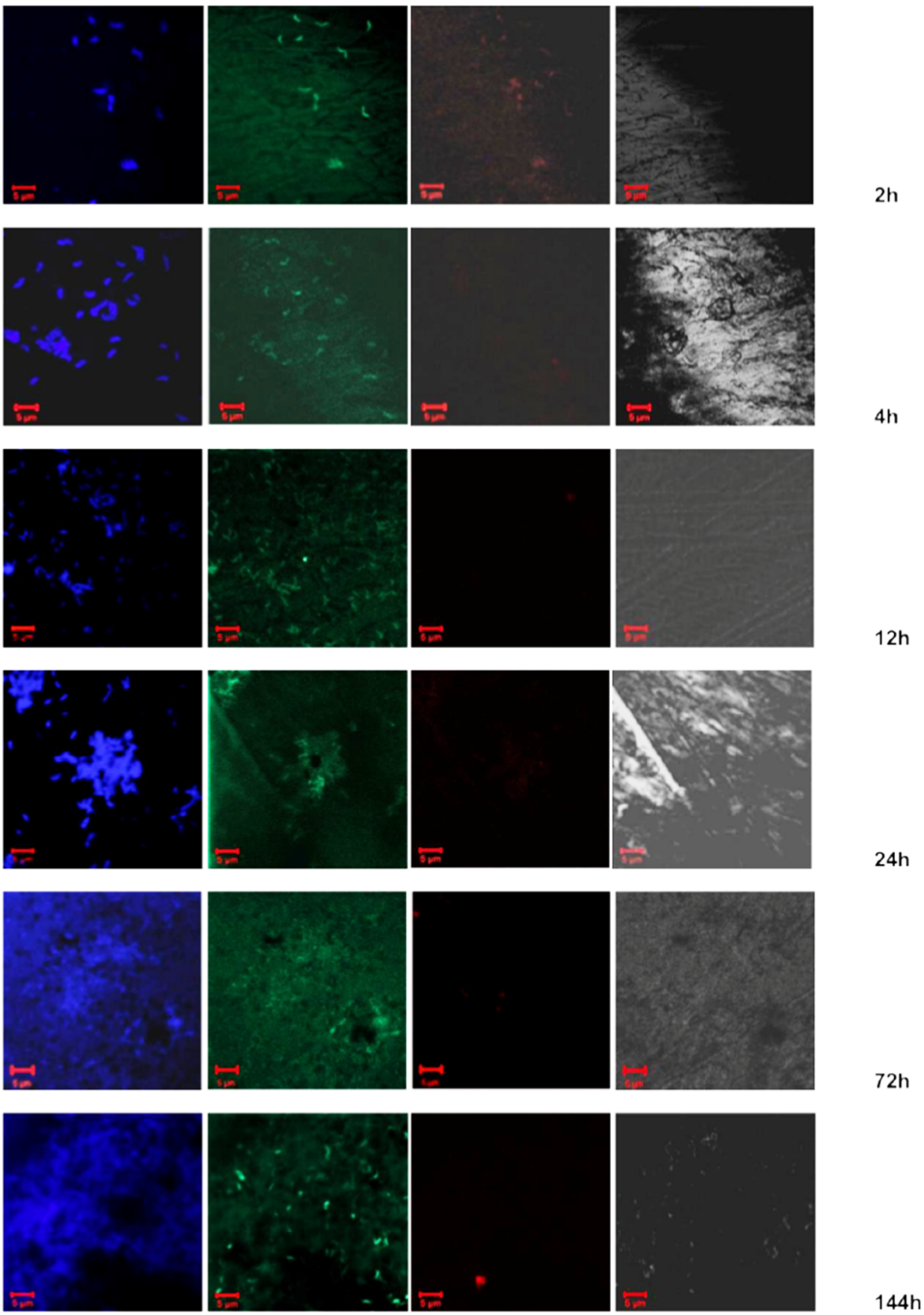

FIG. 4.4. BIOFILM FORMATION OF *D. ALASKENSIS* ON THE CARBON STEEL SURFACE; FROM LEFT: SIGNALS FROM CHANNELS SET FOR DAPI (BLUE), FITC, (GREEN), CONA–TRITC (RED) AND LIGHT SURFACE REFLECTION. SIZE BARS REPRESENT 5 µM.

After 4 h of incubation, cell aggregation became visible and continued to develop during the following hours. Clusters of cells tended to be associated to surface imperfections or polishing traces. This similar pattern of the cells distribution was observed up to 12 h, with the stepwise increase of area covered. At these times, the signal from TRITC–conjugated ConA was hardly detectable, indicating a low amount of α–D–mannosyl and α–D–glucosyl containing sugars being produced during this stage.

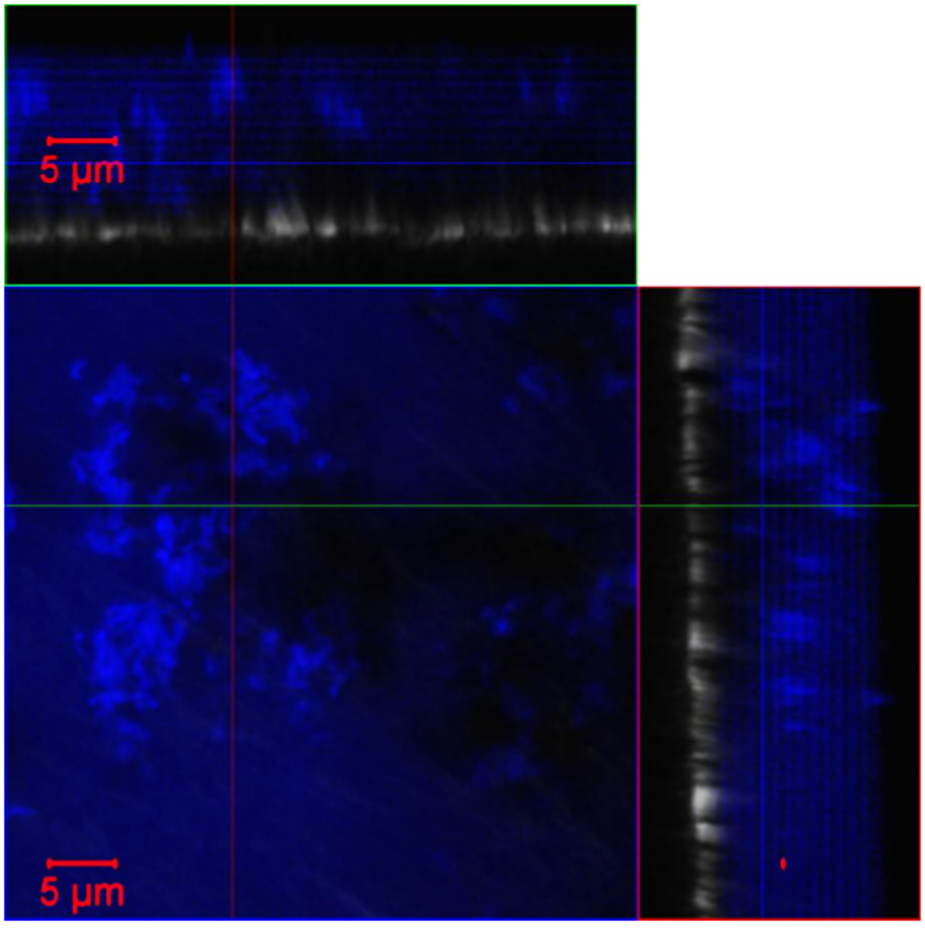

FIG. 4.5. DEPTH PROFILE OF 24 H OLD BIOFILM OF *D. ALASKENSIS* ON CARBON STEEL SURFACE: DAPI SIGNAL (BLUE) AND SURFACE REFLECTION (WHITE).

Biofilms grown for 24 h (**FIG. 4.4**) exhibited a structure with clearly distinguishable microcolonies, which seemed to be supported by proteins. 3D scanning (**FIG. 4.5**) revealed that the biofilm harboured not only big surface–associated clusters of cells, but also smaller aggregations observed in its upper part. These seemed to form an additional layer, suggesting that secondary colonisation and/or cell division had occurred.

After 72 h, a heterogeneous biofilm covered the whole surface. Non–colonised cavities were observed, corresponding to the regions of surface with poor light reflection, which probably was related to these areas, where pits were formed. Interestingly, the edges of these hypothetical pits were intensively colonised. At 144 h the heterogeneity of the biofilm continued to develop. The Con A signal remained weak during all the experimental time, where the biofilm formation was observed.

4. DISCUSSION

Detailed biofilm formation studies of *D. alaskensis* AL1 were performed in order to follow its microbial activity and to characterise its impact on the carbon steel. It was shown that the presence of these SRB had a destructive effect on the surface. Its presence provoked a potential ennoblement, especially within the first days of the growth. In parallel, the impact of metabolic products towards the surface, studied with coupons covered with a 0.22 µm membrane, although aggressive at the beginning, decreased significantly with time. In the latter conditions, sulfides might cause the primary damages. However, after the formation of an iron sulfide layer on the surface, it could be protective. As shown in the literature, both protective and detrimental effects of biogenic sulfide were possible to occur on the steel surface, depending on its concentration in the liquid phase (Lee et al., 1995; Ma et al., 2000). The increment of the potential registered within the first 24 h of surface exposure, might also be related to the sulfide production, which at this time reached its maximal concentration. Furthermore, the primary microbial attachment might additionally influence the corrosion potential variation. Within the next 24 h, a multilayer biofilm was formed. Biofilm growth and maturation combined with bridging between the cells and binding of the iron ions might enhance corrosion failures. Localised microbial attack on the surface finally presented smaller potential ennoblement than the general corrosion attack of marine growth medium. On the other hand local attack disrupted steel integrity, which consequently may become a bigger thread for the stability of the complex installations.

Observed corrosion failures caused by microbial activity appeared in a form of pits of various depths. Pitting corrosion is characterised by the formation of small anodes and corresponding large cathodes, which allow their further development in

the metal matrix**.** It is also considered to be a specific consequence of SRP activity on steel surfaces (Hamilton, 1985)**.** Typical pits caused by these microorganisms are opened and contain a black mixture of the corrosion products, mostly composed of iron sulfide. Among the mechanisms believed to contribute to the localised corrosion development, hydrogenases activity and local chemical gradients due to the biofilm porosity and heterogeneity are considered to be the most important (Castaneda and Benetton, 2008)**.**

Observed corrosion rates and potential increase reached low values, but even though St37–2 carbon steel underwent pitting corrosion in presence of *D. alaskensis* AL1. This behaviour was detected in case of direct contact with the surface as well as while isolating it by the membrane, which allowed only metabolic products to pass.

Thus, the microbial influence on the surface can take place even if the direct contact is restricted. As *D. alaskensis* AL1 EPS added to the medium did not exhibit corrosiveness, the most probable reason of pits formation on the membrane–covered surface was due to sulfide production by SRP. This suggestion coincides with the descriptions of enhanced pitting on carbon steel surface in the presence of a wide range of hydrogen sulfide concentrations (Gupta, 1981)**.** However, in this case damages of the metal protected from bacterial colonisation were less severe. This suggests that the corrosive effect of planktonic cells might be attenuated in flow conditions. Interestingly, addition of EPS to the medium resulted in minor changes of surface structure compared to the control. Protective effects of the biofilms were previously described (Videla and Herrera, 2009), but the role of EPS is still subjected to many discussions. An alternative of discovering and understanding EPS can be found in electrochemical investigations, which are presented in the Chapter VII.

5. CONCLUSIONS

The experimental approach reported in this study allowed to perform a detailed characterisation of microbial biofilms formed on the carbon steel surface. Exposition of the surface to microbial products secreted by *D. alaskensis* AL1 leads to the changes, which were strongly dependent on the sulfide concentration in the liquid phase. Microbial biofilm formation and maturation, being a very complex and dynamic process, as shown by microscopic techniques, became a bigger thread than just H_2S production and its presence in the bulk. The consequences of the biofilm

activity, in form of pitting with its further development, are detrimental for the integrity and stability of the material. This has to be especially considered while evaluating corrosion risks in the field conditions, as, according to presented results, localised corrosion may be the source of serious damages. The role of extracellular molecules requires more attention, as these are fundamental for the bacterial biofilm lifestyle. Proteins may initiate the primary attachment of *D. alaskensis* to the surface. Understanding of the biofilm formation processes and microbial activity may provide a necessary background for developing new strategies for biocorrosion prevention in the future.

6. REFERENCES

Bak, F., Cypionka, H., 1987. A novel type of energy metabolism involving fermentation of inorganic sulphur compounds. 1987 326, 891–892.

Barton, L.L., 1995. Sulfate–Reducing Bacteria. Springer.

Beech, I.B., 2003. Biocorrosion: Role of Sulfate Reducing Bacteria, in: Encyclopedia of Environmental Microbiology. John Wiley & Sons, Inc.

Beech, I.B., Cheung, C.W.S., 1995. Interactions of exopolymers produced by sulphate–reducing bacteria with metal ions. Int. Biodeterior. Biodegrad. 35, 59–72.

Beech, I.B., Gaylarde, C.C., 1999. Recent advances in the study of biocorrosion: an overview. Rev. Microbiol. 30, 117–190.

Beech, I.B., Sunner, J., 2004. Biocorrosion: towards understanding interactions between biofilms and metals. Curr. Opin. Biotechnol. 15, 181–186.

Beech, I.B., Sunner, J.A., 2007. Sulphate–reducing bacteria and their role in corrosion of ferrous materials, in: Sulphate–Reducing Bacteria. Cambridge University Press.

Beech, I.B., Sunner, J.A., Hiraoka, K., 2005. Microbe–surface interactions in biofouling and biocorrosion processes. Int. Microbiol. Off. J. Span. Soc. Microbiol. 8, 157–168.

Bradford, M.M., 1976. Rapid and sensitive method for the quantitation of microgram quantities of protein utilizing the principle of protein–dye binding. Anal. Biochem. 72, 248–254.

Bryant, R.D., Jansen, W., Boivin, J., Laishley, E.J., Costerton, J.W., 1991. Effect of Hydrogenase and Mixed Sulfate–Reducing Bacterial Populations on the Corrosion of Steel. Appl. Environ. Microbiol. 57, 2804–2809.

Busalmen, J.., Vázquez, M., de Sánchez, S.., 2002. New evidences on the catalase mechanism of microbial corrosion. Electrochimica Acta 47, 1857–1865.

Castaneda, H., Benetton, X.D., 2008. SRB–biofilm influence in active corrosion sites formed at the steel–electrolyte interface when exposed to artificial seawater conditions. Corros. Sci. 50, 1169–1183.

Cline, J.D., 1969. Spectrophotometric Determination of Hydrogen Sulfide in Natural Waters. Limnol. Ocean. 454 – 458.

Costerton, J.W., Cheng, K.J., Geesey, G.G., Ladd, T.I., Nickel, J.C., Dasgupta, M., Marrie, T.J., 1987. Bacterial biofilms in nature and disease. Annu. Rev. Microbiol. 41, 435–464.

Costerton, J.W., Lewandowski, Z., Caldwell, D.E., Korber, D.R., Lappin–Scott, H.M., 1995. Microbial biofilms. Annu. Rev. Microbiol. 49, 711–745.

Cypionka, H., Widdel, F., Pfennig, N., 1985. Survival of sulfate–reducing bacteria after oxygen stress, and growth in sulfate–free oxygen–sulfide gradients. Fems Microbiol. Lett. 31, 39–45.

Dunne, W.M., 2002. Bacterial Adhesion: Seen Any Good Biofilms Lately? Clin. Microbiol. Rev. 15, 155–166.

Edyvean, R.G.J., 1987. Biodeterioration problems of North Sea oil and gas production—A review. Int. Biodeterior. 23, 199–231.

Feio, M.J., Zinkevich, V., Beech, I.B., Llobet–Brossa, E., Eaton, P., Schmitt, J., Guezennec, J., 2004. Desulfovibrio alaskensis sp. nov., a sulphate–reducing bacterium from a soured oil reservoir.

Int. J. Syst. Evol. Microbiol. 54, 1747–1752.
Flemming, H.–C., Wingender, J., 2010. The biofilm matrix. Nat. Rev. Microbiol. 8, 623–633.
G01 Committee, 2011. Practice for Preparing, Cleaning, and Evaluating Corrosion Test Specimens. ASTM International.
Goodhew, C.F., Brown, K.R., Pettigrew, G.W., 1986. Haem staining in gels, a useful tool in the study of bacterial c–type cytochromes. Biochim. Biophys. Acta Bba – Bioenerg. 852, 288–294.
Gupta, D.V.S., 1981. Corrosion Behavior of 1040 Carbon Steel. Corrosion 37, 611–616.
Hamilton, W.A., 1985. Sulphate–reducing bacteria and anaerobic corrosion. Annu. Rev. Microbiol. 39, 195–217.
Hamilton, W.A., 2003. Microbially Influenced Corrosion as a Model System for the Study of Metal Microbe Interactions: A Unifying Electron Transfer Hypothesis. Biofouling 19, 65–76.
Hardy, J.A., Hamilton, W.A., 1981. The oxygen tolerance of sulfate–reducing bacteria isolated from North Sea waters. Curr. Microbiol. 6, 259–262.
Karatan, E., Watnick, P., 2009. Signals, regulatory networks, and materials that build and break bacterial biofilms. Microbiol. Mol. Biol. Rev. Mmbr 73, 310–347.
Lee, W., Lewandowski, Z., Nielsen, P.H., Hamilton, W.A., 1995. Role of sulfate-reducing bacteria in corrosion of mild steel: A review. Biofouling 8, 165–194.
Lewandowski, Z., W, D., W, L., 1997. Electrochemical interactions of biofilms with metal surfaces (36) 1, 295–302.
Lovley, D.R., Phillips, E.J.P., 1994. Novel Processes for Anaerobic Sulfate Production from Elemental Sulfur by Sulfate–Reducing Bacteria. Appl. Environ. Microbiol. 60, 2394–2399.
Ma, H., Cheng, X., Li, G., Chen, S., Quan, Z., Zhao, S., Niu, L., 2000. The influence of hydrogen sulfide on corrosion of iron under different conditions. Corros. Sci. 42, 1669–1683.
Miranda, E., Bethencourt, M., Botana, F.J., Cano, M.J., Sánchez–Amaya, J.M., Corzo, A., de Lomas, J.G., Fardeau, M.L., Ollivier, B., 2006. Biocorrosion of carbon steel alloys by an hydrogenotrophic sulfate–reducing bacterium Desulfovibrio capillatus isolated from a Mexican oil field separator. Corros. Sci. 48, 2417–2431.
Odom, J.M., Singleton, R., Jr, R.S., 1993. The Sulfate–reducing Bacteria: Contemporary Perspectives. Springer–Verlag Berlin and Heidelberg.
Padilla–Viveros, A., Garcia–Ochoa, E., Alazard, D., 2006. Comparative electrochemical noise study of the corrosion process of carbon steel by the sulfate–reducing bacterium Desulfovibrio alaskensis under nutritionally rich and oligotrophic culture conditions. Electrochimica Acta 51, 3841–3847.
Postgate, J.R., 1984. The sulphate–reducing bacteria, Cambridge University Press. ed.
Rabus, R., Hansen, T.A., Widdel, F., 2006. Dissimilatory sulfate– and sulfur–reducing prokaryotes, in: The Prokaryotes. pp. 659–768.
Rao, T.S., Sairam, T.N., Viswanathan, B., Nair, K.V.K., 2000. Carbon steel corrosion by iron oxidising and sulphate reducing bacteria in a freshwater cooling system. Corros. Sci. 42, 1417–1431.
Sand, W., Gehrke, T., 2006. Extracellular polymeric substances mediate bioleaching/biocorrosion via interfacial processes involving iron(III) ions and acidophilic bacteria. Res. Microbiol. 157, 49–56.
Sanders, P.F., Stott, J.F.D., 1987. Assessment, monitoring and control of microbiological corrosion hazards in offshore oil production systems.
Thomas, P.E., Ryan, D., Levin, W., 1976. An improved staining procedure for the detection of the peroxidase activity of cytochrome P–450 on sodium dodecyl sulfate polyacrylamide gels. Anal. Biochem. 75, 168–176.
Videla, H.A., Herrera, L.K., 2009. Understanding microbial inhibition of corrosion. A comprehensive overview. Int. Biodeterior. Biodegrad. 63, 896–900.
Zinkevich, Beech, 2000. Screening of sulfate–reducing bacteria in colonoscopy samples from healthy and colitic human gut mucosa. Fems Microbiol. Ecol. 34, 147–155.

CHAPTER V: EXTRACTION STRATEGY OF EPS FROM *D. ALASKENSIS*

In order to find the most suitable protocol for the extraction of EPS from *D. alaskensis* AL1, the efficiency of various extraction compounds was investigated. Five extraction reagents were tested in order to verify which of them caused the lowest cell lysis. Three of them: EDTA with pH=8.0, Dowex cation exchange resin and 18–crown–6 ether (CE) were chosen for further improvement of the extraction protocol. This procedure included a three–step EPS extraction for either 1.5 or 2 h (of each step). Quantification of KDO revealed less than 0.13% cell lysis in first two extraction steps and ~ 1% in the third one. Abiotic controls showed that EDTA and CE significantly contributed to the sugars and uronic acids signals. It was observed that with use of EDTA the highest amounts of humic substances were extracted, while Dowex or CE extracted mainly proteins. Polyacrylamide gels electrophoresis (PAGE) revealed that the protein patterns of all three EPS extracts were very similar. However, EDTA showed the ability to extract a higher amount of low molecular weight proteins, as compared to Dowex and CE. Characterisation of humic substances using UV–Vis spectra showed higher molecular weight compounds present in the EPS extracted by EDTA. In general, it was observed that proteins, humic substances and some amounts of sugars were the main components of *D. alaskensis* AL1 EPS. Uronic acids were extracted with comparable efficiency by all three reagents and together with the extracellular DNA (eDNA) were the minor components of *D. alaskensis* EPS matrix. The extraction with use of Dowex in three 1.5 h time intervals was chosen to be applied for further EPS extraction.

1. INTRODUCTION

Microorganisms are known to produce a great number of extracellular polymeric substances (EPS) with various chemical and functional properties (Rehm, 2010). However, one of the problems when comparing the available data on the role of EPS in biocorrosion is the difference between the experimental approaches. Apart from various methodologies applied for corrosion risks evaluation, EPS isolation strategies differ significantly. In most of the studies only loosely bound EPS, obtained by centrifugation, was used. However, the removal of EPS tightly bound (TB) to the cells cannot be easily obtained and needs special approaches to be done. Especially that this TB fraction seems to be very interesting regarding the metal–microbial interactions.

An appropriate EPS extraction procedure should result in obtaining the highest EPS yields avoiding its contamination with the products of cell lysis. Several extraction methods, both physical and chemical, have been proposed. Physical methods included heating, sonication, high–speed centrifugation, boiling, and use of cationic exchange resins. Among the chemical reagents ethylendiaminetetraacetic acid (sodium edetate / EDTA), sodium hydroxide, aldehydes, phenol, sodium chloride, crown ether (Brown and Lester, 1980; Platt et al., 1985; Karapanagiotis et al., 1989; Azeredo et al., 1998; Aguilera et al., 2008) have been suggested as extractants. Currently, the most widely used physical method for TB EPS extractions consists of employing cationic exchange resins, which results in high exopolymer yields due to the combination of two types of mechanisms: the shear forces on granules applied by the stirring and the further destabilisation of the granule structure by exchange of bivalent cations mainly with sodium ions. The most efficient chemical extractants are considered to be EDTA and crown ether. They allow winning high amounts of exopolymers by means of cation complexing and are comparatively easy to remove (Aguilera et al., 2008; D'Abzac et al., 2010). As the cells of different microorganisms might vary in their resistance to physical and chemical treatment, while optimising the EPS extraction a special attention needs to be paid to controlling cell lysis. This becomes especially important for the precise characterisation of EPS, since its contamination with cell compounds might lead to a false interpretation of results. For Gram–negative–bacteria, 2–keto–3–deoxyoctonate (KDO), which is an

outer membrane component, is often used as a marker for cell damage (Adav et al., 2008).

However, it is important to mention that the universal procedure for EPS extraction does not exist as the properties of exopolymers and, especially the susceptibility of different bacterial genera cells to extraction reagent can differ. Therefore, the quality of each investigation concerning EPS depends greatly on the proper development and utilisation of an extraction procedure. This study focused on the development of the EPS extraction procedure for *D. alaskensis* AL1. Previously, only loosely bound (LB) EPS fraction of this SRP was previously characterised (Zinkevich et al., 1996) and there are no studies focused on the extraction of EPS of SRP, which here were undertaken.

2. MATERIALS AND METHODS

2.1. Microorganisms and growth media

TB and LB EPS were extracted from the model SRP – *D. alaskensis* AL1 (Feio et al., 2004). Its growth conditions and the inoculation procedure were described in the previous chapter. Microorganisms were grown for 3 days under gentle stirring of 100 rpm. After this time, EPS extraction was performed.

2.2. Extraction conditions

2.2.1. Collection of loosely bound EPS

A batch SRP culture was centrifuged at 9400 × g for 12 min at 4°C. 1 L of the supernatant was collected and immediately filtered twice with 0.22 µm pore size cellulose acetate membrane. In order to remove metabolites and salts of low molecular weight, filtered supernatant was dialysed overnight against running deionised water, using Spectra/Por 3.5 kDa dialysis tubing. The volume of water was at least 25 times greater than the total volume of the dialysed EPS. The dialysis was continued for additional 48h at 4°C with stirring at 100 rpm. Water was changed 3 times a day. Afterwards aliquots of LB EPS were stored at –20°C for further use.

Harvested cell pellet was divided in aliquots of 1g (wet weight) and each aliquot was washed with VMN medium mineral salts solution (mVMN). Incorporation of this step was necessary to remove eventual medium residues and products of microbial metabolic activity from the pellet.

2.2.2. Reagents selection for the tightly bound EPS extraction

The primary step in defining the most efficient extraction protocol for TB EPS was to select these extraction reagents (ER), which gave the lowest cell lysis rates. The following reagents (all of analytical grade (p.a.)) were tested: 0.34 M sodium chloride at 80°C (Rougeaux et al., 2001), Dowex® Marathon™C cation exchange resin, Na^+ form, 20–50 mesh size (Frølund et al., 1996). It was advised to use an extraction buffer with an ionic strength/conductivity similar to that of the sample/environment collected (Frølund et al., 1996; Wingender et al., 1999). For that reason phosphate buffer saline (PBS) used as an extraction buffer was modified in a following way: 2 mM $Na_2PO_4 \cdot 12H_2O$, 4 mM $NaH_2PO_4 \cdot H_2O$, 0.34 M NaCl, 1 mM KCl, pH=7.4 (adjusted with NaOH). The proportions between Dowex cation exchange resin and the PBS extraction buffer were 1:2 (w/v). Further on 30 mM dicyclohexyl–18–crown–6–ether (CE) in 50 mM Tris buffer, pH = 8 (Wuertz et al., 2001) and 1M NaOH (modified from Tay et al., 2001) were also examined. In the latter extraction, harvested cell pellet was resuspended in mVMN and NaOH was added dropwise under gentle stirring (100 rpm) until the cell suspension reached pH = 11. Subsequently, it was incubated for 30 min and further on heated at 80°C. Optimisation of the extraction protocol included also tests with EDTA (sodium edetate) as described (Liu and Fang, 2002). This ER was tested in different pH, adapted to the *D. alaskensis* growth conditions (Chapter IV, pH from 7.4 to 9.4). All solutions used during the extraction procedure were sterilised by double filtration with 0.2 µm pore size filters. As *D. alaskensis* is an anaerobic bacterium, all reagents were flushed with nitrogen (30 min) in order to avoid cell contact with oxygen. Washed cell pellets were afterwards resuspended in the ER in the glovebox (except for the procedure with NaOH). Further extraction was performed for 1.5 h under stirring of 100 rpm at required temperatures. For 1 g of cell pellet, 30 mL of ER were used.

2.2.3. Tightly bound EPS extraction procedure

After choosing three ER with the lowest cell lysis ratio, new batch of 3 days old SRP culture was prepared, aliquoted in cell pellets of 1g each and washed with mVMN, as described previously. Comparison of extraction efficiency was done with the cells from the same batch culture. This allowed avoiding intrinsic differences due to the differences in growth that could affect EPS production. Additionally, after washing the cells pellets with mVMN, the supernatant was collected, purified as LB EPS and stored for further analysis.

All extractions were performed in parallel and in duplicate. Two cell pellet aliquots (1 g) were resuspended in 30 mL of each of three ERs (in the anaerobic chamber), and incubated under stirring (100 rpm) at required temperatures for either 1.5 h or 2 h. After the extraction, cell suspensions were centrifuged (9400 × g, 12 min, T = 4°C) and as for LB EPS, the collected supernatant containing TB EPS was purified and stored at –20°C for further analysis. Collected cell pellets were again resuspended in each ER as before, and the extraction procedure was repeated twice. In parallel to this ternary step extraction, abiotic extraction controls were performed with the sterile growth medium, which was mixed with ER in the 1:1 (v/v) ratio. The control trials were performed for 4.5 or 6 h, corresponding to three times 1.5 or 2 h of single extraction step. In total, 6 controls were added to the protocol to assess the extraction reagent and medium contribution to the biochemical analyses. All extraction steps were performed in sterile conditions. Freeze drying (FD) was performed in this study and it was observed that lyophilised material was no more entirely dissolvable in water. It was also reported in the literature that FD may cause compositional changes (Tapia et al., 2011). Thus, FD was excluded from the protocol.

2.3. EPS composition analyses

All EPS aliquots were stored at –20°C and thawed prior to composition analysis. Pure and sterile VMN medium was also investigated. All chemical analyses were carried out in at least in triplicates for each determined parameter using the chemicals of analytical grade. For the determination of absorbances, Varian Cary 50 Bio UV/Visible spectrophotometer was used. All absorbances were measured

against water, and converted to concentrations by use of calibration standards for each method. Phenol–sulphuric acid method was used for polysaccharide content determination (Dubois et al., 1956) with glucose as a standard. Uronic acids levels were determined as described (Filisetti–Cozzi and Carpita, 1991), with glucuronic acid as a standard. Introduction of sulfamate and the diphenyl reagent in the protocol allowed measurements of analysed molecules without the interference from neutral sugars. Blind values were estimated similarly to the samples except that the m–hydroxydiphenyl reagent was substituted with an appropriate NaOH solution. Correction for non–uronic compounds was made by subtraction of blind values. e–DNA was determined as described (Burton, 1956) with DNA from salmon sperm as a standard. Protein concentration was analysed as described (Bradford, 1976) with bovine serum albumin (BSA) standard. An improved Lowry protocol (Frølund et al., 1995) was also incorporated in additional analyses of humic compounds with the correction of protein interference. Total volatile solids (TVL) were determined as described (DIN standard No. 38409–1, 1987), including the evaluation of mass change after drying the sample at 105°C, and its further ignition at 550°C. TVL was performed with use of 10 mL of extracted and dialysed EPS solution.

2.4. Monitoring of cell lysis

In order to determine the cell lysis levels in extracted EPS KDO concentration was determined as described elsewhere (Karkhanis et al., 1978). KDO was used as standard. In parallel, the previously mentioned six complementary abiotic extraction controls were also subjected to KDO tests. This served as an additional verification of possible medium and ERs contribution to the KDO signal.

In addition, a positive control with a defined amount of disrupted cells was analysed for its KDO content. Cell preparation and damage was performed as for the DNA extraction described in the Chapter III, Section 2.3.1 (Aljanabi and Martinez, 1997)). Obtained KDO values were further used to calculate the percentage of cell lysis in extracted EPS.

2.5. Characterisation of proteins from *D. alaskensis* EPS

Proteins from LB and TB EPS extracted in the second extraction step were analysed by sodium dodecyl sulfate polyacrylamide gel electrophoresis technique (SDS–PAGE). Here the protocol from (Schägger and von Jagow, 1987) was followed, with 10% and 15% acrylamide (v/v) concentration and Bio–Rad® Mini Protean apparatus. Gels were stained with Coomassie G–250 (Dyballa and Metzger, 2009). If no bands were observed, the same gel was destained for at least 10 h, and then stained with the silver nitrate solution (2D Electrophoresis Principles and Methods, GE Healthcare® 80–6429–60 AD). Because of low protein concentration for SDS–PAGE experiments, both LB and TB EPS fractions were concentrated with Amicon® Ultra–15 Centrifugal Filters (Milipore®) in 10 mM potassium phosphate buffer (KH_2PO_4/K_2HPO_4). 4 µg of TB EPS and 0.3 µg of LB EPS proteins were loaded in the gel, respectively. Lower LB EPS levels were loaded, because of their precipitation during the concentration. A constant current of 40 mA per slab was applied and the gels were run until the bromophenol blue tracking dye reached 0.5 cm from the bottom of the gel. Low–molecular–weight markers (Bio–Rad®) were used as protein standards.

2.6. UV–Visible spectra of EPS

The UV–Visible absorption spectra of extracted EPS were performed with a Shimadzu® UV–VIS Spectrophotometer model UV–1800, in the wavelength range of 250 until 800 nm at room temperature (RT) with 1 cm optical pathway in the quartz cuvette. Measurements were performed on EPS with equal protein concentration in all TB samples (0.4 mg/mL).

3. RESULTS

3.1. Influence of extraction reagents on cell lysis

The first part of the EPS extraction protocol optimisation (PART1, **FIG. 5.1**) was based on the choice of these ER, which were non–destructive for the cells. The second part (PART2, **FIG. 5.1**) was focused on finding the best ER for the EPS

extraction. Five different reagents were tested: two in high temperature conditions (80°C) – 0.34 M sodium chloride or 1M sodium hydroxide and three at low ones (4°C) – CE, Dowex and EDTA. Furthermore, EDTA binds to metal cations through its two amines and four carboxylates. At very low pH its fully protonated form predominates, whereas at very high pH, the fully deprotonated form is the prevalent one. In consequence the higher the pH, the better the complexing abilities of EDTA and further EPS winning. For that reason EDTA was tested at different pH values (**FIG. 5.1**).

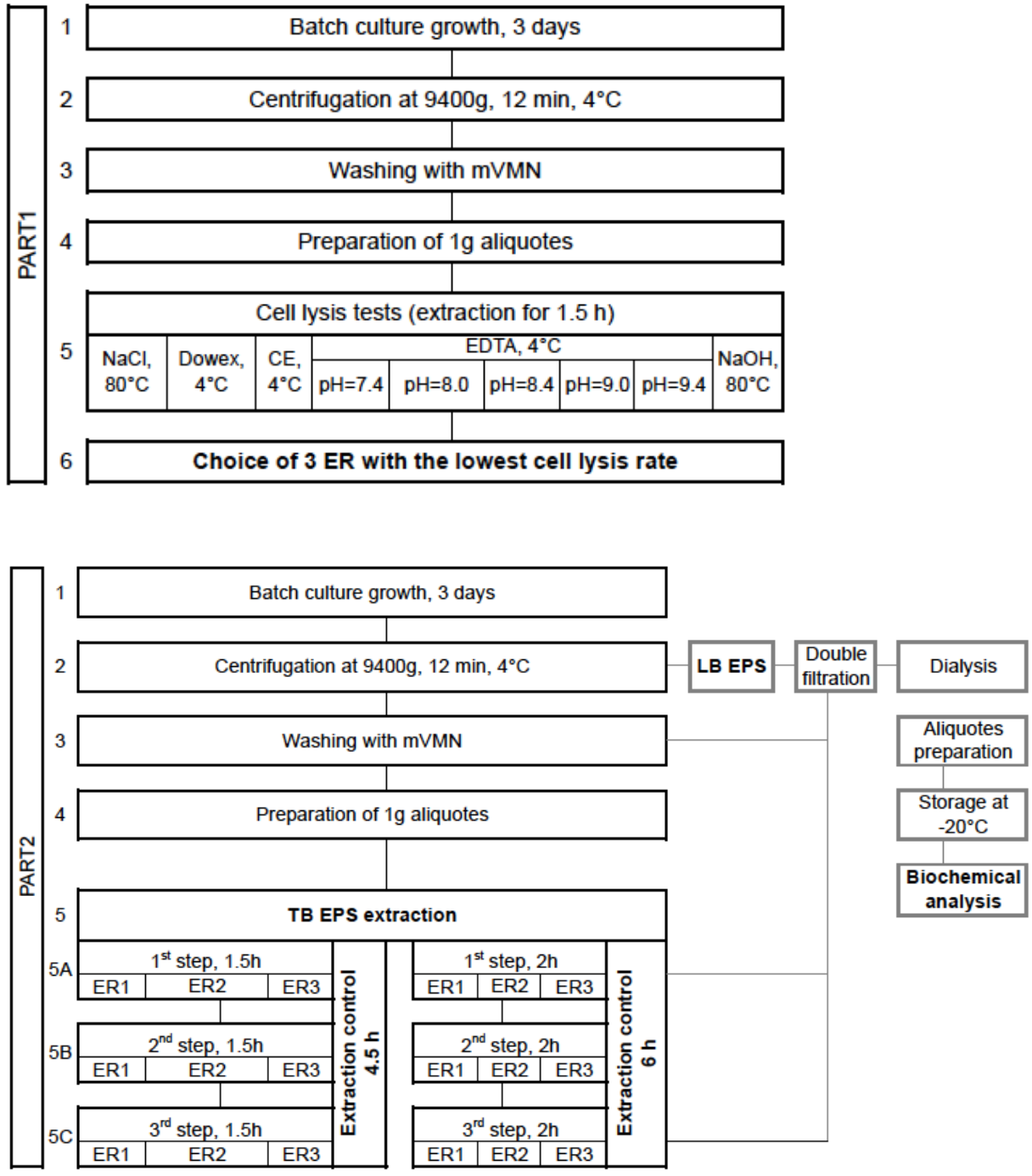

FIG. 5.1. EPS EXTRACTION SCHEME: PART 1 – SELECTION OF EXTRACTION REAGENT (ER) WITH THE LOWEST CELL LYSIS RATE; PART 2 – EXTRACTION REAGENT SELECTION; MVMN – VMN MEDIUM MINERAL SALTS SOLUTION, CE – CROWN ETHER, LB EPS – LOOSELY BOUND EPS, TB EPS – TIGHTLY BOUND EPS.

At the beginning, all ER were tested for cell lysis. As shown in **TABLE 5.1**, increased temperature was very destructive for the cell integrity, what discarded the extraction in these conditions from further considerations. Examination of a proper pH for EDTA solution revealed strong damages of bacterial outer membrane, at pH = 9.4. Its decrease of one pH unit gave cell lysis rates lower than 1%. CE and Dowex

were the least destructive ER with lysis rates lower than 0.1%. In order to have comparable conditions for the assessment of the extraction yield, EDTA at pH = 8 was chosen as the third evaluated ER.

TABLE 5.1. COMPARISON OF CELL LYSIS RATIOS BETWEEN DIFFERENT EXTRACTION REAGENTS AFTER 1.5 H EXTRACTION.

Extraction reagent	% of total cell lysis
NaCl, 80°C	5.15 ± 0.22
NaOH, 80°C	6.25 ± 0.05
EDTA, pH=9.4, 4°C	11.70 ± 0.17
EDTA, pH=9.0, 4°C	1.43 ± 0.51
EDTA, pH=8.4, 4°C	0.22 ± 0.01
EDTA, pH=8.0, 4°C	0.013 ± 0.003
EDTA, pH=7.4, 4°C	0.021 ± 0.007
CE, 4°C	0.052 ± 0.002
Dowex, 4°C	0.052 ± 0.001

3.2. Monitoring of cell lysis in the negative controls and their contribution to the determined parameters

The second part of the EPS extraction protocol optimisation was designed in the way that each chosen reagent was tested in a three-step extraction for either 1.5 h or 2 h, as shown in **FIG. 5.1**. The interval of 30 min between the extractions gave a total time difference of 1.5 h, consequently prolonging the procedure for 1.5 h.

KDO rates were also carefully monitored in this part of the EPS extraction protocol optimisation, as shown in **TABLE 5.2**.

TABLE 5.2. CELL LYSIS RATES OBTAINED IN THE SECOND EXTRACTION PART (CALCULATED BASED ON THE POSITIVE CONTROL).

Extraction reagent	Extraction step	*Extraction time [h]*	
		1.5	2.0
		% cell lysis	
EDTA	1st	0.056 ± 0.036	0.057 ± 0.003
	2nd	0.129 ± 0.018	0.046 ± 0.002
	3rd	0.830 ± 0.308	0.427 ± 0.016
	Control*	0.041 ± 0.002	0.052 ± 0.012
Dowex	1st	BDL**	0.051 ± 0.001
	2nd	0.022 ± 0.002	0.058 ± 0.012
	3rd	0.579 ± 0.074	0.626 ± 0.080
	Control*	0.045 ± 0.011	0.034 ± 0.018
Crown ether	1st	N.D.**	0.091 ± 0.042
	2nd	0.007 ± 0.006	0.085 ± 0.038
	3rd	0.186 ± 0.025	0.513 ± 0.145
	Control*	0.043 ± 0.020	0.022 ± 0.004
	% cell lysis		
LB EPS	0.024 ± 0.001		
Washed fraction	0.065 ± 0.031		
VMN medium	0.122 ± 0.003		

* Extraction time for the controls (VMN medium + ER) was equal to the triplication of single extraction step time
** BDL – below the detection limit

It was observed that the first two Dowex and CE extractions, independently of the extraction time, gave the lowest levels of cell lysis. In the second EDTA extraction, with the shorter extraction times (1.5 h), cell lysis rate slightly increased. No cell lysis increase in 2 h EDTA extraction was observed. However, in the third extraction step it was observed that in all surveys, cell lysis rates increased. Their values increased from approx. 6 up to almost 27 times in comparison to the former extraction step, however they were still lower than 1%. KDO signal in abiotic controls and growth medium was also detected in minor amounts.

The overview of negative controls and growth medium composition is shown in **TABLE 5.3**. None of used ER did influence protein or humic substances signal. However, a contribution to the sugars and uronic acids measurements was recorded. EDTA and CE gave high signals of uronic acids in the controls, which were comparable (EDTA) or even higher than the ones observed with the VMN medium itself (CE).

TABLE 5.3. VALIDATION OF NEGATIVE CONTROLS BY MEANS OF COLORIMETRIC ASSAYS. ALL VALUES WERE EXPRESSED IN µG EPS PER 1 ML OF EXTRACTED MATERIAL.

ER	Total Extraction time [h]	Proteins	Humic substances	Sugars	Uronic acids	DNA
		[µg EPS / mL]				
EDTA–VMN	4.5	BDL*	BDL*	1.65 ± 0.65	110.68 ± 3.61	0.19 ± 0.01
	6.0	BDL*	BDL*	1.41 ± 1.38	119.46 ± 6.80	0.34 ± 0.04
Dowex–VMN	4.5	**BDL***	**BDL***	**BDL***	**13.36 ± 0.84**	**BDL***
	6.0	**BDL***	**BDL***	**BDL***	**BDL***	**0.34 ± 0.02**
CE–VMN	4.5	BDL*	BDL*	0.64±0.43	132.06±13.77	0.35 ± 0.02
	6.0	BDL*	BDL*	0.93±0.01	138.40±16.86	0.25 ± 0.01
VMN medium	–	25.67±0.13	85.95±5.53	5.35±1.92	115.33±7.92	BDL*

* BDL – below the detection limit

3.3. EPS composition analyses

Depending on the different ER used and the time of extraction diverse results were obtained. These are shown in **FIG. 5.2**.

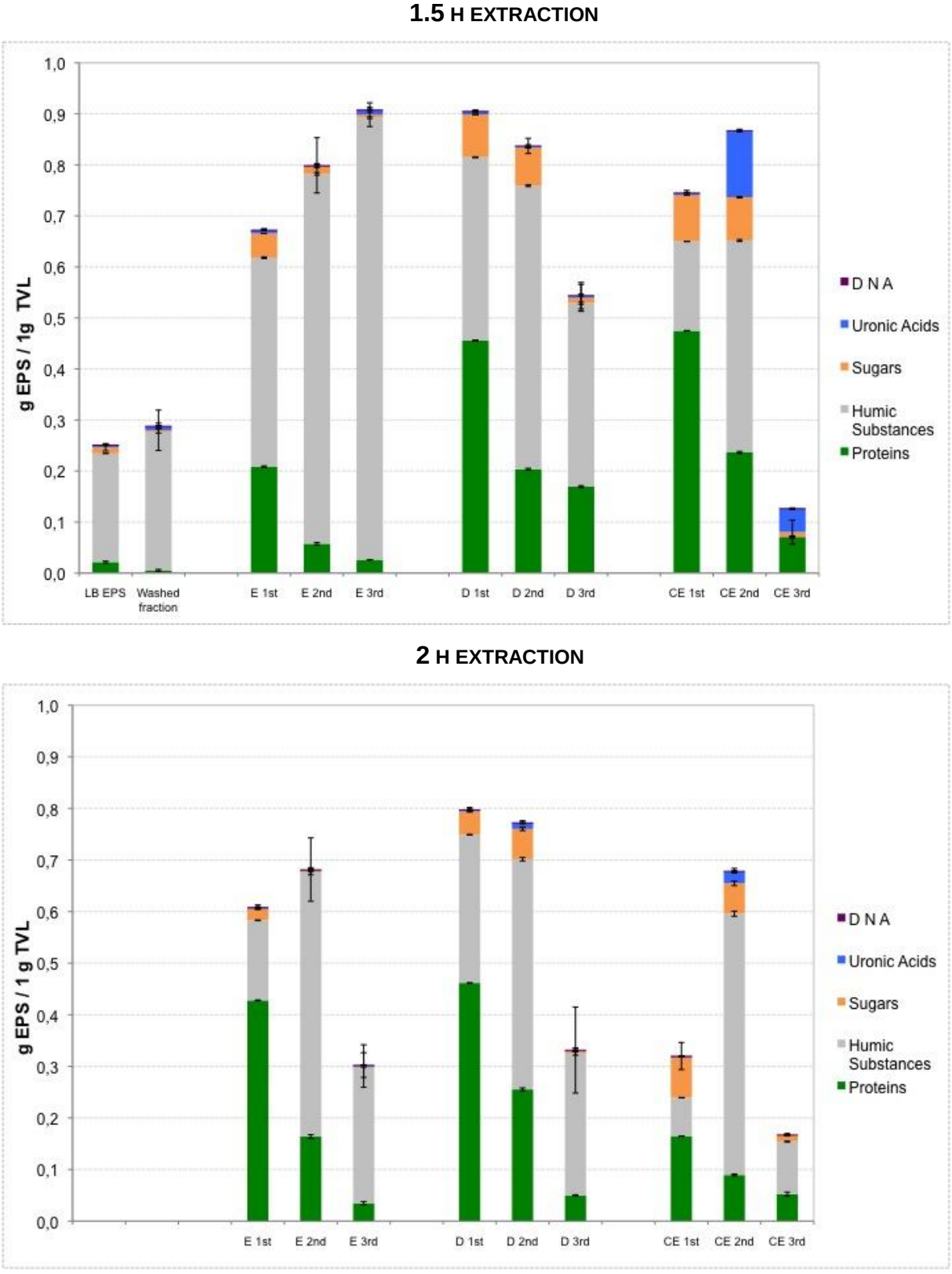

FIG. 5.2. EPS COMPOSITION (PER 1G OF TVL). LB EPS – LOOSELY BOUND EPS, E – EDTA, D – DOWEX, CE – CROWN ETHER, 1ST 2ND AND 3RD REFER TO THE SUBSEQUENT EXTRACTION STEPS.

Proteins and humic substances appeared to be the dominant components of *D. alaskensis* EPS. Within the first 1.5 h of extraction, Dowex and CE delivered similar amounts of extracellular proteins. For the EDTA extraction, 2 h were needed to give a comparable effect. EDTA was the most effective for humic substances extraction. For the sugar content, Dowex and CE gave comparable results and EDTA was about 50% less effective. All ER extracted e–DNA with comparable yield. CE delivered the highest amounts of uronic acids.

Incorporation of three steps of extraction delivered interesting data. The amounts of proteins with each subsequent step decreased. In contrast humic substances levels were either comparable or higher than in the first extraction stage. Sugars were obtained mostly in the first two attempts. It was observed that from 0.7 to almost 0.9 g of EPS per 1g of TVL could be identified, if the extraction was performed for 1.5 h (except of CE), while from only 0.2 g up to maximally 0.8 g were identified when the extraction time was prolonged for additional 30 min.

Only up to 0.3 g EPS per 1g of their TVL was found in the LB and first washed EPS fraction from the cell pellet, containing mainly humic substances, some proteins and very small amounts of sugars, uronic acids and DNA.

Decrease in amounts of EPS correlated with a decrease in the colour of extracted matter, as shown in **FIG. 5.3**.

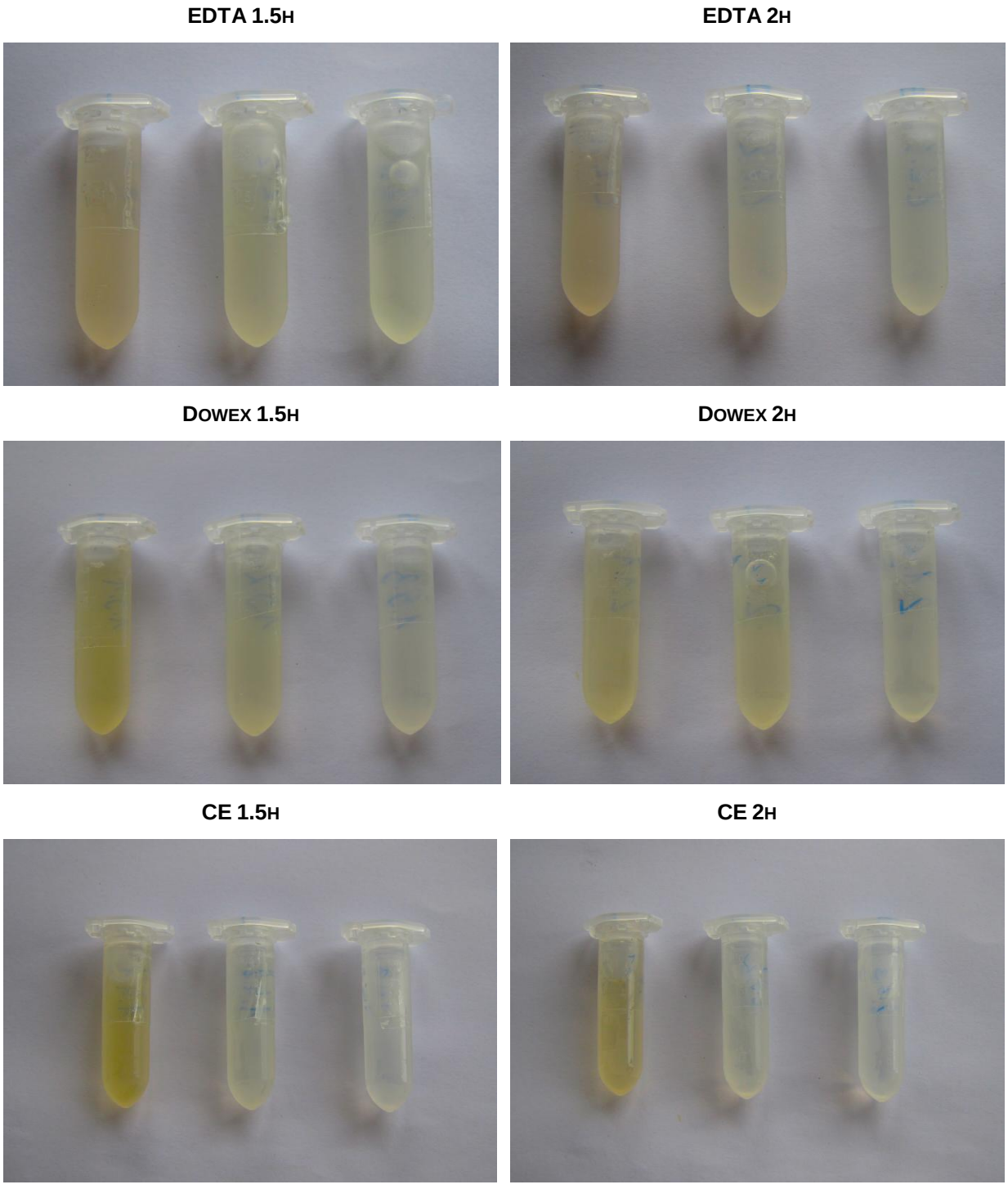

FIG. 5.3. CHANGES IN COLOUR OF TB EPS FRACTIONS AFTER SUBSEQUENT EXTRACTIONS. ON EACH PICTURE FROM LEFT: EPS FROM THE 1ST, 2ND AND 3RD EXTRACTION STEP, RESPECTIVELY.

There was a correlation between the extraction steps and the decrease of the respective EPS colour. Between 1.5 h and 2 h extractions, the colour intensity differed as well, being less intensive in the further ones. These observations were consistent with the determined EPS concentrations. Interestingly, also different

colours were observed between the EPS extracted with Dowex and CE and the ones won by use of EDTA. The former had orange–yellow hue, while the later rather brown tint.

3.4. Characterisation of extracellular proteins from *D. alaskensis* EPS

Proteins, as the molecules present in high concentrations, were additionally analysed by SDS–PAGE, as shown in **FIG. 5.4** (with extracellular proteins from each extraction step analysed separately) and **FIG. 5.5** (total EPS profile of combined fractions). Extracellular proteins from the first two extractions were analysed.

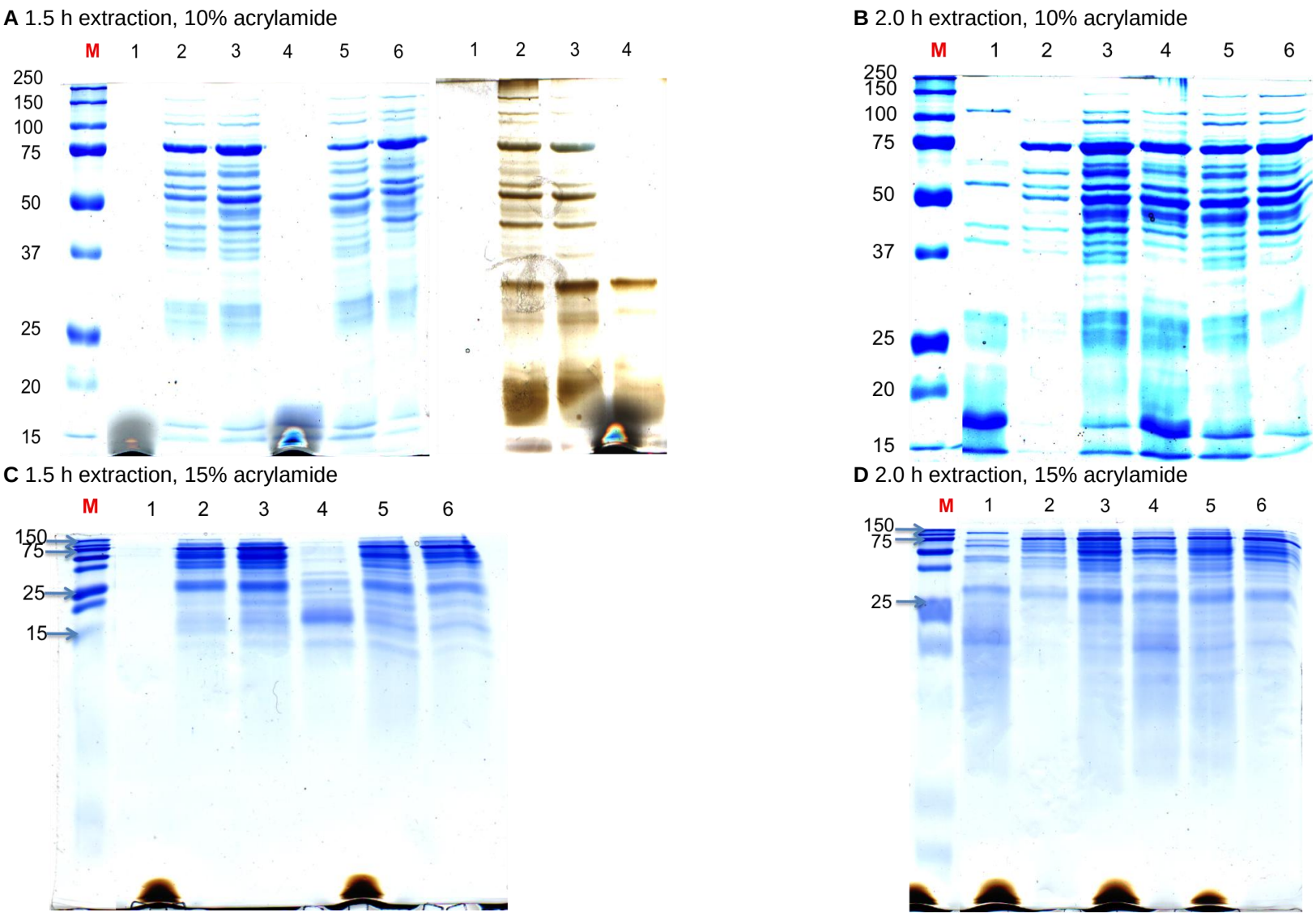

FIG. 5.4. PROTEIN PROFILES OF VARIOUS EXTRACTED EPS FRACTIONS. A – EXTRACTION TIME = 1.5 H, 10% PAGE; B – EXTRACTION TIME = 2 H, 10% PAGE; C – EXTRACTION TIME = 1.5 H, 15% PAGE; D – EXTRACTION TIME = 2 H, 15% PAGE; LANE NUMBERS CORRESPOND TO: 1 – 1ST EXTRACTION STEP, EDTA; 2 – 1ST EXTRACTION STEP, DOWEX; 3 – 1ST EXTRACTION STEP, CE; 4 – 2ND EXTRACTION STEP, EDTA; 5 – 2ND EXTRACTION STEP, DOWEX; 6 – 2ND EXTRACTION STEP, CE; M – MOLECULAR WEIGHT MARKER; GELS WERE STAINED WITH COOMASSIE BLUE G–250 AND ADDITIONALLY WITH SILVER NITRATE (ADDED AT THE RIGHT IN FIG. 5.4 A).

Performed SDS-PAGE trials revealed a big protein diversity in both types of gels. Their profiles from Dowex and CE extracted EPS were identical, containing approximately 20 bands with molecular weights from 35 kDa up to 150 kDa, with the most intensive bands of 75 kDa and 50 kDa. Low molecular weight proteins were not well separated in 10% PAGE and were uncountable and indistinguishable between each other. No bands were detected in the 1.5 h EDTA fractions in 10% PAGE, and only after the silver staining these of low molecular weight could be observed. In contrast, in 15% PAGE 1.5 h EDTA extracted proteins were detected: the first EDTA extract gave a light smear in the top part of the lane, while various proteins were visible in the second extract. This profile was similar to the Dowex and CE extracted EPS. However, more lower molecular weight proteins were observed in EDTA.

EPS extracted with EDTA and Dowex in the first 2 h contained less proteins compared to 2 h CE extract. Extracts from the second step were very similar. The only variation was observed for EDTA extracted EPS, where more low molecular weight EPS were found with predominant bands of approx. 20 and 25 kDa.

The profiles of entirely extracted TB EPS presented in the **FIG. 5.5**, showed comparable patterns of proteins extracted either with cation exchange resin or CE. The lowest protein extraction efficiency was observed when EDTA was used, although the amounts of proteins of 25 kDa and smaller were the highest.

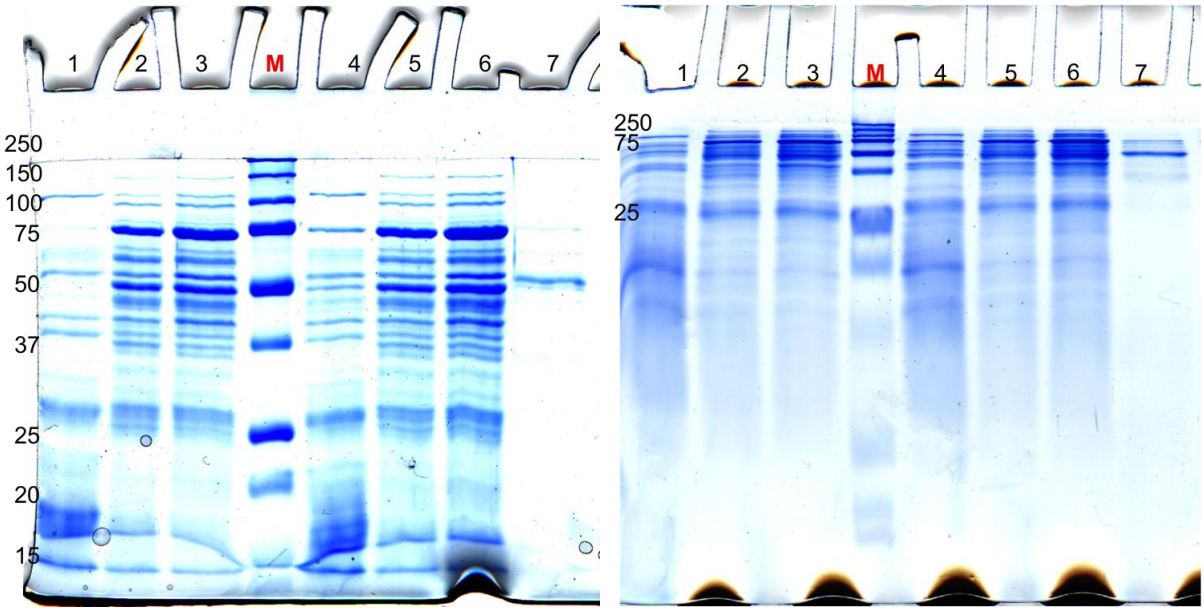

FIG. 5.5. PROTEIN PROFILES OF TOTAL EPS. 10% (A) AND 15% (B) PAGE; LB AND TB EPS EXTRACTED WITH DIFFERENT REAGENTS: 1 – EDTA, 3H; 2 – DOWEX, 3H; 3 – CE, 3H; 4 – EDTA, 4H; 5 – DOWEX, 4H; 6 – CE, 4H; 7 – LOOSELY BOUND EPS; M – MOLECULAR WEIGHT MARKER; GELS STAINED WITH COOMASSIE BLUE G–250.

In the LB EPS lane only 4 protein bands were observed: one of 75 kDa, another of approx. 60 kDa, the dominant 50 kDa one and a week band directly below it. All these protein bands were present in TB EPS profiles from all ER.

3.5. UV–Visible spectra of EPS

Absorbance spectra of extracted EPS are shown in **FIG. 5.6**. TB EPS from EDTA extraction differed from Dowex and CE UV–Vis spectral profiles. EDTA extracted EPS profile started with a plateau and followed with a sharp decline at around 275 nm, continued with a small peak at 335 nm and a well developed peak at 407 nm. Two additional absorption hills were detected at 525 nm and 620 nm. 4.5 h vs. 6 h EDTA extracts differed gently in the absorption intensity. UV–Vis spectra of Dowex and CE extracts started with the maxima of different absorption intensity at 256 nm (Dowex 4.5 h > Dowex 6 h> CE 4.5 h ≈ CE 6h), followed by gentle acclivities at 335 nm, from which Dowex 4.5 was the highest, Dowex and CE (6 h) were almost identical, and CE (4.5 h) was the lowest. 407 nm peaks were present in all four samples with absorbance heights much lower than for EDTA extracts, changing as following: Dowex 4.5 h > Dowex 6h ≈ CE 6 h > CE 4.5 h. Gentle signals at 525 and 620 nm were also recorded, but these were weaker and less visible as in EDTA

extracted samples. In the LB EPS spectrum, very small broad peaks at 270 nm and at 360 nm were observed.

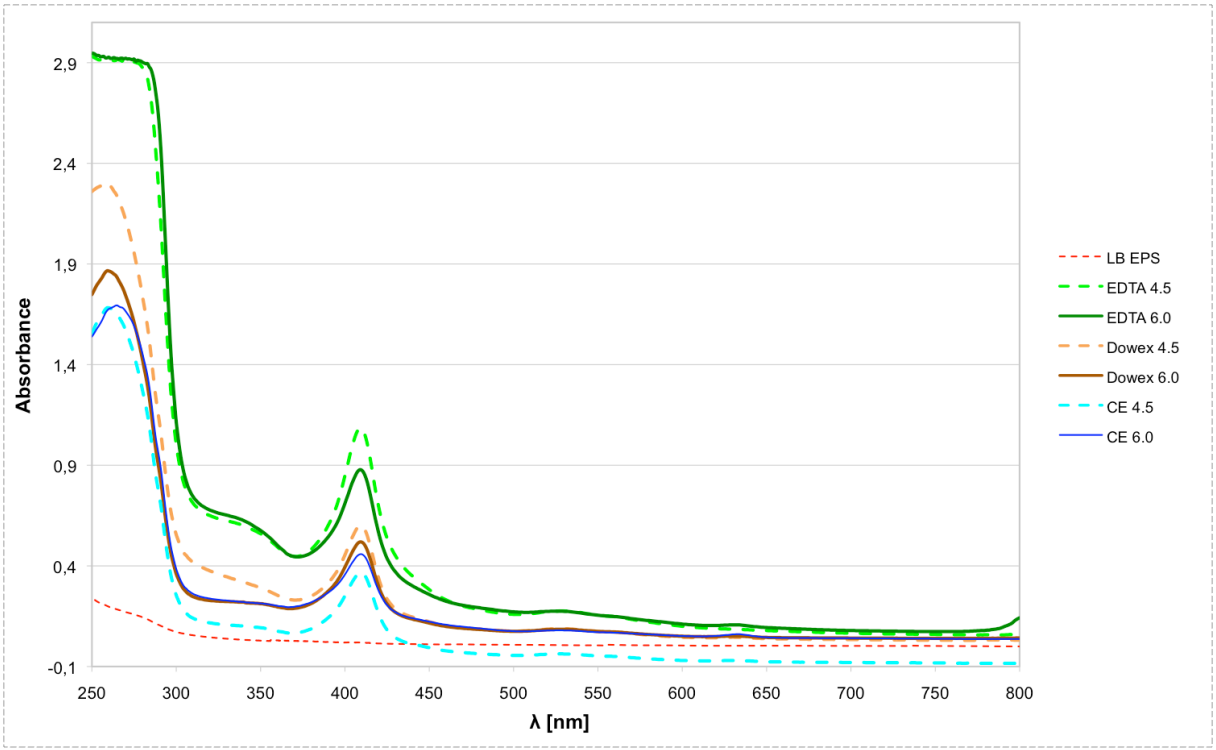

FIG. 5.6. UV–VISIBLE SPECTRA OF EXTRACTED EPS; 4.5 AND 6 RELATES TO THE TOTAL EXTRACTION TIME; LB EPS – LOOSELY BOUND EPS, CE – CROWN ETHER.

4. DISCUSSION

In this study various approaches were applied in order to optimise the extraction protocol for the most effective EPS winning from *D. alaskensis* AL1.

Proper ER selection was based in the first place on the levels of caused cell lysis. In this case, five tested reagents, three with the lowest (and comparable between themselves), lysis ratios were chosen: Dowex, CE and EDTA, pH=8. Further on, the cell pellet was prepared before the implementation of main procedures by washing it. Washing prior to extraction was conducted to remove the medium and metabolic products traces. The washed fraction composition was investigated in order to verify possible EPS losses. The influence of this step on the EPS losses provoked a minor release of humic substances.

The main EPS extraction procedure, included a number of steps, which might have an influence on cell integrity, therefore a careful lysis monitoring was performed after each step. Cell lysis might come not only from the applied extraction reagents

and temperature conditions, but also originate from the mechanical treatment. Therefore decreased stirring forces, extraction under oxygen free conditions and application of deaerated ERs were applied. All these conditions probably helped in obtaining lower KDO levels. At the same time no changes in the e–DNA and protein contents were observed, indicating that small outer cell membrane breakages rather than substantial cell lysis may have occurred.

Monitoring of KDO in the growth medium and performed controls delivered supplementary observations. A positive signal was detected in the control samples, but it was weak (the average value equal to 0.04 ± 0.01%). In the growth medium this value was however 3.1 times higher. Thus, if the dialysis is not performed properly, medium and ER contribution to the KDO signal might occur at any time. For that reason, in each extraction, an additional monitoring of KDO levels in the control and an extensive dialysis, as proposed here, should be performed.

The next feature of the evaluated ERs, also important for the consideration of their usability in EPS extraction protocol, was the level of their interference with the chemicals applied for EPS characterisation. This has a special importance if the removal of ER by dialysis is incomplete. None of the ER contributed to the signal of proteins or humic substances, which were the main components of the *D. alaskensis* EPS. However, while determining sugars and uronic acids concentrations a positive signal occurred in the CE and EDTA samples. It was observed that in the CE controls, levels of determined uronic acids were even higher than in the medium itself. This could possibly be related to the additional presence of the compounds present in the CE solution. Dowex resin grains were separated from the EPS or from the control solution, before the dialysis was performed, and the extraction buffer was composed of only low molecular weight inorganic compounds. Hence, the purification process in these conditions appeared to be much more effective than in the two other ER.

Extraction efficiency was promising while using CE, but the risk of its possible contribution to the signals undermined its extraction values. In order to avoid possible perturbations in the EPS composition, the ER, which does not contribute to the determined parameters, should be chosen. Application of Dowex gave the most appropriate conditions to meet this requirement, since its controls did not give any significant additional signal.

The key part in exploring the most suitable procedure for the EPS extraction from marine SRP was focused on the monitoring of the extraction yields. EPS winning efficiency was based on the determination of EPS compounds, normalised per 1 g of TVL. This information helped also in the estimation of the amounts of unidentified molecules in the EPS. Independently on the extraction time, EDTA was the most effective for humic substances extraction, while CE and Dowex were effective for proteins and sugars winning. Possible reasons for the simultaneous extraction of both molecules will be discussed in Chapter VI. Up to 90% of EPS could be identified from the first two extraction steps when extracting in 90 min intervals.

Application of a defined volume of ER is connected with the risk of improper choice of its volume. Extraction reagent might be even after short extraction time overloaded with cations and thus not able to gain more biopolymers in a single extraction. Thus, the EPS extraction protocol was extended by two supplementary steps, in order to verify if without a risk of cell damage, more EPS could be extracted. It was observed that the addition of fresh ER was beneficial for obtaining higher amounts of humic substances and proteins.

However, in the third 1.5 h extraction step with CE and in all extracts of 2 h trials, the amounts of unidentified EPS were significantly higher. Possibly, the primary release of amphiphilic molecules, allowed also lipids to be further transported to the ER solution. Moreover, CE posses properties, which allow both hydrophobic and hydrophilic molecules to be simultaneously extracted. The oxygen atoms are well situated to coordinate a cation located at the interior of the crown, whereas its exterior is hydrophobic. Consequently, created cations complexes often form salts that are soluble in non – polar chemical environments. In addition, CE have the unique feature of solubility in almost all known solvents, through the phenomenon of "winding" and "expanding", what may be of crucial role in the intensified attracting of hydrophobic lipids. When all hydrophilic molecules can be extracted in first two extractions, a favourable environment for these molecules in the CE solution is created. However this a hypothesis, which needs additional verification.

Finally, it was needed to elucidate the origin of differences between EDTA and two other ER extractions. The chemical nature of these reagents varies and, in consequence, modifies their complexing properties. Crown ethers combine with the cations by relatively weak ion–dipole interactions, which however, after adding many of these interactions provide a stable complex. They are also highly selective ligands

– changing the size and topology of the cyclic systems, these compounds can be prepared to bind very specific ions. 18–crown–6 functioned as a ligand for alkaline metal cations. It can also bind to protonated amines and form very stable complexes, what might help in extracting proteins. The Dowex resin has the corresponding features. In principle, it interchanges the ions between a solid (ion exchange resin) and a liquid. Its selectivity for cations changes accordingly: $Ba^{2+} > Sr^{2+} > Ca^{2+} > Mg^{2+} > Cs^{+} > Rb^{+} > K^{+} > Na^{+} > H^{+} > Li^{+}$. However it is able to exchange to some extend also iron and manganese ions.

EDTA usually binds to any metal cation through its amine and carboxylates groups. It forms especially strong complexes with Mn(II), Cu(II), Fe(III), Pb (II) and Co(III) (Holleman et al., 2001). Thus, its complexing properties to cations are unselective and possibly can deliver more diverse humic substances, whereas in Dowex and CE these properties are limited. The latter compounds contain a complex mixture of many different acids including carboxylic, phenolic, salicylic and phthalate groups. Many humic acids have two or more of these groups arranged in the way to enable the formation of chelate complexes. Their formation is an important aspect of the biological role of humic acids in regulating bioavailability of a wide range metal ions. If humic substances could be bound by various cations, which were complexed by EDTA, then their release will be significantly facilitated. As Dowex can to some extend also complex Fe and Mn cations, it became also possible to cause the release of humic substances.

Subsequently, shorter time extractions delivered more identifiable EPS. It might be possible that the missing substances were extracellular lipids, constituting from 10 up to 30% of EPS. Lipid determination is still a source of many problems. It arises from determining only one type of these molecules. For example the sulfo–phospho–vanillin (SPV) protocol (Cheng et al., 2011; Frings et al., 1972) is a rapid and very simple method for their investigation. However, the basis of this protocol is the presence of a carbon – carbon double bonds (Knight et al., 1972). Unsaturated compounds with more than one double bond do react, but the reaction may vary with the steric hindrance. The method is precise, but its accuracy depends primarily on the reference standard used. And as further shown (Chapter VI), *D. alaskensis* extracellular lipids contain all the types of lipids: saturated, unsaturated and molecules with more than one double bound. Their main component contained 16 carbon atoms (C16) in the saturated hydrocarbon chain. As the fatty acid chain is

saturated, this method could not be applied. However, a general estimation of the lipids levels in the extracted EPS matrix could be performed based on TVL rates analyses.

Application of a multiple step extraction might induce the question, if the qualitative composition of the EPS did change between the steps and between the different ERs applied. In order to answer this question proteins, as the molecules present in higher concentration were analysed by SDS–PAGE. The profiles of LB EPS and various TB EPS extracts from all above described conditions were analysed by SDS–PAGE at different polyacrylamide concentrations. It was observed that EDTA extracted EPS had fewer proteins than two other reagents especially these of higher molecular weight. The advantages of its use appeared in the release of smaller proteins. However, the main protein profile was very similar between all ER, showing a simultaneous extraction of the same proteins, which if not extracted in the first step, were obtained in the further ones.

Main peaks detected in the UV–Vis spectra were recorded at 620, 525, 407 and 335 nm, together with either peaks or plateau starting at approx. 275 nm. The increase of absorbance at 275 nm could be correlated with the proteins presence, which absorb the light at 280 nm. Nevertheless, recorded plateau of 250 to 270 nm could be likewise attributed to the structural conjugation of quinones and/or ketones, therefore indicative of aromatic systems (Ghosh and Schnitzer, 1979). Thus, the main recorded signals probably came from proteins and humic substances.

5. CONCLUSIONS

In this chapter a suitable *D. alaskensis* EPS extraction protocol was developed. This included the selection of ERs, which caused less cell lysis. Also the contribution of each ER to the determination procedures was considered. No significant EPS losses were recorded while washing the cell pellet before the extraction. Finally, a broad spectrum of different trials was applied to find the best extraction reagent. From all proposed approaches, the use of Dowex in three steps of 1.5 h extractions appeared to be the most beneficial for the *D. alaskensis* EPS release. The highest amounts of extracellular polymers were extracted when this cation exchange resin was applied. The lowest levels of interferences of this ER in quantitative studies were reported with low cell lysis rates. Another advantage of using Dowex comes from its

applicability in a wide pH and temperature range, what allows using it in extracting EPS from extremophilic microorganisms. Other reagents demand a defined environment to be used, what narrows the range of their applications. 18–crown–6, despite of its good extraction properties is however toxic, expensive and interferes with sugars and uronic acids determinations, significantly increasing the risk of artefacts in chemical EPS determination. It was also important to adapt the extraction features to the growth and environmental conditions. In this survey, extractions were performed with lack of oxygen, as this may be beneficial to decrease cell lysis. Our multiple extraction step protocol profits from a more efficient EPS winning. The first two steps deliver compounds such as proteins, humic substances or sugars, while the latter one possibly gave an additional amount of extracellular lipids.

Although most of the attention was focused on the SRP *D. alaskensis*, this EPS extraction protocol can be expanded to any other system with a careful consideration of the best ER to be used.

6. REFERENCES

Adav, S.S., Lee, D.–J., Tay, J.–H., 2008. Extracellular polymeric substances and structural stability of aerobic granule. Water Res. 42, 1644–1650.

Aguilera, A., Souza–Egipsy, V., San Martín–Uriz, P., Amils, R., 2008. Extraction of extracellular polymeric substances from extreme acidic microbial biofilms. Appl. Microbiol. Biotechnol. 78, 1079–1088.

Aljanabi, S.M., Martinez, I., 1997. Universal and rapid salt–extraction of high quality genomic DNA for PCR–based techniques. Nucleic Acids Res. 25, 4692–4693.

Azeredo, J., Oliveira, R., Lazarova, V., 1998. A new method for extraction of exopolymers from activated sludges. Water Sci. Technol. 367–370.

Beech, I.B., Zinkevich, V., Tapper, R., Gubner, R., 1998. Direct involvement of an extracellular complex produced by a marine sulfate-reducing bacterium in deterioration of steel. Geomicrobiol. J. 15, 121–134.

Bradford, M.M., 1976. A rapid and sensitive method for the quantitation of microgram quantities of protein utilizing the principle of protein–dye binding. Anal. Biochem. 72, 248–254.

Brown, M.J., Lester, J.N., 1980. Comparison of Bacterial Extracellular Polymer Extraction Methods. Appl. Environ. Microbiol. 40, 179–185.

Burton, K., 1956. A study of the conditions and mechanism of the diphenylamine reaction for the colorimetric estimation of deoxyribonucleic acid. Biochem. J. 62, 315–323.

Chen, Y., Senesi, N., Schnitzer, M., 1977. Information Provided on Humic Substances by E4/E6 Ratios. Soil Sci. Soc. Am. J. 41, 352–358.

Cheng, Y.–S., Zheng, Y., VanderGheynst, J.S., 2011. Rapid quantitative analysis of lipids using a colorimetric method in a microplate format. Lipids 46, 95–103.

D'Abzac, P., Bordas, F., Van Hullebusch, E., Lens, P.N.L., Guibaud, G., 2010. Extraction of extracellular polymeric substances (EPS) from anaerobic granular sludges: comparison of chemical and physical extraction protocols. Appl. Microbiol. Biotechnol. 85, 1589–1599.

DIN standard No. 38409–1, 1987. Deutsche Einheitsverfahren zur Wasser–, Abwasser– und Schlammuntersuchung; Summarische Wirkungs– und Stoffkenngrößen (Gruppe H); Bestimmung des Gesamttrockenrückstandes, des Filtrattrockenrückstandes und des Glührückstandes (H 1).

Dubois, M., Gilles, K.A., Hamilton, J.K., Rebers, P.A., Smith, F., 1956. Colorimetric Method for Determination of Sugars and Related Substances. Anal. Chem. 28, 350–356.

Dyballa, N., Metzger, S., 2009. Fast and sensitive colloidal coomassie G–250 staining for proteins in polyacrylamide gels. J. Vis. Exp. Jove.

Feio, M.J., Zinkevich, V., Beech, I.B., Llobet–Brossa, E., Eaton, P., Schmitt, J., Guezennec, J., 2004. Desulfovibrio alaskensis sp. nov., a sulphate–reducing bacterium from a soured oil reservoir. Int. J. Syst. Evol. Microbiol. 54, 1747–1752.

Filisetti–Cozzi, T.M., Carpita, N.C., 1991. Measurement of uronic acids without interference from neutral sugars. Anal. Biochem. 197, 157–162.

Frings, C.S., Fendley, T.W., Dunn, R.T., Queen, C.A., 1972. Improved determination of total serum lipids by the sulfo–phospho–vanillin reaction. Clin. Chem. 18, 673–674.

Frølund, B., Griebe, T., Nielsen, P.H., 1995. Enzymatic activity in the activated–sludge floc matrix. Appl. Microbiol. Biotechnol. 43, 755–761.

Frølund, B., Palmgren, R., Keiding, K., Nielsen, P.H., 1996. Extraction of extracellular polymers from activated sludge using a cation exchange resin. Water Res. 30, 1749–1758.

Ghosh, K., Schnitzer, M., 1979. Uv and Visible Absorption Spectroscopic Investigations in Relation to Macromolecular Characteristics of Humic Substances. J. Soil Sci. 30, 735–745.

Helms, J.R., Stubbins, A., Ritchie, J.D., Minor, E.C., Kieber, D.J., Mopper, K., 2008. Absorption spectral slopes and slope ratios as indicators of molecular weight, source, and photobleaching of chromophoric dissolved organic matter. Limnol Ocean. 53, 955–969.

Holleman, A.F., Wiber, E., Wiberg, N., 2001. Inorganic Chemistry. Academic Press.

Karapanagiotis, N.K., Rudd, T., Sterritt, R.M., Lester, J.N., 1989. Extraction and characterisation of extracellular polymers in digested sewage sludge. J. Chem. Technol. Biotechnol. 44, 107–120.

Karkhanis, Y.D., Zeltner, J.Y., Jackson, J.J., Carlo, D.J., 1978. A new and improved microassay to determine 2–keto–3–deoxyoctonate in lipopolysaccharide of gram–negative bacteria. Anal. Biochem. 85, 595–601.

Knight, J.A., Anderson, S., Rawle, J.M., 1972. Chemical basis of the sulfo–phospho–vanillin reaction for estimating total serum lipids. Clin. Chem. 18, 199–202.

Liu, H., Fang, H.H.P., 2002. Extraction of extracellular polymeric substances (EPS) of sludges. J. Biotechnol. 95, 249–256.

Mayer, C., Moritz, R., Kirschner, C., Borchard, W., Maibaum, R., Wingender, J., Flemming, H.C., 1999. The role of intermolecular interactions: studies on model systems for bacterial biofilms. Int. J. Biol. Macromol. 26, 3–16.

McDonald, S., Bishop, A.G., Prenzler, P.D., Robards, K., 2004. Analytical chemistry of freshwater humic substances. Anal. Chim. Acta 527, 105–124.

Platt, R.M., Geesey, G.G., Davis, J.D., White, D.C., 1985. Isolation and partial chemical analysis of firmly bound exopolysaccharide from adherent cells of a freshwater sediment bacterium. Can. J. Microbiol. 31, 675–680.

Quiocho, F.A., 1986. Carbohydrate–binding proteins: tertiary structures and protein–sugar interactions. Annu. Rev. Biochem. 55, 287–315.

Rehm, B.H.A., 2010. Bacterial polymers: biosynthesis, modifications and applications. Nat. Rev. Microbiol. 8, 578–592.

Rougeaux, H., Guezennec, M., Che, L.M., Payri, C., Deslandes, E., Guezennec, J., 2001. Microbial Communities and Exopolysaccharides from Polynesian Mats. Mar. Biotechnol. 3, 181–187.

Schägger, H., von Jagow, G., 1987. Tricine–sodium dodecyl sulfate–polyacrylamide gel electrophoresis for the separation of proteins in the range from 1 to 100 kDa. Anal. Biochem. 166, 368–379.

Tapia, J.M., Muñoz, J.A., González, F., Blázquez, M.L., Ballester, A., 2011. Mechanism of adsorption of ferric iron by extracellular polymeric substances (EPS) from a bacterium Acidiphilium sp. Water Sci. Technol. J. Int. Assoc. Water Pollut. Res. 64, 1716–1722.

Tay, J.–H., Liu, Q.–S., Liu, Y., 2001. The role of cellular polysaccharides in the formation and stability of aerobic granules. Lett. Appl. Microbiol. 33, 222–226.

Wingender, J., Neuburger, T.R., Flemming, H.–C., 1999. Microbial Extracellular Polymeric Substances: Characterization, Structure, and Function. Springer.

Wuertz, S., Spaeth, R., Hinderberger, A., Griebe, T., Flemming, H.C., Wilderer, P.A., 2001. A new method for extraction of extracellular polymeric substances from biofilms and activated sludge suitable for direct quantification of sorbed metals. Water Sci. Technol. J. Int. Assoc. Water Pollut. Res. 43, 25–31.

Yang, K., Xing, B., 2009. Adsorption of fulvic acid by carbon nanotubes from water. Environ. Pollut. Barking Essex 1987 157, 1095–1100.

Zinkevich, V., Bogdarina, I., Kang, H., Hill, M.A.W., Tapper, R., Beech, I.B., 1996. Characterisation of exopolymers produced by different isolates of marine sulphate–reducing bacteria. Int. Biodeterior. Biodegrad. 37, 163–172.

CHAPTER VI. COMPARISON OF EPS ORIGINATING FROM *D. ALASKENSIS* GROWN IN VARIOUS CONDITIONS

EPS fills the intercellular space of microbial aggregates and, by various interactions form the architecture of the biofilm matrix. Changes in their secretion, while growing *D. alaskensis* AL1 in various conditions, were investigated. These included tests in static conditions in the VMN growth medium and with a modified VMN medium with 10 times reduced nutrients content. *D. alaskensis* was also grown in the bioreactor with the exchange of the modified medium and presence of carbon steel plates. Seven different EPS were obtained from these conditions. The first four represented the loosely and tightly bound EPS (LB and TB, respectively), extracted from the cells grown in the static conditions. The latter three were obtained from the bioreactor cells, and included LB EPS secreted to the bulk medium, TB EPS from the planktonic cells, and EPS from the biofilm. It was observed that LB EPS were not intensively secreted. They were mainly composed of sugars, secreted in the range from 2.08 ± 0.01 to 8.30 ± 2.10 fg /cell. Protein amounts were from 2 to 4 times lower than sugars. Extracellular DNA and uronic acids were intensively secreted in the TB EPS, grown under starvation in static conditions, and both TB EPS from planktonic cells and from the biofilm. The main components of TB EPS were proteins and humic substances. Additionally, EPS were analysed by SDS-PAGE. From 8 (biofilm EPS) to approx. 30 bands (EPS from the static conditions with non– modified growth medium) were observed in the TB fraction and from 2 to 4 bands in the LB EPS. Fatty acid content of EPS was characterised by GC. This was obtained by the lipid derivatisation of the fatty acid lipid esters (FAME). Unbranched saturated C16 and C18 fatty acids were dominantly secreted.

Transmission electron microscopy experiments showed that EPS components can organise themselves in three main structures, which were compared with existing EPS models. They were identified as probably sugar–protein complex, protein–metal sulfides aggregates and micelle like complexes.

1. INTRODUCTION

Extracellular polymeric substances (EPS) are involved in the formation of microbial aggregates such as sludge, biofilms and flocs, which are referred as the "planktonic biofilms". In this very diverse, self–produced and highly hydrated EPS matrix microorganisms form organised biofilm structures coexisting in a synergistic consortia, and protective against various environmental stresses. Formation of a biofilm allows a lifestyle that is entirely different from the planktonic state. Although planktonic cells produce EPS, its role becomes critical when the microbial biofilm develops and becomes a serious thread for industrial systems.

Biofilm establishment, maturation and maintenance depend on the EPS production and quantities (Sutherland, 2001). Its architecture can also be strongly influenced by anionic EPS, able to entrap various cations. Some EPS, in particular those forming capsules, are associated more closely with cell surfaces than others (Flemming and Wingender, 2010). These discrete polysaccharide – protein layers are tightly bound to the surface of a bacterial cell, closely surrounding it. Less compact, amorphous loosely bound EPS slime is dispersed to the more distant extracellular environment. The schematic organisation of EPS around the cell is shown in **FIG. 6.1**. EPS secretion is dependent on the growth mode, microorganisms present, the shear forces experienced, the temperature and the availability of nutrients.

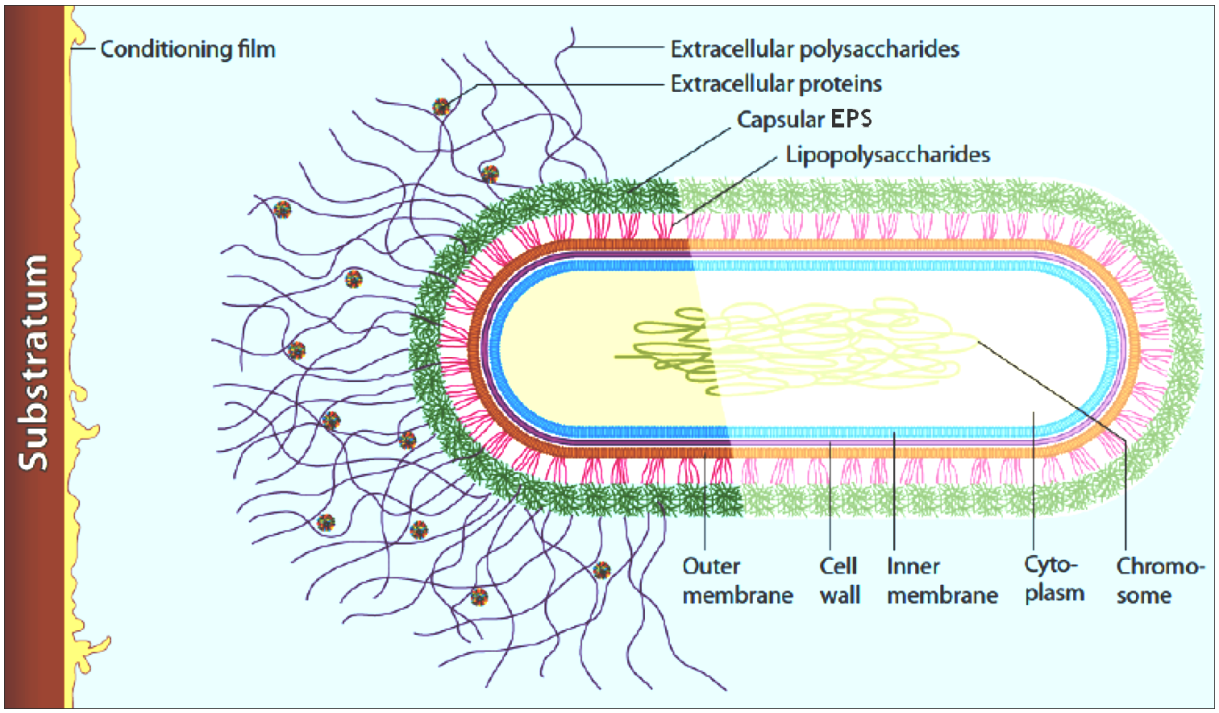

FIG. 6.1. EPS ORGANISATION AROUND THE CELL. A CAPSULE OF TIGHTLY BOUND TO THE SURFACE EXOPOLYMERS WITH DISPERSED LOOSELY BOUND EPS ADEPTED FROM (FLEMMING, 2011).

Beneficial properties of a biofilm growth mode are strongly related to its heterogeneous structure (Davey and O'toole, 2000). Due to the gradients of gases and nutrients within the biofilm, spatial distribution of the representatives of different metabolic groups occurs and thus, the establishment of cooperative relations becomes possible (Stewart and Franklin, 2008). Proteins, in particular the structural ones and those exhibiting enzymatic activity, take part in nutrients sorption. They may also carry out dispersal mechanisms in the conditions of starvation. Furthermore, extracellular redox enzymes play a part in microbially influenced corrosion (Busalmen et al., 2002). Polysaccharides, except their leading structural role maintain a highly hydrated microenvironment around the cells. They may prevent desiccation and serve as a nutrient source on the late stages of biofilm development. The importance of the extracellular DNA was recognised comparatively recently. Apart of facilitating horizontal gene transfer, DNA is believed to contribute to the aggregation of cells and microcolonies formation (Harmsen et al., 2010). Lipids are, probably, the least studied component of exopolymeric matrix. According to some investigations they may be essential for attachment to the hydrophobic surfaces and formation of the water channels, which enable transport of nutrients and metabolites within the biofilm (Espinosa–Urgel, 2003).

In this chapter the changes in bacterial EPS secretion while changing from the laboratory to "field related" conditions were investigated. The function of the extracellular matrix components will be discussed for a better understanding of the biofilm formation processes.

2. MATERIALS AND METHODS

2.1. SRP planktonic growth conditions

The growth conditions for *D. alaskensis* AL1 are shown in Chapter IV. The medium was prepared with either 0.6% or 0.06% (w/v) of sodium lactate (53.6 mM and 5.36 mM, respectively). This reduction of the lactate concentration applied in order to approach to the levels of organic compounds and potential electron donors present in the field conditions (Comanescu et al., 2012). Further annotation of 0.6 and 0.06 will refer to these lactate concentrations in the media. Microorganisms were grown at 30°C under gentle stirring of 100 rpm for three days, and afterwards harvested for EPS extraction.

2.2. Conditions for the biofilm development

In order to simulate oil field related conditions for *D. alaskensis* biofilm growth, the following experimental apparatus in the medium flow–through mode was constructed. The main component of this installation was a 2 L glass bioreactor, interconnected in the circuit with a peristaltic pump. The full scheme of the installation is shown in **FIG. 6.2**. To maintain anoxic conditions and avoid contaminations, a permanent nitrogen flow was kept in the reactor, ensuring a positive pressure throughout the entire survey. Deaeration of the bioreactor was performed with use of a Kobold gas flowmeter. Its application allowed to control the flux of nitrogen flowing through the system and to a constant flux of 10 L/h. Before introducing it to the reactor, applied gas was humidified by passing through a gas–washing bottle filled with sterile deionised water. Nitrogen was supplied through the 0.2 µm filters located between the gas flowmeter and the gas–washing bottle and delivered inside the reactor through the glass frit. Further on, a 2 M zinc acetate trap was mounted to the

bioreactor's gas exit in order to precipitate produced hydrogen sulfide and avoid its escape outside the system.

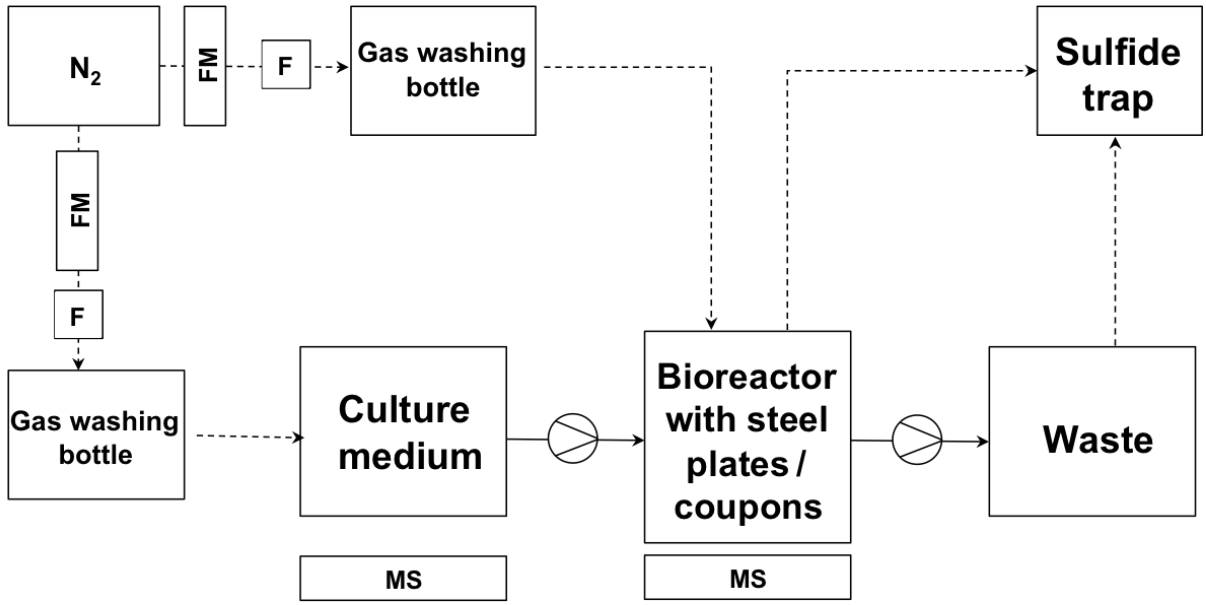

FIG. 6.2. BIOREACTOR SCHEME: DOTTED LINES CORRESPOND TO THE GAS FLOW, WHILE THE CONTINUOUS LINE – LIQUID FLOW; F – GAS FILTER, FM – FLOWMETER, MS – MAGNETIC STIRRING DEVICE.

The dosage of the fresh, sterile growth medium, as well as the removal of the consumed medium took place via the separately connected Ismatec peristaltic pump (IPC). Sterile medium was pumped from the 0.06 VMN stock 10 L bottle. This one was connected to the nitrogen in the same way as in the bioreactor, however with the separate tubing set. The supply vessel was flushed with the gas during the whole survey and stirred as the bioreactor fluids, as further described. The spent culture medium was pumped via separate tubing into the collecting vessels, which were connected to the zinc acetate trap as well. Liquids in the bioreactor were exchanged with a flux of 480 mL/day. For a better distribution of the dosed gas and liquid components an IKA COMBIMAG RCT magnetic stirring device was placed below the reaction vessel. Applied stirring force was uniform for planktonic and sessile cells, as well as for the fresh growth medium supplied to the reactor (100 rpm). Inside the reactor, a 2 cm high teflon stand, able to fit 10 steel plates (5x10x0.2 cm) or 20 steel coupons (2x3x0.2 cm), was mounted. The plates and or coupons, prepared as described further, were oriented parallel to each other and perpendicular to the bioreactors bottom. Pockets for the plates/coupons were wide enough to enable

simple and stable placement of the material, without the risk of scratching the surface. All selected components of the installation were autoclavable. They were disconnected, separately sterilised at 121°C for 30 min and afterwards assembled in a sterile bench. The bioreactor was inoculated as for the planktonic cells with 5% (v/v) inoculum (initial cell number of 10^7 cells/mL). The described survey was performed for 21 days at 30°C. The assembled reactor and the system during its work are shown in **FIG. 6.3**. The pump for medium/waste exchange was switched on 3 days after the inoculation.

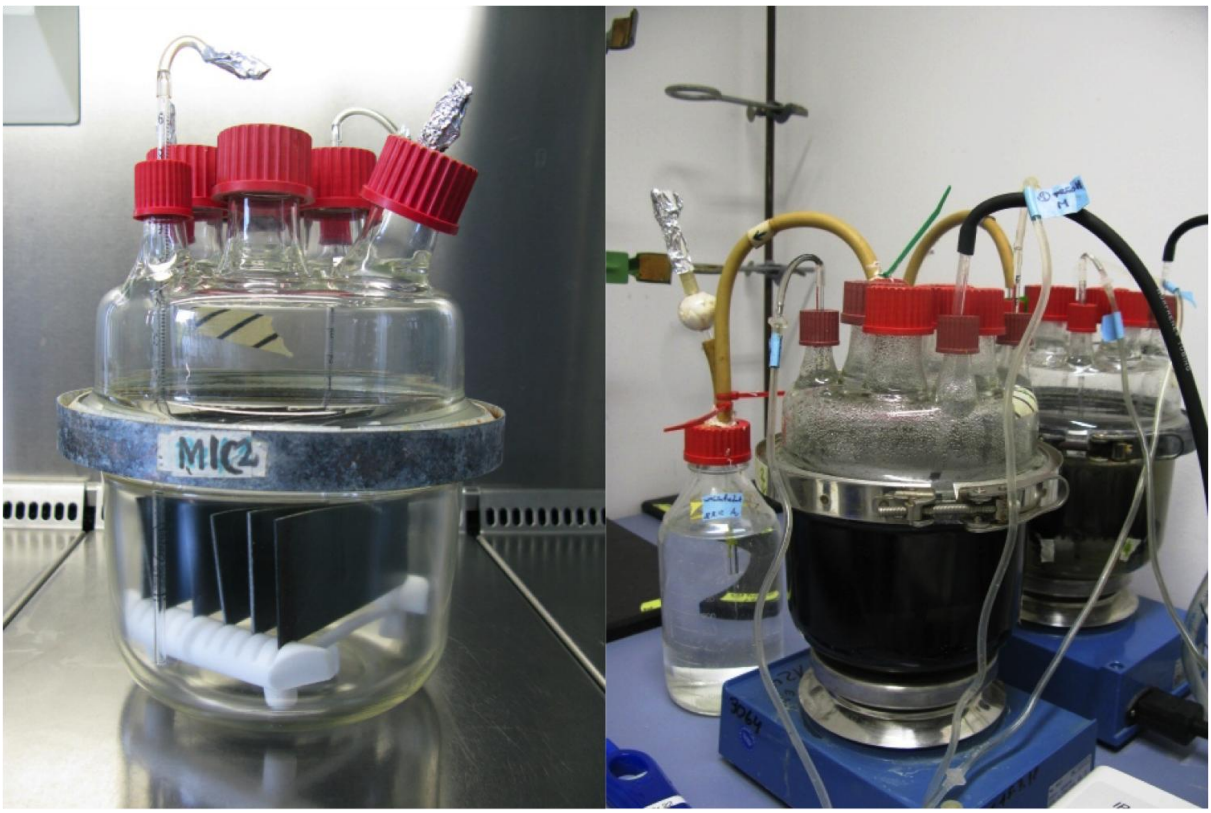

FIG. 6.3. ASSEMBLED BIOREACTOR (LEFT) AND ITS IMPLEMENTATION IN THE SURVEY (RIGHT).

2.3. Specimens preparation

Steel plates (10x5x0.2 cm) and coupons (1x2x0.2cm) used for biofilm winning and weight loss tests were prepared from the same carbon steel sheets as used in Chapter IV (St37–2). Coupons and plates were prepared accordingly.

2.4. Determination of a total cell number in planktonic and biofilm samples

For the determination of total cell numbers in all samples a Z30000 – Helber (Hawksley®) counting chamber was used. Counting was performed using a light microscope (Zeiss®) with the phase contrast at 40x magnification. In case of planktonic cells the sample was directly taken and immediately counted. For estimating the cell number in the biofilm, coupons were removed under sterile conditions and immediately transferred to a Whitley A85 Anaerobic Workstation (Don Whitley Scientific®) with the gas atmosphere of nitrogen, hydrogen and carbon dioxide in the 88:10:2 $v_{N_2}/v_{H_2}/v_{CO_2}$ ratio. Biofilms formed on the steel plates were gathered with a sterile rubber spatula and resuspended in VMN medium. Further on, steel plates were immersed in the same fresh VMN medium and sonicated at 35 kHz (Bandelin Sonorex Digitec DT 510 H–RC sonication bath) at 4°C with a sequence of 2 min sonication and 1 min brake, repeated 3 times. Obtained biofilms were combined, mixed carefully for 2 min and cells were counted as described above.

2.5. EPS extraction and composition analyses

Details of the extraction protocol and its controls, composition and control analyses applied to the investigated EPS samples are found in Chapter V. For the control of the cell lysis 0.6 and 0.06 VMN medium with Dowex were used. Except of previously described composition analyses, sulfide and iron contents were analysed. The former were analysed, as described (Cord–Ruwisch, 1985). For the determination of ferrous iron in the EPS, samples were collected anaerobically, directly after the extraction, filtered and mixed with 1N sulfuric acid in 1:1 (v/v) ratio in anaerobic conditions. Medium residues in the samples for iron and sulfide determination were removed by the centrifugation with Amicon tubes (Chapter V) and 1N sulfuric acid (iron determination) and anaerobic water (sulfide determination). Iron content was measured by means of 1100B Atomic Absorption Spectrometer (AAS) from Perkin Elmer.

EPS composition was calculated and normalised against cell numbers in order to investigate differences in their secretion. Percentages of cell lysis in extracted EPS

were determined based on KDO concentration measurements, as described in the Chapter V.

Seven different EPS fractions were obtained from various experimental approaches (FIG. 6.4). In the static *D. alaskensis* growth conditions four EPS were obtained: LB and TB EPS from the 0.6 VMN medium and LB and TB EPS from the 0.06 VMN medium (later named: 0.6 LB, 0.6 TB, 0.06 LB and 0.06 TB, respectively).

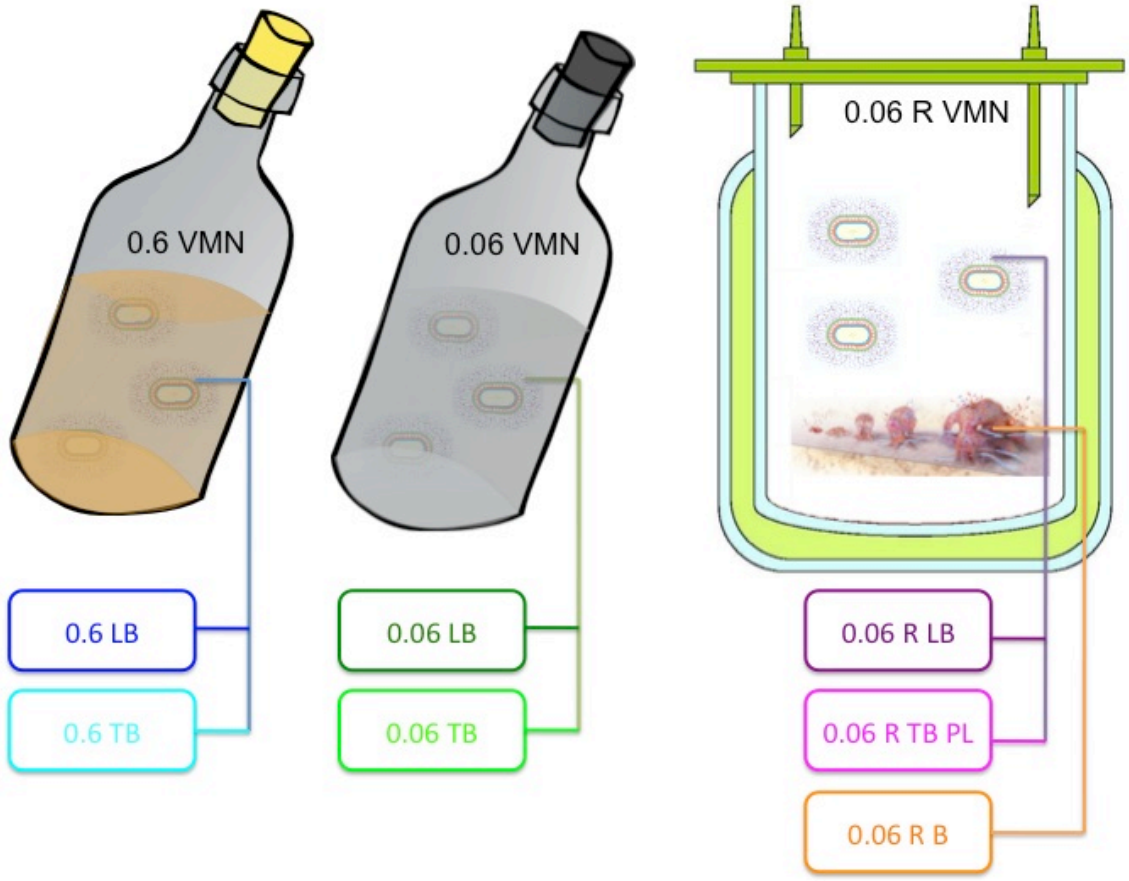

FIG. 6.4. SCHEME OF EPS OBTAINED FROM VARIOUS GROWTH CONDITIONS. 0.6 AND 0.06 CORRESPOND TO THE LACTATE CONCENTRATION WITH 0.6 % AND 0.06% (W/V), RESPECTIVELY; VMN – GROWTH MEDIUM, LB – LOOSELY BOUND EPS, TB – TIGHTLY BOUND EPS, R – REACTOR TRIAL, PL – PLANKTONIC CELLS, B – BIOFILM. CELL SCHEME WAS MODIFIED FROM (FLEMMING, 2011). THE BIOFILM FIGURE WAS TAKEN FROM: WWW.WVLC.UWATERLOO.CA/BIOLOGY447/BIOFILMS.

From the bioreactor survey three types of EPS were collected. The first one was extracted from the biofilm formed on the plates (0.06 R B). For this, the teflon rack with the steel sheets was removed from the bioreactor. The biofilm was gathered in the same way as for the cell count from the coupon biofilms. However, the VMN medium was substituted with the PBS buffer, in order to wash the cells before the extraction. The two other EPS fractions were obtained from the residual cell suspension. This liquid was centrifuged as in the EPS extraction and collected

supernatant was purified (filtration and dialysis, Chapter V). Obtained loosely bound EPS fraction was named as 0.06 R LB. Harvested cell pellet was used to extract the third EPS fraction was extracted (0.06 R TB PL). All obtained EPS were further on investigated for their quantitative and qualitative composition. They were also tested on their influence on the surface (Chapter VII). Protease inhibitors cocktail tablets (cOmplete, EDTA–Free; Roche®) were added as recommended by the manufacturer to all samples directly after their extraction and additionally after the dialysis.

2.6. Characterisation of extracellular proteins

Proteins from LB and TB EPS were analysed by SDS–PAGE as described in Chapter V. Obtained gels were stained with Coomassie G–250 (Dyballa and Metzger, 2009). Furthermore, an attempt was made to verify the presence of heam containing proteins by application of an appropriate staining (Thomas et al., 1976; Goodhew et al., 1986).

2.7. Identification of EPS fatty acids

For these analyses all EPS were concentrated 50x by centrifugation with the Amicon tubes as described in the Chapter V. Then, the samples were mixed with a chloroform – methanol mixture (2:1, v/v), in the 2:3 (v/v, sample to organic mixture) ratio and shaken on a Vortex shaker (Genie 2) at the maximum speed for 10 min. For a better phase separation, the samples were afterwards centrifuged for 5 min at 7000 × g. The organic phase was used for fatty acid derivatisation. Obtained fatty acids methylated esters (FAMEs) were analysed by gas chromatography (GC). Derivatisation and GC protocols can be found elsewhere (Purish et al., 2012).

2.8. EPS visualisation by Transmission Electron Microscopy

The EPS extracted to the organic solvent as described in the Section 2.6 were visualised by JEOL JEM 1011 Transition Electron Microscope (TEM) with cathode made from tungsten, accelerating voltage of 100 kV and resolution of 4–5 Å. Data acquisition was done with slow scans SIS (Megaview III) camera. Images were processed using the iTEM Software. The TEM specimens were prepared by slow

evaporation of droplets of EPS solution of different samples deposited on carbon supported copper grids.

3. RESULTS

3.1. EPS secretion and cell lysis rates

Cell lysis rates, calculated as described in the Chapter V, are shown in TABLE 6.1. The first extraction from the abiotic control (0.6 VMN + Dowex) gave a weak signal while determining the KDO concentration (% of total cell lysis below 0.1%), while the second one (0.6 VMN + Dowex) was equal to 0.64 ± 0.13 %. Cell lysis rates higher than 1% were found in the samples from the reactor survey. In the biofilm sample their amounts reached 3.50 ± 0.54 %.

TABLE 6.1. CELL LYSIS RATES DETECTED IN THE CONTROLS AND IN THE INVESTIGATED EPS.

EPS solution	% of total cell lysis
0.6 VMN + Dowex	0.05 ± 0.01
0.06 VMN + Dowex	0.64 ± 0.13
0.6 LB	0.04 ± 0.01
0.6 TB	0.02 ± 0.01
0.06 LB	0.23 ± 0.03
0.06 TB	0.06 ± 0.01
0.06 R LB	1.04 ± 0.11
0.06 R TB PL	2.09 ± 1.45
0.06 R B	3.50 ± 0.54

EPS composition was normalised per cell amount, in order to compare exopolymers secretion in the different conditions (FIG. 6.5).

All LB EPS were secreted on a comparatively low level. Sugars were secreted in the range from 2.08 ± 0.01 (0.6 LB) to 8.30 ± 0.15 fg / cell (0.06 R LB). Amounts of proteins were approx. 2 to 4 times lower (1.15 ± 0.01 to 2.42 ± 0.17 fg /cell). Uronic acids content in the LB EPS samples was the lowest in the 0.6 LB sample (0.51 ± 0.01 fg / cell). In the 0.06 R LB solution, their quantity was the highest from all EPS (10.43 ± 0.06 fg / cell). Humic substances, among all LB EPS, were the most intensively secreted in 0.06 R LB solution (35.61 ± 2.66 fg / cell).

Proteins and humic substances were the dominant components in the TB EPS. Their concentration was the highest, when the lactate amount was decreased and the carbon steel was absent in the medium (0.06 TB: 135.56 ± 2.82 fg / cell).

Humic substances content in the TB EPS was in the range of 51.4 ± 3.31 fg/cell (0.06 R B EPS) to 221.8 ± 18.6 fg/cell (0.06 R TB EPS), while uronic acids from 1.25 ± 0.01 to 8.40 ± 0.27 fg EPS / cell. Sugar amounts in the 0.06 R B solution reached the value of approx. 11.8 ± 1.1 fg/cell, being approx. twice lower than in other TB EPS.

DNA and sulfides amounts were increased in 2 EPS samples: 0.06 R TB PL and 0.06 R B. Iron was present in 0.06 TB, 0.06 R TB PL and 0.06 R B EPS. In the latter its concentration was equal to 3.05 ± 0.11 fg/cell and it was 3 times higher than in the other EPS.

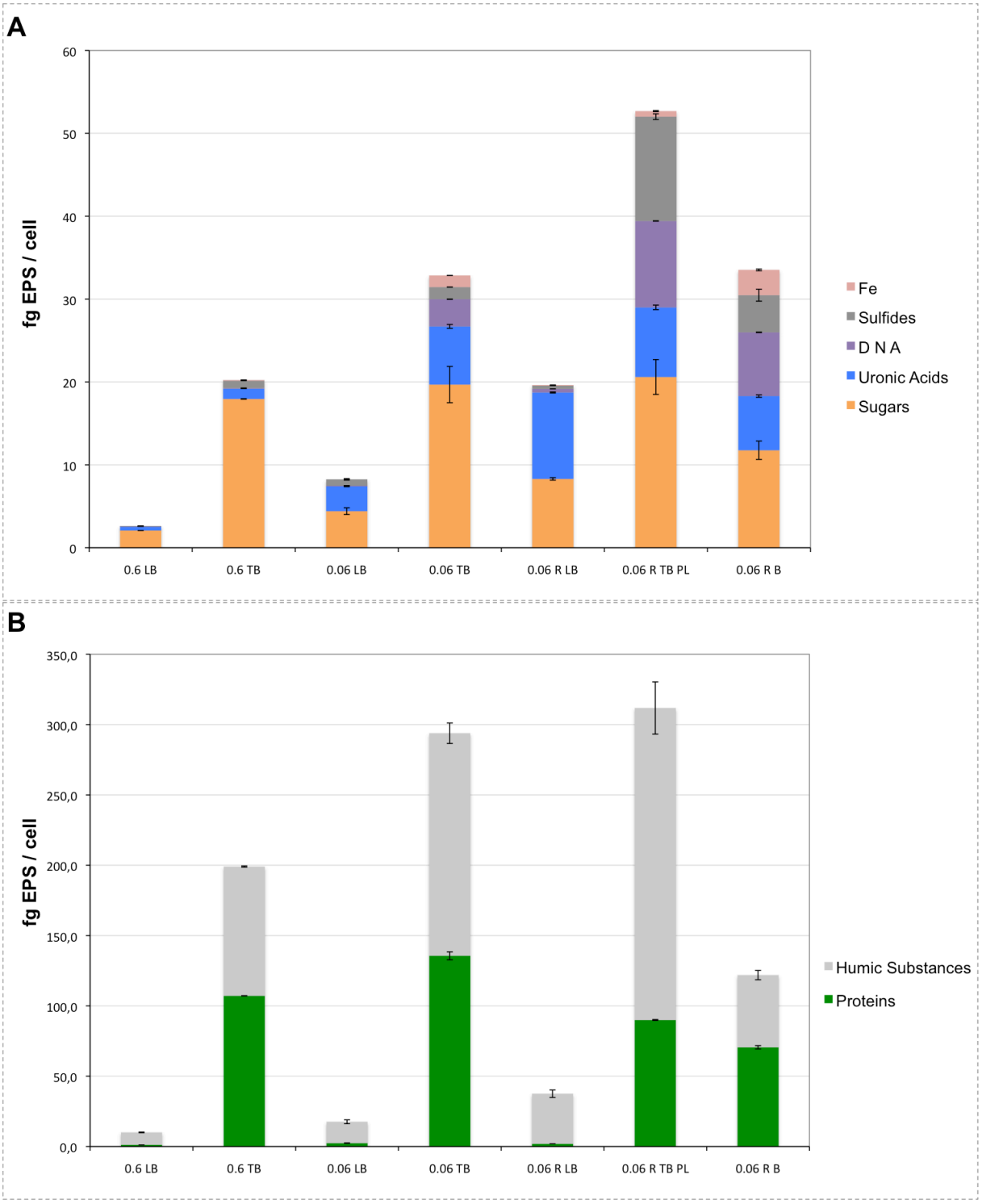

FIG. 6.5. COMPOSITION OD D. ALSKENSIS EPS (IN FG OF EPS PER CELL). A – SUGARS, URONIC ACIDS, DNA, SULFIDES AND IRON CONTENT; B – PROTEINS AND HUMIC SUBSTANCES CONTENT.

3.2. Extracellular proteins profiles

Profiles of all extracellular proteins are shown in the **FIG. 6.6.** The band distribution was similar in all TB EPS. It appeared that the number of secreted TB proteins did decrease when the growth conditions were stepwise modified. The

dominant proteins in the 0.6 TB EPS sample were of approx. 75 and 50–kDa size. In the upper part of this lane two bands of approx. 100 kDa were located very closely to each other. 40, 35 and 27–kDa proteins were also secreted in higher amounts. There were approx. 30 bands observed in this sample. The 0.06 TB EPS profile was similar to the previous one. Some bands were weaker, e.g. 100 kDa or the 50 kDa bands, some did not appear, as observed between 100 and 75 kDa, 75 and 50–kDa, and directly below 50 kDa. In the 0.06 R TB PL EPS the size of the most intensive bands changed. These were approx. 60 and 27 kDa, respectively. A double band, appearing visible only in this EPS, was of approx. 40–kDa size. 0.06 R B EPS had the lowest amounts of EPS, with only approx. 8 bands. These were of 100, 75, 60, 50, 42, 40 and 27–kDa, respectively.

Only 4 protein bands were foundin the 0.6 LB EPS lane: one of 75 kDa, another of approx. 60 kDa, the main one of 50 kDa and week band directly below it. In the 0.06 LB EPS only the double band at approx. 50 kDa was detected. 0.06 LB EPS contained the 75, 60, 50 and 40–kDa bands. All these protein bands were present in TB EPS profile obtained with all ER.

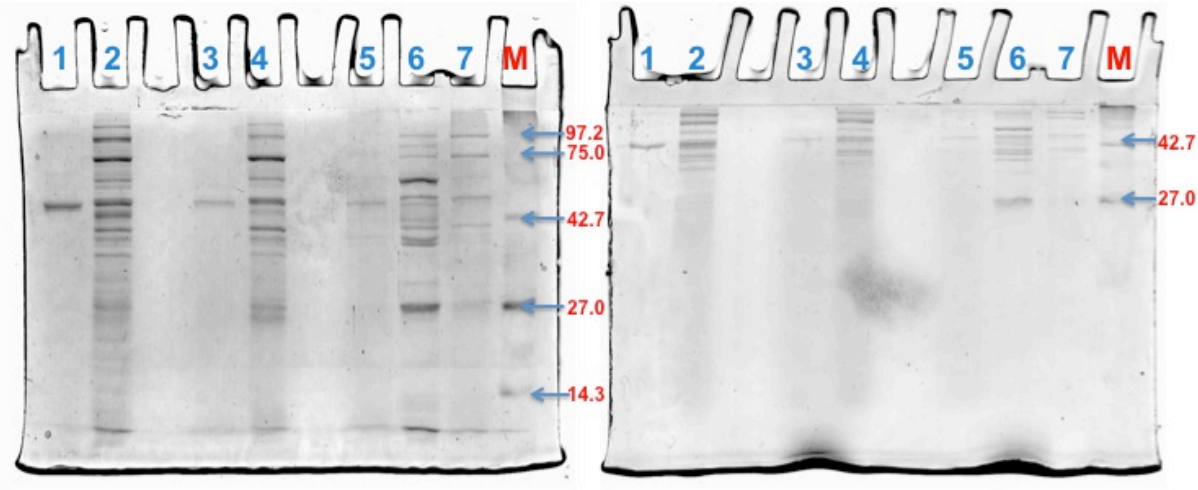

FIG. 6.6. SDS–PAGE PROFILES OF EXTRACELLULAR PROTEINS. ON THE LEFT 10% PAGE, ON THE RIGHT 15% PAGE. NUMBERS CORRESPOND TO THE FOLLOWING EPS SAMPLES: 1 – 0.6 LB; 2 – 0.6 TB; 3 – 0.06 LB; 4 – 0.06 TB; 5 – 0.06 R LB; 6 – 0.06 R PL TB; 7 – 0.06 R B; M – MOLECULAR WEIGHT MARKER.

An attempt was also made to verify the presence of haem containing proteins. The gels were run for either 40 min or 5 to 10 min. In the first approach no bands were detected. However, when this time was reduced, in the upper part of the 0.6 TB and 0.06 TB lanes a weak band was observed (data not shown). It was not possible to attribute it to any protein size.

3.3. Extracellular fatty acids

EPS changes in their FAMEs composition, occuring under the influence of different culturing conditions were investigated by use of GC (FIG. 6.7). Fatty acids content was represented as a percentage of corresponding FAME peak area to the total area of detected peaks. FAMEs were described as C (number of C atoms in the fatty acid chain) : (number of double bonds in this chain); "iso" indicated a branched $–CH(CH3)_2$ structure of FAME.

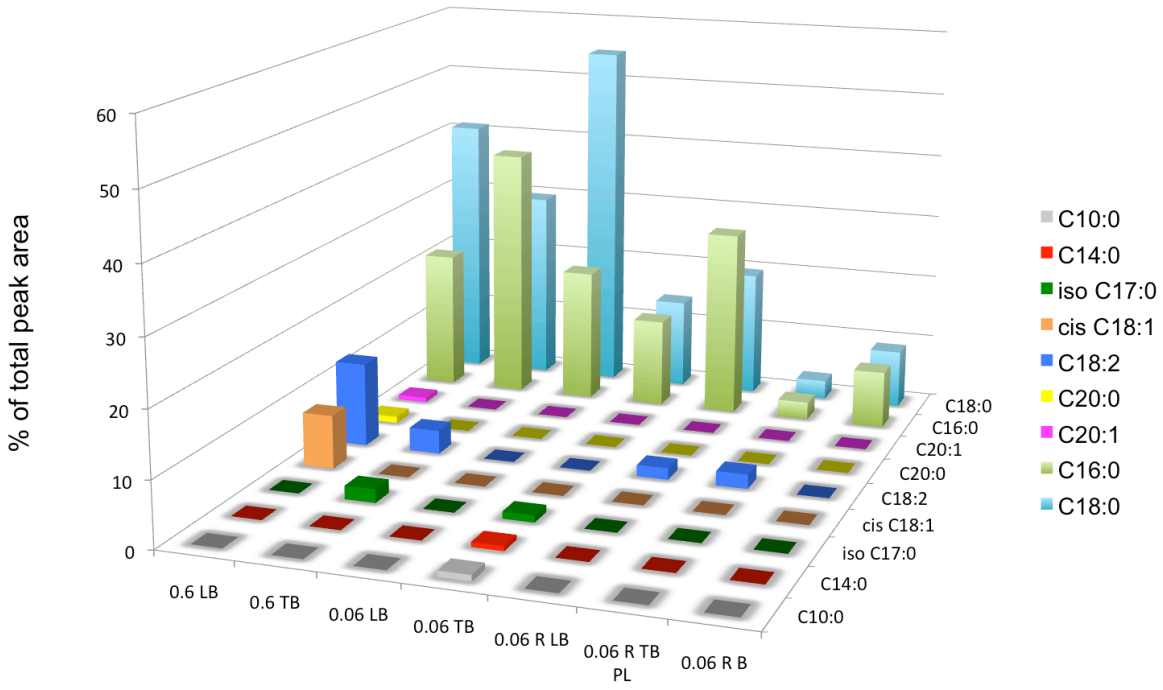

FIG. 6.7. FATTY ACID COMPOSITION OF *D. ALASKENSIS* EPS. FATTY ACID CONTENT WAS REPRESENTED AS A PERCENTAGE OF CORRESPONDING FAME PEAK AREA FROM THE TOTAL AREA OF THE IDENTIFIED PEAKS. FAMES ARE DESCRIBED AS C(NUMBER OF C ATOMS):(NUMBER OF DOUBLE BONDS); "ISO" INDICATES A BRANCHED STRUCTURE OF FAME.

In all kinds of EPS analysed, C18 and C16 were the most abundant fatty acids detected. However, their ratios differed depending on the culturing conditions. Unsaturated fatty acids were found in 0.6 LB and TB and in 0.06 R LB and 0.06 R TB PL EPS. These were mostly C18:1 and C18:2. EPS samples also differed by some minor fatty acids. Interestingly when *D. alaskensis* AL1 was grown in the stationary conditions, branched iso–heptadecanoic acid (iso–C17) was also detected in the

tightly bound EPS fraction (0.6 TB and 0.06 TB). The highest diversity of fatty acids present, with a small shift to the long–chained ones was detected in the 0.6 LB and TB EPS, and 0.06 TB EPS.

3.4. EPS visualisation by TEM

Three EPS structures were observed by TEM microscopy (**FIG. 6.8**). The first one possessed a long, often branched chain with darker amorphous aggregates of various sizes attached to it. In the second form, observed spheres were organised in the branched chains linked with each other by a slimy “rope”. Below these the literature models of similar complexes are presented (the first model related to the sugar–protein and the second one to the protein–metal sulfide complex). The third observed structure contained bigger irregular spheres within a slimy matrix. These were either transparent or contained some dark small grains, as detected in two previous structures.

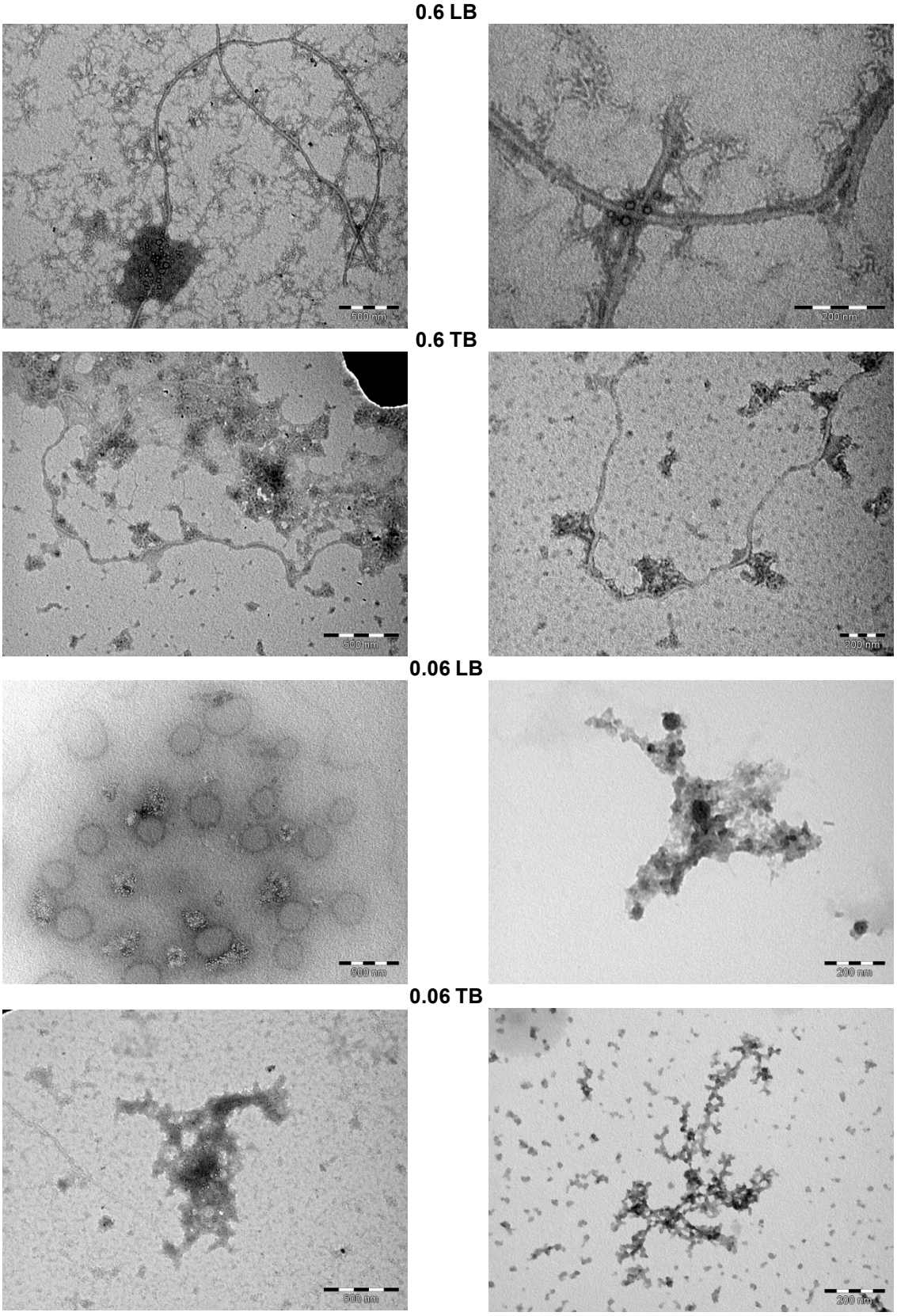

FIG. 6.8 A. EPS FROM THE *D. ALASKENSIS* GROWN IN THE STATIONARY GROWTH CONDITIONS (VISUALISED BY TEM). IN THE LEFT COLUMN OF IMAGES SCALE BARS CORRESPOND TO 500 NM, WHILE IN THE RIGHT TO 200 NM.

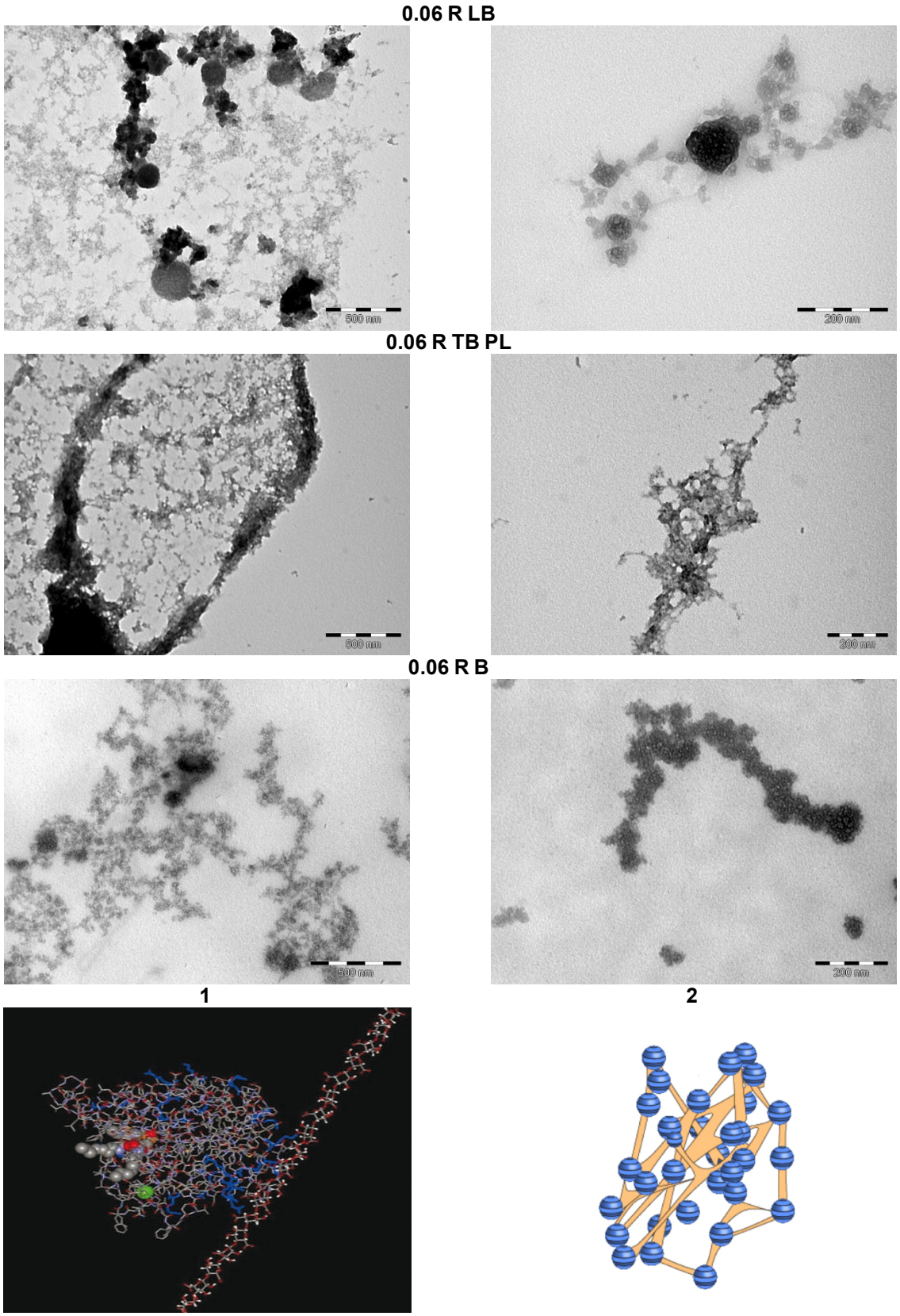

FIG. 6.8 B. EPS FROM THE *D. ALASKENSIS* GROWN UNDER FLOW CONDITIONS (VISUALISED BY TEM). IN THE LEFT COLUMN OF IMAGES SCALE BARS CORRESPOND TO 500 NM, WHILE IN THE RIGHT TO 200 NM. EPS MODELS WERE TAKEN FROM: 1 – (FLEMMING AND WINGENDER, 2010), 2 – WWW.ASKNATURE.ORG/STRATEGY/A1BC03D2AEE740C44F4F38741F8A2469. THE FIRST ONE SHOWED A SUGAR – PROTEIN COMPLEX. THE SECOND ONE SHOWS PROTEINS ENTRAPPING METAL SULFIDES.

4. DISCUSSION

Changes in the EPS from *D. alaskensis* AL1 grown in various conditions, such as the initial decrease of a nutrients and further introduction of a carbon steel to the system, were found.

The first modifications were observed in the sugar secretion. Ten fold lactate decrease in the medium caused twice higher polysaccharides secretion in comparison to the non modifed growth medium. The presence of steel plates also induced further polysaccharides augmentation (in 0.06 R LB EPS) – also by a factor of approx two with respect to 0.06 LB and close to 4 times when compared to the normal medium. Polysaccharides were also the dominant component of the LB EPS. As shown in **FIG. 6.1** (Flemming, 2011), loosely associated polysaccharides seem to be the first molecules, which get in contact with the surface. Thus, higher amounts of this moiety may be needed to create a firm connection with the surface.

Polysaccharides in the TB EPS were secreted on comparable levels between them. Only in the normal VMN medium, these were 9% lower. However in the biofilms, their levels decreased approx. 50% against all TB EPS. In many bacteria, exopolysaccharides are indispensable for biofilm building, and mutants that cannot synthesise them are severely limited or even unable to form mature biofilms (Danese et al., 2000; Ma et al., 2009). Polysaccharides hydrate very quickly in contact with water and link the cells to form these gel like structures (Wotton, 2007). As mentioned earlier, in planktonic bacteria they may help to form stable gel–like flocks, and to maintain this very fragile structure.

Uronic acids were secreted either in comparable or lower amounts than sugars. Again the lowest levels of these substances were reported in the conditions, where SRP were not subjected to any stresses (0.6 LB and TB EPS). The acidic polysaccharides are not related with the primary attachment of bacterial cells, but they are considered to be involved in the time–dependent development of the biofilm (Beech and Gaylarde, 1991). Uronic acids may represent one mechanism, whereby SRP increase corrosion. They can chelate metal ions by forming salt bridges between these ions and the carboxyl groups.

Extracellular DNA was present in the 0.06 TB sample. However, there was no significant change in the protein profile and the cell lysis rate was very low. The highest amounts of eDNA were present in the EPS from the biofilm and planktonic

cells present in the reactor trial. Biofilms of various origins have been found to contain these molecules (Flemming and Wingender, 2010). Extracellular DNA was for a long time believed to be the residual DNA from the lysed cells. However, some similarities but also differences between the eDNA and genomic DNA were reported (Böckelmann et al., 2006). It has been demonstrated that this e–DNA was not simply released by lysed cells. Its possible function may be related to the horizontal gene transfer. However, eDNA has also been reported to be important for the maintenance of the microcolonies, structural integrity and even to serve as adhesin contributing to the conditioning layer formation (Vilain et al., 2009; Nijland et al., 2010; Dominiak et al., 2011).

EPS could also entrap sulfides and iron ions. Sulfides were dominantly found in the tightly bound and biofilm EPS from the reactor survey (0.06 R TB PL and 0.06 R B). Possibly, the flow conditions in the bioreactor allowed SRP to constantly produce sulfides and thus, create the favourable conditions to entrap them in the EPS matrix. Iron (II) ions were found in the same samples, as sulfide. Additionally, it was detected in the 0.06 TB EPS. It appeared that the combination of less lactate and biofilm growth mode provoked higher levels of captured iron. And this can be correlated with increased amount of uronic acids, which were probably one of the cations compexing molecules.

Proteins present in the loosely bound EPS were secreted in small amounts. It was detected, that they were one of the major components of all tightly bound and biofilm EPS. Their secretion varied in the stationary and flow conditions. In the latter from 34% (0.06 R TB PL) to 48 % (0.06 R B) less proteins were observed in comparison to 0.06 TB EPS sample. This also found its response in the lower band numbers in SDS–PAGE gels. Proteins, originating from the cells grown in the stationary conditions, were also more diverse and contained haem groups.

Secretion of large amounts of extracellular proteins, which far exceeded the polysaccharide content has been already reported (Frølund et al., 1996; Conrad et al., 2003). It has been shown in the environmental biofilms, in activated sludge and biofilms in sewers (Jahn and Nielsen, 1998). Extracellular enzymes, such as the SRP hydrogenases are known to stay active within the biofilm matrix, irrespective of the absence of living cells, and can play a significant role in the biocorrosion of iron and ferrous alloys (Beech, 2002).

The other major compounds detected in the investigated EPS were humic substances. The highest levels of these compounds were observed in two TB EPS samples – first one originating from the static conditions with reduced amounts of lactate (0.06 TB) and the second from the planktonic cells grown in the bioreactor conditions (0.06 R TB PL). Humic acids with hydroxyl–, phenoxyl–, and carboxyl–reactive groups can form coordination compounds with various metals (Pandey et al., 2000). They create highly stable complexes especially with copper and iron ions. Thus, they function could be similar to uronic acids. Humic substances are also surface active. They are amphiphilic as well. This may be of high importance, when the conditioning film modifies the surface hydrophilic/hydrophobic properties. Humic acids, similarly like sugars, could mediate the contact between the cell and the surface.

Nevertheless, most of the studies on EPS reported in literature have been focused on its water–soluble part, neglecting its hydrophobic components. In all kinds of EPS analysed, C18 and C16 were the most abundant fatty acids detected. Interestingly, when *D. alaskensis* AL1 was grown in static conditions, branched iso–heptadecanoic acid (iso–C17) was detected in the tightly bound EPS fraction, independent on the lactate levels. These results demonstrate that the environment could influence the composition of extracellular fatty acids. Bacterial fatty acids have been reported to be involved in enzymes activation and protein modification (Kaneda, 1991). These processes might be of high importance for the biofilm formation, metal–microbial interactions and biocorrosion development. These non–polar molecules are believed to contribute to the formation of water channels in the mature biofilm, which allow transporting nutrients and metabolites (Davey et al., 2003). Extracellular fatty acids were also shown to be of high relevance to the fouling layer formation in the membranes from a full–scale membrane bioreactor treating municipal wastewater (Al–Halbouni et al., 2009). A study of the *Acidithiobacillus ferrooxidans* EPS showed that a significant part of it is composed of fatty acids, which might be involved in cell adhesion to sulfide minerals (Kinzler et al., 2003).

The absence of the surface, to which cells could attach and build their “biofilm homes” provoked significant change in the EPS composition. The chemical heterogeneity, observed on the example of proteins and lipids, was lower, when *D. alaskensis* was grown in the presence of the carbon steel. Therefore, two questions arise: why there are less diverse EPS secreted, when the steel is

introduced to the surface and why their amounts decrease so significantly in the biofilm.

Under the flow conditions, metabolites are removed and fresh nutrients are provided. Thus, SRP might not suffer from lack of nutrients or excess of sulfides. In this way EPS may be unnecessary to be secreted in higher amounts.

Another scenario would include the secretion of hydrolitic enzymes, which could degrade EPS. When the conditions in the biofilm become unfavourable, the hydrolytic degradation of EPS becomes the way for the cells to escape the matrix and return to planktonic state. This would allow bacteria to detach and to search for more favourable conditions.

Nevertheless, chemotaxis studies to iron ions were done (Asaulenko et al., 2004). It was shown that some SRP strains were able to migrate to the source of iron. These strains with higher ability to migration caused higher weight loss in experiments with carbon steel coupons. If bacteria can "feel" the surface and use it for colonisation, this can result in a modified EPS composition. Also, the fact that bacteria often live as communities associated with solid surfaces rather than as planktonic individuals is not a recent discovery (Meadows, 1971). Biofilm mode of life is probably the most beneficial and successful form of live for microorganisms (Flemming and Wingender, 2010). If the surface is not yet known, more diverse, molecules might be secreted, reaching a “state of readiness” for the biofilm formation. When the surface is already present and recognised by the first attached cells, they might be able to define more precisely their needs, and thus, secrete and use only these EPS, which will be probably the most appropriate.

Finally, EPS were visualised by TEM, showing very interesting structures. One could be attributed to the polysaccharide – protein complex (Flemming and Wingender, 2010). These were observed in the EPS extracted from cells, grown in static conditions. Sugars and proteins carry a variety of functional groups: carboxyl and amide groups, hydroxyl and acetal groups. Within and between macromolecules carrying these residues, a number of molecular interactions are possible to occur: electrostatic forces between various ionic or non–ionic functional groups, hydrogen bonds and dispersion interactions (London interactions, often referred to as van der Waals forces). The repulsive interactions can be altered by the presence of ions, which either partially compensate or screen the charges. In case of bivalent cations, they also cause bridging between neighbouring chains. The electrostatic interactions

involve divalent cations. In particular Ca^{2+}, which is responsible for a considerable proportion of the overall binding energy (Mayer et al., 1999). However, there are also proteins that can bind carbohydrates and they are present in large numbers in all living cells (Quiocho, 1986). The existence of a sugar–protein complexes in EPS from SRP, capable of accelerating the deterioration of mild steel, has also been reported in the literature (Beech et al., 1998). Thus, the high extraction efficiency, observed for sugars and proteins (Chapter V), may be explained also by above–mentioned factors.

In the 0.06 LB and TB, as well as in the EPS extracted from the cells grown in the bioreactor a second complex was observed. This was attributed to the protein – metal sulfides complex. It was shown that the extracellular proteins of some SRP limit the dispersal of nanoparticles by aggregating them (Moreau et al., 2007). SRP release sulfide, which binds with various cations and sequester them into nanoparticles. Proteins and polypeptides released by SRP create spheres of metal sulfide nanocrystals. The key to the clumping was the inclusion of the proteins into pores on the spheres. Cysteine or cysteine–rich polypeptides were the driving force in this process.

The third observed round structures, present in all samples, could be built from various EPS molecules mixed micelles. These are amphiphilic block polymers, with sizes ranging 10–200 nm (Tan et al., 2013). Their size can vary and may be affected by adsorption of other molecules. As the samples were prepared by the organic solvents extraction, the inverse micelles (with hydrophilic core and hydrophobic shell) would be observed. Micelles containing acid–functional groups should be capable of sequestering amine–containing molecules creating supramolecular nanostructures.

5. CONCLUSIONS

The EPS matrix and its secretion by microorganisms is connected to the environmental factors and changes in microbial surrounding. While adapting the laboratory conditions to the more field related ones, various interesting observations were made. It appears that, independently of the growth conditions sugars were the main component of the LB EPS, while humic substances and proteins were dominant in the TB EPS fraction. Uronic acids were more intensively secreted when SRP were grown under the starvation conditions or steel presence. In this environment also e–

DNA, iron and sulfide presence was detected. Qualitative changes were also detected between various EPS. If bacteria were grown in conditions of optimal nutrition levels, EPS were secreted in the lowest amounts. However, the diversity of their proteins and lipids was the highest among all investigated EPS samples. 10 fold lactate decrease provoked an increase in the EPS amounts, with a slight decrease in protein diversity and shorter chain fatty acids. Approximation to the field conditions in the bioreactor provoked significant changes in the EPS secretion with much fewer proteins and only C16 and C18 saturated fatty acids. This phenomenon was attributed not only to the flow conditions, medium change and removal of toxic metabolic products. The absence of a defined surface might provoke cells, to differentiate their EPS composition, in order to “prepare themselves” to the possible attachment and biofilm formation on different surfaces.

EPS sugars could be responsible for the structural stabilisation of the biofilm. In addition to the uronic acids, humic substances could be also involved in the complexation of cations. As amphiphilic molecules, together with lipids, they could also contribute to the biofilm integrity. It was observed that secreted EPS build very complex structures, probably providing microorganisms to build the some beneficial for their growth and maturation conditions. Interactions between sugars and proteins, between proteins and inorganic matter or the formation of micelle–like aggregates are some of the examples. The influence of these compounds on the steel behaviour will be described in the Chapter VII, in order to assess their corrosive properties.

6. REFERENCES

Al–Halbouni, D., Dott, W., Hollender, J., 2009. Occurrence and composition of extracellular lipids and polysaccharides in a full–scale membrane bioreactor. Water Res. 43, 97–106.

Asaulenko, L.H., Purishch, L.M., Kozlova, I.P., 2004. [Stages of biofilm formation by sulfate–reducing bacteria]. Mikrobiolohichnyĭ Zhurnal Kiev Ukr. 1993 66, 72–79.

Beech, I.B., 2002. Biocorrosion: role of sulfate–reducing bacteria, in: Encyclopedia of Environmental Microbiology. Wiley, New York, pp. 465–475.

Beech, I.B., Coutinho, C., 2003. Biofilms on corroding materials, in: Biofilms in Medicine, Industry and Environmental Biotechnology Characteristics, Analysis and Control. IWA Publishing of Alliance House, London, pp. 115–131.

Beech, I.B., Gaylarde, C.C., 1991. Microbial polysaccharides and corrosion. Int. Biodeterior. 27, 95–107.

Beech, I.B., Zinkevich, V., Tapper, R., Gubner, R., 1998. Direct involvement of an extracellular complex produced by a marine sulfate-reducing bacterium in deterioration of steel. Geomicrobiol. J. 15, 121–134.

Böckelmann, U., Janke, A., Kuhn, R., Neu, T.R., Wecke, J., Lawrence, J.R., Szewzyk, U., 2006. Bacterial extracellular DNA forming a defined network–like structure. Fems Microbiol. Lett. 262, 31–38.

Busalmen, J.., Vázquez, M., de Sánchez, S.., 2002. New evidences on the catalase mechanism of

microbial corrosion. Electrochimica Acta 47, 1857–1865.
Comanescu, I., Melchers, R.E., Taxen, C., 2012. Correlation between MIC and water quality, pigging frequency and biocide dosing in oil field water injection pipelines. Eur. Corros. Congr. Paper No.: 1527 (in press).
Conrad, A., Suutari, M.K., Keinänen, M.M., Cadoret, A., Faure, P., Mansuy–Huault, L., Block, J.–C., 2003. Fatty acids of lipid fractions in extracellular polymeric substances of activated sludge flocs. Lipids 38, 1093–1105.
Cord–Ruwisch, R., 1985. A quick method for the determination of dissolved and precipitated sulfides in cultures of sulfate–reducing bacteria. J. Microbiol. Methods 4, 33–36.
Dominiak, D.M., Nielsen, J.L., Nielsen, P.H., 2011. Extracellular DNA is abundant and important for microcolony strength in mixed microbial biofilms. Environ. Microbiol. 13, 710–721.
Danese, P.N., Pratt, L.A., Kolter, R., 2000. Exopolysaccharide production is required for development of Escherichia coli K–12 biofilm architecture. J. Bacteriol. 182, 3593–3596.
Davey, M.E., Caiazza, N.C., O'Toole, G.A., 2003. Rhamnolipid Surfactant Production Affects Biofilm Architecture in Pseudomonas aeruginosa PAO1. J. Bacteriol. 185, 1027–1036.
Davey, M.E., O'toole, G.A., 2000. Microbial biofilms: from ecology to molecular genetics. Microbiol. Mol. Biol. Rev. Mmbr 64, 847–867.
Dyballa, N., Metzger, S., 2009. Fast and sensitive colloidal coomassie G–250 staining for proteins in polyacrylamide gels. J. Vis. Exp. Jove.
Espinosa–Urgel, M., 2003. Resident parking only: rhamnolipids maintain fluid channels in biofilms. J. Bacteriol. 185, 699–700.
Flemming, H.–C., 2011. Microbial Biofouling: Unsolved Problems, Insufficient Approaches, and Possible Solutions, in: Flemming, H.–C., Wingender, J., Szewzyk, U. (Eds.), Biofilm Highlights, Springer Series on Biofilms. Springer Berlin Heidelberg, pp. 81–109.
Flemming, H.–C., Wingender, J., 2010. The biofilm matrix. Nat. Rev. Microbiol. 8, 623–633.
Frølund, B., Palmgren, R., Keiding, K., Nielsen, P.H., 1996. Extraction of extracellular polymers from activated sludge using a cation exchange resin. Water Res. 30, 1749–1758.
Goodhew, C.F., Brown, K.R., Pettigrew, G.W., 1986. Haem staining in gels, a useful tool in the study of bacterial c–type cytochromes. Biochim. Biophys. Acta Bba – Bioenerg. 852, 288–294.
Harmsen, M., Yang, L., Pamp, S.J., Tolker–Nielsen, T., 2010. An update on Pseudomonas aeruginosa biofilm formation, tolerance, and dispersal. Fems Immunol. Med. Microbiol. 59, 253–268.
Jahn, A., Nielsen, P.H., 1998. Cell biomass and exopolymer composition in sewer biofilms. Water Sci. Technol. 37, 17–24.
Kaneda, T., 1991. Iso– and anteiso–fatty acids in bacteria: biosynthesis, function, and taxonomic significance. Microbiol. Rev. 55, 288–302.
Kinzler, K., Gehrke, T., Telegdi, J., Sand, W., 2003. Bioleaching—a result of interfacial processes caused by extracellular polymeric substances (EPS). Hydrometallurgy 71, 83–88.
Ma, L., Conover, M., Lu, H., Parsek, M.R., Bayles, K., Wozniak, D.J., 2009. Assembly and development of the Pseudomonas aeruginosa biofilm matrix. Plos Pathog. 5, e1000354.
Mayer, C., Moritz, R., Kirschner, C., Borchard, W., Maibaum, R., Wingender, J., Flemming, H.C., 1999. The role of intermolecular interactions: studies on model systems for bacterial biofilms. Int. J. Biol. Macromol. 26, 3–16.
Meadows, P.S., 1971. The attachment of bacteria to solid surfaces. Arch. Für Mikrobiol. 75, 374–381.
Moreau, J.W., Weber, P.K., Martin, M.C., Gilbert, B., Hutcheon, I.D., Banfield, J.F., 2007. Extracellular Proteins Limit the Dispersal of Biogenic Nanoparticles. Science 316, 1600–1603.
Nijland, R., Hall, M.J., Burgess, J.G., 2010. Dispersal of Biofilms by Secreted, Matrix Degrading, Bacterial DNase. Plos One 5, e15668.
Pandey, A.K., Pandey, S.D., Misra, V., 2000. Stability constants of metal–humic acid complexes and its role in environmental detoxification. Ecotoxicol. Environ. Saf. 47, 195–200.
Purish, L.M., Asaulenko, L.G., Abdulina, D.R., Vasil'ev, V.N., Iutinskaia, G.A., 2012. Role of polymer complexes in the formation of biofilms by corrosive bacteria on steel surfaces. Prikl. Biokhim. Mikrobiol. 48, 294–301.
Quiocho, F.A., 1986. Carbohydrate–binding proteins: tertiary structures and protein–sugar interactions. Annu. Rev. Biochem. 55, 287–315.
Stewart, P.S., Franklin, M.J., 2008. Physiological heterogeneity in biofilms. Nat. Rev. Microbiol. 6, 199–210.
Sutherland, I.W., 2001. The biofilm matrix—an immobilized but dynamic microbial environment. Trends Microbiol. 9, 222–227.
Tan, C., Wang, Y., Fan, W., 2013. Exploring Polymeric Micelles for Improved Delivery of Anticancer Agents: Recent Developments in Preclinical Studies. Pharmaceutics 5, 201–219.
Thomas, P.E., Ryan, D., Levin, W., 1976. An improved staining procedure for the detection of the peroxidase activity of cytochrome P–450 on sodium dodecyl sulfate polyacrylamide gels. Anal.

Biochem. 75, 168–176.
Vilain, S., Pretorius, J.M., Theron, J., Brözel, V.S., 2009. DNA as an Adhesin: Bacillus cereus Requires Extracellular DNA To Form Biofilms. Appl. Environ. Microbiol. 75, 2861–2868.
Wotton, R.S., 2007. The ubiquity and many roles of exopolymers (EPS) in aquatic systems. Sci. Mar. 68.

CHAPTER VII. INFLUENCE OF EPS ON THE ELECTROCHEMICAL BEHAVIOUR OF CARBON STEEL IN MARINE CONDITIONS

In this study an attempt was made to investigate the influence of EPS from *D. alaskensis* AL1 on carbon steel surface behaviour. To understand better surface changes corrosion potential (E_{corr}) monitoring together with Electrochemical Impedance Spectroscopy (EIS) and Linear Polarisation (LP) were used to monitor surface response to the presence of loosely and tightly bound EPS extracted from the cells grown in planktonic and biofilm state, in presence or absence of carbon steel. More protective behaviour was observed for loosely bound EPS in comparison to artificial seawater (ASW), while the impact of tightly bound EPS was comparable to ASW. From the surface tension measurements it was observed that *D. alaskensis* EPS contained significant amounts of surface–active molecules. Further on, EPS attached to the carbon steel surface was characterised by X–ray Photoelectron Spectroscopy (XPS). These macromolecules, which showed low inhibitory effects on the steel deterioration, were mainly consisting of proteins. The remaining EPS had high levels of hydrocarbons. Observed aggressiveness of extracellular proteins highlights their importance in MIC processes.

1. INTRODUCTION

Any surface in contact with a biological matter is a potential target for microbial cell adhesion. Especially, industrial plants are ideal incubators for microbial activity and biofilm development, providing optimal conditions for their growth. This includes an appropriate temperature, pH between 6 and 9 and being a continuous source of nutrients – inorganic or organic. Life in biofilms happens in a very complex microenvironment. EPS generation is initiated with the coating of a surface with the conditioning layer and reversible attachment of microorganisms. The conditioning layer may influence microbial adhesion by affecting the physico–chemical interactions at interfaces or by its involvement in specific interactions with the cells (Schneider and Leis, 2003). The EPS biomolecules secreted by the microorganisms present in the environment can influence the initial bacterial attachment (Dufrěne et al., 1996) and further biofilm formation and biocorrosion process (Beech and Sunner, 2004; Beech et al., 2005). Since all the other cells within a biofilm rely on the interaction between the surface and mother cells for their survival, this phase of the biofilm life cycle is critical for their existence (Palmer et al., 2007). It is thought that a multitude of factors are involved in the primary attachment, including the surface characteristics, microorganisms involved, exopolymeric cell cover, as well as environmental conditions.

Biofouling is a natural consequence of the biofilm formation. Its significant negative effects include blockage of fluids transport in the system with its subsequent mechanical damage and MIC (Rajagopal S. et al., 1996; Thierry and Sand, 2002; Flemming, 2011). An understanding of EPS function and their effect on the surface behaviour may help in development of MIC mitigation approaches. Therefore, the main focus of this work was to investigate the influence of adsorbed EPS on the electrochemical behaviour carbon steel, widely used in the O&G industry. As the seawater is an inherent environment of the oil platforms, artificial seawater (ASW) was chosen as the basic milieu for these tests and served as the control for further EPS assessment. The chemical nature of the surface–active molecules present in EPS was complementarily investigated with use of X–ray photoelectron spectroscopy and surface tension measurements.

2. MATERIALS AND METHODS

2.1. Electrochemical experiments

2.1.1. Carbon steel and EPS preparation

As for all previous studies, the St37–2 carbon steel was used. The surface area of steel disks exposed to the solution was equal to 0.454 cm^2, and the tightness between the disk and the sample holder was ensured by an inert Viton® O–ring. Before electrochemical measurements, samples were mechanically polished with SiC papers down to the grit 600, then degreased in acetone in an ultrasonic bath (f = 50 Hz; Branson 1510) for three times during 5 min, dried under an argon flow, and finally exposed to UV/ozone chamber (UV/ozone Pro Cleaner, Bioforce nanoscience) for 20 min.

ASW with pH = 8.0 (Berglin and Elwing, 2008) was used as a control solution. Further on, all 7 EPS samples, as described in the previous chapter and shown in the **FIG. 6.4**, were investigated. After their extraction, EPS were additionally dialysed against ASW, to ensure the same basic environment as for the control. Subsequently, EPS samples were diluted with ASW to obtain in all of them an equal protein concentration of 20 mg/L. Applied protein concentration was unified with parallel studies performed by the network partner from the Centre National de la Recherche Scientifique, Laboratoire de Physico–Chimie des Surfaces (CNRS – LPCS), Chimie ParisTech Paris, France, where investigations of influence of various proteins and EPS from *Pseudomonas* sp. 2021 were performed. Comparable experimental conditions allowed correlating the influence of various EPS on the steel surface.

2.1.2. Measurements

The electrochemical measurements were performed with a three–electrode cell, designed and manufactured at CNRS – LPCS, with a volume of approx. 100 mL, as shown in **FIG. 7.1**. The working electrode (WE) was the St37 – 2 disc, the counter–electrode (CE) was a graphite sheet, and the reference electrode (RE) was a

saturated calomel electrode (SCE). Experiments were carried out in stagnant conditions (static working electrode and solution).

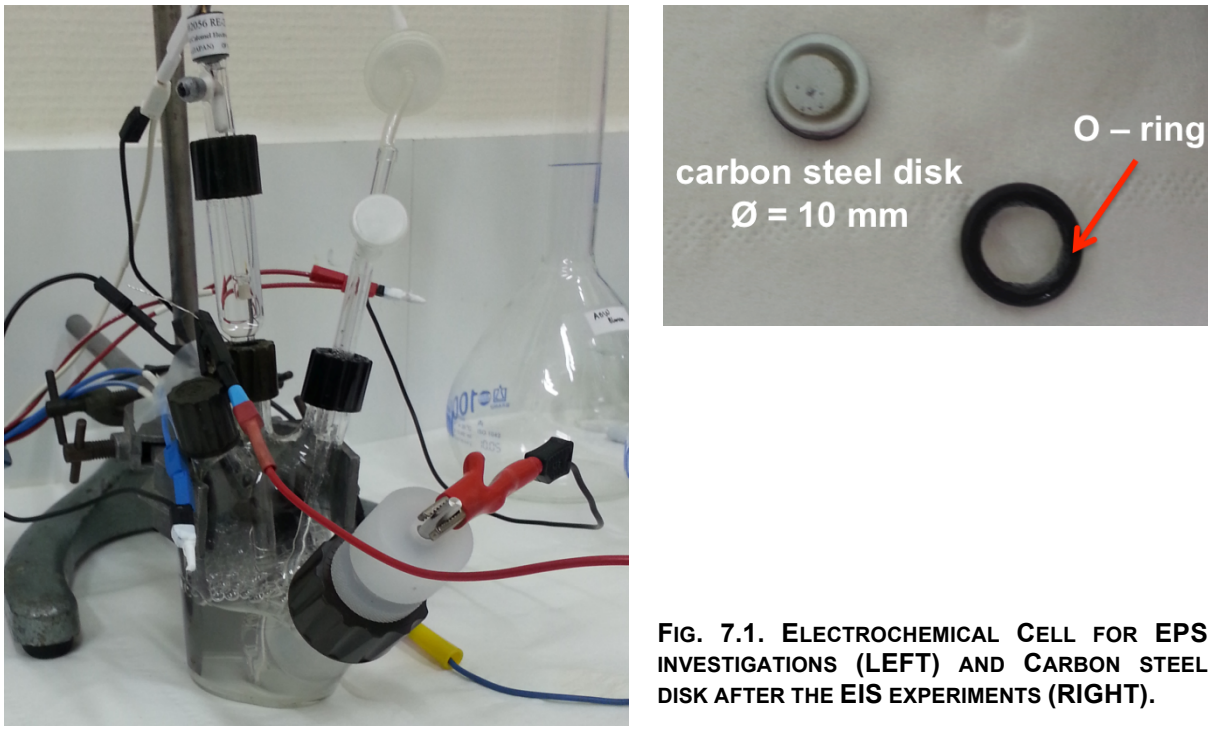

FIG. 7.1. ELECTROCHEMICAL CELL FOR EPS INVESTIGATIONS (LEFT) AND CARBON STEEL DISK AFTER THE EIS EXPERIMENTS (RIGHT).

The corrosion potential (E_{corr}) was measured for 2 h directly after the immersion, then either a cathodic or anodic polarisation curve was plotted separately starting from + 20 or – 20 mV *vs.* E_{corr}, respectively, using a scan rate of 0.5 mV/s. Electrochemical impedance diagrams were plotted at E_{corr} after 2 h of immersion, with a frequency domain ranging from 10^5 Hz to 10^{-3} Hz, 7 points per decade, and an amplitude of 10 mV peak–to–peak. Electrochemical measurements were performed with the EC–Lab SP–200 System from Bio–Logic® or Autolab PG STAT 30 potentiostat. All the experiments were performed in duplicate, at room temperature under anaerobic conditions. The later ones have been provided by argon bubbling in the vessel for at least 1 h before the beginning of the experiment. Gas purging was performed during the whole measurement. The gas was filtered with a 0.2 µm pore size filter. In case of EIS measurement, the gas tube was raised up above the solution level 15 minutes before starting the plotting, in order not to induce noise on the impedance data. Additionally, cathodic polarisation curves were also plotted in aerated ASW (solution in equilibrium with air).

2.2. Surface investigations

2.2.1. Substrates and extracellular polymers

Two approaches were applied for the investigations of surface–active EPS molecules. Firstly the glass disks (Gl) with diameter of 1.2 cm (Menzel–Gläser, Germany) were cleaned using a piranha solution (7:3 v/v mixture of 97% sulfuric and 30% hydrogen peroxide) for 30 s, further on rinsed with ultrapure water and dried under nitrogen flow. They were used immediately after cleaning. St37–2 carbon steel (CS) coupons of 1.0 x 1.0 x 0.1 cm size were polished first with SiC paper up to grade 1200, then with 6 µm, 3 µm, and 1 µm diamond paste. Their subsequent cleaning treatment was the same as before electrochemical measurements. EPS samples used for this study were dialysed against deionised water in order to avoid the contribution of other than EPS molecules to the XPS signal.

2.2.2. XPS analyses

Two kinds of samples were analysed by XPS (FIG. 7.2): substrates conditioned by adsorption from EPS solutions and residues of evaporation of these solutions. To prepare residues of evaporation (EVAP), an aliquot of 100 µl of EPS was deposited onto Gl substrate and left drying at room temperature (RT). This process was repeated additionally 2 times to form a visible EPS layer. For these samples it was verified that the substrate did not contribute significantly to the obtained signals (Si content < 4%). In order to prepare substrate with adsorbed macromolecules (ADS) CS coupons were immersed in 0.6 ml of EPS solution in a well plate for 2 h at RT and subsequently rinsed. Rinsing procedure was carried out by performing 3 times the following operation: 1.5 mL of ultrapure water was introduced, homogeneously and very gently stirred, and 1.5 mL of obtained mixture was removed. This provided a dilution by a factor of 43 and avoided the repeated coupon removal from the liquid. Finally, the conditioned coupon was removed and quickly dried under a nitrogen flow. In case of carbon steel samples the whole procedure was performed anaerobically under nitrogen atmosphere with all solutions deaerated prior to use.

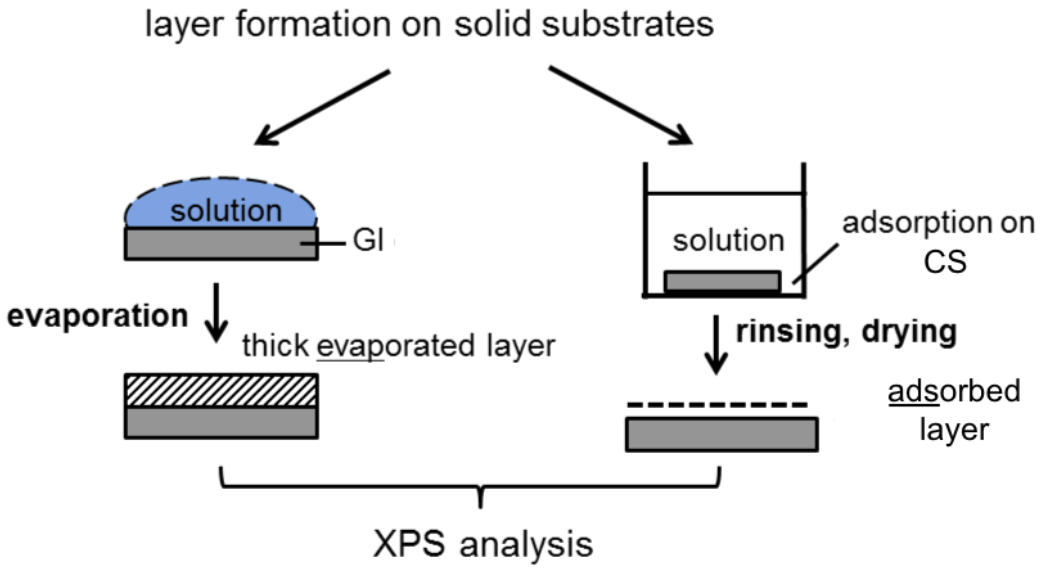

FIG. 7.2. SCHEME OF SAMPLE PREPARATION FOR XPS ANALYSES.

XPS measurements were carried out with a Kratos Axis Ultra spectrometer (Kratos Analytical, UK), using monochromated Al Kα radiation (powered at 10 mA and 15 kV) and an eight–channeltrons detector. The analysed area was 700 × 300 μm^2. The vacuum in the analysis chamber was about 10^{-6} Pa. The direction of photoelectron collection was perpendicular to the sample surface. Charge stabilisation was insured by using the Kratos Axis device. Survey spectra were recorded with 160 eV pass energy and for the narrow scans with the pass energy of 40 eV. In the latter conditions, the full width at half maximum (FWHM) of the Ag $3d_{5/2}$ peak of a standard silver sample was about 0.9 eV. The C 1s peak component due to carbon exclusively bound to carbon or hydrogen [**C**–(C,H)] was fixed at 284.8 eV to set the binding energy scale. The survey spectrum was recorded on each sample and the individual peaks were recorded at the high resolution when the element was detected on the survey spectrum. The C 1s peak was always recorded thrice (at the beginning, in the middle and at the end of the measurement) to check the charge stability and absence of sample evolution as a function of time. Quantification was made after using linear background subtraction and peak area normalisation on the basis of the acquisition parameters, using experimental sensitivity factors and transmission factors given by the manufacturer. This provided elemental mole fractions, excluding hydrogen, which is not detected by XPS. The C 1s, O 1s and N 1s peaks were decomposed with the Casa XPS program (Casa Software Ltd., U.K) using a Gaussian/Lorentzian (70/30) product function.

2.3. Surface tension

The surface tension, γ of EPS was measured at RT, using the du Nouy's ring method (Huh and Mason, 1975), by means of a Kruss K100 tensiometer (Kruss GmbH, Hamburg, Germany). The solutions were examined at increasing dilutions prepared with ultrapure water, until γ reached the values close to water (measured value of γ_{H2O} = 71.7 mN/m).

3. RESULTS

3.1. Electrochemical measurements

It was observed that the corrosion potential (E_{corr}) of WE decreased very rapidly after the immersion in the ASW solution with or without EPS to further stabilise within 1 h. Only in case of E_{corr} monitoring before EIS measurement, a gentle potential increase was observed after rising up the purging gas tube above the solution level. However, this change did not exceed 4 mV and stabilised within 10 min. The results of E_{corr} monitoring before EIS experiments are shown in **FIG. 7.3.** The average E_{corr} values after 2 h of immersion, calculated from the whole electrochemical experiments (E_{corr} monitoring before performing cLP, aLP or EIS), are summarised in **TABLE 7.1**. The corrosion potential of carbon steel in ASW was equal to – 0.777 ± 0.011 V. The presence of EPS did not induce significant changes in E_{corr} values.

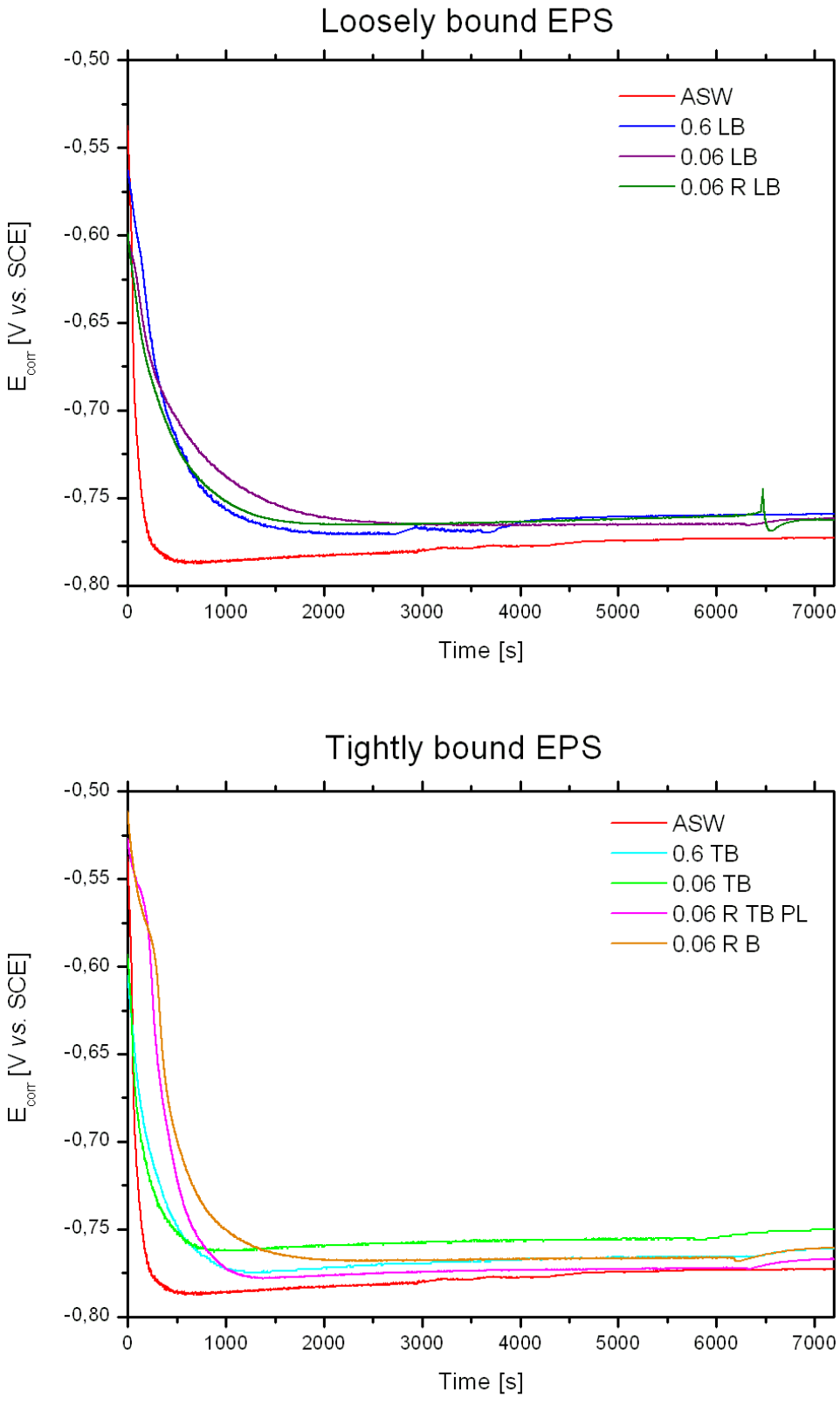

FIG. 7.3. MONITORING OF THE CORROSION POTENTIAL *VS.* IMMERSION TIME OF ST37–2 CARBON STEEL IN DIFFERENT EPS SOLUTIONS (BEFORE EIS MEASUREMENTS). 0.6 AND 0.06 CORRESPOND TO THE LACTATE CONCENTRATION WITH 0.6 % AND 0.06% (W/V), RESPECTIVELY; LB – LOOSELY BOUND EPS, TB – TIGHTLY BOUND EPS, R – REACTOR TRIAL, PL – PLANKTONIC CELLS, B – BIOFILM.

TABLE 7.1. AVERAGE E_{CORR} VALUES OF ST37–2 CARBON STEEL AFTER 2 H OF IMMERSION IN ALL TESTED EPS SOLUTIONS.

Solution	E_{corr} [V *vs.* SCE]
ASW	– 0.777 ± 0.011
0.6 LB	– 0.757 ± 0.016
0.6 TB	– 0.766 ± 0.009
0.06 LB	– 0.761 ± 0.007
0.06 TB	– 0.759 ± 0.010
0.06 R LB	– 0.761 ± 0.005
0.06 R TB PL	– 0.770 ± 0.005
0.06 R B	– 0.769 ± 0.010

FIG. 7.4 shows the cathodic polarisation curves obtained in ASW in aerated or deaerated conditions i.e. in presence or absence of dissolved oxygen. The corrosion potential was more anodic in the aerated solution. In these conditions, a pseudo–plateau was observed near E_{corr} down to – 0.91 V *vs.* SCE, then the current density (in absolute value) increased linearly with decreasing potential for – 1.02 < E < – 0.91 V *vs.* SCE, and below – 1.02 V *vs.* SCE the current density increased significantly but no more linearly. In deaerated conditions, the shape of the curve was similar except for the absence of the pseudo–plateau near E_{corr}. The two curves overlapped in the potential range of – 1.02 < E < – 0.91 V *vs.* SCE (same slope observed). This linear variation of the current density illustrated a cathodic Tafel behaviour (reaction totally limited by charge transfer).

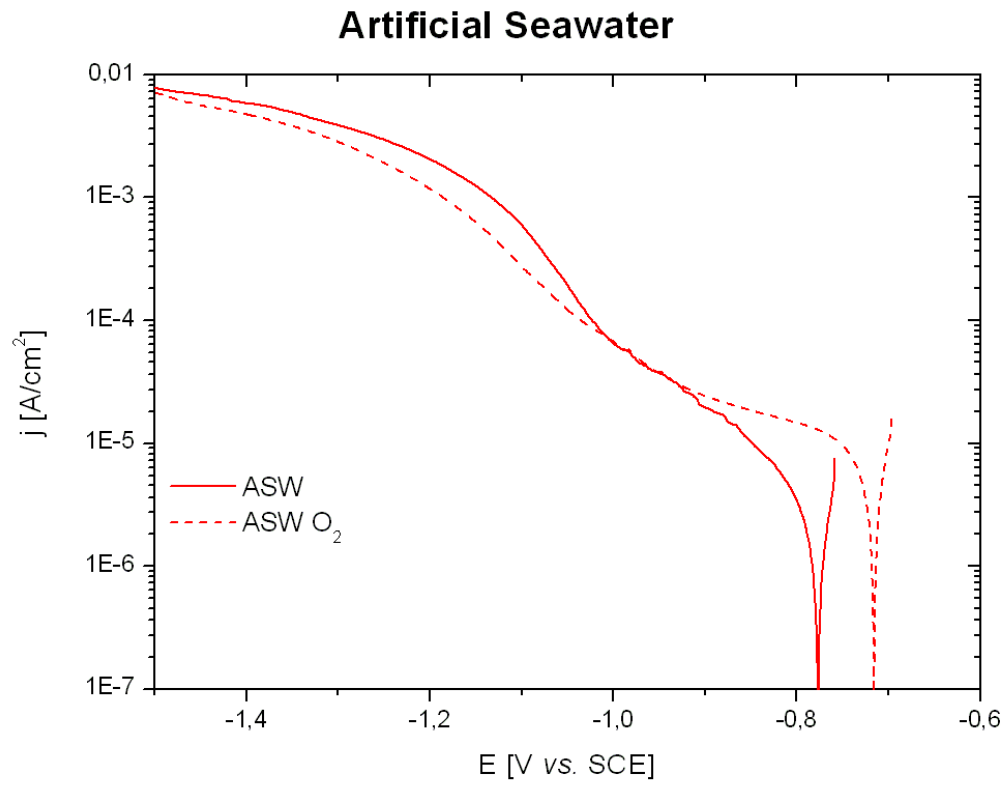

FIG. 7.4. CATHODIC POLARISATION CURVES OF ST37–2 CARBON STEEL AFTER 2 H OF IMMERSION IN AERATED (O_2) AND DEAERATED ASW. SCAN RATE: 0.5 MV/S.

In **FIG. 7.5,** cathodic polarisation curves recorded in the different EPS solutions are shown. The difference between linear (Tafel behaviour) and non–linear variation of the current density *vs*. potential, as clearly observed in ASW, was more or less pronounced depending on the EPS solution. In some cases, a single straight line was visible in a very wide potential range (e.g. down to –1.4 V vs. SCE for 0.06 LB). In the case of LB EPS, cathodic currents were always lower in absolute value than those for ASW. In the case of TB EPS, cathodic currents for 0.6 TB and 0.06 TB were only slightly lower than those for ASW. The lowest cathodic currents were observed for 0.06 LB, 0.06 R TB PL and 0.06 R B (about one decade lower in comparison to ASW).

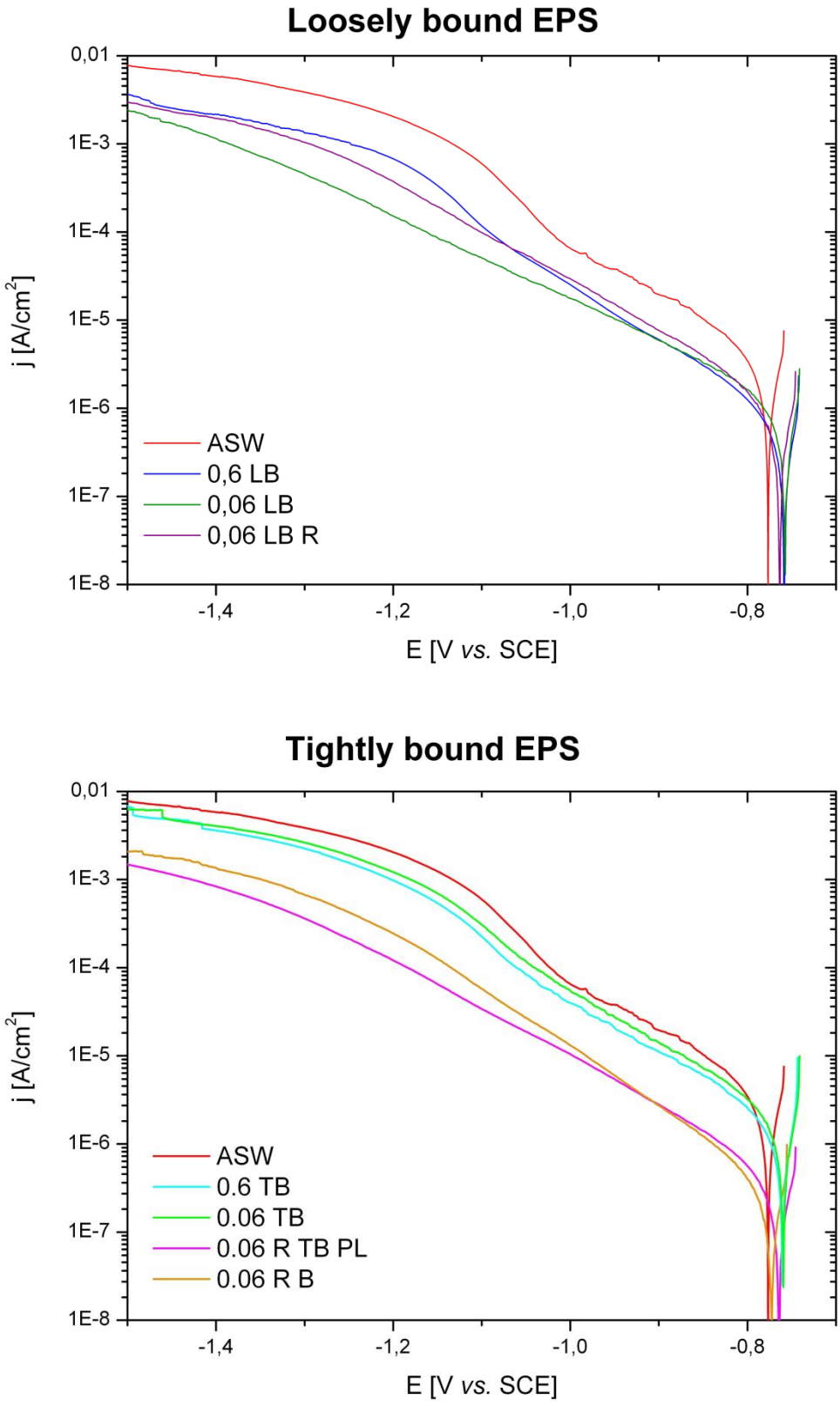

FIG. 7.5. CATHODIC POLARISATION CURVES OF ST37–2 CARBON STEEL AFTER 2 H OF IMMERSION IN DEAERATED EPS SOLUTIONS (LB AND TB). SCAN RATE: 0.5 MV/S. 0.6 AND 0.06 CORRESPOND TO THE LACTATE CONCENTRATION WITH 0.6 % AND 0.06% (W/V), RESPECTIVELY; LB – LOOSELY BOUND EPS, TB – TIGHTLY BOUND EPS, R – REACTOR TRIAL, PL – PLANKTONIC CELLS, B – BIOFILM.

Anodic polarisation curves recorded in ASW and in the different EPS solutions are shown in **FIG. 7.6**. In ASW, the current density continuously increased with the potential, with a linear variation in a narrow potential domain close to E_{corr}. This linear increase of the current density illustrated an anodic Tafel behaviour (reaction totally limited by charge transfer).

In the presence of EPS, two different shapes were observed for $E_{corr} < E < –0.2$ V *vs*. SCE, even for two measurements performed in the same solution: 1) one with a linear increase of the current density close to E_{corr}, followed by a pseudo–plateau between – 0.6 and – 0.5 V *vs*. SCE, corresponding to current densities between 30 and 100 mA/cm^2; and 2) a second one with a linear variation of the current density over several current decades. Both shapes were obtained for 0.6 LB, 0.06 LB and 0.06 R B EPS; the shape 1 (with the pseudo–plateau) was exclusively observed for 0.06 R LB and 0.06 R TB PL EPS, and shape 2 (wide Tafel domain) for 0.6 TB and 0.06 TB EPS. Whatever the shape, anodic current densities were lower in the presence of EPS compared to ASW, for $E_{corr} < E < – 0.2$ V *vs*. SCE. For $E > – 0.2$ V *vs*. SCE, the shape of the anodic curves was similar without and with EPS; current densities were similar without and with LB EPS, except for 0.06 R LB for which current densities were lower. Current densities were also lower with TB EPS compared to ASW.

From the cathodic and the anodic polarisation curves, it could be concluded that the presence of *D. alaskensis* EPS, whatever the EPS, decreased both the cathodic current and the anodic current (for $E_{corr} < E < –0.2$ V vs. SCE) i.e. slowed down the corresponding reactions. In particular, all the tested EPS induced lower dissolution currents at not too high anodic potentials.

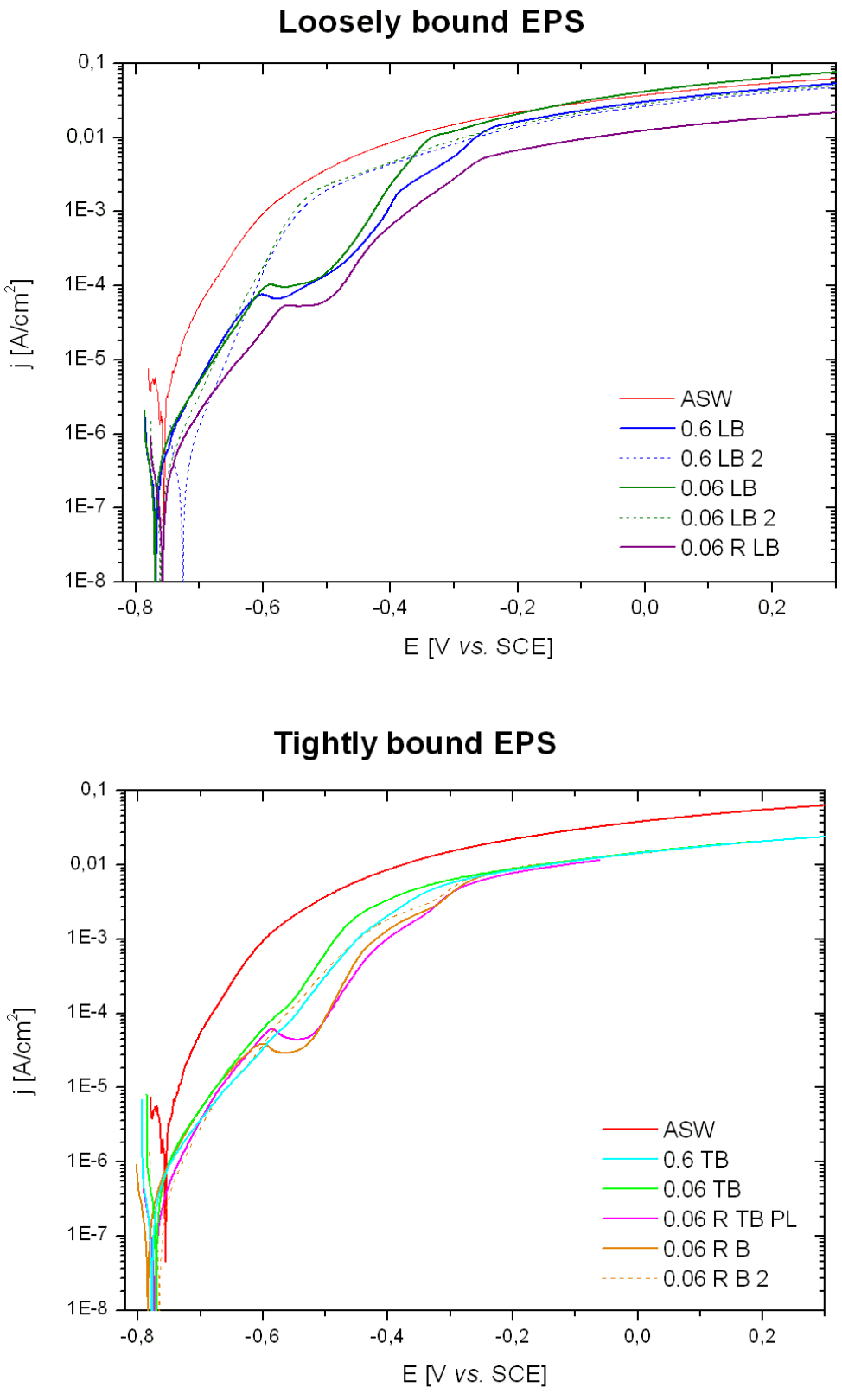

FIG. 7.6. ANODIC POLARISATION CURVES OF ST37–2 CARBON STEEL AFTER 2 H OF IMMERSION IN DEAERATED EPS SOLUTIONS (LB AND TB). SCAN RATE: 0.5 MV/S. 0.6 AND 0.06 CORRESPOND TO THE LACTATE CONCENTRATION WITH 0.6 % AND 0.06% (W/V), RESPECTIVELY; LB – LOOSELY BOUND EPS, TB – TIGHTLY BOUND EPS, R – REACTOR TRIAL, PL – PLANKTONIC CELLS, B – BIOFILM. DASHED LINES CORRESPOND TO THE SECOND SHAPE OBSERVED IN THE SAME EPS SOLUTION.

EIS measurements were performed at E_{corr} after 2 h of immersion in deaerated artificial seawater, without and with EPS. The impedance data are presented as Nyquist diagrams (opposite of the imaginary part of the impedance *vs.* real part) in **FIG. 7.7** and as Bode plots in **FIG. 7.8** (modulus *vs.* frequency in logarithmic coordinates) and **FIG. 7.9** (phase angle *vs.* frequency). One single capacitive loop, looking like a depressed semi–circle, was observed for all solutions. The diameter of this loop was higher in the presence of EPS compared to ASW, showing a protective effect of EPS. The lowest protective effect was obtained for 0.6 TB and 0.06 TB EPS, and the highest effect was obtained for 0.6 LB EPS.

In **FIG. 7.10**, the absolute value of the imaginary part of the impedance (Z_J) was plotted as a function of frequency in logarithmic coordinates (Orazem *et al.*, 2006). In the high frequency (HF) range, a straight line with a slope lower than 1 in absolute value was observed, showing a non–ideal capacitive behaviour.

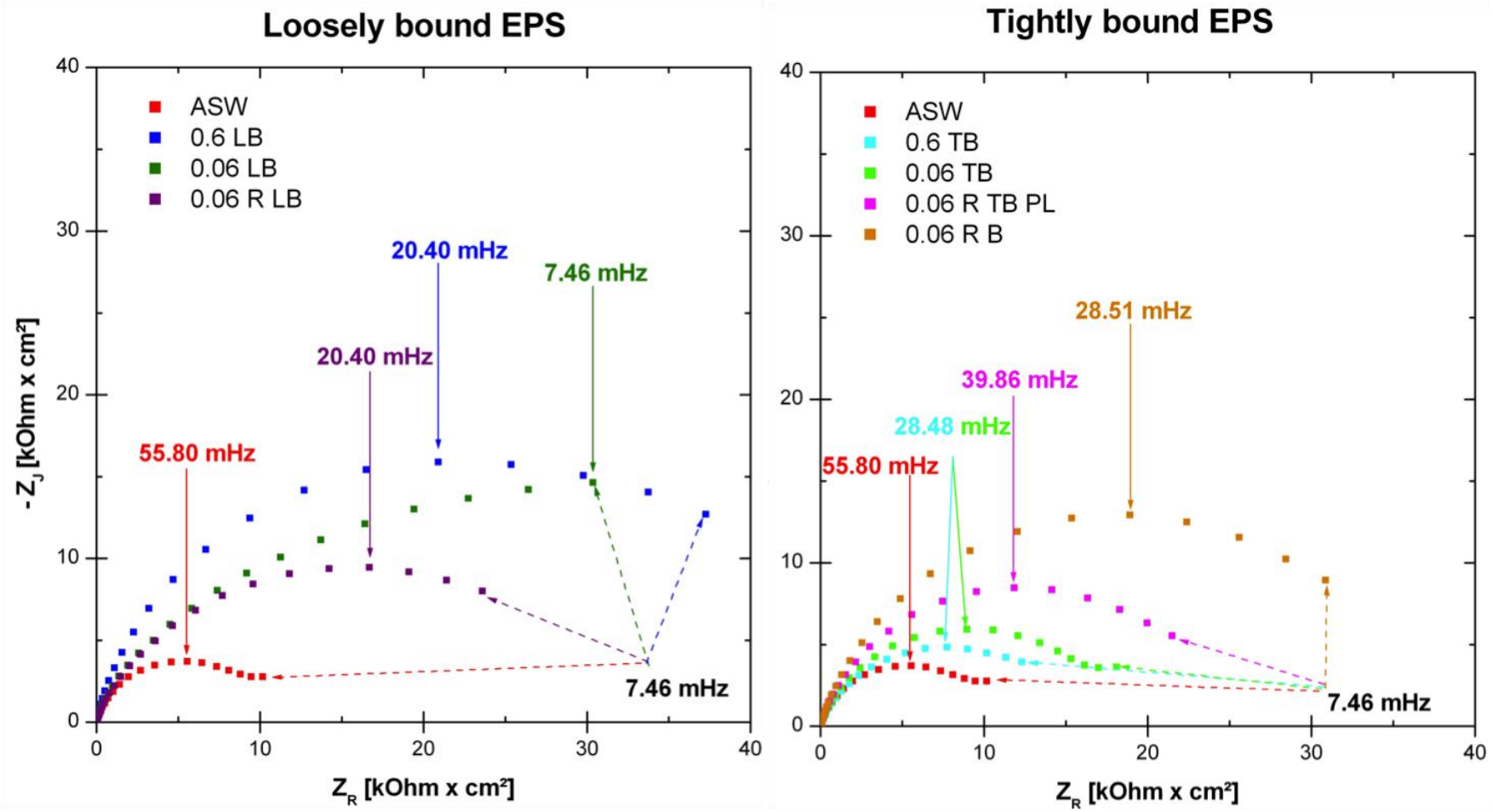

FIG. 7.7. EIS DATA. NYQUIST DIAGRAMS OF ST37–2 CARBON STEEL PLOTTED AT E_{CORR} AFTER 2 H OF IMMERSION IN DEAERATED EPS SOLUTIONS. 0.6 AND 0.06 CORRESPOND TO THE LACTATE CONCENTRATION WITH 0.6 % AND 0.06% (W/V), RESPECTIVELY; LB – LOOSELY BOUND EPS, TB – TIGHTLY BOUND EPS, R – REACTOR TRIAL, PL – PLANKTONIC CELLS, B – BIOFILM.

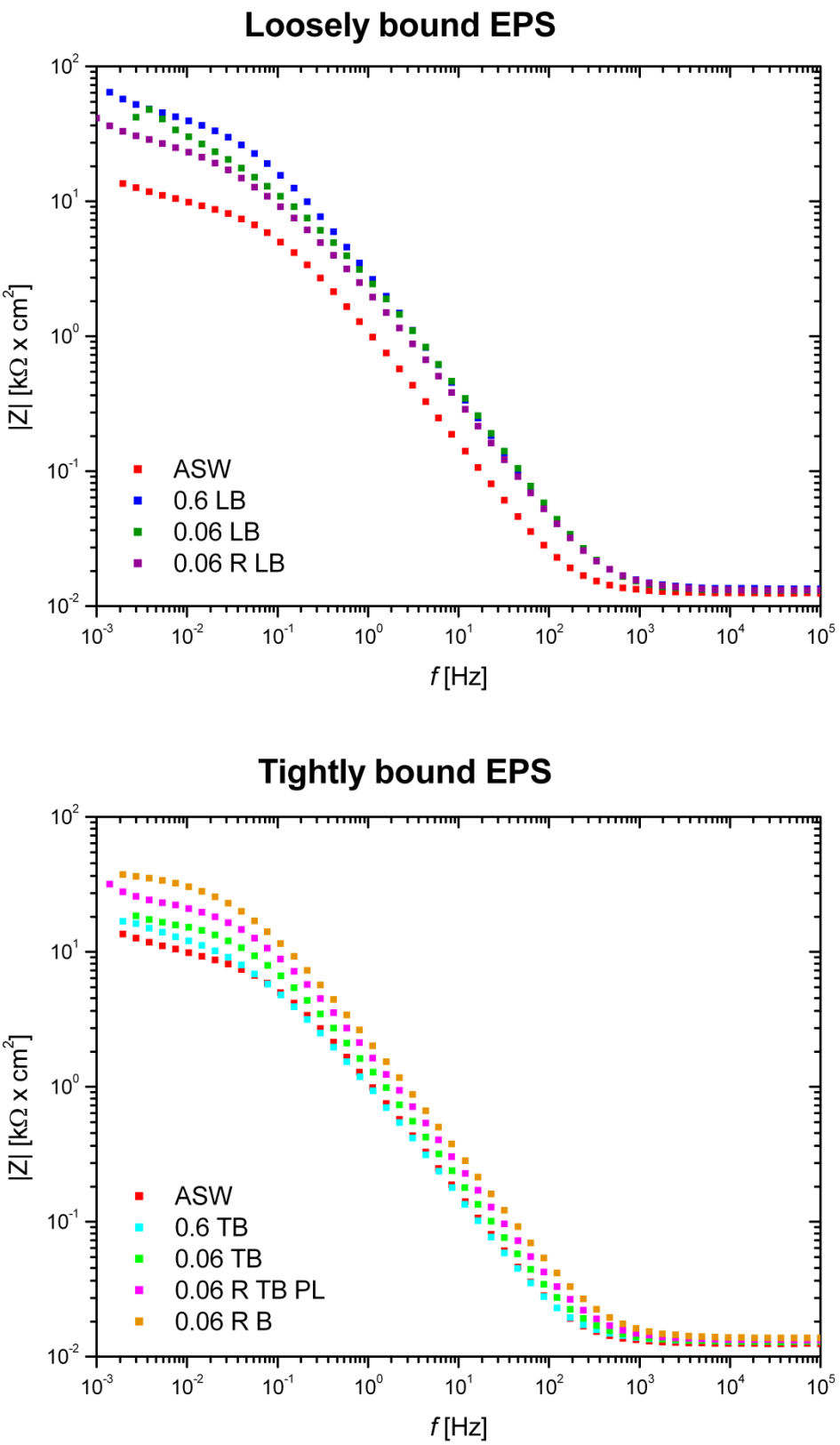

FIG. 7.8. EIS DATA. BODE PLOTS (MODULUS Z *VS.* FREQUENCY IN LOGARITHMIC COORDINATES) OF ST37–2 CARBON STEEL AT E_{CORR} AFTER 2 H OF IMMERSION IN DEAERATED EPS SOLUTIONS (LB AND TB).

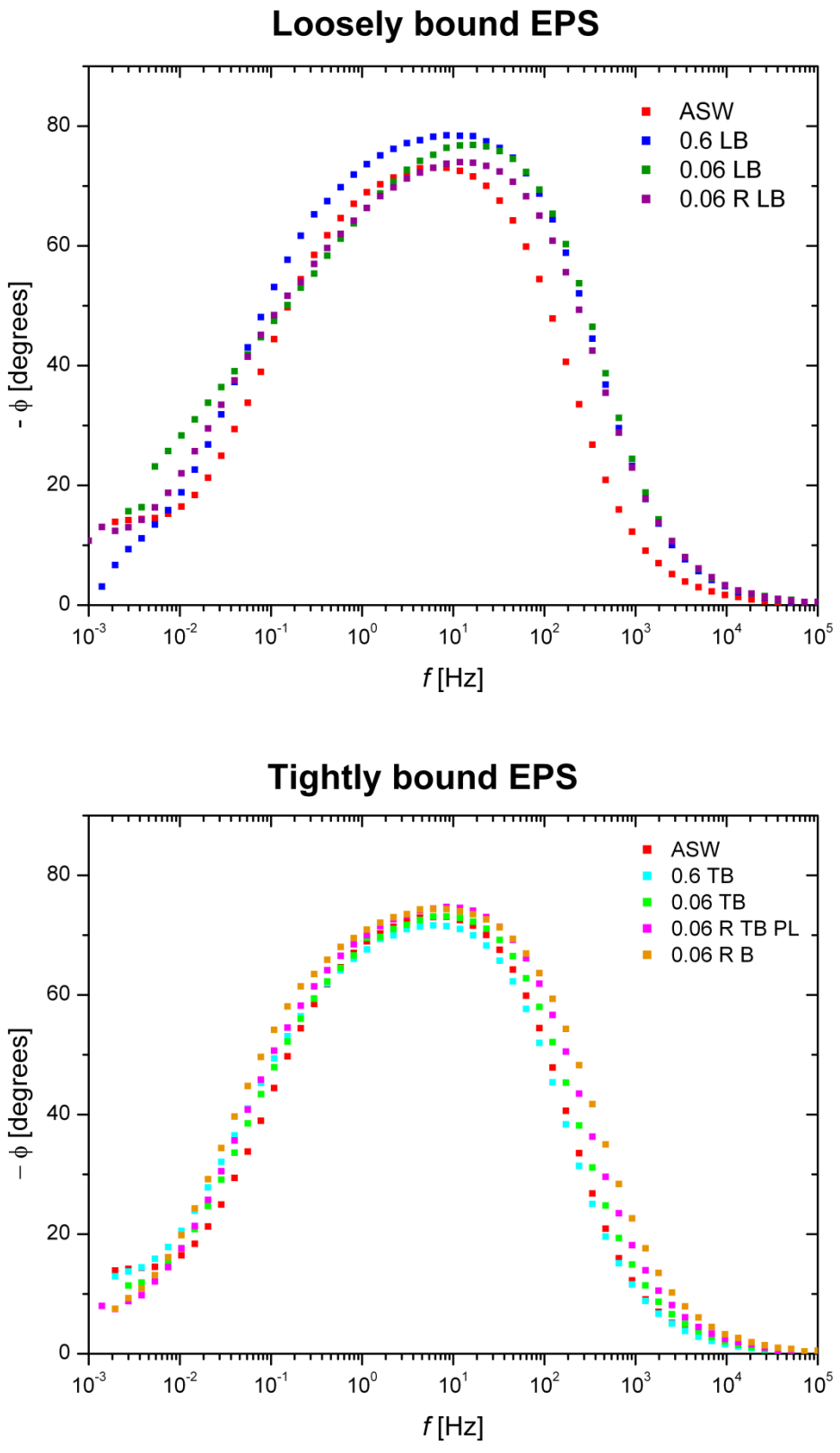

FIG. 7.9. EIS DATA. BODE PLOTS (OPPOSITE OF THE PHASE ANGLE *VS.* FREQUENCY) OF ST37–2 CARBON STEEL AT E_{CORR} AFTER 2 H OF IMMERSION IN DEAERATED EPS SOLUTIONS (LB AND TB).

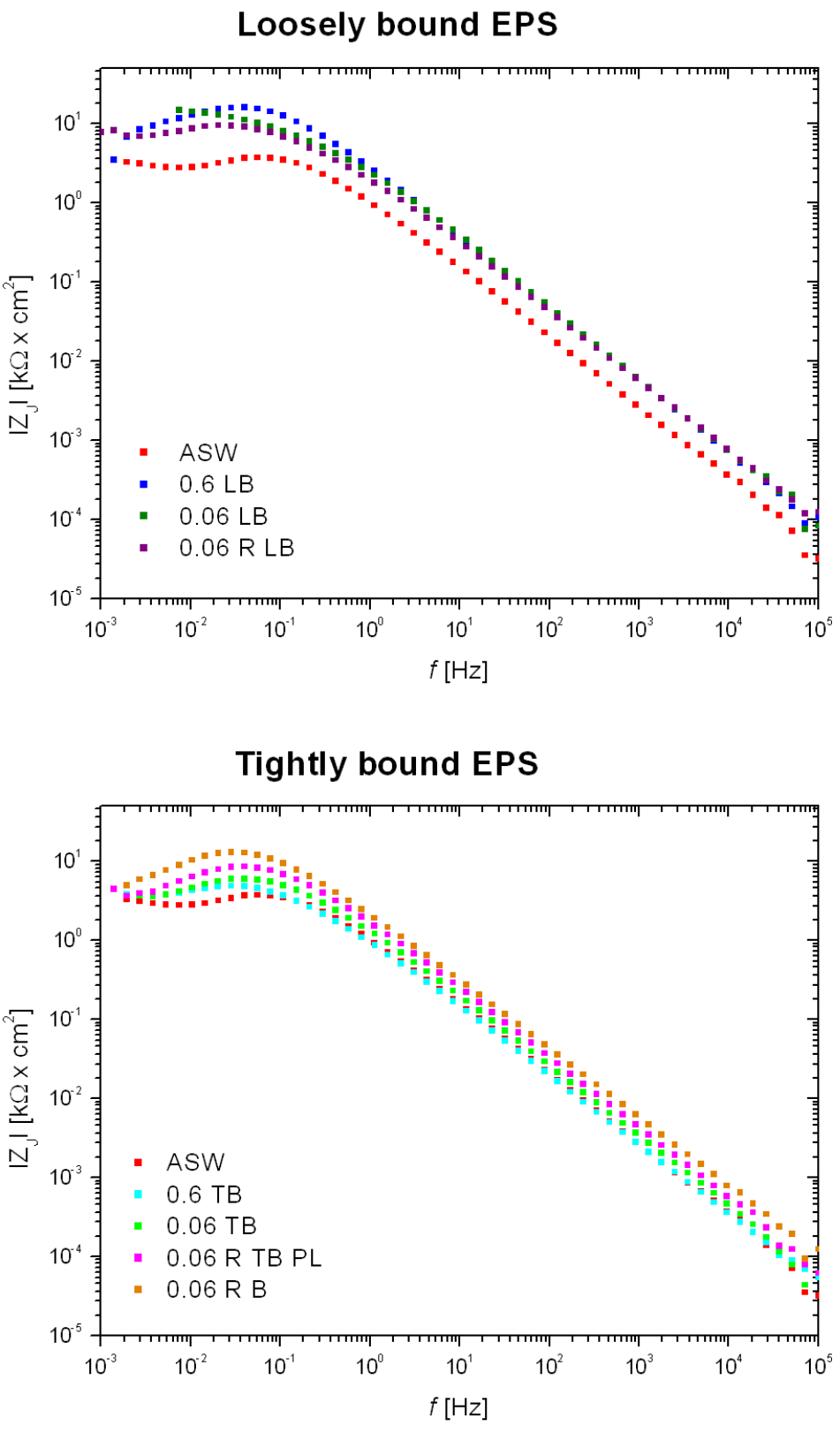

FIG. 7.10. EIS DATA. IMAGINARY PART OF THE IMPEDANCE *VS.* FREQUENCY IN LOGARITHMIC COORDINATES OF ST37–2 CARBON STEEL AT E_{CORR} AFTER 2 H OF IMMERSION IN DEAERATED EPS SOLUTIONS (LB AND TB).

3.2. Surface analysis

The chemical composition of the surface – active molecules present in EPS was investigated. Therefore, the composition of the adlayer formed by conditioning the carbon steel with these EPS was determined by X–ray photoelectron spectroscopy (XPS) and was compared with the residue of evaporation of their solution (Aguié–Béghin et al., 2009). The approach was focused on the information concerning chemical functional groups of organic compounds and on the expression of the chemical composition in terms of model compounds obtained from the elemental molar concentrations, from the XPS spectra (Boonaert et al., 2003; Ahimou et al., 2007; Landoulsi et al., 2008; Rouxhet and Genet, 2011; Rouxhet et al., 2008).

Primarily acquired XPS spectra were decomposed in order to observe the species present on the carbon steel surface or on the EVAP layer. **FIG. 7.12** shows the range of obtained shapes for O 1s, N 1s and C 1s peaks in the carbon steel surface.

The C 1s peak was decomposed with constraints insuring the consistency required to make quantitative comparison between samples (Genet et al., 2008; Rouxhet and Genet, 2011). The summary of observed peaks, their position in the recorded spectrum and possible relations between the peaks from various spectra (e.g. C 1s and O 1s, or C 1s N 1s) were presented in **TABLE 7.2**. The C 1s component typical of carbon bound only to carbon and hydrogen [**C**–(C,H)] was fixed at 284.8 eV, ($\mathbf{C_{284.8}}$). A second component was found at 286.1 – 286.8 eV, which was due to carbon making a single bond with oxygen or nitrogen in alcohol, amine or amides, or carbon making a single bond with oxygen in the ester group [**C**–(O,N)] ($\mathbf{C_{286.2}}$). A third component was close to 288.0 eV, due to carbon making two single bonds with oxygen in acetal [C–O–**C**–O–C, one per hexose unit in polysaccharides] or making one double bond with oxygen in amide [N–**C**=O], ($\mathbf{C_{288}}$). Some samples showed a fourth component at 289 eV, due to carbon making one double bond and one single bond with oxygen [O=**C**–O] in carboxyl or ester functions, ($\mathbf{C_{289}}$) (Genet et al., 2008; Rouxhet et al., 2008; Rouxhet and Genet, 2011). The total carbon present on the surface was designated as C_{tot}.

The O 1s peak was decomposed as follows. The major components at 531.2 eV and 531.8 eV were due to oxygen double bound to carbon [**O**=C] in amide or carboxyl and ester group, respectively. Another components near 533.0 eV were due

to oxygen singly bound to the carbon atom [**O**–C] in alcohol, carboxyl and ester or oxygen of ether [C–**O**–C]. Below 530.0 eV, inorganic oxides or hydroxides were found.

The N 1s peak was decomposed for 2 components. The main N 1s component was found at 399.8 – 400.2 eV, typical of non – protonated amine and amide. The second component at lower binding energy (<399.0 eV) was probably due to the presence of a nitrogen atom bound to the carbon in aromatic ring with single or double bound (Wanger et al., 1981). The sum of these components was the total organic nitrogen, N_{org}.

TABLE 7.2. BINDING ENERGY OF ELEMENTS IN CHEMICAL FUNCTIONAL GROUPS OF BIOCHEMICAL COMPOUNDS (ROUXHET AND GENET, 2011). COLOURS USED IN THIS TABLE CORRESPONDED TO THE COLOURS FROM THE XPS SPECTRA (FIG. 7.11).

Element and function	Position [eV]	Compound of reference	Related data
CARBON			
C–(C,H)	284.8	Hydrocarbon, adventitious contamination	
C–N, (C=O)–NH–C	286.1	Amine; amide, peptidic link	
C–O	286.3	Alcohol	**
(C=O)–O–C	286.8	Ester [a]	*
C=O, O–C–O	287.8	Aldehyde, (hemi)acetal	
(C=O)–NH–C, O=C–O^-	288.0	Amide, peptidic link; carboxylate	***
(C=O)–O–C	289.0	Ester [a]	*
(C=O)–OH	289.0	Carboxylic acid	
OXYGEN			
O=C–O^-	531.1	Carboxylate	
(C=O)–NH–C	531.3	Amide, peptidic link	***
P=O, P–O^-	531.2	Phosphodiester [b]	
(C=O)–OH	531.8	Carboxylic acid	
(C=O)–O–C	531.9	Ester [a]	*
C–OH, C–O–C–O–C	532.6	Alcohol, (hemi)acetal	**
(C=O)–O–C	533.4	Ester [a]	*
(C=O)–OH	533.4	Carboxylic acid	
NITROGEN			
N – Ar	**< 399.0**	**Nitrogen linked to aromatic carbon rings***	
C–NH_2	399.3	Amine	
(C=O)–NH–C	399.8	Amide, peptidic link	***
C–NH_3^+	401.3	Protonated amine	
R_4– N^+	402.4	Quaternary ammonium [c]	

*** (WANGER ET AL., 1981)**

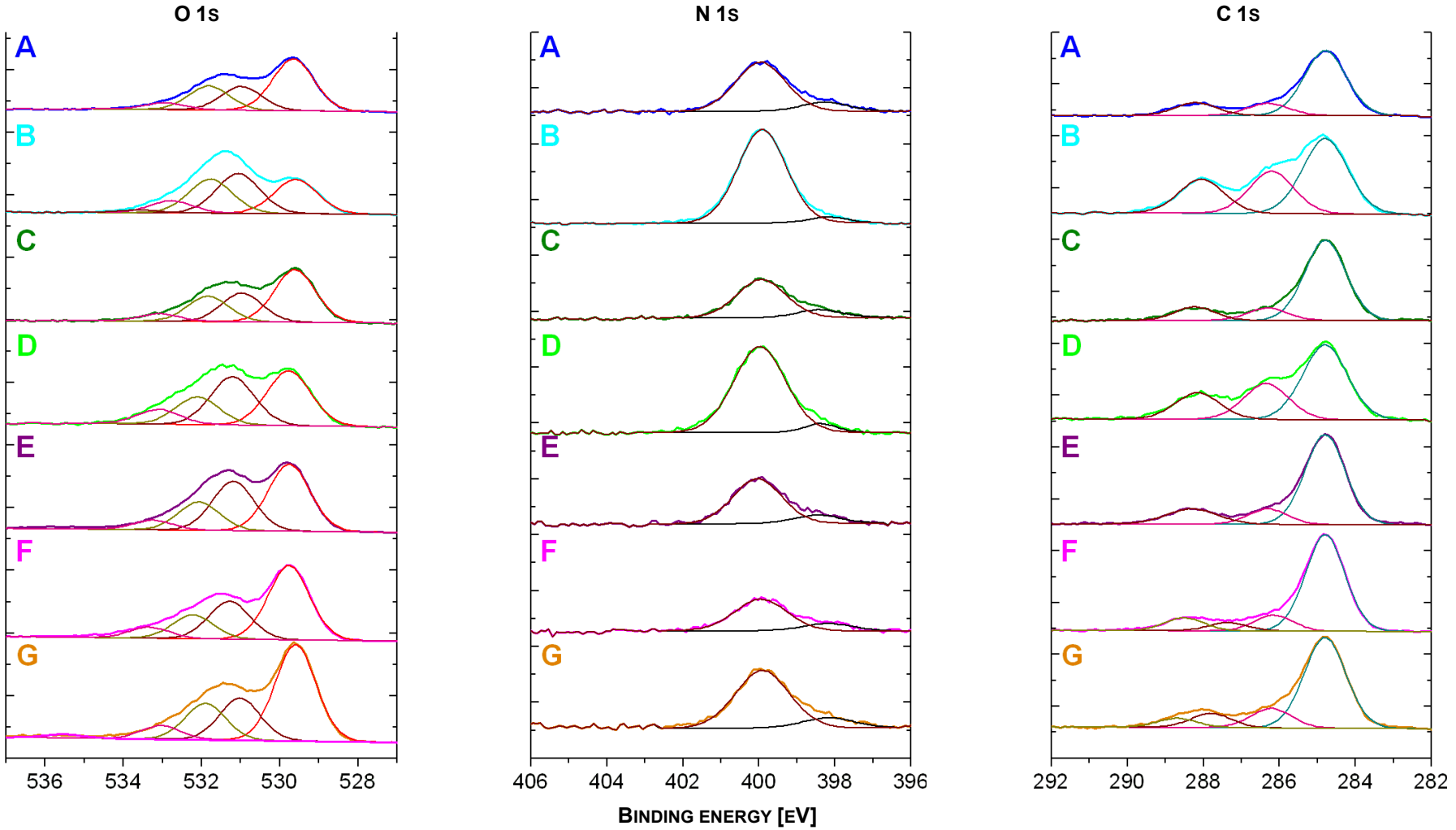

FIG. 7.11. XPS SPECTRA FROM EPS ADSORBED ON THE CARBON STEEL SURFACE. EPS IDENTIFICATION: BLUE – 0.6 LB, CYAN – 0.6 TB, OLIVE – 0.06 LB, GREEN – 0.06 TB, PURPLE – 0.06 R LB, MAGENTA – 0.06 R TB PL, ORANGE – 0.06 R B EPS. C 1S COMPONENTS: MARINE BLUE – C–(C,H), PINK – C–(O,N), BROWN – (C=O)–NH–C, O–C–O, DARK YELLOW – O=C–(O,H); N 1S COMPONENTS: BLACK – N–AR, BROW – (C=O)–NH–C; O 1S COMPONENTS: RED – IRON OXIDES, BROWN – (C=O)–NH–C, DARK YELLOW – O=C–(O,H).

It was observed that most of the identified peaks were linked with nitrogen. However, a significant difference in the peak intensity was reported for two EPS samples: 0.6 TB and 0.06 TB. Particularly amide peaks ((C=O)–NH–C) were higher in all spectra in comparison to five other EPS samples.

Moreover, the composition of the adlayers and drying residues examined here (ADS and EVAP, respectively, **FIG. 7.2**) was expressed in terms of 4 chemical entities: amide [HC–NH–(C=O)] quantified by N_{org} as a marker, CH_2 quantified from the $C_{284.8}$ component, additional carbon quantified by $C_{add} = C_{ox} – 2\times N_{org}$ and additional organic oxygen quantified by $O_{add} = O_{org} – N_{org} = C_{ox} – 2\times N_{org}$ (Yang et al., in preparation). C_{ox} was defined as:

$$C_{ox} = C_{286.2} + C_{288} + C_{289} = C_{tot} – C_{284.8} \quad (7.1)$$

where $\mathbf{C_{284.8}}$ = [**C**–(C,H)]; $\mathbf{C_{286.2}}$ = [**C**–(O,N)]; $\mathbf{C_{288}}$ = [C–O–**C**–O–C] and [N–**C**=O]; $\mathbf{C_{289}}$ = [O=**C**–O]; C_{tot} = total carbon.

The elemental molar concentrations, obtained from the XPS spectra, were converted into weight percentage of these chemical entities (Yang et al., in preparation). The scheme of the procedure used for converting the concentration of markers (mole %) into concentration of relevant chemical moieties (mass %), which provide a more practical representation of the surface composition, is shown in the **TABLE 7.3**. Multiplying the molar concentration of markers (X, mol/100 mol) by the molar mass (MM) of the relevant constituent or model compound provided the concentration of each compound (W, in g/100 mol). Dividing W of each compound by the sum of W for all compounds (Tot) and multiplying by 100 gave the mass concentration in % of the constituent in the volume analysed by XPS.

TABLE 7.3. SCHEME OF THE PROCEDURE USED FOR CONVERTING MARKER CONCENTRATIONS (MOLAR PERCENTAGE OF RELEVANT ELEMENT) INTO MASS CONCENTRATION (%) OF MODEL COMPOUNDS IN THE EPS (YANG ET AL., IN PREPARATION).

Model constituents			$W = X \times MM^c$	(W × 100) / Tot Constituents concentration (mass %)
Nature	MM^a	Name and concentration X^b		
HC–NH–(C=O)	56.02	N_{org}	•••	•••
CH_2	14.01	$C_{284.8}$	•••	•••
Additional C	12.01	$C_{ox} – 2\times N_{org}$	•••	•••
Additional O_{org}	16.00	$C_{ox} – 2\times N_{org}$	•••	•••
Total	–	–	Tot = •••	Tot=•••

[a] molar mass of constituent
[b] name of marker, concentration X obtained from the XPS spectra [mole / 100 moles excluding hydrogen]
[c] in gram of constituent / 100 moles of elements other than hydrogen
••• concentration read from the spectra

The results of the XPS analysis converted into weight % of amide, as defined above, CH_2 and additional carbon C_{add} combined with the additional organic oxygen O_{add} are presented in **FIG.7.12** in the form of a ternary composition diagram (Graham and Midgley, 2000). The vertices of the triangle represent 100 weight (wt) % of amide, 100 wt % CH_2 and 100 wt % additional (C + O).

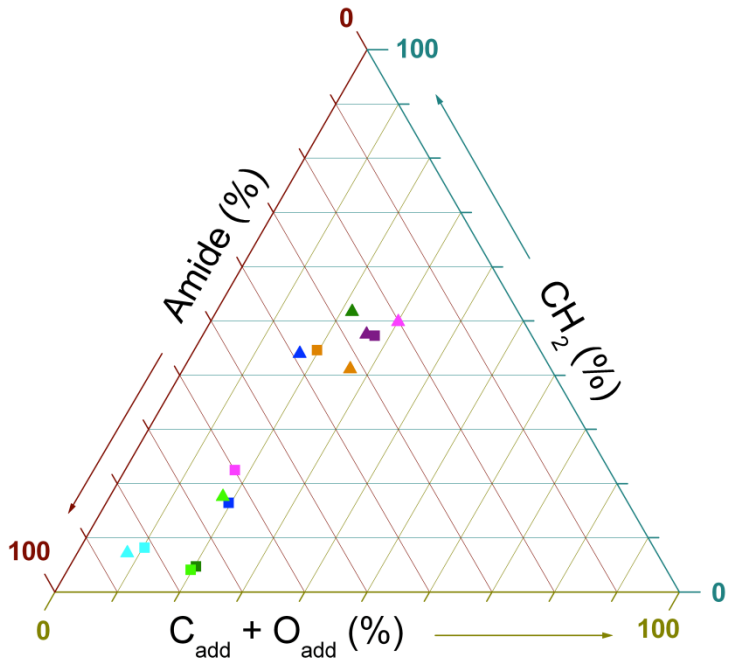

FIG. 7.12. EPS COMPOSITION ON THE SURFACE (TERNARY COMPOSITION DIAGRAMS). RELATIVE MASS CONCENTRATION OF AMIDE (CH–NH=C–O), HYDROCARBON CH_2 AND OTHER OXYGEN CONTAINING MOLECULES, INCLUDING POLYSACCHARIDES (C_{OX}+O_{ORG}) FROM EPS EVAPORATED ON GLASS SURFACE (■) OR ADSORBED ON CARBON STEEL (▲) EPS. CORRESPONDING EPS COLOUR ID: BLUE – 0.6 LB, CYAN – 0.6 TB, OLIVE – 0.06 LB, GREEN – 0.06 TB, PURPLE – 0.06 R LB, MAGENTA – 0.06 R TB PL, ORANGE – 0.06 R B EPS.

As in elemental XPS spectra, the ternary diagram revealed a significant difference in the adsorption abilities between the tightly bound EPS from the static conditions (0.6 TB and 0.06 TB) and five remaining EPS. The main component of the former, obtained from the EVAP samples (which accumulated at the liquid–air interface, generating the analysed layer), as well as from the EPS adsorbed on the carbon steel, appeared in form of proteins.

Further on, three samples (0.6 LB, 0.06 LB and 0.06 R TB PL) in the EVAP form contained mainly proteins; however, the molecules, which were adsorbed on the carbon steel surface (ADS) after 2 h immersion, contained increased amounts of hydrocarbon species.

Other EPS samples (0.06 R LB and 0.06 R B) in both forms (EVAP and ADS) contained mostly hydrocarbons, with some proteins and polysaccharides.

Measurements of the surface tension data (**TABLE 7.4**) indicated the presence of surface – active compounds in LB and TB EPS. The lowest γ values were found in 0.06 TB EPS; however only after the 6 times dilution the solution reached γ value of water.

TABLE 7.4. SURFACE TENSION (γ) MEASUREMENT OF THE EPS FROM *D. ALASKENSIS*.

Solution	Surface tension γ [mN/m]	Dilution at which γ ≈ 71.7 mN/M
0.6 LB	64.07 ± 0.25	24x
0.6 TB	58.01 ± 1.10	48x
0.06 LB	62.62 ± 0.46	12x
0.06 TB	70.24 ± 0.11	6x
0.06 R LB	58.11 ± 0.34	96x
0.06 R TB PL	63.85 ± 0.28	24x
0.06 R B	61.72 ± 0.42	48x

4. DISCUSSION

Various approaches were applied in this study in order to better understand the EPS influence on carbon steel behaviour in marine environment. First, the environment itself was validated. St37–2 carbon steel was cathodically polarised in ASW in two various conditions (aerated and deaerated) in order to verify if residual oxygen was present in degassed solutions. In aerated conditions, the pseudo–plateau observed for – 0.91 V *vs.* SCE < E < E_{corr} corresponded to the reduction of dissolved oxygen with transfer of 4 electrons, that can be written at pH = 8.0 as follows:

$$O_2 + 2\ H_2O + 4\ e^- \rightarrow 4\ OH^- \qquad (7.2)$$

The linear variation of the current density for – 1.02 < E < – 0.91 V *vs.* SCE (cathodic Tafel behaviour) possibly corresponded to the reduction of the oxide layer formed on the steel surface at the air, after polishing and in the solution during the 2 h of immersion. Further increase of the current density below –1.02 V *vs.* SCE corresponded to the reduction of water (hydrogen evolution reaction), that can be written at pH = 8.0 as follows:

$$2\ H_2O + 2e^- \rightarrow H_2 + 2\ OH^- \qquad (7.3)$$

The absence of pseudo–plateau near E_{corr} in the deaerated solution showed that the residual oxygen concentration was very low and could be neglected.

Back to the EPS, it was observed that exopolymers had no effect on the corrosion potential value, independently of the EPS type. The first differences emerged while cathodically polarising the carbon steel in their presence. In the EPS

– containing solutions, the cathodic currents were decreased, *i.e.* the corresponding cathodic reactions were slowed down. A similar effect was observed in the anodic potential domain with the decrease of anodic current and subsequent slow–down of the corresponding reactions for not too high potentials (for $E_{corr} < E < -0.2$ V *vs.* SCE). Subsequently, lower metal dissolution occurred if EPS were present in the solution. Thus, in both cathodic and anodic potential domains, a protective effect of EPS is observed.

Looking further at EIS data, from the plots of the imaginary part of the impedance *vs.* frequency (**FIG. 7.10**), a straight line with a slope lower than 1.0 in absolute value was observed in the high frequency range. This indicated the presence of a constant phase–element (CPE) behaviour (non ideal capacitive behaviour).

The impedance of a CPE is given by:

$$Z_{CPE}(\omega) = \frac{1}{Q(j\omega)^2} \tag{7.4}$$

with $\omega = 2\pi f$. The CPE parameters α and Q could be graphically obtained, following the method presented by Orazem et al. (Orazem *et al.*, 2006). The parameter α was calculated from the slope of the log $|Z_j|$ *vs*. log(f) curve (**FIG. 7.10**) in the HF range (opposite of the slope), and Q was obtained from α as follows:

$$Q = \frac{1}{Z_J(F)(2\pi f)^{\alpha}} \sin(\frac{\alpha\pi}{2}) \tag{7.5}$$

Assuming that this CPE behaviour was associated with surface distributed time constants for charge–transfer reactions (time–constant distribution along the electrode surface), then it was possible to apply the Brug equation (Brug *et al.*, 1984) to calculate the effective capacitance (C_{eff}) associated with the CPE (Hirschorn et al., 2010):

$$c_{eff} = Q^{\frac{1}{\alpha}}(R_e^{-1} + R_t^{-1})^{\frac{\alpha-1}{\alpha}} \tag{7.6}$$

where R_e was the electrolyte resistance and R_t the charge transfer resistance. R_e was estimated from the high frequency limit of impedance diagrams, and R_t was assumed to be the diameter of the capacitive loop.

The α (slope) and *Q* (admittance) values determined from **FIG. 7.10**, as well as the effective capacitance values calculated by application of equation (Eq.) 7.6 are shown in **TABLE 7.5**.

TABLE 7.5. CPE PARAMETERS EXTRACTED FROM THE IMPEDANCE DATA OF ST37–2 CARBON STEEL IN VARIOUS EPS SOLUTIONS, AND CALCULATED EFFECTIVE CAPACITANCE. GIVEN RESULTS ARE MEAN VALUES FROM TWO INDEPENDENT MEASUREMENTS.

Solution	α	Q_{eff} [F×cm^{-2}×s$^{(\alpha-1)}$]	C_{eff} [μF/cm^2]
ASW	0.87	1.75×10^{-4}	78
0.6 LB	0.89	7.02×10^{-5}	31
0.6 TB	0.87	1.88×10^{-4}	75
0.06 LB	0.88	7.06×10^{-5}	30
0.06 TB	0.88	1.31×10^{-4}	54
0.06 R LB	0.87	9.77×10^{-5}	42
0.06 R TB PL	0.87	1.08×10^{-4}	42
0.06 R B	0.86	8.99×10^{-5}	30

These capacitance values, of the order of several tens of μF/cm^2, were typical of those for a double layer capacitance, which validated the assumption that the capacitive loop illustrated charge transfer phenomenon and that its diameter was equal to the charge transfer resistance.In this work, R_t was not extracted from a fitting procedure but estimated graphically from the Nyquist diagrams as: $R_t = 2 \times Z_R^{max}$, where Z_R^{max} was the real part of the impedance corresponding to the maximum of $-Z_J$ (top of the depressed semi–circle). The values assessed for R_t in the different EPS solutions are presented in **TABLE 7.6**. R_t was always higher in the presence of EPS compared to ASW; the R_t ratio (R_t(EPS)/R_t(ASW)) varied from *ca.* 1.2 for 0.6 TB EPS up to *ca.* 3.9 for 0.6 LB EPS.

The corrosion current i_{corr}, was calculated from the charge transfer resistance by application of the modified Stern and Geary relationship (Stern and Geary, 1957; Epelboin et al., 1981):

$$i_{corr} = \frac{1}{R_t} \cdot \frac{b_a b_c}{2.303 \cdot (b_a + b_c)} \tag{7.7}$$

with i_{corr} in A/cm^2, R_t the global charge transfer resistance in Ω × cm^2, and b_a and b_c the anodic and cathodic Tafel constants, respectively, in V/dec ($b_{a,c} > 0$). Here, i_{corr}

was calculated by combining EIS data and polarisation curves: R_t was the diameter of the capacitive loop of impedance diagrams, and b_a and b_c were the inverse of the slopes (in absolute value) of the anodic and cathodic polarisation curves (log |j| *vs.* E representation), respectively, in the linear variation domain (Tafel behaviour). The values assessed for R_t, b_a and b_c in the different EPS solutions were presented in **TABLE 7.6**.

At E_{corr}, both the anodic and the cathodic reactions occurred on the same surface but the net current is equal to zero (same magnitude for the anodic and the cathodic currents). By principles of summation of currents, the anodic and cathodic impedances must be in parallel. Therefore, the global charge transfer resistance R_t was equal to the anodic charge transfer resistance R_t^a in parallel with the cathodic charge transfer resistance R_t^c. If $R_t^c >> R_t^a$, then $R_t = R_t^a$ and the corrosion current can be calculated from the single b_a and R_t^a, as follows:

$$i_{corr} = \frac{1}{R_t^a} \cdot \frac{b_a}{2.303} \tag{7.8}$$

If $R_t^a >> R_t^c$, then $R_t = R_t^c$ and the corrosion current can be calculated from the single b_c and R_t^c, as follows:

$$i_{corr} = \frac{1}{R_t^c} \cdot \frac{b_c}{2.303} \tag{7.9}$$

The corrosion current was estimated by application of Eq. 7.7, 7.8 or 7.9, assuming that the diameter of the capacitive loop of impedance diagrams was equal to R_t, R_t^a or R_t^c, respectively (R_t, R_t^a or $R_t^c = 2 \times Z_R^{max}$). The corresponding values are presented in **TABLE 7.6**.

TABLE 7.6. CHARGE TRANSFER RESISTANCE, ANODIC AND CATHODIC TAFEL CONSTANTS, AND CORROSION CURRENT EITHER CALCULATED FROM COMBINED EIS DATA AND POLARISATION CURVES (EQS. 7.7, 7.8 AND 7.9) OR ESTIMATED GRAPHICALLY FROM THE ANODIC OR CATHODIC POLARISATION CURVES. GIVEN RESULTS ARE MEAN VALUES FROM TWO INDEPENDENT MEASUREMENTS.

Solution	b_a [mV/dec]	b_c [mV/dec]	R_t [$\Omega \times cm^2$]	i_{corr} [$\mu A/cm^2$]				
				Calculated values			Values estimated graphically	
				Global (Eq. 7.7)	Anodic (Eq. 7.8)	Cathodic (Eq. 7.9)	Anodic	Cathodic
ASW	0.08	0.18	11 500	2.1	3.0	6.7	2.0	3.5
0.6 LB	0.06	0.16	45 000	0.4	0.6	1.6	0.5	0.7
0.6 TB	0.09	0.18	14 500	1.8	2.7	5.4	0.7	2.3
0.06 LB	0.06	0.20	37 300	0.6	0.8	2.3	0.5	1.0
0.06 TB	0.09	0.17	18 400	1.3	2.0	4.0	0.9	2.0
0.06 R LB	0.09	0.19	29 600	0.9	1.3	2.8	0.7	1.2
0.06 R TB PL	0.07	0.17	29 100	0.8	1.0	2.6	0.3	0.5
0.06 R B	0.07	0.16	40 100	0.5	0.7	1.7	0.4	0.4

The values of i_{corr} calculated by application of Eqs. 7.7, 7.8 and 7.9 were compared to each other. It was observed that all computed data were of the same order of magnitude. However, the values calculated from Eq. 7.7 (calculated "global" i_{corr}) and 7.8 (calculated "anodic" i_{corr}) were similar (ratio between calculated "anodic" and "global" i_{corr} of *ca.* 1.5), while the calculated "cathodic" i_{corr} (Eq. 7.9) was even 4 times higher in comparison to the global i_{corr}. Thus, the capacitive loop of impedance diagrams illustrated mainly the anodic charge transfer, and its diameter was equal to R_t^a ($R_t \approx R_t^a$).

The calculated values of i_{corr} were then compared to i_{corr} values estimated graphically from the anodic or the cathodic polarisation curves, by extrapolation of the anodic or the cathodic Tafel straight lines, respectively, down to E_{corr} (**TABLE 7.6**). It could be noticed that estimated "cathodic" i_{corr} values were higher than estimated "anodic" i_{corr} ones. The same order of magnitude was obtained for calculated and graphically estimated i_{corr} values, showing the good agreement between polarisation curves and EIS data.

In order to compare the corrosion inhibition effect of the different EPS, i_{corr} values calculated from Eq. 7.8 were plotted as a function of the solution (**FIG. 7.13).**

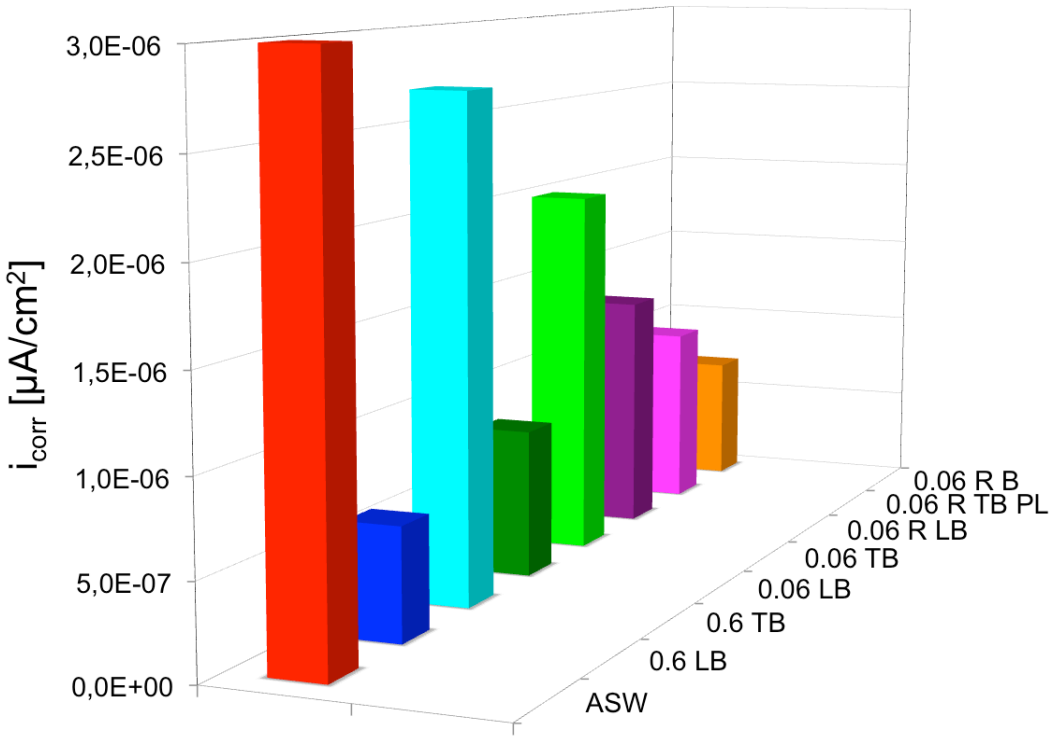

FIG. 7.13. COMPARISON OF CORROSION CURRENTS IN DIFFERENT EPS SOLUTIONS (LB AND TB) CALCULATED FROM THE EQ. 7.8. GIVEN RESULTS WERE THE MEAN VALUE FROM TWO INDEPENDENT SAMPLES.

While comparing i_{corr} in the EPS–containing solutions and in the EPS–free solution (ASW), it could be concluded that LB EPS were always protective whatever the conditions; thus, an important corrosion inhibition effect was observed for 0.6 and 0.06 LB EPS, with a ratio of corrosion currents without and with EPS (i_{corr} (ASW) / i_{corr} (EPS)) comprised between ca. 4 and 5. A similar effect was also shown for the EPS from the bioreactor survey (ratio of corrosion currents without and with EPS equal to ca. 3 – 4). A negligible or poor corrosion inhibition effect was recorded for 0.6 and 0.06 TB EPS (ratio of corrosion currents without and with EPS equal to *ca.* 1.1 and 1.5, respectively).

Recorded XPS spectra and modelling of surface – active compounds in terms of proteins, polysaccharides and hydrocarbons, helped to better understand this phenomenon. Despite some differences in the general composition, adsorption properties of two particular EPS (0.6 TB and 0.06 TB) distinguished themselves among all investigated molecules. Poor corrosion inhibition effect was assigned mainly to the proteins adsorption layer created on the carbon steel surface from these EPS samples. As shown in the Chapter VI, these were also the only samples, in which detectable amounts of heam containing proteins were found. Heamproteins

are involved in the oxygen transport or the electron transfer. Cytochromes are an example of the latter proteins. Involvement of extracellular proteins in the redox reactions may be of high importance for the acceleration of biocorrosion processes.

Later on, it was observed that *D. alaskensis*, while growing in the presence of carbon steel, secreted more hydrocarbon molecules. These were further observed on the carbon steel surface. EPS composition may change in order to respond to surface features and to provide the cell surface with the properties optimal for the attachment. At the expense of protein diversity, these intensively produced amphiplihic molecules could facilitate the attachment to the carbon steel surface.

EPS became less invasive for the carbon steel surface than ASW. This behaviour, in which EPS were more protective, with the difference of LB EPS being more beneficial for the steel stability than TB EPS, was in parallel detected in EPS from a marine aerobic strain of *Pseudomonas* sp. 2021 (Torres–Bautista, 2013). In this study, observed TB EPS properties were attributed to the protein adsorption.

5. CONCLUSIONS

EPS secretion by *D. alaskensis* grown in various conditions can evolve very dynamically. Proteins were found to be present in very high concentrations in most of the dried EPS residues. These layers were mainly composed of proteins, either because these were the major bulk constituent, as shown by biochemical analysis, or because they were accumulated at the liquid – air interface, which generated this solid surface, subsequently analysed by XPS. The second class of adsorbed EPS components at high concentrations was identified as hydrocarbon containing molecules. These may be attributed to the lipid and humic substances fractions from *D. alaskensis* EPS. Polysaccharides were also detected, but generally their levels were low and did not significantly change with varying growth conditions, as it was observed for other EPS components.

EPS adsorption to the carbon steel surface processed very rapidly and comparably for all samples, as deduced from the E_{corr} measurements. Nevertheless, EPS adsorptive properties spreaded in two directions. Either proteins were dominantly adsorbed on the carbon steel surface (80–90 % of EPS) or a mixture of hydrocarbons, proteins and residual polysaccharides (in the average rate of approximately 50:30:20, respectively) was detected.

All loosely bound EPS, belonging to the latter group, were protective independently of their origin. In their presence, the highest corrosion inhibition effect was observed. EPS extracted from *D. alaskensis,* grown in the bioreactor conditions, showed similar properties. Two tightly bound EPS from the planktonic cells (grown in absence of carbon steel) were less inhibitive than other solutions properties, but still they were slightly lower than ASW.

At E_{corr}, it can be concluded from combined polarisation curves (anodic and cathodic) and EIS data that EPS did not enhance corrosion and induced a decrease of the dissolution rate with decreased currents, and thus slowed down corresponding reactions.

6. REFERENCES

Aguié–Béghin, V., Adriaensen, Y., Péron, N., Valade, M., Rouxhet, P., Douillard, R., 2009. Structure and Chemical Composition of Layers Adsorbed at Interfaces with Champagne. J. Agric. Food Chem. 57, 10399–10407.

Ahimou, F., Boonaert, C.J.P., Adriaensen, Y., Jacques, P., Thonart, P., Paquot, M., Rouxhet, P.G., 2007. XPS analysis of chemical functions at the surface of Bacillus subtilis. J. Colloid Interface Sci. 309, 49–55.

Beech, I.B., Sunner, J., 2004. Biocorrosion: towards understanding interactions between biofilms and metals. Curr. Opin. Biotechnol. 15, 181–186.

Beech, I.B., Sunner, J.A., Hiraoka, K., 2005. Microbe–surface interactions in biofouling and biocorrosion processes. Int. Microbiol. Off. J. Span. Soc. Microbiol. 8, 157–168.

Berglin, M., Elwing, H., 2008. Erosion of a model rosin–based marine antifouling paint binder as studied with quartz crystal microbalance with dissipation monitoring (QCM–D) and ellipsometry. Prog. Org. Coatings 61, 83–88.

Boonaert, C.J.P., Dufrêne, Y.F., Rouxhet, P.G., 2003. Adhesion (Primary) of Microorganisms onto Surfaces, in: Encyclopedia of Environmental Microbiology. John Wiley & Sons, Inc.

Brug, G.J., van den Eeden, A.L.G., Sluyters–Rehbach, M., Sluyters, J.H., 1984. The analysis of electrode impedances complicated by the presence of a constant phase element. J. Electroanal. Chem. Interfacial Electrochem. 176, 275–295.

Dufrêne, Y.F., Vermeiren, H., Vanderleyden, J., Rouxhet, P.G., 1996. Direct evidence for the involvement of extracellular proteins in the adhesion of Azospirillum brasilense. Microbiology 142, 855–865.

Epelboin, I., Gabrielli, C., Takenouti, H., 1981. Alternating–Current Impedance Measurements Applied to Corrosion Studies and Corrosion–Rate Determination, in: Electrochemical Corrosion Testing, ASTM STP 727, American Society for Testing and Materials. p. 150.

Flemming, H.–C., 2011. Microbial Biofouling: Unsolved Problems, Insufficient Approaches, and Possible Solutions, in: Flemming, H.–C., Wingender, J., Szewzyk, U. (Eds.), Biofilm Highlights, Springer Series on Biofilms. Springer Berlin Heidelberg, pp. 81–109.

Flemming, H.–C., Wingender, J., 2010. The biofilm matrix. Nat. Rev. Microbiol. 8, 623–633.

Genet, M.J., Dupont–Gillain, C.C., Rouxhet, P.G., 2008. XPS Analysis of Biosystems and Biomaterials, in: Medical Applications of Colloids. Springer, New York, pp. 177–307.

Graham, D.J., Midgley, N.G., 2000. Graphical representation of particle shape using triangular diagrams: an Excel spreadsheet method. Earth Surf. Process. Landforms 25, 1473–1477.

Hirschorn, B., Orazem, M.E., Tribollet, B., Vivier, V., Frateur, I., Musiani, M., 2010. Determination of effective capacitance and film thickness from constant–phase–element parameters. Electrochimica Acta 55, 6218–6227.

Huh, C., Mason, D.S.G., 1975. A rigorous theory of ring tensiometry. Colloid Polym. Sci. 253, 566–580.

Landoulsi, J., Genet, M.J., Richard, C., El Kirat, K., Pulvin, S., Rouxhet, P.G., 2008. Evolution of the passive film and organic constituents at the surface of stainless steel immersed in fresh water. J. Colloid Interface Sci. 318, 278–289.

Orazem, M.E., Pébère, N., Tribollet, B., 2006. Enhanced Graphical Representation of Electrochemical Impedance Data. J. Electrochem. Soc. 153, B129–B136.

Rajagopal S., Nair K.V.K., Azariah J., van der Velde G., Jenner H.A., 1996. Chlorination and Mussel Control in the Cooling Conduits of a Tropical Coastal Power Station. Mar. Environ. Res. 41, 201–221.

Rouxhet, P.G., Genet, M.J., 2011. XPS analysis of bio–organic systems. Surf. Interface Anal. 43, 1453–1470.

Rouxhet, P.G., Misselyn–Bauduin, A.M., Ahimou, F., Genet, M.J., Adriaensen, Y., Desille, T., Bodson, P., Deroanne, C., 2008. XPS analysis of food products: toward chemical functions and molecular compounds. Surf. Interface Anal. 40, 718–724.

Schneider, R.P., Leis, A., 2003. Conditioning Films in Aquatic Environments, in: Encyclopedia of Environmental Microbiology. John Wiley & Sons, Inc.

Stern, M., Geary, A.L., 1957. Electrochemical Polarization I . A Theoretical Analysis of the Shape of Polarization Curves. J. Electrochem. Soc. 104, 56–63.

Thierry, D., Sand, W., 2002. Microbially Influenced Corrosion, in: Marcus, P. (Ed.), Corrosion Mechanisms in Theory and Practice. CRC Press, pp. 583–603.

Torres–Bautista, B.E., 2013. Effect of biomolecules adsorption and bacterial adhesion on oxide layers

developed on metallic materials used in cooling water systems. PhD Thesis. Centre National de la Recherche Scientifique, Laboratoire de Physico–Chimie des Surfaces, Chimie ParisTech, France.

Wanger, C.D., Riggs, W.M., Davis, L.E., Moulder, J.F., Muilenberg, G.E., (eds) Briggs, D., 1981. Handbook of X–ray Photoelectron Spectroscopy. Perkin–Elmer Corp., Physical Electronics.

Yang, Y., Wikieł, A.J., Dall'Agnal, L.T., Eloy, P., Genet, M.J., Moura, J.J.., Sand, W., Dupont–Gillain, C.C., Rouxhet, P.G., in preparation. Proteins dominating in conditioning layers formed by extracellular polymeric substances.

SUMMARY AND GENERAL CONCLUSIONS

Oil and gas industry is build of complex systems, vulnerable to microbial activity. The consequences of the latter, occurring in the form of microbially influenced corrosion (MIC) were investigated in this study. A special attention was paid to the characteristics of extracellular polymeric substances (EPS) and their influence on MIC processes on the carbon steel. The industry suffers from the complex microbial interactions with corrosive various metabolites, able to stimulate surface deterioration in a complex way.

Microbial diversity in the oil production and water injection pipelines were investigated by means of culture–dependent and molecular approaches. Aerobic and anaerobic microorganisms involved in the sulfur, nitrogen, iron and manganese cycles were found in the investigated field samples. With use of the epifluorescence microscopy the dynamics of attachment of the SRP field enrichment to the carbon steel was monitored. It was observed that within one week these microorganisms were able to form a thick, multilayer biofilm, revealing how actively these organisms can develop.

A model organism, *D. alaskenis* AL1, a sulfate reducing bacterium isolated from the oil field, was chosen for the further studies. In order to assess its corrosive properties, this SRB was subjected to the electrochemical, corrosion rate and microscopic investigations. Corrosion potential (E_{corr}) ennoblement was observed with two potential peaks of –720 mV (after 24h of inoculation) and –710 mV (after approx. 48h of inoculation). Corrosion rates were slightly lower than in the abiotic control and did not exceed 0.05 mmpy. Carbon steel surface after the exposure to the SRP biofilm and its metabolic products was visualised by use of the atomic force microscopy, revealing the importance of attached microorganisms in the pitting corrosion. Confocal laser scanning microscopy suggested importance of extracellular proteins in the biofilm formation.

The core part of this work was focused on the investigations of extracellular polymeric substances (EPS) on the corrosion processes. Analyses in this direction begun with the optimisation of an appropriate *D. alaskensis* EPS extraction protocol. Various reagents were tested to assess the rate of caused cell lysis. Three, 18–crown–6 ether (CE), Dowex cation exchange resin, and EDTA, pH=8 were chosen, as the lysis levels were lower than 1%. The optimal protocol included a three–step

EPS extraction for either 1.5 or 2 h. Additionally, for each extraction adequate sterile abiotic controls were prepared. In the EDTA and CE controls a positive signal was detected for sugars and uronic acids signals. It was observed, that with use of EDTA the highest amounts of humic substances were extracted, while with Dowex and CE mainly proteins were isolated. Based on the protein profiles analyses, performed by sodium dodecyl sulfate polyacrylamide gel electrophoresis (SDS–PAGE), it was shown that proteins extracted in different steps EPS did not differ in their qualitative composition. Only EDTA showed the ability to extract higher numbers of lower molecular weight proteins, as compared to Dowex and CE. The extraction with use of Dowex in the 1.5 h time intervals was applied for the further EPS isolation.

Changes in the EPS secretion, while growing *D. alaskensis* AL1 in various conditions, were investigated. These included tests in static conditions with non–modified growth medium and the medium with 10 times reduced nutrients content. SRP were also grown in the bioreactor with the exchange of the modified medium and presence of the carbon steel plates. It was observed that loosely bound (LB) EPS were not intensively secreted. They were mainly composed of sugars. Proteins amounts were 2 to 4 times lower than sugars. Extracellular DNA and uronic acids were intensively secreted in the tightly bound (TB) EPS, obtained from the cells, grown under starvation in static conditions, and both TB EPS from planktonic cells and from the biofilm (i.e. grown in the presence of carbon steel). The main components of TB EPS were proteins and humic substances. Extracellular fatty acid methyl esters (FAME) were also investigated. Unbranched, saturated C16 and C18 FAME chain lipids were dominantly secreted.

It was also found, using transmission electron microscopy that EPS components could organise themselves in three main structures, which were compared with existing EPS models. They were identified as probably sugar–protein complex, protein–metal sulfides aggregates and micelle like complexes.

For the corrosion studies in the marine conditions EPS were dialysed in the artificial seawater (ASW). Their influence on the carbon steel surface behaviour was analysed by means of E_{corr} monitoring together with Electrochemical Impedance Spectroscopy (EIS) and Linear Polarisation (LP). A protective behaviour was observed for LB EPS and the biofilm EPS (corrosion current, i_{corr} was in the range of 0.6 – 1.3 μA/cm^2) in comparison to artificial seawater (ASW, i_{corr} = 3.0 μA/cm^2), while the impact of TB EPS from the static conditions was only slightly lower in comparison

to ASW (i_{corr} = 2.0–2.7 μA/cm^2). From the surface tension measurements it was observed that *D. alaskensis* EPS contained a significant amount of surface–active molecules. Further on EPS attached to the carbon steel surface was characterised by means of X–ray Photoelectron Spectroscopy (XPS). These macromolecules, which showed low inhibitory effects on the steel deterioration, were mainly consisting of proteins. Remaining EPS revealed high levels of hydrocarbons.

This study presented the insights into the biocorrosion problems related to the oil and gas field. The complexity of the corrosive biofilm development and its interactions with the metal surface were highlighted. Special attention was paid to the isolation, composition, function and corrosiveness of EPS in order to deliver new insights into the MIC studies.

This work proposed a different way of approaching the problem of MIC. The emphasis was put on the multidisciplinary approach of two scientific fields, chemistry and microbiology, which are the basis for MIC examination. The problem is very advanced; thus, innovative actions should be undertaken to deal with it.

Investigations presented in this work open new perspectives for the future corrosion investigations. First of all, the attention needs to be paid to the EPS research, as these molecules posses potential to affect MIC processes in many various ways. EPS did not enhance corrosion and induced a decrease of the dissolution rate with decreased currents. Thus, it slowed down corresponding reactions. However, this effect was different among various EPS fractions tested. When a low inhibitory effect was observed, protein moieties were mainly detected on the surface. The highest inhibitory effects were obtained, while the steel surface was covered with the hydrocarbon molecules. Thus, more attention needs to be paid to target these compounds. Mass spectrometry should be more intensively applied for these studies. A major attention also should be paid in the EPS proteins, as they have started to be considered as relevant to the biodeterioration (Busalmen et al., 2002). A potential of using loosely bound EPS, as the inhibitors of MIC should also be considered, especially that they are easy to isolate.

More electrochemical studies should be incorporated in the EPS investigations. From a large number of analytical methods, electrochemistry provides promising reagentless methods capable of miniaturisation. They have a decreased response time with low energy requirements. Electrochemistry offers also insights to the mechanisms occurring on the surface.

Finally, an attempt was made to move the corrosion problems from the field to the laboratory, in order to give a feedback for the industry. Industrial samples were successfully analysed and provided many data for further application in the field. EPS analyses delivered not only the understating of their potential functions in the corrosion processes, but also some of them were observed on the carbon steel. To supplement this research work and obtain a global view of the MIC problem, more MIC related microorganisms need to be investigated. It will be of utmost interest to perform the studies, which will incorporate the field isolates and mixed cultures, with an emphasis on the field related experimental conditions.

REFERENCES

Busalmen, J., Vázquez, M., de Sánchez, S.., 2002. New evidences on the catalase mechanism of microbial corrosion. Electrochimica Acta 47, 1857–1865.

APPENDIX

PUBLIKATIONSLISTE

A. J. Wikieł, I. Datsenko, M. Vera, W. Sand *Impact of Sulfate Reducing Prokaryotes Biofilms on Corrosion Behaviour of Low Carbon Steel in Marine Environment,* Bioelectrochemistry Journal (under review)

A. J. Wikieł, I. Datsenko, L.T. Dall'Agnol J.J.G. Moura, M. Vera, W. Sand *Comparative Study on EPS Extraction Strategies from Sulfate Reducing Prokaryotes* (in preparation)

Y. Yang, A.J. Wikieł, L.T. Dall'Agnol, P. Eloy, M.J. Genet, J.J.G. Moura, W. Sand, C.C. Dupont–Gillain, P.G. Rouxhet *Proteins dominance in conditioning layers formed by extracellular polymeric substances* (in preparation)

POSTER UND VORTRÄGE

A. J. Wikieł, M. Vera, W. Sand *Influence of Extracellular Polymeric Substances on Biocorrosion Processes*

- Euroscience Open Forum 2010, Torino, Italy (Poster)

A. J. Wikieł, M. Vera, W. Sand *Influence of Extracellular Polymeric Substances on Biocorrosion Processes*

- International Symposium on Applied Microbiology and Molecular Biology in Oil Systems 2011, Calgary, Canada (Vortrag)

A. J. Wikieł, M. Vera, W. Sand *Biofilm formation studies and EPS analysis within the oil & gas industry*

- The European Corrosion Congress, Eurocorr 2011, Stockholm, Sweden (Vortrag)

A. J. Wikieł, I. Datsenko, M. Vera, W. Sand *Impact of Sulfate Reducing Prokaryotes and Extracellular Polymeric Substances on corrosion behaviour of low carbon steel in marine environment*

- The European Corrosion Congress, Eurocorr 2012, Istanbul, Turkey (Vortrag)

CURRICULUM VITAE

Der Lebenslauf ist in der Online – Version
aus Gründen des Datenschutzes nicht enthalten.

DEKLARATION

Hiermit versichere ich, dass ich die vorliegende Arbeit mit dem Titel

„Role of extracellular polymeric substances on biocorrosion initiation or inhibition"

selbst verfasst und keine außer den angegebenen Hilfsmitteln und Quellen benutzt habe, und dass die Arbeit in dieser oder ähnlicher Form noch bei keiner anderen Universität eingereicht wurde.

Essen, im Juli 2013

AGATA JOANNA WIKIEŁ

Agata Joanna Wikieł

Role of extracellular polymeric substances on biocorrosion initiation or inhibition

PhD Supervisor: Prof. Dr. Wolfgang Sand
Co–Supervisor: Dr. Mario Vera
Biofilm Centre, Aquatische Biotechnologie
Universität Dusiburg–Essen

ABSTRACT

Oil and gas industry is built of complex systems, which are vulnerable to microbial activity. Investigating microbially influenced corrosion (MIC) in order to improve the understating of this process constitutes an immense challenge. Microorganisms accumulate on the steel surface, forming biofilms embedded in extracellular polymeric substances (EPS). EPS provide the reaction space for the metal–surface interactions. The serious economic impact of MIC has lead to the understanding that development of efficient solutions strongly depends on application of multidisciplinary approaches. This study was focused on characterising the diversity of microorganisms present in the oil and gas field and on the assessment of the influence of bacterial EPS on biocorrosion processes. The first main goal was achieved by use of culture–dependent and molecular biology techniques. For the second goal, the sulfate reducing bacterium *Desulfovibrio alaskensis* AL1, was used as a model organism. An extraction protocol of EPS secreted by this bacterium was developed. Isolated EPS were used for further investigations, which included i) its composition analysis, ii) studies of the influence of carbon steel and flow conditions in a bioreactor on its secretion patterns and iii) its influence on the steel stability, which was investigated by means of corrosion potential monitoring, linear polarisation and electrochemical impedance spectroscopy. EPS moieties adsorbed to the carbon steel were identified with use of X–ray photoelectron spectroscopy.

Key words: microbially influenced corrosion, sulfate reducing prokaryotes, biofilms, extracellular polymeric substances, oil and gas industry

The research leading to these results has received funding from the European Community's Seventh Framework Programme (FP7/2007–2013) under grant agreement n°238579. Project website: www.biocor.eu/ip4 (RSP1&2).